

**QCD Factorisation in Exclusive
Semileptonic B Decays**
**New Applications and Resummation of
Rapidity Logarithms**

DISSERTATION
zur Erlangung des Grades eines Doktors
der Naturwissenschaften

vorgelegt von
M.Sc. Philipp Böer

eingereicht bei der Naturwissenschaftlich-Technischen Fakultät
der Universität Siegen

Siegen 2018

gedruckt auf alterungsbeständigem holz- und säurefreiem Papier

Betreuer und erster Gutachter: Prof. Dr. Thorsten Feldmann (Universität Siegen)

Zweiter Gutachter: Prof. Dr. Guido Bell (Universität Siegen)

Tag der mündlichen Prüfung: 23. August 2018

Promotionskommission: Prof. Dr. Thomas Becher (Universität Bern, Schweiz)

Prof. Dr. Guido Bell (Universität Siegen)

Prof. Dr. Thorsten Feldmann (Universität Siegen)

Prof. Dr. Markus Risse (Universität Siegen)

Abstract

Exclusive charmless decays of heavy B -mesons play an important role both in testing the Standard Model of particle physics as well as in searches for new physics. Due to the non-perturbative nature of the strong interactions, reliable predictions for hadronic decay rates are intrinsically difficult to estimate. Exploiting the simplifications of the strong interaction dynamics that arise in the heavy-quark limit, the “QCD factorisation approach” (QCDF) allows for a separation of perturbative and non-perturbative effects in these decays. In this thesis we present new applications of the QCDF approach and investigate cases where the factorisation is not yet understood.

In a first project, we introduce a novel factorisation formula for form factors in semileptonic multi-body $B \rightarrow \pi\pi\ell\nu$ decays that is valid for large pion energies and a large dipion invariant mass. We present phenomenological implications in the form of approximate form factor relations, which can be used to interpolate between different phase-space regions. Theoretically, a careful consideration of endpoint-divergent moments is crucial in the confirmation of the factorisation formula. They either cancel in factorisable contributions or can be absorbed into simpler and more universal $B \rightarrow \pi$ form factors.

For the $B \rightarrow \pi$ form factors themselves, a complete factorisation of scales is presently not understood as a consequence of ill-defined convolution integrals. We investigate these so-called “endpoint divergences” in a perturbative toy model, in which the hadronic states are approximated as non-relativistic bound states of two heavy quarks. The relativistic QCD dynamics is then calculable in perturbation theory, and by employing the method of regions the factorisation properties can be studied. Fairly new methods that go under the names *rapidity renormalisation group* and *collinear anomaly* have been successfully applied to handle endpoint divergences in collider physics observables. In this thesis we apply these techniques to heavy-to-light form factors at large hadronic recoil. As a first step on the way to establish an all-order factorisation theorem, we present an improved factorisation that contains a resummation of all leading logarithms within the perturbative model. Due to operator mixing, the structures that arise in the resummed expression are more complicated but also more interesting than in collider physics applications of these methods.

Zusammenfassung

Exklusive Zerfälle schwerer B -Mesonen in leichte Mesonen spielen eine wichtige Rolle, um das Standardmodell der Elementarteilchenphysik zu testen, sowie nach Neuer Physik zu suchen. Aufgrund der nicht-perturbativen Natur der starken Wechselwirkung sind verlässliche Vorhersagen für hadronische Observablen schwer zu bestimmen. Vereinfachungen der Dynamik treten jedoch im Limes unendlich großer Masse des b -Quarks auf. Darauf basierend erlaubt der “QCD Faktorisierungsansatz” (QCDF) eine systematische Trennung von perturbativen und nicht-perturbativen Effekten in oben genannten Zerfällen. In dieser Arbeit präsentieren wir neue Anwendungen des QCDF Zugangs und untersuchen im Speziellen Fälle, in denen die Faktorisierung noch unverstanden ist.

In einem ersten Projekt führen wir ein neues Faktorisierungstheorem für die Formfaktoren in semileptonischen $B \rightarrow \pi\pi\ell\nu$ Zerfällen ein, welches für große Pionenergien sowie für große invariante Masse des Dipion Systems gültig ist. Phänomenologische Implikationen in Form von näherungsweise gültigen Relationen zwischen den Formfaktoren werden untersucht, und können in zukünftigen Studien genutzt werden, um zwischen verschiedenen Phasenraumregionen zu interpolieren. In der Herleitung des Faktorisierungstheorems spielen endpunkt-divergente Momente eine entscheidende Rolle. Diese heben sich teilweise zwischen verschiedenen Beiträgen weg, oder aber können in universellere $B \rightarrow \pi$ Formfaktoren absorbiert werden.

Eine vollständige Faktorisierung von Skalen in den $B \rightarrow \pi$ Formfaktoren ist aufgrund von divergenten Faltungsintegralen derzeit noch unverstanden. Wir untersuchen diese sogenannten Endpunktdivergenzen in einem störungstheoretischen Modell, in welchem die hadronischen Zustände als nicht-relativistische Bindungszustände zweier schwerer Quarks genähert werden können. Die relativistische Dynamik ist dann störungstheoretisch berechenbar und die Faktorisierungseigenschaften können mit Hilfe der Methode der Regionen untersucht werden. In dieser Arbeit wenden wir die neuen Methoden der “kollinearen Anomalie” sowie der “Rapiditäts-Renormierungsgruppe”, welche bisher noch nicht im Kontext der Flavourphysik benutzt wurden, auf die Formfaktoren in exklusiven schwer-nach-leicht Prozessen an. Als ersten Schritt auf dem Weg, ein Faktorisierungstheorem zu etablieren, wird eine verbesserte Faktorisierung der Formfaktoren in diesem Modell präsentiert, welche eine Resummation von allen führenden großen Logarithmen beinhaltet. Aufgrund von mehreren Operatoren, welche untereinander mischen, ist unser Ergebnis komplizierter als in Anwendungen dieser Methoden in der Collider Physik.

Contents

Introduction	3
1 Introduction	3
1.1 General Introduction	3
1.2 Factorisation	5
1.3 The QCD Factorisation Approach	9
1.4 Outline of this Thesis	13
Project I: QCD Factorisation Theorem for $B \rightarrow \pi\pi\ell\nu$ Decays	17
2 Factorisation of Hadronic Matrix Elements	19
2.1 Kinematics and Power Counting	19
2.2 The Factorisation Formula	20
2.2.1 The kernel T^{I}	21
2.2.2 The kernel T^{II}	24
3 $B \rightarrow \pi\pi$ Form Factors and Observables	31
3.1 Constraining the Phase Space	31
3.2 Reduction of Independent Form Factors	32
3.3 Numerical Results	34
4 Summary	41
Project II: Endpoint Divergences in Exclusive B Decays	45
5 Theoretical Foundations and the Massive On-Shell Sudakov Problem	47
5.1 One-Loop Calculation in QED with a Massive Photon	47
5.2 The Strategy of Regions	51
5.3 Soft-Collinear Effective Theory	58
5.4 Factorisation and Resummation	63
6 Factorisation of Heavy-to-Light Form Factors at Large Recoil	71
6.1 Preliminary Discussion	71
6.2 (Incomplete) Factorisation Formula	74

6.3	Matching the A -Type Current onto SCET _{II}	76
6.3.1	Operator Basis	77
6.3.2	Tree-Level Matching	77
6.3.3	Leading Poles in One-Loop Corrections to $D_{m,1}$	81
6.4	Light-Cone Distribution Amplitudes	86
6.4.1	Heavy Mesons	86
6.4.2	Light Mesons	89
6.5	Naive Factorisation Formula for ξ_π	92
7	Heavy-to-Light Form Factors for Non-Relativistic Bound States	95
7.1	Setup	95
7.2	Non-Factorisable Double Logarithms at One-Loop	96
7.2.1	ξ_π at Tree-Level	97
7.2.2	Cancellation of Double Poles at One-Loop Order	98
7.3	Resummation of Leading Logarithms	102
7.3.1	Recursion Relations for Inverse Moments	103
7.3.2	Rapidity Renormalisation Group Treatment of Inverse Moments	108
8	Beyond the Resummation of Leading Logarithms	117
8.1	The Soft-Collinear Mode	118
8.2	Endpoint Re-Factorisation	119
9	Summary	127
	Conclusion and Outlook	131
10	Conclusion and Outlook	131
	Appendix	135
A	Details on $B \rightarrow \pi\pi$ Form Factors at Large Dipion Invariant Masses	135
A.1	Definition of Dipion Form Factors	135
A.2	Twist-3 Contributions to the Kernel T^I	137
A.3	Detailed Calculation for the Kernel T^{II}	139
A.3.1	Recapitulation: the $B \rightarrow \pi$ Form Factor F_+	139
A.3.2	Expressions for $b \rightarrow d\pi^+g\ell^-\bar{\nu}_\ell$ Amplitudes	140
A.3.3	Contributions to $B \rightarrow \pi\pi$ Matrix Elements	142
A.4	More on Kinematics	146
B	Details on the Sudakov Form Factor	149
B.1	Details on the RG Evolution Kernels	149
B.2	Details on the Renormalisation of F and R	150

C	Details on the Factorisation of Heavy-to-Light Form Factors	151
C.1	QCD \rightarrow SCET _I Matching of $B \rightarrow \pi$ Form Factors	151
C.2	Details on the One-Loop Hard-Collinear Kernel	152
C.3	Matrix Element of the Collinear Current $\bar{\chi} \frac{\not{p}}{2} \gamma_5 i \not{\phi}_\perp \chi$	154
C.4	Contributions of the Individual Operators to ξ_π	156
D	Details on Heavy-to-Light Form Factors for NR Bound States	157
D.1	LCDAs for Non-Relativistic Bound States	157
D.1.1	Tree-Level	157
D.1.2	One-Loop Corrections	157
D.2	Leading Endpoint Contributions of Two-Loop Moments	160
D.3	Solutions of the Recursion Relations	165
D.4	The Collinear Anomaly Argument in the Presence of Operator Mixing . .	167
	Bibliography	171

Introduction

Chapter 1

Introduction

1.1 General Introduction

The Standard Model (SM) of elementary particle physics is a relativistic and renormalisable quantum field theory that comprises our current knowledge about the constituents of matter that are believed to be fundamental as well as three of the four known fundamental forces of nature: the electroweak interaction – a unification of the electromagnetic interaction and the weak nuclear force – and the strong nuclear force. These interactions are implemented through the principle of local gauge invariance. The fourth known force, gravity, is at large scales well-described by the general theory of relativity. Whereas the SM is a quantum theory, general relativity is a classical field theory whose quantised nature is unknown. Thus (and due to various other phenomena that are not explained by the SM, like the existence of dark matter and dark energy, the matter-antimatter asymmetry in the universe, etc.) the SM is not the one physical theory that encompasses all interactions and phenomena observed in the universe. It nevertheless has proven to describe the observed phenomena at very small distances with intriguing precision and has been tested up to energies of several TeV. The most recent example for the success of the SM is the discovery of the Higgs boson in 2012 by the experiments ATLAS [1] and CMS [2] at the European Organization for Nuclear Research (CERN) in Geneva (Switzerland). About 50 years earlier the existence of this particle was predicted [3, 4] and before its discovery it was the last missing piece in the set of elementary particles incorporated in the SM. Consequently, the discovery led to a Nobel Prize in Physics awarded to Higgs and Englert in 2013. In this thesis we refrain from giving a detailed introduction into the mathematical formulation of the SM and its explicit gauge structure, which nowadays is presented in many textbooks, e.g. [5–9].

The matter particles in the SM are classified into quarks and leptons, which are organised in multiplets of the various gauge groups. Each multiplet comes in three copies (“families”) with identical gauge couplings. The only way to distinguish between different families is through their Yukawa coupling to the Higgs field, which after spontaneous symmetry breaking results in different fermion masses. *Flavour physics* is the branch of particle physics investigating transitions between the various quarks and leptons (“flavours”) contained in the SM. Whereas gauge symmetry enforces the couplings of the strong and electroweak interactions to be universal, the Yukawa matrices are not fixed by symmetry arguments. This allows in particular a mixing of quarks of the up-type with quarks of the down-type with their relative couplings being parametrised by the unitary CKM matrix

(named after Cabibbo, Kobayashi und Maskawa [10, 11]). Flavour-changing processes provide a unique possibility to determine some of the fundamental parameters of the SM, such as the CKM-matrix elements and thus to test the SM for its consistency. On the other hand, certain decays that are strongly suppressed in the SM (“rare decays”) are highly sensitive to physics beyond the Standard Model, and can indirectly test much higher energies than currently accessible in experiments. The ultimate goal of flavour physics is to explain the origin of flavour and to answer the question why the number of families occurring in nature is exactly three. Due to their extremely rich phenomenology, B -meson decays currently play the most important role in the field of flavour physics.

The strong interactions, however, prevent direct tests of the fundamental interactions between quarks. A main part of current research in elementary particle physics is thus the study of effects related to quantum chromodynamics (QCD), the gauge theory of the strong interactions, based on an $SU(3)_c$ gauge group. Due to the properties that will be discussed below, these effects are intrinsically difficult to determine, but are necessary for a precise prediction for a large class of observables. The non-abelian nature of the symmetry group yields gluon self-interactions which – in contrast to quantum electrodynamics (QED; the gauge theory of the electromagnetic interactions) – leads to an “anti-screening” of colour-charges: the running coupling constant $\alpha_s(\mu) \equiv g_s(\mu)^2/4\pi$ decreases with increasing energy scale. This behaviour is captured in the β -function,

$$\beta(\alpha_s(\mu)) \equiv \frac{d\alpha_s(\mu)}{d \log \mu} = -2\beta_0 \frac{\alpha_s(\mu)^2}{4\pi} + \mathcal{O}(\alpha_s^3), \quad (1.1)$$

where β_0 can be calculated in perturbation theory:

$$\beta_0 = \frac{11}{3}C_A - \frac{2}{3}n_f > 0. \quad (1.2)$$

Here C_A is defined by the Casimir operator in the adjoint representation (for $SU(3)_c$ we have $C_A = 3$) and n_f is the number of active flavours. The solution to the differential equation gives the one-loop running coupling

$$\alpha_s(\mu) = \frac{\alpha_s(\mu_0)}{1 + \frac{\alpha_s(\mu_0)}{4\pi} \beta_0 \log \frac{\mu^2}{\mu_0^2}}. \quad (1.3)$$

The energy behaviour of $\alpha_s(\mu)$ has profound consequences and results in different “phases” of QCD. At large energy scales (or equivalently short distances) the coupling tends to zero, $\alpha_s(\mu \rightarrow \infty) \rightarrow 0$, and QCD is “*asymptotically free*” [12, 13], which justifies a perturbative treatment in this energy region. Thus, if one resolves very short distances, quarks can be viewed as quasi-free particles. On the other hand, for small values of μ the coupling becomes large and eventually leads to a breakdown of the perturbative expansion. This is related to the “*confinement*” of quarks into hadrons: observable in nature are only colour-neutral bound states of quarks and gluons, which are classified into mesons (hadronic states with two valence quarks) and baryons (three valence quarks). (Recently also bound states with more valence quarks have been observed at the LHCb experiment, see e.g. [14].) The intrinsic QCD parameter Λ_{QCD} gives an estimate of the energy scale where non-perturbative physics dominate. It is defined as the value where the coupling

constant (formally) diverges, $\alpha_s(\mu = \Lambda_{\text{QCD}}) \rightarrow \infty$. Measuring α_s at higher energies gives $\Lambda_{\text{QCD}} \approx 200 - 300 \text{ MeV}$.

To relate partonic amplitudes with hadronic observables is in general challenging. In the following, we will see how this goal can be systematically accomplished in many relevant situations.

1.2 Factorisation

Processes in experiments often involve several widely separated energy scales which simplifies the QCD dynamics to a certain approximation. For example, beam energies in modern particle accelerators are a factor of 10^4 – 10^5 greater than the intrinsic QCD-scale Λ_{QCD} ,¹ but also the mass of a heavy particle can define a “hard scale.” According to the above discussion, the QCD dynamics associated with the different energy scales is qualitatively different. Due to the asymptotic freedom of QCD, quarks at high energies can be viewed as quasi-free particles. The hard dynamics can thus be described by a partonic process and is accessible in perturbation theory. On the other hand, effects related to the hadronisation happen at low energies and need to be treated non-perturbatively. The main goal in the treatment of QCD effects is thus the systematic separation (“*factorisation*”) of effects associated with different energy scales. The hard process happens at small timescales $\tau_{\text{hard}} \sim (\text{large energy})^{-1}$, whereas the hadronisation effects happen at much larger timescales $\tau_{\text{had.}} \sim 1/\Lambda$. Here $\Lambda \sim$ a few $\Lambda_{\text{QCD}} \lesssim 1 \text{ GeV}$ characterises typical momentum transfers of the confined partons inside a hadron. It is thus intuitive that the different effects should decouple in the limit where the hard scale goes to infinity. Upon factorisation, quantities related to the different energy scales can then be studied independently using different (perturbative and non-perturbative) methods.

In the following, we briefly illustrate with two simple observables how a factorisation can be realised technically. Although the idea is very general and can be applied to a variety of different scenarios, in this thesis we focus on effects related to the strong-interaction dynamics. Furthermore, whenever we consider processes that happen at energy scales much smaller than the electroweak scale, $\mu_{\text{EW}} \sim 100 \text{ GeV}$, we implicitly consider the situation where physics associated to μ_{EW} has already decoupled. This is in particular assumed in decays of B mesons, with $\mu_{\text{EW}} \gg M_B \simeq 5.3 \text{ GeV}$.

Example 1: Operator Product Expansion in $e^+e^- \rightarrow \text{Hadrons}$

The analysis presented in the following is based on Chapter 18.4 in [5]. As an introductory example we study electron-positron annihilation into an inclusive hadronic final state at centre-of-mass energies $\sqrt{s} \gg \Lambda$. For simplicity, we furthermore assume $\sqrt{s} \ll M_Z$, such that the process happens through the electromagnetic quark current only. The total

¹The most powerful currently running machine is the Large Hadron Collider (LHC) at CERN. At the LHC (primarily) two beams of protons are accelerated and brought to collision in four different interaction points where the four main experiments are located: ATLAS, CMS, LHCb and ALICE. In 2015 the LHC has started its second run and since then has been running at a centre-of-mass energy of 13 TeV.

cross section can be related to the imaginary part of the hadronic vacuum polarisation using the optical theorem. For massless electrons one finds

$$\sigma(e^+e^- \rightarrow \text{hadrons}) \equiv \sigma(s) = -\frac{4\pi\alpha}{s} \text{Im} \Pi_{\text{had.}}(s), \quad (1.4)$$

with

$$i \Pi_{\text{had.}}^{\mu\nu}(s = q^2) \equiv -e^2 \int d^4x e^{iq \cdot x} \langle 0 | T \{ J^\mu(x) J^\nu(0) \} | 0 \rangle \equiv (q^2 g^{\mu\nu} - q^\mu q^\nu) i \Pi_{\text{had.}}(q^2), \quad (1.5)$$

and $J^\mu = \sum_q Q_q \bar{q} \gamma^\mu q$ being the electromagnetic quark current. Since the probability of the final-state quarks to hadronise is one, one would expect that the inclusive *partonic* cross section describes the observed shape of $\sigma(s)$ fairly well for large q^2 . Corrections to the partonic picture can be systematically incorporated by performing an operator product expansion² (OPE) of $J^\mu(x) J^\nu(0)$ in the limit $x \rightarrow 0$:

$$J_\mu(x) J_\nu(0) = C_{\mu\nu}^{(1)}(x) \cdot \mathbb{1} + C_{\mu\nu}^{(\bar{q}q)}(x) \cdot (\bar{q}q)(0) + C_{\mu\nu}^{(G^2)}(x) \cdot (G_{\mu\nu}^A)^2(0) + \dots, \quad (1.6)$$

where $G_{\mu\nu}^A$ is the QCD field-strength tensor. The operators on the right-hand side are gauge invariant Lorentz scalars with non-vanishing vacuum expectation value. From a dimensional analysis one can infer the scaling behaviour of the Wilson coefficients for small x :

$$C_{\mu\nu}^{(1)} \sim x^{-6}, \quad C_{\mu\nu}^{(\bar{q}q)} \sim m_q x^{-2}, \quad C_{\mu\nu}^{(G^2)} \sim x^{-2}. \quad (1.7)$$

Since the operator $\bar{q}q$ violates chiral symmetry, the coefficient $C_{\mu\nu}^{(\bar{q}q)}$ must be proportional to a quark-mass m_q that we made explicit. Fourier transforming Eq. (1.6) to momentum-space gives

$$\begin{aligned} & -e^2 \int d^4x e^{iq \cdot x} J^\mu(x) J^\nu(0) \\ &= -ie^2 (q^2 g^{\mu\nu} - q^\mu q^\nu) \left[c^{(1)}(q^2) \cdot \mathbb{1} + c^{(\bar{q}q)}(q^2) \cdot m_q (\bar{q}q)(0) + c^{(G^2)}(q^2) \cdot (G_{\mu\nu}^A)^2(0) + \dots \right], \end{aligned} \quad (1.8)$$

where now the coefficient functions $c^{(\mathcal{O})}$ have the following scaling in q^2 :

$$c^{(1)} \sim (q^2)^0, \quad c^{(\bar{q}q)} \sim (q^2)^{-2}, \quad c^{(G^2)} \sim (q^2)^{-2}. \quad (1.9)$$

On dimensional grounds, the coefficients multiplying higher-dimensional operators become less relevant for large q^2 . Combining Eqs. (1.4), (1.5) and (1.8), we find for the total cross section:

$$\begin{aligned} \sigma(e^+e^- \rightarrow \text{hadrons}) &= \frac{4\pi\alpha^2}{s} \left[\text{Im} c^{(1)}(q^2) + \text{Im} c^{(\bar{q}q)}(q^2) \langle 0 | m_q \bar{q}q | 0 \rangle \right. \\ &\quad \left. + \text{Im} c^{(G^2)}(q^2) \langle 0 | (G_{\mu\nu}^A)^2 | 0 \rangle + \dots \right]. \end{aligned} \quad (1.10)$$

²The OPE holds rigorously only for spacelike momenta, $Q^2 \equiv -q^2 \gg \Lambda_{\text{QCD}}^2$, which does not correspond to the physical situation under consideration. However, the result that we will derive in Eq. (1.10) can be analytically continued to the region of timelike momentum. A further investigation would go beyond the scope of this introductory example and for details we refer to [5].

The Wilson coefficients $c^{(\mathcal{O})}$ capture the short-distance physics related to the energy scale $s = q^2$. They are defined through the operator identity Eq. (1.6), which in particular implies that they can be computed with unphysical free quark and gluon states and are accessible in a perturbative expansion in $\alpha_s(\sqrt{s})$. The first term $\sim \text{Im } c^{(1)}(q^2)$ exactly reproduces the naive perturbative QCD result for the inclusive partonic cross section. Corrections to this approximation are accompanied by vacuum expectation values of *local* operators. They parametrise long-distance effects from the non-trivial QCD vacuum and are called quark and gluon condensates. As they do not depend on the hard scale, the condensates are of purely non-perturbative nature. Together with the scaling of the Wilson coefficients, we find that the corrections to the partonic cross section are suppressed by $(\Lambda/\sqrt{s})^4$.

In summary, the result in Eq. (1.10) exactly shows the desired factorisation, since the physics related to \sqrt{s} and Λ is disentangled. Technically, this is achieved by introducing a factorisation scale μ_F with $\sqrt{s} \gg \mu_F \gg \Lambda$. Effects from hard gluon virtualities $\mu^2 > \mu_F^2$ contribute to the Wilson coefficients, $c^{(\mathcal{O})}(q^2) \equiv c^{(\mathcal{O})}(q^2; \mu_F)$, whereas effects from soft gluon virtualities $\mu^2 < \mu_F^2$ are part of the condensates, $\langle \mathcal{O} \rangle \equiv \langle \mathcal{O} \rangle(\mu_F)$. The cross section, as a physical quantity, must not depend on the artificial scale μ_F , which thus has to cancel in the product of the Wilson coefficients and the condensates.

Example 2: Heavy-Quark Effective Theory

The complexity of the strong interaction dynamics in a bound state of quarks and gluons simplifies, when it contains one heavy quark with a mass much greater than the hadronic scale. This situation is for example realised in B mesons (and baryons), where the mass of the b quark, $m_b \approx 4.2 \text{ GeV} \gg \Lambda$, defines a hard scale. In some applications, the charm quark with $m_c \approx 1.3 \text{ GeV}$ is considered heavy as well. Similar to the observation that we made in the previous example, a factorisation of scales can be achieved through an expansion in the small parameter $\Lambda/m_Q \ll 1$, where m_Q is the heavy-quark mass. Formally, this can be realised in an effective field theory (EFT) called *Heavy-Quark Effective Theory* (HQET) (reviews are e.g. given in [15–18]).

In the course of this thesis, we will mainly consider the heavy-quark limit $m_Q \rightarrow \infty$, in which the rest frame of the heavy quark coincides with the meson’s rest frame and we can identify their masses, e.g. $M_B \simeq m_b + \mathcal{O}(\Lambda)$. In analogy to the hydrogen atom for $m_e \ll m_p \rightarrow \infty$, the heavy quark acts as a static source of a colour field that determines the wave function of the light constituents. This field configuration, however, is independent of the mass and the spin orientation of the heavy quark. Thus, the properties of the light degrees of freedom are flavour-symmetric and spin-symmetric in this approximation.

We will not give a detailed derivation of the HQET Lagrangian in this thesis and refer to the literature mentioned above. It can be constructed by removing the heavy degrees of freedom from the QCD Lagrangian. Formally, this can be accomplished by “integrating out” highly oscillating fields in the generating functional (see e.g. [19]). At tree-level, the same result can be obtained by employing the equations of motion. The main idea is to split the QCD field of the heavy quark $Q(x) = e^{-im_Q(v \cdot x)}(h_v(x) + H_v(x))$ into a small component H_v and a large component h_v , the former being removed from the

theory. Here v^μ , with $v^2 = 1$, is the four-velocity of the heavy meson. After eliminating the small components H_v , one can use an OPE to expand the Lagrangian in powers of $D^\mu/m_Q \sim \Lambda/m_Q$, with D^μ being the covariant derivative. Including the first corrections in Λ/m_Q , the tree-level Lagrangian then becomes

$$\mathcal{L}_{\text{HQET}} = \bar{h}_v i(v \cdot D) h_v + \frac{1}{2m_Q} \bar{h}_v (iD_\perp)^2 h_v + \frac{g_s}{4m_Q} \bar{h}_v \sigma_{\mu\nu} G^{\mu\nu} h_v + \mathcal{O}(1/m_Q^2). \quad (1.11)$$

The first term corresponds to the heavy-quark limit $m_Q \rightarrow \infty$ and reflects the flavour and spin symmetry. The last term describes the leading chromo-magnetic coupling of the heavy-quark spin to the gluon field. In the second term, the index “ \perp ” of a Lorentz vector X^μ refers to the component perpendicular to the velocity v^μ , i.e. $X_\perp^\mu = X^\mu - (v \cdot X)v^\mu$.

To illustrate the factorisation at the level of an observable, we consider the form factors F_i that parametrise the hadronic matrix elements in the decay $B \rightarrow D\ell\nu$. The decay of a heavy B meson can be treated in HQET as long as the recoil energy of the final-state meson is small. In this case the typical momentum transfer between heavy and light degrees of freedom is still of order Λ . (The case of large recoil energy will be discussed in detail in Section 1.3 and in the main part of this thesis.) In the following, we consider both the b quark as well as the c quark as heavy quarks in the static limit. The underlying effective $b \rightarrow c$ current can then be matched onto *local* HQET operators through a matching relation $\bar{c} \Gamma b \rightarrow \sum_i C_{\Gamma_i} \bar{h}_v^{(c)} \Gamma_i h_v^{(b)} + \mathcal{O}(\Lambda/m_Q)$, with $m_Q = m_{b,c}$ and v^μ is the four-velocity of the heavy D meson. Furthermore, the Γ_i are a set of Dirac-structures and the C_{Γ_i} are Wilson coefficients depending on the hard scale m_Q only and can thus be computed in a perturbative series in $\alpha_s(m_Q)$. Heavy-quark symmetries limit the number of independent hadronic matrix elements and at leading power all form factors can be related to a single universal function $\xi(v \cdot v')$, the Isgur-Wise function [20, 21]. Thus, at leading power, all form factors F_i in $B \rightarrow D$ transitions factorise according to

$$F_i(q^2) = H_i(\mu_F) \xi(v \cdot v'; \mu_F) + \mathcal{O}(\Lambda/m_Q), \quad (1.12)$$

where the hard perturbative coefficient function H_i captures effects from gluon virtualities larger than μ_F , and the Isgur-Wise function correspondingly captures effects from gluon virtualities smaller than μ_F .

In the course of this thesis, we investigate yet another case where a hard scale is set by light but energetic final-state particles, which in experiments are visible as jets; many hadrons and other particles that are clustered into a narrow cone. The factorisation for these observables is more involved as it cannot be achieved through a local OPE, and furthermore, is in certain situations not (yet) fully understood. We focus on a particular class of such observables, namely exclusive charmless B -meson decays. These decays are of great phenomenological interest in the investigation of quark-flavour transitions in the SM or its possible new physics (NP) extensions (see e.g. the reviews in [22–26]). They allow, for example, for an extraction of the CKM-parameter $|V_{ub}|$, which is one of the least precisely known of the CKM-matrix elements. Moreover, a lot of attention is currently attracted by the so-called B anomalies: several observables in exclusive B decays are in slight tension with the SM predictions (summaries can be found e.g. in [22–24]). Most prominently, certain angular observables in the rare heavy-to-light decay $B \rightarrow K^* \ell^+ \ell^-$

could maybe give a hint towards NP. An approach that accomplishes a separation of long- and short-distance physics and allows for a systematic implementation of QCD radiative corrections for exclusive heavy-to-light B -meson decays is the so-called “QCD factorisation” approach, which will be presented in the following.

1.3 The QCD Factorisation Approach

The QCD factorisation (QCDF) approach was first introduced by Beneke, Buchalla, Neubert and Sachrajda (BBNS) around 2000 [27–29] in the context of exclusive hadronic two-body decays of B mesons. Within this framework, two distinct previously known approaches were merged: the Heavy-Quark Expansion (HQE) (see Example 2 from above) and the factorisation of hard exclusive processes [30–32], also known as collinear factorisation. Whereas the HQE relies on the fact that the mass of the b quark is much greater than typical hadronic scales, collinear factorisation is applicable to exclusive processes with highly energetic final-state particles that move almost on the light-cone (e.g. pion form factors at large momentum transfer). It seems natural that the description of decays of heavy B mesons into light (charmless) energetic mesons should feature elements of both formalisms. The QCD dynamics of the initial-state B meson can be tackled within the HQE, whereas the dynamics of the energetic final-state mesons is approached using collinear factorisation. The physical reason behind the factorisation is the so-called colour-transparency argument [33]: to first approximation soft gluons in the B meson see the fast moving final-state particles as colour singlets. A coupling between those is thus suppressed by the large mass m_b .

The QCDF approach is based on first principles and makes use of an expansion in $\Lambda/m_b \ll 1$ and $\Lambda/E \ll 1$, where $E \sim \mathcal{O}(m_b)$ is the large energy of a light final-state particle (in the B -meson rest frame). Along the lines of the discussion from above, the main achievement is that effects associated with the hard energy scale m_b and effects associated with the soft energy-scale Λ are (at least partially) disentangled. Hadronic matrix elements of effective dimension-six flavour-changing operators are related to simpler and more universal objects in a *factorisation theorem*. Long-distance physics is encoded in non-perturbative objects like decay constants and light-cone distribution amplitudes (LCDAs) which are process-independent. The hard contribution emerges as process-dependent matching coefficients and scattering kernels that can be computed in an expansion in $\alpha_s(m_b) \simeq 0.22$. Higher-order perturbative corrections have been calculated for example in [34–41] (see also [42] for a brief overview).

Factorisation theorems for exclusive B decays can be derived and proven on a field-theoretical footing using Heavy-Quark Effective Theory and Soft-Collinear Effective Theory (SCET), effective field theories designed to study the limits $m_b \rightarrow \infty$ and $E \rightarrow \infty$ respectively. In this context, the scattering kernels emerge as Wilson coefficients multiplying effective *non-local* operators whose hadronic matrix elements define the non-perturbative quantities. We refrain from giving an introduction to SCET at this point and postpone this discussion to the second part of this thesis in Section 5.3, where more formal developments will be discussed.

Factorisation theorems have been derived for a variety of different processes, including purely hadronic, semileptonic and radiative decays of B mesons. More recently, the case of multiparticle final-states also has been tackled (one example will be investigated in the first research project of this thesis; another example is the study in [43]). In the following, we briefly discuss three examples of factorisation formulas without explaining their formal derivation.

Example 1: Radiative Leptonic $B \rightarrow \gamma \ell \nu$ Decays

In the kinematic region where the photon carries large energy, $E_\gamma \sim \mathcal{O}(m_b)$ in the B -meson rest frame, QCDF is applicable to describe the QCD dynamics of $B \rightarrow \gamma \ell \nu$ decays. These decays are probably the simplest process to study within the QCDF approach, and in particular, they are the simplest setup to study power corrections in Λ/m_b . At leading order in the electromagnetic coupling, but to all orders in α_s , the decay amplitude can be decomposed into two form factors $f_{V,A}(E_\gamma)$, which incorporate a photon emission from the lepton as well as from the meson constituents. For energetic photons the form factors obey the factorisation formula (see e.g. [44–48]):

$$f_V(E_\gamma) \simeq f_A(E_\gamma) \simeq \frac{QM_B f_B}{2E_\gamma} C(E_\gamma) \int_0^\infty \frac{d\omega}{\omega} \phi_B^+(\omega) T(\omega, E_\gamma) + \xi(E_\gamma) + \text{symm.-breaking power-corrections}. \quad (1.13)$$

The first line is the leading-power expression in Λ/m_b and the second line corresponds to the leading power-corrections. At leading power, the form factors factorise into a convolution of the B -meson light-cone distribution amplitude ϕ_B^+ with a scattering kernel $T = 1 + \mathcal{O}(\alpha_s)$. The integration variable ω amounts to a certain light-cone projection of the spectator-quark momentum. Moreover, $C = 1 + \mathcal{O}(\alpha_s)$ is a hard matching coefficient, f_B is the B -meson decay constant and Q is the electric charge of the spectator quark in units of $|e|$. Since $\phi_B^+(\omega)$ vanishes linearly for $\omega \rightarrow 0$, the convolution integral in Eq. (1.13) is well-defined. At subleading power in Λ/m_b , convolution integrals that are ill-defined in the limit $\omega \rightarrow 0$ – so-called “endpoint divergences” – may arise. They spoil a factorisation similar to the leading-power term and a consistent treatment of these contributions is presently not understood.³ However, it turns out that they preserve the spin-symmetry, i.e. they are identical for both form factors $f_{V,A}$, and at first subleading power can be absorbed into a single unknown hadronic function $\xi(E_\gamma)$. The remaining terms, which are not explicitly given in Eq. (1.13), are well-defined but break this symmetry.

Phenomenologically, this decay is interesting, since the amplitude strongly depends on the first inverse moment of the LCDA ϕ_B^+ , which can thus be determined experimentally. This parameter – usually denoted as λ_B^{-1} – is also an essential input for semileptonic and nonleptonic decays in the QCDF approach. Experimental analyses of $B \rightarrow \gamma \ell \nu$ decays by the BABAR collaboration set lower bounds on λ_B between 300–700 MeV [50, 51], while the value $\lambda_B = 460 \pm 110$ MeV has been obtained using sum rules [52]. However, in [49]

³In a recent work Beneke and Braun et al. found that the endpoint-divergent moments cancel in the higher-twist contributions at tree-level [49]. This however does not necessarily remain true once one includes radiative corrections.

the authors showed that the decay amplitude also strongly depends on the first logarithmic moment σ_1 and future experimental determinations should thus aim at extracting correlated values for λ_B and σ_1 .

Example 2: Semileptonic $B \rightarrow \pi \ell \nu$ Decays

In the limit of large pion energies $E_\pi \sim \mathcal{O}(m_b)$ (“large hadronic recoil”) and at leading power in Λ/m_b , the form factors F_i (with $i = +, -, T$) that parametrise the $B \rightarrow \pi \ell \nu$ decay amplitude factorise according to [53, 54]

$$F_i(E_\pi) \simeq H_i(E_\pi) \xi_\pi(E_\pi) + \int_0^\infty d\omega \int_0^1 du f_B \phi_B^+(\omega) T_i(u, \omega; E_\pi) f_\pi \phi_\pi(u). \quad (1.14)$$

Even the leading-power contribution suffers from endpoint divergences, which are again spin-symmetry preserving and can be absorbed in the “soft-overlap” form factor ξ_π . The form factors thus split into the sum of a factorisable and a non-factorisable contribution. Whereas the hard matching coefficient H_i that multiplies ξ_π is obtained through hard interactions that do not involve the spectator-quark, the factorisable part includes “spectator scattering”. It is again given by a convolution of the LCDA ϕ_B^+ and a perturbative and spin-symmetry breaking scattering kernel T_i . The latter one, however, is also sensitive to the partonic structure of the pion and is thus convoluted with the leading-twist pion LCDA ϕ_π as well (f_π is the pion decay constant). The soft form factor ξ_π on the other hand describes the situation where the final-state pion picks up the spectator quark of the B meson, which results in a highly asymmetric partonic configuration of the energetic pion.

Even at tree-level, the kernel T_i requires one gluon exchange. Hence, at leading order in the strong coupling α_s and at leading power in Λ/m_b , all three independent QCD form factors reduce to a single function ξ_π [55]. Deviations from this limit can be computed systematically in perturbation theory [53]. This is used in phenomenological studies to construct so-called optimised observables, in which the only hadronic function ξ_π drops out to first approximation in ratios of observables.

Example 3: Hadronic $B \rightarrow \pi\pi$ Decays

Historically, the QCDF approach has been introduced as a first systematic treatment of the purely hadronic $B \rightarrow \pi\pi$ (and also $B \rightarrow \pi K$ and $B \rightarrow D\pi$) decays [27–29]. The kinematics of two-body decays is completely fixed and in the B -meson rest frame both pions share the same energy $E_\pi = M_B/2 \sim \mathcal{O}(m_b)$. At leading power in the Heavy-Quark Expansion, the decay amplitude for a given effective operator \mathcal{O}_i factorises according to

$$\begin{aligned} \langle \pi_1 \pi_2 | \mathcal{O}_i | B \rangle &\simeq \xi_{\pi_1}(M_B/2) \int_0^1 du T_i^{\text{I}}(u) f_\pi \phi_{\pi_2}(u) + (\pi_1 \leftrightarrow \pi_2) \\ &+ \int_0^\infty d\omega \int_0^1 du dv T_i^{\text{II}}(\omega, u, v) f_B \phi_B^+(\omega) f_\pi \phi_{\pi_1}(u) f_\pi \phi_{\pi_2}(v). \end{aligned} \quad (1.15)$$

(Note that this is a slightly different form than proposed by BBNS, where we made the soft overlap contained in the $B \rightarrow \pi$ form factors explicit.) The first (second) term in

the factorisation formula corresponds to the situation where the first (second) pion picks up the spectator quark of the B meson, which is described by the soft form factor. The respective other pion factorises into a well-defined convolution involving a hard scattering kernel T_i^I . The second line factorises completely into a convolution of the B -meson LCDA ϕ_B^+ and both leading-twist pion LCDAs ϕ_{π_1, π_2} with a second scattering kernel T_i^{II} that is determined by spectator-scattering contributions. In addition to the endpoint divergences contained in ξ_π , also so-called chirally enhanced twist-3 contributions in the second line give rise to endpoint divergent convolutions.

Independent of the final-state, factorisation formulas for exclusive decays suffer from the conceptual problem of endpoint divergences that spoil a complete factorisation. Whereas they arise at subleading power in Λ/m_b in radiative leptonic $B \rightarrow \gamma \ell \nu$ decays, even the leading-power expression for heavy-to-light form factors has ill-defined convolution integrals. The preservation of spin-symmetry, however, still guarantees the predictive power of the QCDF approach. A complete factorisation would nevertheless be desirable. We dedicate the main part of this thesis to the investigation of an improved factorisation of ξ_π . To this end, we study the endpoint divergences in a perturbative setup where even the hadronic quantities, in particular the LCDAs, can be computed in an expansion in α_s . With new methods that have been successfully applied to certain collider physics observables we try to shed some new light on this long-standing problem.

1.4 Outline of this Thesis

This thesis is subdivided into four parts: an introductory Part, a first research Project I that can be considered as a preliminary work for the main topic of this thesis, which will be discussed in Project II. In the fourth part we conclude. The content of the research projects can be outlined as follows.⁴

Based on the rather superficial introduction to QCDF that we gave in this section, we derive a novel leading-power factorisation formula for four-body semileptonic $B \rightarrow \pi\pi\ell\nu$ decays in Chapter 2. The factorisation of short and long-distance physics holds in the kinematical region where both pions move nearly back-to-back with large energies, and features elements of both semileptonic $B \rightarrow \pi\ell\nu$ decays as well as nonleptonic $B \rightarrow \pi\pi$ decays within QCDF. We will not present an all-order proof within the framework of SCET, but rather calculate the leading non-trivial contributions to the various scattering kernels in perturbation theory. The crucial part in the verification of the factorisation formula is the universality of endpoint divergences, which again can be completely absorbed into the soft $B \rightarrow \pi$ form factor ξ_π . As an application we study approximate form factor relations, and furthermore, present numerical estimates of certain observables in the desired phase-space region in Chapter 3. We summarise this part in Chapter 4.

A more thorough and formal discussion of factorisation, particularly with regard to endpoint divergences, will be presented in the third part. In Chapter 5 we begin this discussion with the investigation of the on-shell Sudakov form factor in a massive $U(1)$ theory. The main objective of this chapter is, exemplified by a simple observable, to provide the necessary theoretical foundations in view of factorisation and resummation that will be used in the subsequent chapters. This includes an introduction to the method of regions, to Soft-Collinear Effective Theory and also a brief introduction to the collinear anomaly and the rapidity renormalisation group. Chapter 6 is dedicated to derive a “naive” – still containing endpoint-divergent convolution integrals – factorisation formula for the soft form factor ξ_π . To this end, we perform a matching calculation onto SCET_{II} operators which is followed by a detailed summary of the various LCDAs for heavy and light mesons, and eventually results in the desired factorisation formula. Compared to previous works, we include a non-zero (but small) quark mass in our calculation. In Chapter 7 we study the emerging endpoint-divergent convolution integrals in a perturbative toy model, which can be considered as the decay $B_c \rightarrow \eta_c\ell\nu$ in the non-relativistic approximation. Applying the methods discussed in Chapter 5 to heavy-to-light form factors at large recoil, we achieve a resummation of all leading logarithms in the product $H_i \xi_\pi$. In Chapter 8 we point out open questions that prevent a complete factorisation of modes and a resummation beyond the leading logarithmic approximation with these methods. We address some of these points by means of scalar toy integrals. We summarise this part in Chapter 9.

Finally, in Chapter 10, we conclude and give a brief outlook on future developments. Necessary details regarding the first project are collected in Appendix A, whereas Appendices B–D are devoted to substantiate the calculations presented in Chapters 5–8.

⁴The work that will be presented in Project I has been published in [56]. This is an open access article distributed under a Creative Commons license. Chapters 2 and 3 have a large overlap with this article. Except the creation of numerical estimates through an implementation in the EOS software, P. Böer has performed all the calculations presented in these chapters, and furthermore, has contributed in the preparation of all parts of the article.

Project I

QCD Factorisation Theorem for $B \rightarrow \pi\pi\ell\nu$ Decays at Large Dipion Masses

The results of this project have been published in:

Philipp Böer, Thorsten Feldmann, and Danny van Dyk. “QCD Factorization Theorem for $B \rightarrow \pi\pi\ell\nu$ Decays at Large Dipion Masses”. *JHEP*, 02:133, 2017.

Introductory Remarks

In this project we study exclusive semileptonic $B \rightarrow \pi\pi\ell\nu$ decays within the QCD factorisation framework, which is applicable in the kinematic situation where both pions recoil against each other with large energies of order $m_b/2$ (in the B -meson rest frame). At the partonic level, $B \rightarrow \pi\pi\ell\nu$ decays are induced by $b \rightarrow u\ell^-\bar{\nu}_\ell$ transitions, which in the SM involve only one effective operator originating from tree-level W -boson exchange. The main phenomenological motivation lies in an independent extraction of the CKM-matrix element $|V_{ub}|$. The advantage of $B \rightarrow \pi\pi\ell\nu$ decays compared to the nonleptonic counterpart $B \rightarrow \pi\pi$ is the richer kinematic structure. Similar to other multi-body decay modes like $B \rightarrow K\pi\ell\ell$ [57–59], $B_s \rightarrow K\pi\ell\nu$ [60, 61], and also baryonic decay modes, such as $\Lambda_b \rightarrow N\pi\ell\ell$ [62], the full angular distribution of the four-body final state can be analysed, which allows one to disentangle the spin-structure of the underlying operators [63]. Hence, $B \rightarrow \pi\pi\ell\nu_\ell$ decays are also well suited for NP searches in charged current $b \rightarrow u$ transitions.

Moreover, knowledge about the form factors that parametrise the hadronic matrix elements in $B \rightarrow \pi\pi\ell\nu$ decays is desirable for multi-body B -meson decays within the QCDF approach. For example, it has been shown in [43] that the factorisation of non-leptonic three-body $B \rightarrow \pi\pi\pi$ decays, in certain phase-space regions, requires the dipion form factors as non-perturbative input.

The factorisation of hadronic matrix elements in $B \rightarrow \pi\pi\ell\nu$ decays features elements known from the analysis of nonleptonic $B \rightarrow \pi\pi$ decays [64, 65] as well as semileptonic $B \rightarrow \pi\ell\nu$ decays [53] and leads to a very similar leading-power factorisation formula (cf. examples 2 and 3 in Section 1.3). One contribution can be described in terms of the universal soft $B \rightarrow \pi$ form factor and the convolution of a short-distance kernel T^{I} with the respective light-cone distribution amplitude of the pion that does not pick up the spectator quark. The second contribution completely factorises, with a short-distance kernel T^{II} convoluted with the leading-twist LCDAs for both pions and the B meson. The objective of this work is the confirmation of the factorisation formula by an explicit calculation of the leading contributions to the scattering kernels in fixed-order perturbation theory. The non-trivial task here is to show that endpoint divergences are again universal and can be absorbed into the soft $B \rightarrow \pi$ form factor. A rigorous proof within the context of Soft-Collinear Effective Theory along the lines of [54, 66] is left for future work.

The remainder of this part is organised as follows. After a brief review of the kinematics as well as the power-counting in the relevant phase-space region, we introduce the novel factorisation formula for the dipion form factors in Chapter 2. Subsequently, we derive the leading contributions to the scattering kernels and show the cancellation of the occurring endpoint divergences with the soft $B \rightarrow \pi$ form factor. In Chapter 3 we discuss phenomenological implications including approximate form factor relations as well as numerical estimates for two different observables. We conclude this part with a brief summary in Section 4. Detailed information on our definitions of the dipion form factors and on the calculation of individual diagrams are collected in Appendix A.

Chapter 2

Factorisation of Hadronic Matrix Elements

In this chapter we introduce the factorisation formula for hadronic matrix elements in $B \rightarrow \pi\pi\ell\nu$ decays and present the calculation of the leading perturbative contributions to the scattering kernels.

2.1 Kinematics and Power Counting

We define the kinematics for the decay

$$B^-(p) \rightarrow \pi^+(k_1) \pi^-(k_2) \bar{\nu}_\ell(q_1) \ell^-(q_2)$$

following the conventions in [63]. In the kinematic regime that we are interested in, it is safe to neglect the pion mass compared to the large B -meson mass and pion energies at large hadronic recoil. We will therefore set $m_\pi^2 = 0$ throughout the discussion of this project. Defining the sums and differences of hadronic and leptonic momenta as

$$\begin{aligned} q &= q_1 + q_2, & k &= k_1 + k_2, \\ \bar{q} &= q_1 - q_2, & \bar{k} &= k_1 - k_2, \end{aligned} \quad (2.1)$$

the hadronic system can be described by three kinematic Lorentz invariants which can be chosen as the momentum transfer q^2 , the dipion invariant mass k^2 , and the scalar product

$$q \cdot \bar{k} = \frac{\sqrt{\lambda}}{2} \cos \theta_\pi. \quad (2.2)$$

Here θ_π refers to the polar angle of the π^+ meson in the dipion rest frame, and

$$\lambda \equiv M_B^4 + q^4 + k^4 - 2(M_B^2 q^2 + M_B^2 k^2 + q^2 k^2) \quad (2.3)$$

is the Källén function. For the following discussion it is sometimes more convenient to use the independent variables

$$E_{1,2} \equiv \frac{p \cdot k_{1,2}}{M_B} = \frac{M_B^2 + k^2 - q^2 \pm \cos \theta_\pi \sqrt{\lambda}}{4M_B} \quad \text{and} \quad k^2, \quad (2.4)$$

where $E_{1,2}$ denote the energies of the individual pions in the B -meson rest frame, with

$$q^2 = M_B^2 - 2M_B(E_1 + E_2) + k^2, \quad q \cdot \bar{k} = M_B(E_1 - E_2), \quad (2.5)$$

and

$$\lambda = 4M_B^2 \left((E_1 + E_2)^2 - k^2 \right). \quad (2.6)$$

The power counting that underlies the factorisation of hadronic matrix elements follows from the requirements that:

- (i) The energies of both pions in the B -meson rest frame are large to allow for the factorisation of soft modes in the B -meson and collinear modes in the pions,

$$E_{1,2} \gg \Lambda, \quad (2.7)$$

where Λ is a typical hadronic scale;

- (ii) The invariant mass of the dipion system k^2 is large, in order to allow for the factorisation of collinear modes in the two different pion directions:

$$k^2 \gg \Lambda^2. \quad (2.8)$$

Allowing for generic values of q^2 , k^2 and $|\cos \theta_\pi|$, the minimal pion energy corresponds to

$$E_{1,2} \geq E_{\min}(q^2, k^2, |\cos \theta_\pi|) = \frac{M_B^2 + k^2 - q^2 - |\cos \theta_\pi| \sqrt{\lambda}}{4M_B}. \quad (2.9)$$

Criterion (i) is therefore fulfilled if $E_{\min} \gg \Lambda$.

2.2 The Factorisation Formula

In the kinematical limit discussed above the hadronic matrix elements for generic $b \rightarrow u$ currents in the SM or beyond are expected to factorise in a similar way as the hadronic matrix elements of 4-quark and chromomagnetic penguin operators appearing in non-leptonic $B \rightarrow \pi\pi$ decays [27, 29] (cf. Eq. (1.15)). The notable difference between the two cases stems from the fact that the perturbative expansion for the short-distance kernels in $B \rightarrow \pi\pi\ell\nu$ requires at least one hard gluon exchange to generate the additional quark-antiquark pair ending up in the final-state pions. We thus introduce the following factorisation formula:

$$\begin{aligned} & \langle \pi^+(k_1) \pi^-(k_2) | \bar{\psi}_u \Gamma \psi_b | B^-(p) \rangle \\ &= \frac{2\pi f_\pi}{k^2} \left\{ \xi_\pi(E_2; \mu) \int_0^1 du \phi_\pi(u; \mu) T_\Gamma^{\text{I}}(u, k^2, E_1, E_2; \mu) \right. \\ & \quad + \frac{\pi^2 f_B f_\pi M_B}{N_C E_2^2} \int_0^1 du \int_0^1 dv \int_0^\infty \frac{d\omega}{\omega} \\ & \quad \left. \times \phi_\pi(u; \mu) \phi_\pi(v; \mu) \phi_B^+(\omega; \mu) T_\Gamma^{\text{II}}(u, v, \omega, k^2, E_1, E_2; \mu) \right\} \\ & \quad + \text{power corrections}. \end{aligned} \quad (2.10)$$

In the first term, $\xi_\pi(E_2)$ denotes the universal non-factorisable (“soft”) $B^- \rightarrow \pi^-$ form factor in SCET [53, 54, 67], which can be defined as

$$\langle \pi^-(k_2) | \bar{\xi}^{(u)} \Gamma_X h_v^{(b)} | B(v) \rangle = \xi_\pi(E_2) \text{tr} [k_2 \Gamma_X P_v] . \quad (2.11)$$

Here

$$P_v \equiv \frac{\not{v} + M_B}{2M_B} \simeq \frac{1 + \not{v}_b}{2} \quad (2.12)$$

is the usual projector on the large components $h_v^{(b)}$ of the heavy-quark spinor in Heavy-Quark Effective Theory with the heavy-quark velocity v_b^μ . Moreover, $\xi^{(u)}$ denotes the large component of an energetic up-quark spinor field in SCET. ϕ_π is the leading-twist LCDA of the pion and ϕ_B^\pm of the B -meson respectively. Their arguments u (v) refer to momentum fractions of the valence quarks in the positively (negatively) charged pion, whereas ω is a light-cone projection of the soft spectator-quark momentum in the B meson. We do not discuss more details about the non-perturbative objects at this point since they will be investigated in detail in the second part of this thesis (see Section 6.4). On the perturbative side, T_Γ^{I} denotes the short-distance kernel from hard gluon interactions with the constituents of the pions in the final state, and T_Γ^{II} contains the contributions from hard-collinear gluon exchange with the (would-be) spectator quark in the B meson, as well as additional hard-gluon corrections. (The normalisation factors in (2.10) have been chosen for convenience.) The terms “hard” and “hard-collinear” refer to different virtualities of the exchanged gluons. Hard gluons have $\mu_h \sim M_B$ whereas hard-collinear gluons have $\mu_{hc} \sim \sqrt{M_B \Lambda}$. Both are considered to be in the perturbative regime.

Whereas the second term factorises completely into leading-twist LCDAs convoluted with a short-distance kernel, the first term still contains the non-factorisable soft form factor ξ_π . As we will see in the explicit calculation below, a complete factorisation is spoiled since endpoint-divergent convolution integrals arise in the calculation of T^{II} that exactly arrange in such a way that the factorisation formula Eq. (2.10) holds. An exhaustive discussion of the problem of endpoint divergences will be given in the second part of this thesis. In the following, we are going to confirm this factorisation structure by explicit calculation of the leading contributions to the kernels T^{I} and T^{II} .

2.2.1 The kernel T^{I}

The kernel T^{I} contains the short-distance QCD effects that *do not* involve the spectator quarks (and gluons) in the B -meson. The non-trivial tasks are then to show that

1. the leading-power contributions indeed only involve the leading-twist pion distribution amplitude of the π^+ meson,
2. additional spectator interactions that would formally lead to endpoint divergences in T^{II} are indeed universal and can be absorbed into the soft form factor ξ_π .

We are going to address the first issue in this subsection by computing the leading amplitude term for the semi-partonic process $b \rightarrow \pi^+ d \ell^- \bar{\nu}_\ell$. The second problem is left for the next subsection when we discuss the leading spectator-scattering diagrams.

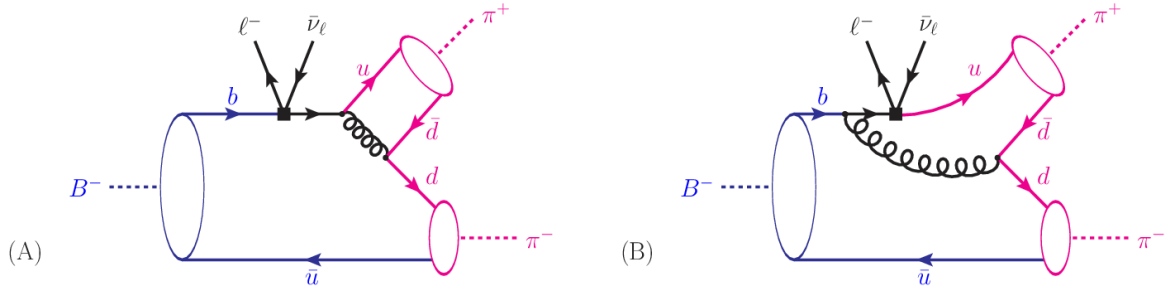


Figure 2.1: Sketch of QCD factorisation in $B^- \rightarrow \pi^+ \pi^- \ell^- \bar{\nu}_\ell$ decays at large dipion mass: Diagrams (i) and (ii) show the leading decay mechanism from hard gluon exchange. Radiative corrections, including factorisable and non-factorisable spectator interactions (see below) are not shown. (The colour coding refers to soft momentum modes in blue and collinear momentum modes in magenta.)

At leading order (LO) in the strong coupling constant, and projecting onto the 2-particle Fock state for the energetic pion, the process $b \rightarrow \pi^+ d \ell^- \bar{\nu}_\ell$ is described by the two diagrams in Fig. 2.1. The relevant non-perturbative dynamics of the initial and final state mesons is parametrised by their respective LCDAs. By Fourier transforming the position-space matrix element that defines the LCDAs and performing the expansion around the dominant light-cone components, the non-perturbative dynamics can be encoded in momentum-space projectors, which can be used in the familiar momentum-space calculation of Feynman diagrams. Again we will not go into the technical details here and refer to Section 6.4 for the operator definition of the various LCDAs and to [53] for the derivation of the respective projectors.

The leading-twist momentum space projector for the final-state pion reads

$$\mathcal{M}_{\pi^+}^{(2)}(u) = i f_\pi \frac{\mathbb{1}}{N_C} \frac{\not{k}_1 \gamma_5}{4} \phi_\pi(u), \quad \text{with } (k_1)^2 = 0, \quad (2.13)$$

where u and $\bar{u} = 1 - u$ are the longitudinal momentum fractions of the quark and antiquark in a 2-particle Fock state, i.e.

$$k_{q1}^\mu \simeq u k_1^\mu, \quad k_{\bar{q}1}^\mu \simeq \bar{u} k_1^\mu. \quad (2.14)$$

Using Eq. (2.13), one obtains for a generic Dirac matrix Γ

$$\langle \pi^+(k_1) d(k_{q2}) | \bar{\psi}_u \Gamma \psi_b | b(p_b) \rangle = 4\pi\alpha_s C_F \int_0^1 du [\bar{u}(k_{q2}) \Gamma_X u(p_b)] \quad (2.15)$$

with

$$\Gamma_X = -\frac{\gamma_\alpha \mathcal{M}_{\pi^+}^{(2)}(u) \gamma^\alpha (\not{p}_b - \not{q}) \Gamma}{(p_b - q)^2 (p_b - q - uk_1)^2} - \frac{\gamma_\alpha \mathcal{M}_{\pi^+}^{(2)}(u) \Gamma (uk_1 + \not{q} + m_b) \gamma^\alpha}{[(uk_1 + q)^2 - m_b^2] (p_b - q - uk_1)^2}, \quad (2.16)$$

in Feynman gauge.¹ Here we used momentum conservation to replace $k_{q2}^\mu = p_b^\mu - q^\mu - k_1^\mu$. In the heavy-quark limit, we can further approximate $m_b \simeq M_B$, and $p_b^\mu \simeq p^\mu$, such that

¹One should not confuse the momentum fractions $u, \bar{u} = 1 - u$ with the on-shell Dirac spinors $u(p), \bar{u}(p)$.

the denominators of the propagators can be expressed in terms of the hadronic Lorentz invariants defined above,

$$\begin{aligned}
 (p_b - q)^2 &\simeq (p - q)^2 = k^2, \\
 (p_b - q - uk_1)^2 &\simeq (k_2 + \bar{u}k_1)^2 = \bar{u}k^2, \\
 (uk_1 + q)^2 - m_b^2 &\simeq (p - \bar{u}k_1 - k_2)^2 - M_B^2 = \bar{u}(k^2 - 2M_B E_1) - 2M_B E_2. \quad (2.17)
 \end{aligned}$$

Assuming the Feynman mechanism to work, i.e. all endpoint divergences from hard-collinear spectator scattering can be absorbed into the universal form factor ξ_π (which will be shown by explicit calculation of T_Γ^{II} below), we can replace the semi-partonic amplitude (2.16) by the hadronic one via (2.11),

$$\langle \pi^+(k_1) \pi^-(k_2) | \bar{\psi}_u \Gamma \psi_b | B^-(p) \rangle = 4\pi\alpha_s C_F \xi_\pi(E_2) \int_0^1 du \text{tr} [k_2 \Gamma_X P_v]. \quad (2.18)$$

From this we can read off the leading order contribution to the hard-scattering kernel for a given Dirac structure Γ . For the presentation of the results, we find it convenient to define a basis of Dirac traces,²

$$\begin{aligned}
 s_1 &\equiv \text{tr}[k_1 \gamma_5 \Gamma P_v], & s_2 &\equiv \text{tr}[k_2 \gamma_5 \Gamma P_v], \\
 s_3 &\equiv \text{tr}[k_1 \gamma_5 \Gamma], & s_4 &\equiv \text{tr}[k_2 \gamma_5 \Gamma], \\
 s_5 &\equiv \frac{1}{M_B} \text{tr}[k_2 k_1 \gamma_5 \Gamma P_v], & s_6 &\equiv \frac{1}{M_B} \text{tr}[k_1 k_2 \gamma_5 \Gamma P_v], \\
 s_7 &\equiv \frac{1}{M_B} \text{tr}[k_2 k_1 \gamma_5 \Gamma], & s_8 &\equiv \frac{1}{M_B} \text{tr}[k_1 k_2 \gamma_5 \Gamma]. \quad (2.19)
 \end{aligned}$$

(Note that in case of vector and axial-vector currents, one has $s_3 = 2s_1$, $s_4 = 2s_2$, and $s_7 = s_8 = 0$.) In the leading order expression for T_Γ^{I} following from (2.18), we find that only two independent functions of the quark momentum fraction u appear, which can be defined as³

$$f_1(u) \equiv \frac{-k^2}{\bar{u}(k^2 - 2E_1 M_B) - 2E_2 M_B}, \quad f_2(u) \equiv \frac{2E_2 M_B}{\bar{u} k^2} f_1(u). \quad (2.20)$$

The moment $\langle \bar{u}^{-1} \rangle_\pi$ (where the symbol $\langle \dots \rangle_\pi$ means integration $\int_0^1 du \dots \phi_\pi(u)$) can be obtained from a linear combination,

$$\frac{1}{\bar{u}} = \left(\frac{2E_1 M_B}{k^2} - 1 \right) f_1(u) + f_2(u). \quad (2.21)$$

²The corresponding structures without γ_5 do not appear due to parity invariance of QCD.

³With this choice we obtain simple expressions in the limit $k^2 \rightarrow 2E_1 M_B$, namely $f_1(u) \rightarrow E_1/E_2$ and $f_2(u) \rightarrow 1/\bar{u}$.

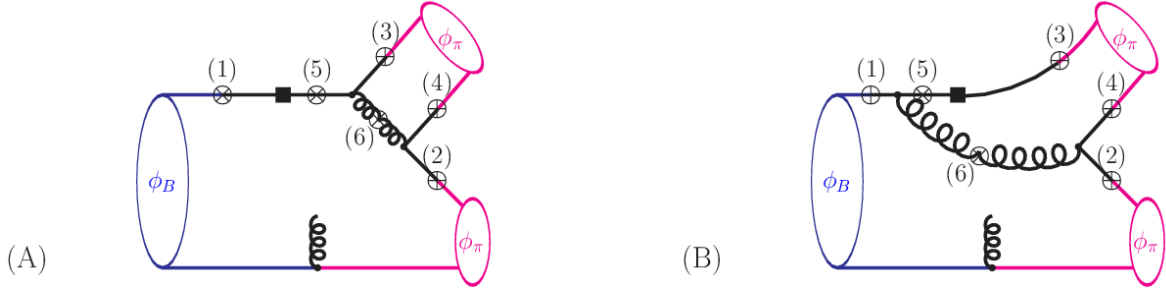


Figure 2.2: Diagrams contributing at leading order to the kernel T^{II} . The hard-collinear gluon emitted from the lower quark line can be connected to any of the crosses numbered by (1)-(6).

With these definitions we obtain

$$\begin{aligned}
 T_{\Gamma}^{\text{I}}(u, k^2, E_1, E_2) \Big|_{\text{LO}} &= i \frac{\alpha_s C_F}{N_C} \left\{ f_1(u) \left[\left(\frac{2E_1 M_B}{k^2} - 1 \right) s_2 + \frac{1}{2} s_3 \right] \right. \\
 &\quad \left. + f_2(u) \left[s_1 + s_2 - \frac{M_B}{2E_2} s_5 - \frac{1}{2} s_7 \right] \right\} \\
 &\equiv i \frac{\alpha_s C_F}{N_C} \frac{S_A + S_B^{(i)}(u) + S_B^{(ii)}(u)}{\bar{u}}, \quad (2.22)
 \end{aligned}$$

where, for later use, we have defined the abbreviations

$$S_A = s_2, \quad \frac{S_B^{(i)}(u)}{\bar{u}} = \frac{f_1(u)}{2} s_3 - \frac{M_B f_2(u)}{2E_2} s_5, \quad \frac{S_B^{(ii)}(u)}{\bar{u}} = f_2(u) \left[s_1 - \frac{s_7}{2} \right]. \quad (2.23)$$

Note that in the individual contributions to T_{Γ}^{I} , different projections of the Dirac matrix Γ in the original $b \rightarrow u$ transition current appear. In particular, at LO, the hard-gluon exchange involves the “small” spinor components, $(1 - P_v) \psi_b$ for the heavy quark (in the Dirac structures $s_{3,7}$), and $\frac{\not{k}_1 \not{k}_2}{k^2} \psi_u$ for the emitted u -quark (in the Dirac structures $s_{2,6}$), but not both of them simultaneously (i.e. the structures s_4 and s_8 do not appear).

Despite their formal power-suppression in Λ/M_B , it is known that due to the large prefactor $\mu_{\pi} = m_{\pi}^2/(m_u + m_d) \sim 2.5$ GeV twist-3 contributions can be numerically important. We thus should include these “chirally-enhanced” contributions in numerical estimates. In the computation of the kernel T_{Γ}^{I} they arise from the twist-3 two-particle LCDAs of the π^+ meson. The derivation of this contribution is presented in Appendix A.2.

2.2.2 The kernel T^{II}

The leading contribution to the kernel T^{II} in the QCD factorisation formula (2.10) arises from diagrams where – in addition to the hard-gluon process in Fig. 2.1 – a hard-collinear gluon connects to the (would-be) spectator quark in the B meson. The relevant Feynman diagrams are shown in Fig. 2.2 and will be discussed in turn in Appendix A.3.

A comment is in order about the definition of the transverse plane related to the underlying light-cone expansion for the *negatively* charged pion state: The hard-collinear gluon propagator associated to the separation of the quark fields in the $|\pi^-\rangle$ state involves the large momenta $p_b^\mu \sim p^\mu$ and k_2^μ . The transverse momenta in the light-cone expansion for the π^- matrix elements are therefore conveniently chosen as transverse to p and k_2 . The parton momenta in the two-particle Fock state are then expanded as

$$\begin{aligned} \text{down-quark in } \pi^-: & \quad k_{q2}^\mu \simeq vk_2^\mu + \bar{k}_\perp^\mu, \\ \text{anti-up-quark in } \pi^-: & \quad k_{\bar{q}2}^\mu \simeq \bar{v}k_2^\mu - \bar{k}_\perp^\mu, \quad \text{with } k_2 \cdot \bar{k}_\perp = p \cdot \bar{k}_\perp \equiv 0, \end{aligned}$$

with v ($\bar{v} = 1 - v$) denoting the longitudinal momentum fraction of the quark (antiquark), and $|\bar{k}_\perp|$ scaling as a hadronic momentum of order Λ . (A similar discussion about the transverse plane and the partonic kinematics in the $|\pi^+\rangle$ state is required for the calculation of twist-3 contributions to the kernel T^1 ; see Appendix A.2.) The corresponding twist-3 momentum-space projector then reads

$$\mathcal{M}_{\pi^-}^{(3)}(v) = \frac{if_{\pi}\mu_\pi}{4} \frac{\mathbb{1}}{N_C} \gamma_5 \left\{ -\phi_P(v) + i\sigma_{\mu\nu} \frac{k_2^\mu p^\nu}{p \cdot k_2} \frac{\phi'_\sigma(v)}{6} - i\sigma_{\mu\nu} \frac{\phi_\sigma(v)}{6} k_2^\mu \frac{\partial}{\partial \bar{k}_{\perp\nu}} \right\} \Big|_{\bar{k}_\perp \rightarrow 0}. \quad (2.24)$$

Neglecting 3-particle contributions, the corresponding LCDAs are fixed by the equations of motion (see e.g. [68], and also Section 6.4). In this approximation one finds

$$\frac{u}{2} \left(\phi_P(u) + \frac{\phi'_\sigma(u)}{6} \right) \simeq \frac{\bar{u}}{2} \left(\phi_P(u) - \frac{\phi'_\sigma(u)}{6} \right) \simeq \frac{\phi_\sigma(u)}{6}, \quad (2.25)$$

leading to

$$\phi_P(u) \simeq 1, \quad \phi_\sigma(u) \simeq 6u\bar{u}, \quad (\text{“Wandzura-Wilczek approx.”}) \quad (2.26)$$

which can easily be verified using Eqs. (6.57) and (6.58).

With the same argument as above, we define the transverse momenta l_\perp of the light antiquark in the B meson, such that the momentum-space projector for the 2-particle distribution amplitudes can be written as in [53],

$$\mathcal{M}_B^{(WW)}(\omega) = -\frac{if_B M_B}{4} \frac{\mathbb{1}}{N_C} \left[P_v \left\{ \phi_B^+(\omega) \not{n}_+ + \phi_B^-(\omega) \left(\not{n}_- - \omega \gamma_\perp^\nu \frac{\partial}{\partial l_\perp^\nu} \right) \right\} \gamma_5 \right] \Big|_{l_\perp \rightarrow 0}, \quad (2.27)$$

where $v_b^\mu = p^\mu/M_B$, $n_-^\mu = k_2^\mu/(v_b \cdot k_2)$ and $n_+^\mu = 2v_b^\mu - n_-^\mu$, and $\omega = (n_- \cdot l)$ is the light-cone projection of the light antiquark momentum. As indicated, we again work in the Wandzura-Wilczek approximation and neglect the 3-particle LCDAs.

The individual contributions from a given diagram X to the $B \rightarrow \pi\pi$ matrix element are decomposed as follows,

$$\begin{aligned} & \langle \pi^+(k_1) \pi^-(k_2) | \bar{\psi}_u \Gamma \psi_b | B^-(p) \rangle \Big|_{(\text{Diagram X})} \\ &= \frac{2\pi f_\pi}{k^2} \frac{i\alpha_s^2 C_F}{4\pi N_C} \frac{\pi^2 f_B f_\pi M_B}{N_C E_2^2} \int_0^1 du \phi_\pi(u) \int_0^1 dv \int_0^\infty d\omega \left(g_{(X)}^{\text{finite}} + g_{(X)}^{\text{endpoint}} \right). \quad (2.28) \end{aligned}$$

Detailed inspection of the diagrams in Fig. 2.2 reveals that the corresponding contributions can be calculated in a similar way as the spectator-scattering contributions to the $B \rightarrow \pi$ form factors considered in [53] at leading non-vanishing order. In particular, we find that all the endpoint sensitive (formally divergent) contributions from 2-particle Fock states at leading power in the $1/M_B$ expansion can be absorbed into the universal form factor ξ_π , with the definition of the associated hard kernel T_Γ^I derived in Eq. (2.23). The details of the calculation for the individual subdiagrams can be found in Appendix A.3.

Endpoint-Divergent Terms

In Table 2.1 we summarise the results for the endpoint-divergent terms as appearing in the individual diagrams when calculated in Feynman gauge. Here, we have introduced the additional abbreviations

$$-v_\perp^2 = \frac{4E_1 E_2}{k^2} - 1, \quad (2.29)$$

where v_\perp^μ denotes the transverse components of the b -quark velocity with respect to the k_1 - k_2 plane, and

$$C_{FA} = \frac{C_A}{2} - C_F = \frac{1}{2N_C}, \quad (2.30)$$

for the coefficient of the sub-leading colour structure. We further use Eq. (2.26) to replace

$$\frac{\mu_\pi}{2E_2} \left(\phi_P(v) - \frac{\phi'_\sigma(v)}{6} \right) \simeq \frac{\mu_\pi \phi_\sigma(v)}{6\bar{v}E_2}. \quad (2.31)$$

We observed that some obvious cancellations (of sometimes rather complicated structures) appear between diagrams (A3,A4) and (B3,B5), respectively. For the sake of readability, we only show the combined results. The final expression for the endpoint-divergent terms arises as the result of rather non-trivial cancellations among the individual diagrams, see Table 2.1. This also involves the cancellation of endpoint divergences related to the momentum fraction $\bar{u} \rightarrow 0$ of the antiquark in the *positively* charged pion, as expected from colour-transparency arguments [27]. We obtain

$$\begin{aligned} & \langle \pi^+(k_1) \pi^-(k_2) | \bar{\psi}_u \Gamma \psi_b | B^-(p) \rangle \Big|_{(A1-A6, B1-B6)} \\ &= \frac{2\pi f_\pi \xi_\pi^{(\text{HSA})}(E_2)}{k^2} \int_0^1 du \phi_\pi(u) T_\Gamma^I(u, k^2, E_1, E_2) + \text{finite terms}, \end{aligned} \quad (2.32)$$

where the corresponding endpoint-divergent contributions in $\xi_\pi^{(\text{HSA})}(E_2)$ have been calculated in [53] (see also Appendix A.3):

$$\begin{aligned} \xi_\pi^{(\text{HSA})}(E_2) \Big|_{\text{endpoint}} &= \frac{\alpha_s}{4\pi} \frac{\pi^2 f_B f_\pi M_B}{N_C E_2^2} \int_0^1 dv \int_0^\infty d\omega \\ & \left\{ C_F \frac{(1+\bar{v}) \phi_\pi(v)}{\bar{v}^2} \frac{\phi_B^-(\omega)}{\omega} + 2\mu_\pi \frac{\phi_p(v)}{\bar{v}} \frac{\phi_B^+(\omega)}{\omega^2} + \frac{\mu_\pi}{2E_2} \left(\frac{\phi_p(v) - \phi'_\sigma(v)/6}{\bar{v}^2} \right) \frac{\phi_B^+(\omega)}{\omega} \right\}. \end{aligned} \quad (2.33)$$

structure	A1	A2	A3 + A4	A5	A6	A1-A6
$\frac{2E_2 M_B}{\bar{u}^2 k^2} S_5 \frac{\phi_B^+(\omega)}{\omega} \frac{\phi_\pi(v)}{2v\bar{v}}$	0	0	$-C_{FA} 2v$	0	$C_A \frac{v-\bar{v}}{2}$	$2vC_F - \frac{C_A}{2}$
$\frac{S_A}{\bar{u}} \frac{\phi_B^-(\omega)}{\omega} \frac{\phi_\pi(v)}{\bar{v}^2}$	$C_F \frac{1}{v}$	$C_F \bar{v}$	$C_{FA} \frac{\bar{v}}{v}$	0	$-\frac{C_A}{2} \frac{\bar{v}}{v}$	$C_F (1 + \bar{v})$
$\frac{S_A}{\bar{u}} \frac{\phi_B^+(\omega)}{\omega} \frac{\mu_\pi \phi_\sigma(v)}{6\bar{v}^3 E_2}$	C_F	0	0	0	0	C_F
$2\mu_\pi \frac{S_A}{\bar{u}} \frac{\phi_B^+(\omega)}{\omega^2} \frac{\phi_P(v)}{\bar{v}}$	0	C_F	0	0	0	C_F

structure	B1	B2	B3+B5	B4	B6	B1-B6
$\frac{2E_2 M_B}{\bar{u}^2 k^2} S_5 \frac{\phi_B^+(\omega)}{\omega} \frac{\phi_\pi(v)}{2v\bar{v}}$	0	0	0	$C_{FA} 2v$	$C_A \frac{\bar{v}-v}{2}$	$\frac{C_A}{2} - 2vC_F$
$\frac{S_B^{(i)}}{\bar{u}} \frac{\phi_B^+(\omega)}{\omega} \frac{\phi_\pi(v)}{\bar{v}^2}$	0	0	$-C_{FA} v_\perp^2$	$C_{FA} v_\perp^2$	0	0
$\frac{S_B^{(i)} + S_B^{(ii)}}{\bar{u}} \frac{\phi_B^-(\omega)}{\omega} \frac{\phi_\pi(v)}{\bar{v}^2}$	$C_F \frac{1}{v}$	$C_F \bar{v}$	$C_{FA} \frac{1}{v}$	$-C_{FA}$	$-\frac{C_A}{2} \frac{\bar{v}}{v}$	$C_F (1 + \bar{v})$
$\frac{S_B^{(i)} + S_B^{(ii)}}{\bar{u}} \frac{\phi_B^+(\omega)}{\omega} \frac{\mu_\pi \phi_\sigma(v)}{6\bar{v}^3 E_2}$	C_F	0	$-C_{FA} v_\perp^2$	$C_{FA} v_\perp^2$	0	C_F
$\frac{S_B^{(i)}}{\bar{u}} \frac{\phi_B^-(\omega)}{\omega} \frac{\mu_\pi \phi_\sigma(v)}{6\bar{v}^3 E_2}$	0	0	$C_{FA} v_\perp^2$	$-C_{FA} v_\perp^2$	0	0
$2\mu_\pi \frac{S_B^{(i)} + S_B^{(ii)}}{\bar{u}} \frac{\phi_B^+(\omega)}{\omega^2} \frac{\phi_P(v)}{\bar{v}}$	0	C_F	0	0	0	C_F

Table 2.1: Endpoint-divergent contributions $g_{(X)}^{\text{endpoint}}$ from diagrams (A1-A6) and (B1-B6) in Feynman gauge.

We thus recover the very same structures as in (2.22), confirming the assumptions that we made in the derivation of T_Γ^{I} in Section 2.2.1. Note that in Feynman gauge all diagrams (except for A5) contribute and the correct cancellation/combination of endpoint divergences provides a useful cross-check of our calculation and a non-trivial aspect for the confirmation of the factorisation hypothesis.

Finite Terms

The remaining (endpoint finite) terms can then be associated to the kernel T_Γ^{II} , thus verifying the factorisation formula (2.10) to leading order in the perturbative expansion. For bookkeeping reasons, we classify our results in non-vanishing and vanishing terms in the large N_C limit.

Large- N_C limit: Neglecting corrections that vanish in the limit $N_C \rightarrow \infty$ (which amounts to setting $C_A = 2C_F$), the hadronic information in the leading order expression

for T_{Γ}^{II} can be encoded in terms of the functions

$$\begin{aligned} f_3(u, v) &= \frac{\phi_{\pi}(v)}{\bar{u}v}, & f_4(u, v) &= \frac{\phi_{\pi}(v)}{\bar{u}v\bar{v}}, \\ f_5(u, v) &= \frac{4vE_2(k^2 - E_1M_B) + \bar{v}k^2M_B}{v\bar{v}k^2M_B} f_1(u), \\ f_6(u, v) &= \frac{4vE_2(k^2 - E_1M_B) + \bar{v}k^2M_B}{v\bar{v}k^2M_B} f_2(u). \end{aligned} \quad (2.34)$$

Note that only three of these functions are linearly independent, since

$$\begin{aligned} f_6(u, v) + \left(\frac{2E_1M_B}{k^2} - 1 \right) f_5(u, v) \\ + \left(\frac{4E_1E_2}{k^2} - \frac{4E_2}{M_B} \right) f_4(u, v) - \left(1 - \frac{4E_2}{M_B} + \frac{4E_1E_2}{k^2} \right) f_3(u, v) = 0. \end{aligned} \quad (2.35)$$

The explicit computation of the individual diagrams in Feynman gauge (see Appendix A.3) yields

$$\begin{aligned} g_{(A1-A6)}^{\text{finite}} \Big|_{C_A=2C_F} &= C_F \left\{ f_3(u, v) \left(s_2 - \frac{2E_2M_B}{k^2} s_6 \right) \right. \\ &\quad \left. + f_4(u, v) \left(\frac{E_2}{M_B} s_4 + \frac{2E_2M_B}{k^2} s_5 \right) \right\} \frac{\phi_B^+(\omega)}{\omega}, \end{aligned} \quad (2.36)$$

and

$$\begin{aligned} g_{(B1-B6)}^{\text{finite}} \Big|_{C_A=2C_F} &= C_F \left\{ -f_3(u, v) \frac{2E_2}{M_B} s_3 + f_4(u, v) \frac{E_2}{M_B} s_3 \right. \\ &\quad \left. + f_5(u, v) \frac{s_3}{2} - f_6(u, v) \frac{M_B}{2E_2} s_5 \right\} \frac{\phi_B^+(\omega)}{\omega}. \end{aligned} \quad (2.37)$$

As a consequence of Eq. (2.35), the results only depend on *three* new independent Dirac structures, which can be chosen as

$$\begin{aligned} \left[s_2 + \frac{M_B(4E_1E_2 - k^2)}{2E_2k^2} s_5 - \frac{2E_2M_B}{k^2} s_6 \right], \\ \left[s_3 - \frac{M_B(k^2 - 2E_1M_B)}{E_2k^2} s_5 \right], \quad \left[s_4 - \frac{M_B(k^2 - 2E_2M_B)}{E_2k^2} s_5 \right]. \end{aligned}$$

Subleading terms in $1/N_C$: Including finite terms of order $(\frac{C_A}{2} - C_F) = \frac{1}{2N_C}$, which arise from the diagrams B_3 and B_5 , we encounter two more hadronic functions,

$$\begin{aligned} f_7(u, v) &\equiv \frac{-2E_2M_B}{\bar{u}(vk^2 - 2E_1M_B) - 2vE_2M_B} f_4(u, v), \\ f_8(u, v) &\equiv \frac{\bar{u}k^2(M_B - 2vE_2) + 4vE_2^2M_B}{2E_2(\bar{u}(k^2 - 2E_1M_B) - 2E_2M_B)} f_7(u, v), \end{aligned} \quad (2.38)$$

entering as

$$g_{(B1-B6)}^{\text{finite}} \Big|_{\frac{C_A}{2}-C_F} = \left(\frac{C_A}{2} - C_F \right) \left\{ - (f_7(u, v) + f_8(u, v)) \frac{E_2}{M_B} \left[s_3 - \frac{M_B(k^2 - 2E_1 M_B)}{E_2 k^2} s_5 \right] - f_7(u, v) \left[\frac{s_7}{2} - \frac{M_B}{2E_2} s_5 \right] \right\} \frac{\phi_B^+(\omega)}{\omega}. \quad (2.39)$$

This involves another independent Dirac structure, $\left[\frac{s_7}{2} - \frac{M_B}{2E_2} s_5 \right]$.

Final result for T_Γ^{II} : For the very definition of T_Γ^{II} , we have to specify the factorisation prescription for the soft form factor $\xi_\pi(E_2)$. If we identify $\xi_\pi(E_2)$ with the physical form factor $F_+((p - k_2)^2)$ for $B \rightarrow \pi$ transitions (as in [53]), with $(p - k_2)^2 = M_B^2 - 2M_B E_2$, we obtain

$$\begin{aligned} & \phi_\pi(v) \frac{\phi_B^+(\omega)}{\omega} T_\Gamma^{\text{II}}(u, v, \omega, k^2, E_1, E_2) \\ &= g_{(A1-A6)}^{\text{finite}} + g_{(B1-B6)}^{\text{finite}} - g_+^{\text{finite}}(v, \omega, E_2) T_\Gamma^{\text{I}}(u, k^2, E_1, E_2). \end{aligned} \quad (2.40)$$

Here the functions $g_{(A1-A6)}^{\text{finite}}$ and $g_{(B1-B6)}^{\text{finite}}$ can be found in Eqs. (2.36), (2.37), (2.39), and the finite contributions to the $B \rightarrow \pi$ form factor $F_+(E_2)$ are encoded in the function g_+^{finite} as given in Eq. (A.20) in the appendix.

Chapter 3

$B \rightarrow \pi\pi$ Form Factors and Observables

In this chapter we discuss phenomenological implications, on the one hand in terms of approximate relations between the individual $B \rightarrow \pi\pi$ form factors and their partial-wave expansion, and on the other hand in terms of numerical estimates for two observables: the integrated decay rate and the pionic forward-backward asymmetry in bins of the invariant dilepton and dipion masses.

3.1 Constraining the Phase Space

First, we briefly discuss the phase-space region in which we expect the factorisation formula to be a valid approximation, i.e. the region where the two requirements discussed in Section 2.1 are fulfilled. A conservative benchmark case would be, for instance, to require $E_{\min} = M_B/3 \simeq 1.76$ GeV. Without any additional cuts on $|\cos\theta_\pi|$ and regardless of the value of q^2 , this can be achieved by setting $k_{\min}^2 = 2M_B^2/3$ (see Appendix A.4). This defines

$$\begin{aligned} \text{Scenario A: } k_{\min}^2 &= 2M_B^2/3 \simeq 18.6 \text{ GeV}^2 \\ &\Rightarrow E_{\min} = M_B/3 \simeq 1.76 \text{ GeV} \quad (\text{for } |\cos\theta_\pi| \leq 1). \end{aligned} \quad (3.1)$$

Note that in this case one finds that $|E_1 - E_2| \leq 0.9$ GeV, i.e. one is very close to the kinematic endpoint, where

$$k^2 \simeq (E_1 + E_2)^2 \sim M_B^2, \quad |E_1 - E_2| \sim \Lambda \ll M_B, \quad \sqrt{\lambda} \ll M_B^2.$$

For $q^2 \rightarrow 0$ this includes the special case for the kinematics in nonleptonic $B \rightarrow \pi\pi$ decays [27]. In a still reasonable benchmark scenario we allow for slightly smaller values of E_{\min} , which can be achieved (again for all values of q^2 and $|\cos\theta_\pi|$) by a somewhat relaxed bound on k^2 , ending up with

$$\begin{aligned} \text{Scenario B: } k_{\min}^2 &= M_B^2/2 \simeq 13.9 \text{ GeV}^2, \\ &\Rightarrow E_{\min} = M_B/4 \simeq 1.32 \text{ GeV} \quad (\text{for } |\cos\theta_\pi| \leq 1). \end{aligned} \quad (3.2)$$

The range of k^2 can be further extended by restricting the size of $|\cos\theta_\pi|$, which yields a non-trivial lower-bound on the size of k^2 . For the case considered in the following, the

bound reads

$$E_{\min} < \frac{\sqrt{a^2 - 1}}{2a} \sqrt{k_{\min}^2}, \quad (3.3)$$

where $|\cos\theta| \leq 1/a$. (Further details and the derivation of this bound are relegated to Appendix A.4.) Aiming, as an example, at a value $k_{\min}^2 = M_B^2/4$ for an angular bound $|\cos\theta_\pi| \leq 1/3$, we obtain

$$\begin{aligned} \text{Scenario C: } k_{\min}^2 &= M_B^2/4 \simeq 7 \text{ GeV}^2, \quad |\cos\theta_\pi| \leq 1/3 \\ \Rightarrow E_{\min} &= \frac{1}{3\sqrt{2}} M_B \simeq 1.24 \text{ GeV}. \end{aligned} \quad (3.4)$$

This includes the so-called ‘‘mercedes-star’’ configuration in $B \rightarrow 3\pi$ decays [43], for which $E_1 = E_2 = M_B/3$, $k^2 = M_B^2/3$ and $\cos\theta_\pi = 0$.

Note that in each scenario above the maximal value of the momentum transfer is given by

$$q_{\max}^2 = (M_B - \sqrt{k_{\min}^2})^2,$$

such that

$$\frac{q_{\max}^2}{M_B^2} \simeq 0.03 \quad (\text{scenario A}), \quad \frac{q_{\max}^2}{M_B^2} \simeq 0.09 \quad (\text{B}), \quad \frac{q_{\max}^2}{M_B^2} \simeq 0.25 \quad (\text{C}).$$

In scenarios A and B the numerical values of q^2 are sufficiently small that one can further approximate the results by only keeping the linear term of a Taylor expansion in $\sqrt{q^2}/M_B$.

3.2 Reduction of Independent Form Factors

In the limit where the form factors are reasonably well described by the factorisation formula Eq. (2.10), the number of independent hadronic quantities is reduced. We first observe that the leading-twist contribution to the leading order expression for the kernel T_Γ^I involves only two independent Dirac structures, see Eq. (2.22). Introducing

$$S_1(\Gamma) \equiv \left(\frac{2E_1 M_B}{k^2} - 1 \right) s_2 + \frac{1}{2} s_3, \quad S_2(\Gamma) \equiv s_1 + s_2 - \frac{M_B}{2E_2} s_5 - \frac{1}{2} s_7, \quad (3.5)$$

we thus have

$$\begin{aligned} & \langle \pi^+(k_1) \pi^-(k_2) | \bar{\psi}_u \Gamma \psi_b | B^-(p) \rangle \Big|_{\text{twist-2}} \\ & \simeq \frac{2\pi f_\pi}{k^2} \{ S_1(\Gamma) F_1(k^2, q^2, q \cdot \bar{k}) + S_2(\Gamma) F_2(k^2, q^2, q \cdot \bar{k}) \}, \end{aligned} \quad (3.6)$$

up to higher-order corrections in the strong coupling. The form factors $F_{1,2}(k^2, q^2, q \cdot \bar{k})$ follow from the leading order expression for the kernel T_Γ^I in (2.22),

$$F_{1,2}(k^2, q^2, q \cdot \bar{k}) \equiv \xi_\pi(E_2, \mu) \frac{i\alpha_s(\mu) C_F}{N_C} \int_0^1 du \phi_\pi(u, \mu) f_{1,2}(u), \quad (3.7)$$

where the functions $f_{1,2}(u)$ are defined in Eq. (2.20), and the dependence on the kinematic variables follows from Eq. (2.5).

As explained above, the twist-3 contributions, given in the appendix in Eq. (A.15), are formally power suppressed but numerically of the same size as the twist-2 terms. They should thus be included in numerical predictions as well. On the other hand, the spectator interactions contributing to the kernel T_{Γ}^{II} are suppressed by the strong coupling constant and can be neglected to first approximation.

Relations among partial-wave form factors

	<i>S</i> -wave	<i>P</i> -wave	<i>D</i> -wave
F_0	$\sqrt{\lambda}$	1	$\sqrt{\lambda}$
F_t	1	$\sqrt{\lambda}$	λ
F_{\perp}	–	$\sqrt{\lambda}$	λ
F_{\parallel}	–	1	$\sqrt{\lambda}$

Table 3.1: Scaling of partial-wave form factors as defined in Appendix A.1 with $\sqrt{\lambda}$.

From Eqs. (2.18), (2.23) and (A.15) we can easily compute the leading contributions to vector and axial-vector form factors. To this end, we first project onto helicity form factors as defined in [63] and summarised in Eq. (A.5) in the appendix. Using that for the phase space scenarios A and B

$$q^2 \sim \sqrt{\lambda} \ll M_B^2,$$

each helicity form factor can then be expanded in the small parameter $\Delta E_{\pi}/M_B \sim \sqrt{\lambda}/M_B^2$, which, via Eq. (2.4), translates into a power series in the angular variable $z \equiv \cos \theta_{\pi}$. From this it is a straightforward task to identify the leading contributions to particular partial waves where – as a general rule, with one exception,¹ see Table 3.1 – higher partial waves will be suppressed by increasing powers of $\sqrt{\lambda}/M_B$. The leading-twist LCDA of the pion can be expanded in Gegenbauer polynomials which diagonalise the one-loop renormalisation group evolution (see also Section 6.4). Performing this expansion up to second order, the leading twist-2 and twist-3 contributions to the partial-wave form factors are obtained as

$$F_0^{(S)} \approx \frac{\sqrt{\lambda}}{2M_B\sqrt{q^2}} F_t^{(S)} \approx \frac{i\alpha_s C_F}{N_C} \frac{2\pi f_{\pi}}{M_B} \frac{2\sqrt{\lambda}}{M_B\sqrt{q^2}} \left(1 + \frac{3a_2^{\pi}}{4} + \frac{\mu_{\pi}}{M_B}\right) \xi_{\pi}\left(\frac{M_B}{2}\right), \quad (3.8)$$

and

$$F_0^{(P)} \simeq \frac{1}{\sqrt{2}} F_{\parallel}^{(P)} \approx \frac{2M_B\sqrt{q^2}}{\sqrt{\lambda}} F_t^{(P)} \approx -\frac{i\alpha_s C_F}{N_C} \frac{2\pi f_{\pi}}{M_B} \frac{2}{\sqrt{3}} \left(1 + \frac{3a_2^{\pi}}{2}\right) \xi_{\pi}\left(\frac{M_B}{2}\right), \quad (3.9)$$

¹Note that in the considered kinematic region the *S*-wave contribution to the form factor F_0 is suppressed compared to the *P*-wave and of the same order as the *D*-wave. This differs from other kinematic situations as considered e.g. in [63]. In particular, the form factor $F_0^{(D)}$ will now also provide a leading contribution to the forward-backward asymmetry with respect to the polar angle θ_{π} .

and

$$\begin{aligned}
 F_0^{(D)} &\simeq \sqrt{\frac{2}{3}} F_{\parallel}^{(D)} \approx \frac{2M_B \sqrt{q^2}}{\sqrt{\lambda}} F_t^{(D)} \\
 &\approx -\frac{i\alpha_s C_F}{N_C} \frac{2\pi f_\pi}{M_B} \frac{\sqrt{\lambda}}{6\sqrt{5}M_B^2} \left((5 + 6a_2^\pi + \frac{2\mu_\pi}{M_B}) \xi_\pi\left(\frac{M_B}{2}\right) - (2 + 3a_2^\pi) M_B \xi'_\pi\left(\frac{M_B}{2}\right) \right),
 \end{aligned} \tag{3.10}$$

together with

$$F_{\perp}^{(P)} \approx \frac{i\alpha_s C_F}{N_C} \frac{2\pi f_\pi}{M_B} \frac{\sqrt{3}\sqrt{\lambda}}{\sqrt{2}M_B^2} \left(1 + a_2^\pi - \frac{\mu_\pi}{M_B} \right) \xi_\pi\left(\frac{M_B}{2}\right). \tag{3.11}$$

Note that some of the above relations are a simple consequence of Lorentz invariance, as discussed in [69], since the number of independent four-momentum vectors is reduced at the kinematic endpoint $\sqrt{\lambda} \rightarrow 0$. In particular, we recover in that limit

$$F_0 \simeq \cos\theta_\pi F_{\parallel} \left(1 + \mathcal{O}\left(\frac{\sqrt{\lambda}}{M_B^2}\right) \right), \tag{3.12}$$

which implies $F_{\parallel}^{(P)} \simeq \sqrt{2} F_0^{(P)}$, $F_{\parallel}^{(D)} \simeq \frac{\sqrt{3}}{\sqrt{2}} F_0^{(D)}$ etc.

3.3 Numerical Results

In the following we will discuss numerical results for

- the partial-wave expansion of the form factors,
- and two observables in the differential decay width of $B^- \rightarrow \pi^+ \pi^- \mu^- \bar{\nu}_\mu$.

As already mentioned above, the corrections from spectator-scattering encoded in T_{Γ}^{II} are a subleading effect and will be neglected for simplicity. Our prediction for the absolute values of the form factors and decay width is still rather uncertain because of the overall factors of $\alpha_s(\mu)$ and $\xi_\pi(E_2, \mu)$. A reduction of the uncertainties induced by ξ_π and α_s can be achieved through suitable arithmetic combinations of form factors or observables. For all numerical evaluations we use the central values and uncertainty intervals for the input parameters as listed in Table 3.2, as well as the correlated results of [70] for the parameters describing the $B \rightarrow \pi$ form factor $F_+(\tilde{q}^2)$ in the region $0 \leq \tilde{q}^2 \leq 12 \text{ GeV}^2$. We find that the uncertainties due to the soft-form-factor parameters are in all cases smaller in size than the remaining parametric uncertainties, ranging from roughly 30%–90% of the non-form-factor uncertainties. (Note that we do not account for correlations between the $B \rightarrow \pi$ form factor parameters and the parameters listed in Table 3.2.) The computations are made using the EOS software [71], which has been extended for this purpose.

parameter	value/interval	unit	prior	source/comments
QCD input parameter				
$\alpha_s(m_Z)$	0.1184 ± 0.0007	—	gaussian @ 68%	[72]
μ	$M_B/2 \pm M_B/4$	GeV	gaussian [†] @ 68%	
$\overline{m}_{u+d}(2 \text{ GeV})$	7.8 ± 0.9	MeV	uniform @ 100%	see [70]
hadron masses				
m_B	5279.58	MeV	—	[72]
m_π	139.57	MeV	—	[72]
parameters of the pion DAs				
f_π	130.4	MeV	—	[72]
$a_2^\pi(1 \text{ GeV})$	[0.09, 0.25]	—	uniform @ 100%	[73]
$\mu_\pi(2 \text{ GeV})$	2.5 ± 0.3	GeV	—	$m_\pi^2/(\overline{m}_{u+d})$

Table 3.2: The input parameters that were used in our numerical analysis. We express the prior distribution as a product of individual priors that are either uniform or gaussian. The uniform priors cover the stated intervals with 100% probability. The gaussian priors cover the stated intervals with 68% probability, and the central value corresponds to the mode of the prior. For practical purposes, variates from the gaussian priors are only drawn from their respective 99% probability intervals. The prior for the parameters describing the $B \rightarrow \pi$ form factor F_+ are not listed here, and taken from [70]. †: We artificially restrict the support of the renormalization scale μ to the interval $[M_B/4, M_B]$.

Partial-wave expansion: We choose a benchmark point ($q^2 = 0.6 \text{ GeV}^2, k^2 = 18.6 \text{ GeV}^2$), which corresponds to

$$\frac{q^2}{M_B^2} \approx 0.02, \quad \frac{\sqrt{\lambda}}{M_B} \approx 0.20,$$

in order to illustrate our results for the partial-wave expanded form factors. Each form factor is expanded up to its three leading partial waves, i.e. as a function of $z \equiv \cos \theta_\pi$:

$$F_{0(t)}^{S+P+D}(z) = F_{0(t)}^S + \sqrt{3} F_{0(t)}^P z + \sqrt{5} F_{0(t)}^D \frac{3z^2 - 1}{2}, \quad (3.13)$$

$$F_{\perp(\parallel)}^{P+D+F}(z) = \sqrt{\frac{3}{2}} F_{\perp(\parallel)}^P + \sqrt{\frac{15}{2}} F_{\perp(\parallel)}^D z + \sqrt{\frac{21}{4}} F_{\perp(\parallel)}^F \frac{5z^2 - 1}{2}, \quad (3.14)$$

where we have suppressed the q^2 and k^2 dependence of the form factors and partial-wave coefficients for brevity. One can now define relative residues

$$r_\lambda(z) \equiv \frac{F_\lambda(z) - F_\lambda^{S+P+D}(z)}{F_\lambda(z)}, \quad \text{with } \lambda = 0, t, \quad (3.15)$$

$$r_\lambda(z) \equiv \frac{F_\lambda(z) - F_\lambda^{P+D+F}(z)}{F_\lambda(z)}, \quad \text{with } \lambda = \perp, \parallel,$$

in order to determine whether or not the form factors can be well approximated by their partial wave expansion. We find that

$$|r_0(z)| \leq 0.6\%, \quad |r_t(z)| \leq 3.0\%, \quad (3.16)$$

$$|r_\perp(z)| \leq 1.2\%, \quad |r_\parallel(z)| \leq 0.8\%. \quad (3.17)$$

We therefore conclude that the first three partial waves approximate the total $\cos\theta_\pi$ dependence of the form factors well. These results are visualised in Fig. 3.1.

Decay width and pionic forward-backward asymmetry: Writing the 3-fold differential decay rate in terms of the kinematic variables ($k^2, q^2, \cos\theta_\pi = \frac{2q\bar{k}}{\sqrt{\lambda}}$), we obtain in the SM (for unexpanded dipion form factors, $F_i = F_i(k^2, q^2, q \cdot \bar{k})^2$)

$$\begin{aligned} & \frac{d^3\Gamma(k^2, q^2, \cos\theta_\pi)}{dq^2 dk^2 d\cos\theta_\pi} \\ &= \frac{1}{4} |\mathcal{N}|^2 \beta_\ell \left[(3 - \beta_\ell) |F_0|^2 + (1 - \cos^2\theta_\pi)(3 - \beta_\ell) (|F_\parallel|^2 + |F_\perp|^2) + \frac{3m_\ell^2}{q^2} |F_t|^2 \right], \end{aligned} \quad (3.18)$$

where the normalisation factor reads

$$|\mathcal{N}|^2 = G_F^2 |V_{ub}|^2 \frac{\beta_\ell q^2 \sqrt{\lambda}}{3 \cdot 2^{10} \pi^5 M_B^3}, \quad \text{with} \quad \beta_\ell = 1 - \frac{m_\ell^2}{q^2}. \quad (3.19)$$

The triple-differential branching ratio $\mathcal{B}(k^2, q^2, \cos\theta_\pi)$ can be used to define the two observables that we wish to discuss: the partially-integrated branching ratio, as well as the pionic forward-backward asymmetry for the decay:

$$A_{\text{FB}}^\pi(k^2, q^2) \equiv \frac{\int_{-1}^{+1} d\cos\theta_\pi \text{sign}(\cos\theta_\pi) \mathcal{B}(k^2, q^2, \cos\theta_\pi)}{\int_{-1}^{+1} d\cos\theta_\pi \mathcal{B}(k^2, q^2, \cos\theta_\pi)}. \quad (3.20)$$

In order to avoid controversies with the choice of the input value for $|V_{ub}|$, we provide estimates for the branching ratio only in units of $|V_{ub}|^2$. Due to the smallness of the differential branching ratio, we prefer to provide our numerical estimates in the form of binned observables. We consider the three phase-space bins following from our discussion in Section 3.1 for our numerical calculation (see also Fig. 3.2 for a visualisation in the

²Our result slightly disagrees with the β_ℓ dependence in Eqs. (4.11) and (4.12) of [61] in the arXiv version v2.

phase space region	result			
	central	δ_{param}	δ_{F_+}	unit
$\mathcal{B}(B^- \rightarrow \pi^+ \pi^- \mu^- \bar{\nu}_\mu) / V_{ub} ^2$				
(A)	2.93	+0.87 -0.40	+0.49 -0.35	10^{-8}
(B)	9.31	+2.70 -1.30	+1.77 -0.69	10^{-7}
(A+B)	9.60	+2.80 -1.30	+1.89 -0.79	10^{-7}
(C)	3.18	+0.63 -0.63	+0.48 -0.33	10^{-5}
$A_{\text{FB}}^\pi(B^- \rightarrow \pi^+ \pi^- \mu^- \bar{\nu}_\mu)$				
(A)	-1.96	+0.15 -0.19	+0.04 -0.07	10^{-1}
(B)	-0.29	+0.21 -0.19	+0.06 -0.11	10^{-1}
(A+B)	-0.32	+0.19 -0.21	+0.07 -0.11	10^{-1}
(C)	+1.25	+0.07 -0.07	+0.03 -0.08	10^{-1}

Table 3.3: Numerical estimates for the partially-integrated branching ratio (in units of $|V_{ub}|^2$) and the pionic forward-backward asymmetry in different phase-space bins. Note that our estimate for A_{FB}^π in the region (C) has been obtained for $|\cos \theta_\pi| < 0.33$. The variation of all parameters, except the $B \rightarrow \pi$ form factor F_+ , comprise the uncertainty denoted as δ_{param} . The total uncertainty δ_{tot} is then obtained as $\delta_{\text{tot}}^2 = \delta_{\text{param}}^2 + \delta_{F_+}^2$.

q^2 - k^2 plane):

$$(A) : \begin{cases} 0.02 \text{ GeV}^2 \leq q^2 \leq (M_B - \sqrt{k^2})^2, \\ 18.60 \text{ GeV}^2 \leq k^2 \leq (M_B - \sqrt{q^2})^2, \\ -1 \leq \cos \theta_\pi \leq +1, \end{cases} \quad (3.21)$$

$$(B) : \begin{cases} 0.02 \text{ GeV}^2 \leq q^2 \leq (M_B - \sqrt{k^2})^2, \\ 13.90 \text{ GeV}^2 \leq k^2 \leq 18.60 \text{ GeV}^2, \\ -1 \leq \cos \theta_\pi \leq +1, \end{cases} \quad (3.22)$$

$$(C) : \begin{cases} 0.02 \text{ GeV}^2 \leq q^2 \leq (M_B - \sqrt{k^2})^2, \\ 7.00 \text{ GeV}^2 \leq k^2 \leq (M_B - \sqrt{q^2})^2, \\ -0.33 \leq \cos \theta_\pi \leq +0.33. \end{cases} \quad (3.23)$$

Region (A) corresponds to the phase space region in which the QCD-improved factorisation results are expected to hold. Region (B) extrapolates to somewhat smaller values of k^2 (and the quoted uncertainties for this region might be underestimated). Finally, region (C) limits the phase space for the helicity angle of the pions to $|\cos \theta_\pi| \leq 0.33$. This allows for using a larger part of the q^2 - k^2 plane, while still enforcing large pion energies in the B -meson rest frame, $E_{1,2} > 1.24 \text{ GeV}$. Our results for both observables are listed in Table 3.3. Moreover, we show the behaviour of the normalised single-differential decay rate as a function of $\cos \theta_\pi$ in Fig. 3.3. As can be seen, the decay features a sizeable pionic forward-backward asymmetry in the bins (A) and (C). Note, that the asymmetry switches sign when enlarging the phase space towards bin (C). As a consequence, in the intermediate bin (B) A_{FB}^π is one order of magnitude smaller than in either (A) or (C).

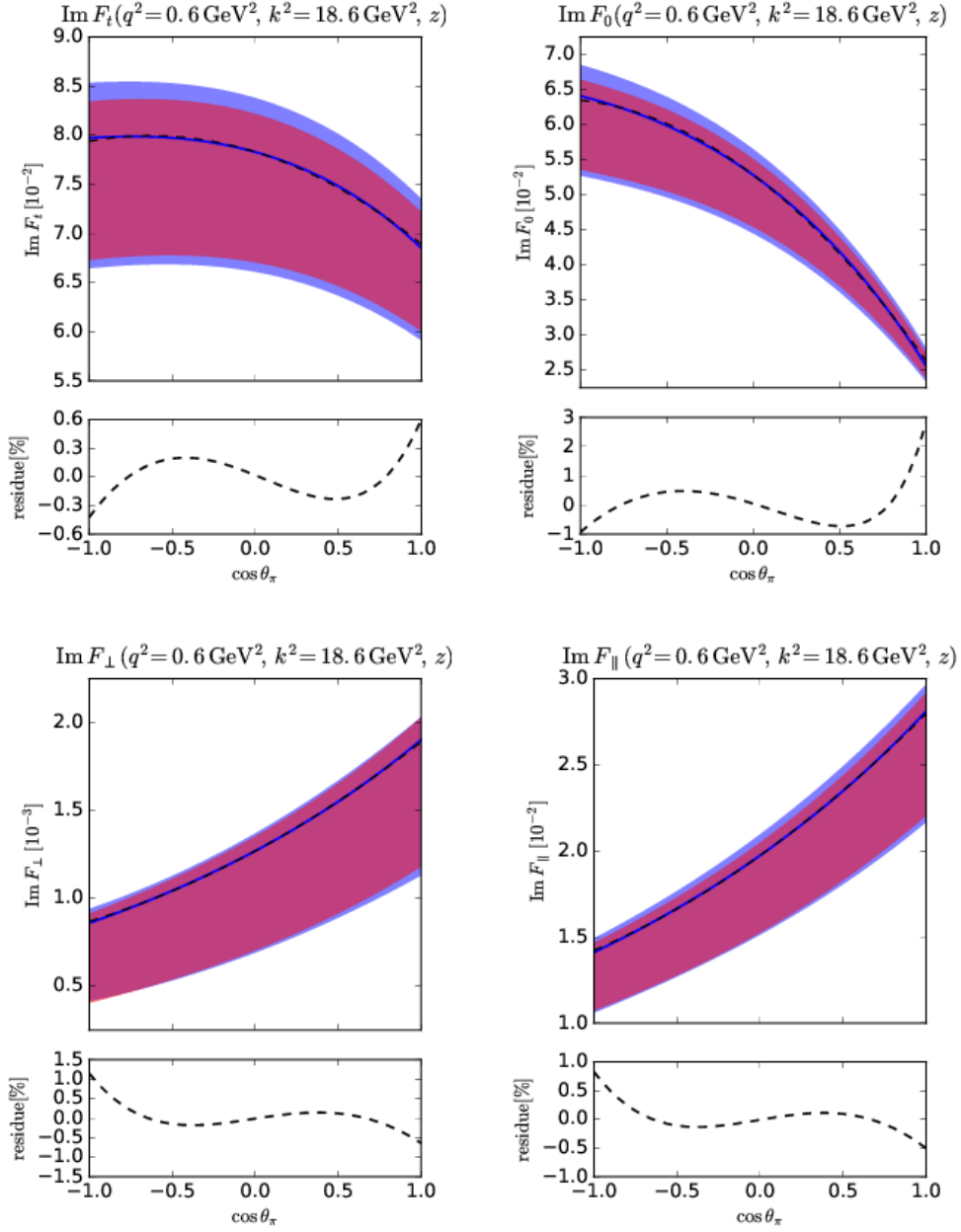


Figure 3.1: Plots of the $\cos \theta_\pi$ dependence of the form factors in the phase space point ($q^2 = 0.6 \text{ GeV}^2, k^2 = 18.6 \text{ GeV}^2$). The blue solid lines show the results at leading order in α_s , including both the twist-2 and twist-3 contributions. The blue shaded areas correspond to central 68% intervals of the posterior-predictive distributions, which arise from the variation of the input parameters as listed in Table 3.2 as well as the parameters for the $B \rightarrow \pi$ form factor F_+ . The red shaded area is the same as the blue area, except for the F_+ variation. The black dashed lines show the approximation of each form factor by its first three partial waves. In the lower parts of each plot, the black dashed lines show the relative residue between the form factors and their partial-wave approximations. (Note that in our convention the form factors are purely imaginary at leading order.)

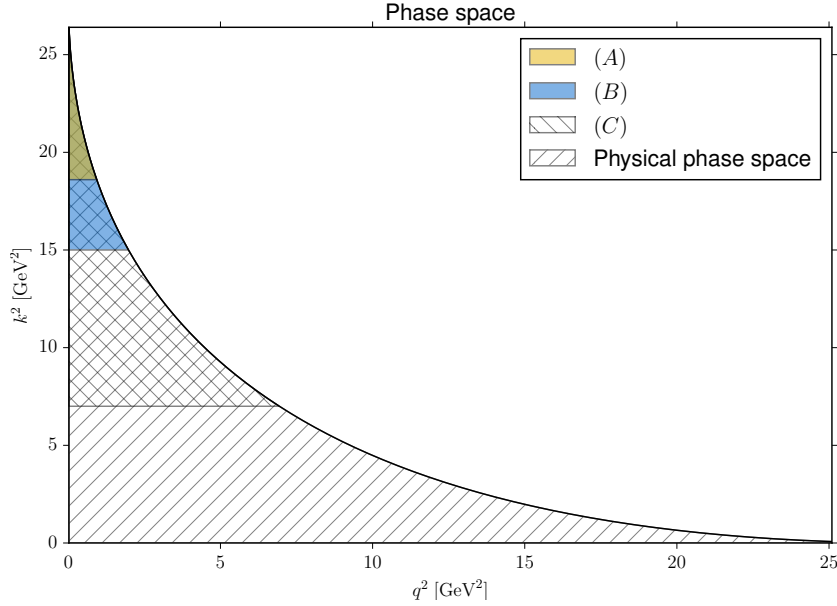


Figure 3.2: We show our choices of phase space bins for the QCDF region (A: gold) and the extrapolation (B: blue). The region C, which has additionally limitations on the magnitude of $\cos\theta_\pi$, is illustrated as the ‘\’-hatched region. The remainder of the physical phase space is highlighted as the ‘//’-hatched area. Estimates for the integrated $B^- \rightarrow \pi^+\pi^-\mu^-\bar{\nu}_\mu$ observables in different bins are shown in Table 3.3.

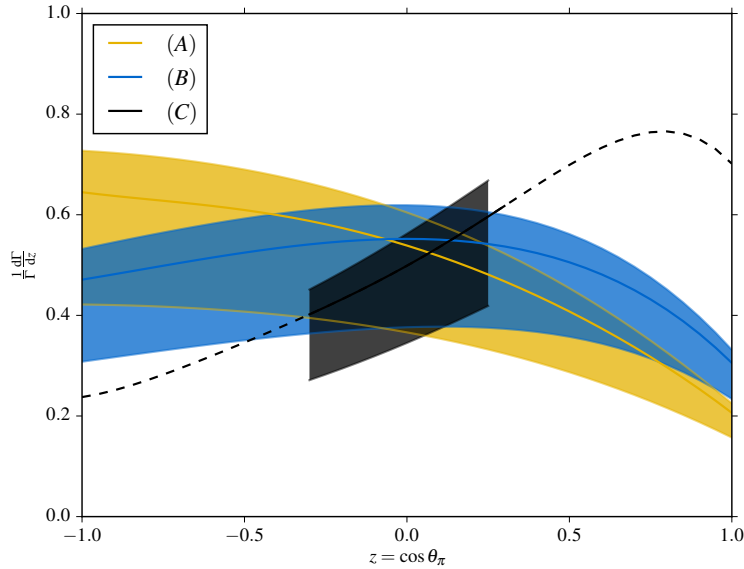


Figure 3.3: Plot of the single-differential normalised decay rate as a function of $z \equiv \cos\theta_\pi$. The gold and blue shaded areas correspond to the phase space bins (A) and (B) as defined in the text. The bin (C) has additional restrictions on the size of $|z|$. An extrapolation beyond these restrictions is indicated by the dashed curve. The shaded areas correspond to the 68% intervals as obtained from variation of all input parameters. The uncertainty is dominated by the parameters listed in Table 3.2.

Chapter 4

Summary

In this work we have investigated the semileptonic four-body decay $B^- \rightarrow \pi^+\pi^-\ell^-\bar{\nu}_\ell$ in the context of QCD factorisation. To this end, we have established a novel factorisation formula for the $B \rightarrow \pi\pi$ form factors that is valid for large dipion invariant mass and large pion energies. The factorisation formula combines features from semileptonic $B \rightarrow \pi$ and nonleptonic $B \rightarrow \pi\pi$ transitions and has a similar structure as known from these decays. One contribution factorises completely into a convolution of a scattering kernel T^{II} with leading-twist LCDAs of both pions and the B meson. The second term involves the non-factorisable soft $B^- \rightarrow \pi^-$ form factor ξ_π . In this contribution only the positively charged pion factorises, involving a hard-scattering kernel T^{I} . The leading contributions to the short-distance kernels T^{I} and T^{II} have been calculated in fixed-order perturbation theory for arbitrary Dirac structures of the $b \rightarrow u$ transition current. The main result of this calculation is the verification of the anticipated factorisation structure, i.e. that the endpoint-divergent contributions arrange exactly in such a way that they can be absorbed into ξ_π , which is multiplied with the convolution involving the kernel T^{I} .

The creation of a final-state quark-antiquark pair with a large recoil requires at least one hard gluon exchange. Contributions from spectator-scattering, contained in the kernel T^{II} , involve an additional hard-collinear gluon exchange and are thus suppressed by a factor of α_s relative to T^{I} . Hence, to first approximation, all dipion form factors are proportional to the soft $B \rightarrow \pi$ form factor ξ_π . The leading-order contribution to T^{I} involves only two independent hadronic structures given by certain moments of the leading-twist LCDA of the positively charged pion. As a consequence, at LO the dipion form factors fulfil approximate relations that have been worked out for the full form factors as well as their partial wave components. Here we have also included “chirally enhanced” twist-3 corrections for the positively charged pion. In the limit of vanishing 3-particle contributions, the corresponding LCDAs are completely fixed by the equations of motion and thus do not introduce new unknown hadronic parameters.

Concerning the calculation of spectator-scattering corrections in T^{II} , a delicate and non-trivial cancellation of endpoint-divergent terms between the individual diagrams and the soft form factor ξ_π confirmed the structure of the factorisation formula, at least to leading order in the perturbative expansion. Since spectator-scattering contributions also probe the partonic structure of the B meson, the first inverse moment of the B -meson LCDA arises as a new hadronic parameter. On the pion side, we find somewhat more complicated convolution integrals, which for $N_C \rightarrow \infty$ reduce to three independent functions that depend on the leading-twist pion LCDA.

A numerical analysis of two different observables in three phase-space bins has been performed. However, due to the phase-space limitation and the perturbative suppression the rate turned out to be too small to be measured with reasonable precision. Nevertheless, our results, in particular the approximate form factor relations, can be used for an interpolation between different phase-space regions utilising results obtained by other methods (see e.g. [74–76]). To this end, one can use a proper form factor parametrisation similar to the one proposed in [77]. Our results can also easily be generalised to other decay modes like $B^- \rightarrow K^+ K^- \ell^- \bar{\nu}_\ell$ or $\bar{B}_s \rightarrow \pi^+ K^0 \ell^- \nu_\ell$, and also $B \rightarrow K \pi \ell^+ \ell^-$. Additionally, this work is interesting from a theoretical point of view since the factorisation emphasises the universal structure of endpoint divergences in exclusive decays.

Project II

Endpoint Divergences in Exclusive *B* Decays

Theoretical Foundations and a Perturbative Toy Model

Introductory Remarks

In the theoretical description of exclusive charmless B -meson decays the conceptual problem of endpoint divergences arises. These contributions spoil a complete factorisation of modes at subleading power (e.g. in $B \rightarrow \gamma \ell \nu$) or even at leading power (for heavy-to-light form factors) in the large-mass expansion. Presently, one eludes a deeper theoretical understanding by absorbing endpoint-sensitive terms into new unknown hadronic functions. The spin-symmetry of these contributions then still guarantees the predictive power of the QCDF approach.

In this second project we aim at improving the factorisation in exclusive B -meson decays. A deeper theoretical understanding of endpoint divergences would be desirable for several reasons. First, one would expect that the process-dependent soft form factors reduce to more universal process-independent hadronic objects, which would increase the predictive power. And second, the mass of the B meson is not extremely large and power corrections are a major source of hadronic uncertainties, which are difficult to estimate. However, endpoint divergences are the very reason that power corrections are not accessible in QCDF. A solution to this long-standing problem is thus vital for an increased precision of SM predictions for exclusive decays, and furthermore, would be of general interest in the context of power corrections in SCET_{II}. To make a step in that direction, we study the soft form factor ξ_π in a perturbative setup where even the hadronic quantities, in particular the LCDAs, can be computed in an expansion in α_s . With fairly new methods that go under the names “collinear anomaly” and “rapidity renormalisation group,” which both have been successfully applied to tackle endpoint divergences in various collider physics observables, we try to gain new insights on this long-standing problem.

This part is organised in three chapters. In Chapter 5 we begin the discussion with an investigation of the on-shell Sudakov form factor in a massive $U(1)$ theory. A comprehensive discussion of an EFT treatment of this simple observable is presented at leading power. To this end, we first introduce the method of regions as a tool to asymptotically expand Feynman integrals and calculate the leading-power contribution to the Sudakov form factor at one-loop. Consecutively, we give an introduction to Soft-Collinear Effective Theory with a focus on SCET_{II}, one of two incarnations of the effective theory. Within SCET_{II}, we formulate a “naive” leading-power factorisation theorem for the Sudakov form factor that holds to all orders in perturbation theory. Endpoint divergences, which require additional regularisation to render the loop integrals well-defined, arise in certain sectors. We reorganise the factorised expression in a way that is manifestly free of endpoint divergences and allows to resum a subset of large logarithms. In this form, the individual quantities can be treated with standard renormalisation group (RG) methods to resum all large logarithms. Finally, we compare the collinear anomaly and the rapidity renormalisation group and show that they give equivalent results for the resummed expression of the Sudakov form factor. In Chapter 6 we study a complete factorisation of heavy-to-light $B \rightarrow \pi$ form factors at large hadronic recoil. After a short summary on how one obtains the factorised form given in Eq. (1.14), this chapter is dedicated to the derivation of a “naive” — still containing ill-defined convolution integrals — factorisation formula for the soft form factor ξ_π within SCET_{II}. To this end, we perform a matching

calculation and compute the leading order (LO) Wilson coefficients of four-quark operators in SCET_{II}. The new ingredient compared to the existing literature is that we include a non-zero (but small) quark mass in our calculation. We, furthermore, compute the leading poles of one-loop corrections to a certain subset of Wilson coefficients that is required in Chapter 7. This calculation is followed by a detailed summary of the various LCDAs for heavy- and light-mesons, which includes their operator definition, equations of motion, and their respective endpoint behaviour. We finally present the naive factorisation of ξ_π for the fixed-order scattering kernels calculated in this chapter. Chapter 7 is dedicated to study the soft form factor ξ_π in a perturbative setup, which can be considered as the decay $B_c \rightarrow \eta_c \ell \nu$ in the non-relativistic approximation. This setup allows us to explicitly calculate the LCDAs, and hence, the convolution integrals, in perturbation theory. We aim at applying the methods discussed in Chapter 5 to heavy-to-light form factors at large recoil. After introducing the setup, we compute ξ_π at tree-level, and furthermore, show the cancellation of all leading divergences at one-loop in the product of ξ_π and the hard matching coefficient H_i . Based on a recursive behaviour, we derive (rapidity-) renormalisation group equations on the level of inverse moments, that, together with the renormalisation of the scattering kernel and the hard matching coefficient, allow us to resum all leading logarithms in the product $H_i \xi_\pi$. We conclude this chapter with a critical discussion about the achievements that we have made. Finally, in Chapter 8, we discuss open questions that prevent a complete factorisation of modes in exclusive decays. To this end, we illustrate how the factorisation changes when we include an additional low-energy mode in the effective theory. Furthermore, we present some ideas how to resum large logarithms beyond the leading logarithmic approximation with the help of toy integrals. However, these ideas have not yet been worked out completely in the realistic scenario. Necessary details to the various chapters can be found in Appendices B-D.

Chapter 5

Theoretical Foundations and the Massive On-Shell Sudakov Problem

We investigate the origin of endpoint divergences in loop integrals. As a toy example, we study the massive on-shell Sudakov form factor at large energies in a $U(1)$ theory with a massive gauge boson. We present all the various steps from the one-loop calculation in fixed-order perturbation theory, to a resummation of large logarithms based on an EFT treatment at leading power.

5.1 One-Loop Calculation in QED with a Massive Photon

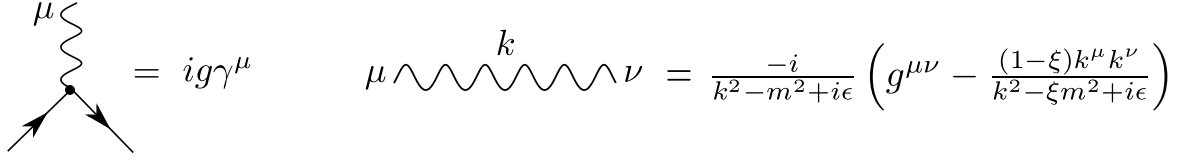
As a toy theory let us consider QED with massless fermions but a non-zero photon mass m :

$$\mathcal{L}_{\text{toy}} = \bar{\psi} i \not{D} \psi - \frac{1}{4} F_{\mu\nu} F^{\mu\nu} + \frac{m^2}{2} A_\mu A^\mu. \quad (5.1)$$

Here $F^{\mu\nu} = \partial^\mu A^\nu - \partial^\nu A^\mu$ is the usual field-strength tensor, $iD^\mu = i\partial^\mu + gA^\mu$ is the covariant derivative and g is the coupling constant of the theory. The last term in the Lagrangian (5.1) is a mass term for the gauge field A^μ which breaks the local $U(1)$ gauge symmetry of QED. Including explicit mass terms in a non-abelian gauge theory spoils the consistency of the theory, since unphysical polarisation states no longer cancel. However, this is not an issue in the abelian case. Using standard gauge fixing, one can show that the Lagrangian with a photon mass term is still invariant under BRST-transformations (Becchi, Rouet, Stora and Tyutin [78, 79]), and unphysical degrees of freedom cancel. Moreover, in an abelian theory, Faddeev-Popov ghosts decouple completely from any physical quantity and can safely be omitted. Thus we can simply write

$$\mathcal{L} \rightarrow \mathcal{L} + \mathcal{L}_{\text{gauge-fix}} = \mathcal{L} - \frac{1}{2\xi} (\partial_\mu A^\mu)^2. \quad (5.2)$$

Inverting the kinetic term of the gauge field gives the ξ -dependent photon propagator. (See Fig. 5.1 for the Feynman rules of the theory). The $k^\mu k^\nu$ term has worse ultraviolet (UV) behaviour than the photon propagator in QED and could potentially spoil the renormalisability of the theory. Equations of motion, however, reveal that $(\partial_\mu A^\mu)$ is a free field and thus the ξ dependence, accompanied by the bad UV behaviour, drops out in



$$\begin{aligned}
 \text{Vertex} &= ig\gamma^\mu & \text{Propagator} &= \frac{-i}{k^2 - m^2 + i\epsilon} \left(g^{\mu\nu} - \frac{(1-\xi)k^\mu k^\nu}{k^2 - \xi m^2 + i\epsilon} \right)
 \end{aligned}$$

Figure 5.1: Feynman Rules resulting from the Lagrangian (5.1) and the gauge-fixing term given in Eq. (5.2). The fermion propagator is as usual.

all physical quantities. In summary, an abelian theory with an explicit gauge-boson mass term is still renormalisable and has predictive power. Although the mass term breaks the gauge-invariance, we still have a cross-check of the ξ -independence of observables. We refer to [80, Ch. 12.9] for a more detailed and formal discussion of $U(1)$ theories with and without a photon mass.

We now study the scattering of on-shell (massless) fermions with an external vector current $J^\mu(x) = \bar{\psi}(x)\gamma^\mu\psi(x)$ in the Euclidean region. The amplitude for such a process is given by the matrix element

$$\langle f(p_c) | J^\mu(x=0) | f(p_{\bar{c}}) \rangle \equiv [\bar{u}_f(p_c)\gamma_\perp^\mu u_f(p_{\bar{c}})] \times \mathcal{F}(Q^2), \quad (5.3)$$

which can be parametrised by a single form factor $\mathcal{F}(Q^2)$. We call the momenta of the fermions p_c and $p_{\bar{c}}$, with $p_c^2 = p_{\bar{c}}^2 = 0$. The square of the momentum transfer is given by $-q^2 = -(p_c - p_{\bar{c}})^2 = 2p_c \cdot p_{\bar{c}} \equiv Q^2 > 0$ and the index “ \perp ” denotes a Lorentz vector in the plane perpendicular to p_c and $p_{\bar{c}}$.

In this section, we calculate $\mathcal{F}(Q^2)$ in perturbation theory up to $\mathcal{O}(\alpha)$, with $g^2 = 4\pi\alpha$, and in particular focus on the limit of large momentum transfer, $Q^2 \gg m^2$. For all n -loop corrections throughout the rest of this chapter we adopt the notation with a superscript (n) for the factor that is multiplied with n -th power of $\frac{\alpha(\mu)}{4\pi}$. At tree-level one simply finds $\mathcal{F}^{(0)}(Q^2) = 1$:

$$\mathcal{F}(Q^2) = 1 + \frac{\alpha(\mu)}{4\pi} \mathcal{F}^{(1)}(Q^2) + \mathcal{O}(\alpha^2). \quad (5.4)$$

There is a single one-particle irreducible Feynman diagram that contributes to $\mathcal{F}^{(1)}(Q^2)$; the vertex correction diagram shown in Fig. 5.2. The corresponding amplitude can be calculated with standard techniques. The loop integral is analytically continued to $d = 4 - 2\epsilon$ dimensions (“*dimensional regularisation*”) to regulate ultraviolet divergences, which show up as poles in ϵ . Note that the amplitude is finite in the infrared (IR) limit because the gauge-boson mass acts as an IR-regulator. Then the integral can be solved easily using, for example, Feynman parameters.

We choose to work in bare perturbation theory and express the bare coupling α_0 through the $\overline{\text{MS}}$ -renormalised coupling via $Z_\alpha\alpha(\mu)\mu^{2\epsilon} = (4\pi)^\epsilon e^{-\epsilon\gamma_E}\alpha_0$, with $\gamma_E \simeq 0.57721$ being the Euler–Mascheroni constant and $Z_\alpha = 1 + \mathcal{O}(\alpha)$. Note that at one-loop order this replacement does not cancel any UV divergences. We find the following expression

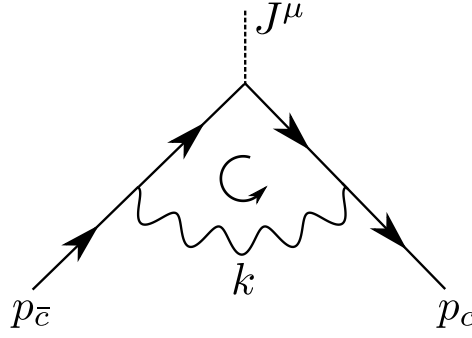


Figure 5.2: One-particle irreducible diagram that contributes to the matrix element defined in Eq. (5.3) at one-loop accuracy.

for the vertex-correction diagram in terms of Feynman parameters x and y :

$$\begin{aligned}
 & \langle f(p_c) | J^\mu(x) | f(p_{\bar{c}}) \rangle \Big|_{\mathcal{O}(\alpha, 1\text{PI})} \\
 &= -ig^2 \int \frac{d^d k}{(2\pi)^d} \frac{\bar{u}_f(p_c) \gamma^\beta (-\not{k} + \not{p}_c) \gamma^\mu (-\not{k} + \not{p}_{\bar{c}}) \gamma^\alpha u_f(p_{\bar{c}})}{[k^2 - m^2 + i\varepsilon] [(k - p_c)^2 + i\varepsilon] [(k - p_{\bar{c}})^2 + i\varepsilon]} \left(g_{\alpha\beta} - \frac{(1 - \xi) k_\alpha k_\beta}{k^2 - \xi m^2 + i\varepsilon} \right) \\
 &= \frac{\alpha(\mu)}{4\pi} e^{\varepsilon\gamma_E} \bar{u}_f(p_c) \gamma_\perp^\mu u_f(p_{\bar{c}}) \left\{ \right. \\
 & \quad 2\Gamma(\varepsilon) \left(\frac{\mu^2}{Q^2} \right)^\varepsilon \int_0^1 dx \int_0^{1-x} dy \left[(\varepsilon - 1)^2 \Delta(x, y; \lambda)^{-\varepsilon} - \varepsilon (\bar{x}\bar{y} - \varepsilon xy) \Delta(x, y; \lambda)^{-1-\varepsilon} \right] \\
 & \quad \left. + \Gamma(\varepsilon - 1) \left(\frac{\mu^2}{m^2} \right)^\varepsilon (1 - \xi^{1-\varepsilon}) \right\}. \tag{5.5}
 \end{aligned}$$

Here $\Delta(x, y; \lambda) = xy + \lambda^2(1 - x - y)$ and $\lambda^2 \equiv m^2/Q^2$ is the dimensionless ratio of the two scales of the problem.¹ Throughout this thesis we make use of the “bar” notation, e.g. $\bar{x} \equiv 1 - x$. Note that the parameter integrals do not give rise to additional poles and the integrand can be expanded around $\varepsilon = 0$. After using the equations of motion for the on-shell spinors and Dirac algebra in d dimensions, all Dirac structures reduce to the form given in Eq. (5.3). The integrals in Eq. (5.5) then yield dilogarithms in λ . The dilogarithm is defined as $\text{Li}_2(z) = \sum_{k=1}^{\infty} \frac{z^k}{k^2}$, for $|z| < 1$ and has the integral representation

$$\text{Li}_2(z) = - \int_0^1 dt \frac{\log(1 - tz)}{t}, \quad |z| < 1, \tag{5.6}$$

which can be analytically continued to the complex plane except for a cut on $[1, \infty)$. However, here we restrict ourselves to values $\lambda \in (0, 1)$ in order to avoid dealing with imaginary parts.

The contribution in the last line of Eq. (5.5) stems from the $k_\alpha k_\beta$ part of the gauge-boson propagator which reduces to so-called massive tadpole integrals and is independent

¹This λ is not to be confused with the Källén function defined in the first part of this thesis.

of the external kinematics Q^2 . We will see now that this contribution exactly drops out as it was argued in the beginning of this section. According to the LSZ formula (Lehmann, Symanzik, Zimmermann [81]), we have to multiply our result Eq. (5.5) with the field-strength renormalisation constant Z_2 , which can be computed from the one-loop fermionic self-energy diagram and is in the on-shell renormalisation scheme given by

$$Z_2 = 1 - \frac{\alpha(\mu)}{4\pi} e^{\epsilon\gamma_E} \left(\frac{\mu^2}{m^2}\right)^\epsilon \left(2\Gamma(\epsilon) \frac{1-\epsilon}{2-\epsilon} + \Gamma(\epsilon-1)(1-\xi^{1-\epsilon})\right) + \mathcal{O}(\alpha^2). \quad (5.7)$$

One immediately sees, that the second term is exactly minus the last line in Eq. (5.5), and hence, the form factor is ξ -independent. Furthermore, Z_2 cancels all UV-divergences and thus the expression for the physical form factor $\mathcal{F}(Q^2)$ is finite in the limit $\epsilon \rightarrow 0$. The one-loop expression reads:

$$\begin{aligned} \mathcal{F}(Q^2) &= 1 + \frac{\alpha(\mu)}{4\pi} \left[-\frac{7}{2} - 6\log\lambda + 2\lambda^2(1+2\log\lambda) \right. \\ &\quad \left. - (1-\lambda^2)^2 \left(\frac{\pi^2}{3} + 2\text{Li}_2(1-\lambda^2) + 4\log^2\lambda \right) \right] + \mathcal{O}(\alpha^2) \\ &\simeq 1 + \frac{\alpha(\mu)}{4\pi} \left[-\frac{7}{2} - \frac{2\pi^2}{3} - 6\log\lambda - 4\log^2\lambda \right] + \mathcal{O}(\alpha\lambda^2, \alpha^2). \end{aligned} \quad (5.8)$$

The second line of this result corresponds to an expansion in the high-energy limit, $\lambda \ll 1 \Leftrightarrow Q^2 \gg m^2$, the so-called Sudakov limit. In general, in fixed-order perturbation theory one encounters logarithms in λ of the form $\alpha^{n_1} \cdot \log^{2n_2} \lambda$, with $n_2 \leq n_1$. A double logarithm of the form $\alpha \cdot \log^2 \lambda$ is typically referred to as a Sudakov (double) logarithm. For small λ the product $\alpha^{n_1} \cdot \log^{2n_2} \lambda$ becomes large and the fixed-order perturbative expansion is no longer a good approximation. This is the typical situation that one can tackle in an EFT. Whenever we have a physical problem with two (or more) widely separated mass scales, EFT methods allow us to resum large logarithms to all orders in perturbation theory using renormalisation group evolution. The proper EFT applicable to the Sudakov problem is Soft-Collinear Effective Theory.

Before moving on, a last comment is in order about the massive $U(1)$ model, in which we calculate the Sudakov form factor. Although the calculation presented here only serves as a toy model, the computation is nevertheless very close to actual applications at the LHC. The LHC currently runs with a centre-of-mass energy of $\sqrt{s} = 14$ TeV, so even the partons can have a centre-of-mass energy of several TeV, which is much higher than the masses of the electroweak gauge bosons, $M_{W,Z} \sim 100$ MeV. Radiative corrections of scattering processes have a similar structure as our result in Eq. (5.8), and in particular also contain large Sudakov logarithms, with $\lambda \sim s/M_{W,Z}^2$. Similar methods and resummation techniques that will be presented in the next sections can be applied in this case. Nonetheless, we are rather interested in formal aspects and in the end we want to transfer some of the methods to exclusive B -meson decays rather than making reliable SM predictions for high-energy processes.

In [82, 83] the Sudakov form factor has been studied in a spontaneously broken $SU(2)$ model (proposed in [84]) which is somewhat closer to the Standard Model. However, it turns out that the one-loop amplitudes are the same in the $SU(2)$ and the $U(1)$ theory. Our results are consistent with the literature.

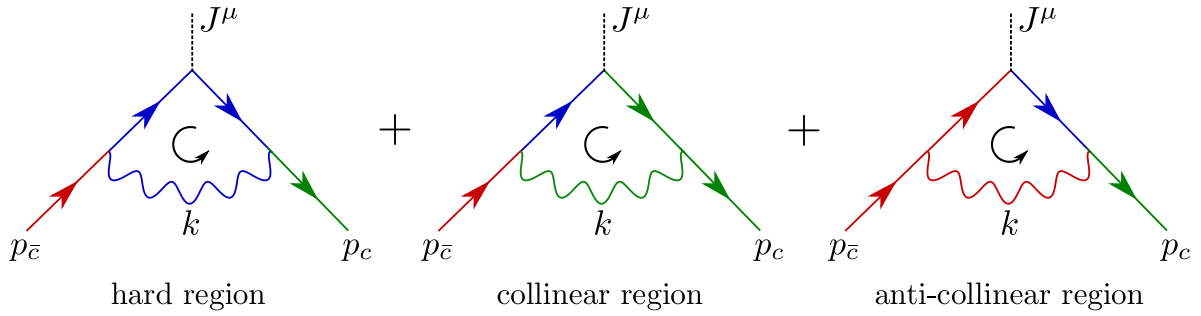


Figure 5.3: Regions that contribute to $\mathcal{F}^{(1)}(Q^2)$ at leading power in λ when using $\nu^\delta/k_\perp^\delta$ as an analytic regulator. Here blue colour indicates hard propagators, green colour collinear, and red colour anti-collinear propagators.

5.2 The Strategy of Regions

The strategy of regions (or method of regions) is a method for an asymptotic expansion of Feynman integrals proposed in [85]. Whenever there is a strong hierarchy of parameters, a given integral can be expanded in a small ratio by expanding the integrand according to certain rules (see below). The remaining integrals then depend on less mass scales and are thus in general much simpler to evaluate. Numerous examples show the validity of the method and it has been formalised to some extent in [86], but a rigorous mathematical proof is at the moment still missing. Following the recipe given e.g. in [86, 87], we have to go through the following steps to obtain an approximate expression for a dimensionally regularised integral:

1. Divide the integration domain of a given multi-loop integral into various regions, each of which is characterised by a specific scaling behaviour of the loop-momenta.
2. Expand the integrand in each region to the desired order in the parameters that are considered small. Then integrate over the whole phase space.
3. Set scaleless integrals to zero.

The sum of integrals calculated in the various regions reproduces the full integral to the desired approximation. However, there is no general algorithm how to find all relevant regions. They often can be determined by the structure of poles of the propagators in the loop, see e.g. [85].

The Sudakov problem is characterised by a single small dimensionless parameter $\lambda \ll 1$. Our aim is to reproduce the expression for $\mathcal{F}^{(1)}(Q^2)$ at leading power in λ , given in the second line of Eq. (5.8). Let us assume that only three regions give contributions that do not give scaleless integrals. We call them the *collinear region* (or *c-collinear*), when the loop-momentum k is (nearly) collinear to p_c , the *anti-collinear region* (or *c-bar-collinear*) for $p_{\bar{c}}$ respectively, and the *hard region*, when k scales as the momentum transfer q . For a graphical depiction see Fig. 5.3. Then we have the identity

$$\mathcal{F}^{(1)}(Q^2) = \mathcal{F}_h^{(1)} + \mathcal{F}_c^{(1)} + \mathcal{F}_{\bar{c}}^{(1)} + \mathcal{O}(\lambda^2). \quad (5.9)$$

The arguments of the different contributions have been omitted for brevity. We will see below that each region only knows its characteristic scale in such a way that in the sum we

end up with the correct logarithms in λ . Since we already showed the “gauge-invariance” of $\mathcal{F}^{(1)}(Q^2)$, let us from now on set $\xi = 1$ for simplicity.²

Before moving on to the calculation of the integrals in the regions, we briefly revisit the kinematics of the process and define some notation that will be used throughout the remainder of the thesis. We can always choose a frame in which both particles move back-to-back along the z -axis and share the same energy $\sqrt{Q^2}/2$ (the Breit-frame). We define two light-like reference vectors n and \bar{n} that point in the direction of the momenta p_c and $p_{\bar{c}}$, i.e. along the z -axis:

$$n^\mu = (1, 0, 0, 1) \quad \text{and} \quad \bar{n}^\mu = (1, 0, 0, -1), \quad (5.10)$$

so that

$$p_c^\mu = \frac{Q}{2} n^\mu \quad \text{and} \quad p_{\bar{c}}^\mu = \frac{Q}{2} \bar{n}^\mu, \quad (5.11)$$

with $Q \equiv \sqrt{Q^2}$. These reference vectors obey $n^2 = \bar{n}^2 = 0$ and $n \cdot \bar{n} = 2$. As mentioned earlier, the index “ \perp ” indicates a vector in the plane perpendicular to n and \bar{n} , so that $n \cdot x_\perp = \bar{n} \cdot x_\perp = 0$ holds for any Lorentz vector x^μ . Let us further define the abbreviations $(n \cdot x) \equiv x_+$ and $(\bar{n} \cdot x) \equiv x_-$, so that x^μ can be decomposed as

$$x^\mu = \frac{x_-}{2} n^\mu + x_\perp^\mu + \frac{x_+}{2} \bar{n}^\mu, \quad (5.12)$$

which in shorthand notation is usually written as the tuple

$$x^\mu \equiv (x_-, x_\perp^\mu, x_+). \quad (5.13)$$

The scalar product of two vectors x^μ and y^μ can then be expressed as

$$x \cdot y = \frac{x_+ y_-}{2} + \frac{x_- y_+}{2} + x_\perp \cdot y_\perp, \quad x^2 = x_+ x_- + x_\perp^2. \quad (5.14)$$

For example, the square of the momentum transfer is given by $Q^2 = p_c \cdot p_{\bar{c}}$.

The phrase “a vector scales as” (denoted by the \sim symbol), means that every light-cone component has a specific power counting in $\lambda = m/Q$:

$$x^\mu \sim (\lambda^a, \lambda^b, \lambda^c) Q \quad \Leftrightarrow \quad (x_- \sim \lambda^a Q, x_\perp^\mu \sim \lambda^b Q, x_+ \sim \lambda^c Q). \quad (5.15)$$

For example, by definition the external momenta scale as

$$p_c^\mu \sim (1, 0, 0) Q \quad \text{and} \quad p_{\bar{c}} \sim (0, 0, 1) Q. \quad (5.16)$$

With these definitions at hand, we now calculate the various terms in Eq. (5.9).

²Note that for $\xi \neq 1$ massive tadpole integrals appear in the calculation. Then the overlap of some regions is no longer scaleless and Eq. (5.9) has to be modified in such a way, that overlapping regions have to be subtracted explicitly in order to avoid double-counting (see discussion in [86]).

Hard region: The loop-momentum scales as $k^\mu \sim (1, 1, 1) Q$ with virtuality $\sqrt{k^2} \sim Q$. At leading power in λ , we can simply neglect the gauge-boson mass, $k^2 - m^2 \simeq k^2$. Hence, we end up with the full integral in terms of Feynman parameters in Eq. (5.5) (with $\xi = 1$) with the replacement $\Delta(x, y; \lambda) \rightarrow \Delta^{(h)}(x, y) = xy$:

$$\begin{aligned} & \langle f(p_c) | J^\mu(x) | f(p_{\bar{c}}) \rangle \Big|_{\mathcal{O}(\alpha), 1\text{PI}, \text{hard}} \\ & \simeq \frac{\alpha(\mu)}{4\pi} e^{\varepsilon\gamma_E} 2\Gamma(\varepsilon) \left(\frac{\mu^2}{Q^2} \right)^\varepsilon \bar{u}_f(p_c) \gamma_\perp^\mu u_f(p_{\bar{c}}) \\ & \int_0^1 dx \int_0^{1-x} dy \left[(\varepsilon - 1)^2 \Delta^{(h)}(x, y)^{-\varepsilon} - \varepsilon (\bar{x}\bar{y} - \varepsilon xy) \Delta^{(h)}(x, y)^{-1-\varepsilon} \right]. \end{aligned} \quad (5.17)$$

The integrals can be evaluated easily and in contrast to the full one-loop amplitude does not involve polylogarithms. Due to the missing mass m , the hard region suffers from new IR-singularities that are regularised in d dimensions. Thus, a double pole in ε emerges that has to cancel with appropriate poles from other regions. We find

$$\mathcal{F}_h^{(1)} = \left(\frac{\mu^2}{Q^2} \right)^\varepsilon \left[-\frac{2}{\varepsilon^2} - \frac{3}{\varepsilon} + \frac{\pi^2}{6} - 8 + \mathcal{O}(\varepsilon) \right] \equiv \mathcal{F}_h^{(1)}(L_{\mu, Q}), \quad (5.18)$$

where we introduced the abbreviation $L_{x, y} \equiv \log \frac{x}{y}$.

Collinear region: $k^\mu \sim (1, \lambda, \lambda^2) Q$ with virtuality $\sqrt{k^2} \sim \lambda Q$.

In the collinear region the fermion propagator attached to the anti-collinear leg has hard virtuality (see Fig. 5.3) and we can approximate $(k - p_{\bar{c}})^2 + i\varepsilon \simeq -Q(k_- - i\varepsilon)$. Furthermore, the numerator structure simplifies to some extent which amounts to replacing the hard fermion propagator and the adjacent vertex by their eikonal limit,

$$\frac{(-\not{k} + \not{p}_{\bar{c}})\gamma^\alpha}{(k - p_{\bar{c}})^2 + i\varepsilon} \rightarrow \frac{\bar{n}^\alpha}{-k_- + i\varepsilon}. \quad (5.19)$$

We find for the leading-power expression:

$$\begin{aligned} & \langle f(p_c) | J^\mu(x) | f(p_{\bar{c}}) \rangle \Big|_{\mathcal{O}(\alpha), 1\text{PI}, \text{coll.}} \\ & \simeq -g^2 \int \frac{d^d k}{(2\pi)^d} \frac{\bar{u}_f(p_c) \gamma^\beta (-\not{k} + \not{p}_{\bar{c}})\gamma^\mu u_f(p_{\bar{c}})}{[(k - p_c)^2 + i\varepsilon]} \frac{\bar{n}^\alpha}{k_- - i\varepsilon} \frac{-i g_{\alpha\beta}}{k^2 - m^2 + i\varepsilon} \\ & \simeq +2ig^2 \bar{u}_f(p_c) \gamma_\perp^\mu u_f(p_{\bar{c}}) \int \frac{d^d k}{(2\pi)^d} \frac{Q - k_-}{[k^2 - m^2 + i\varepsilon] [(k - p_c)^2 + i\varepsilon] [k_- - i\varepsilon]}. \end{aligned} \quad (5.20)$$

Note that the integration measure scales as $d^d k \sim \lambda^d Q^d$, so that the overall integral is of leading power in λ . The factor $1/k_-$ from the eikonal propagator renders the integral ill-defined for $k_- \rightarrow 0$, even in d dimensions. We encounter a so-called rapidity divergence or endpoint divergence. Rapidity divergences arise from momentum regions where the ratio k_+/k_- (or k_-/k_+) diverges but the invariant mass k^2 is fixed. An additional regularisation

prescription is needed to give the integral a meaning. We choose to introduce an ad hoc *analytic regulator* and write a factor of $(\nu/k_-)^\delta$ in the integrand [88]. Similar to the role of the 't Hooft scale μ in dimensional regularisation, the scale ν restores the correct dimensionality. The result of Eq. (5.20) then contains poles in δ in addition to the ones in ε .

To evaluate the integral we rewrite the integration measure in terms of light-cone components

$$d^d k = \frac{1}{2} dk_- dk_+ d^{d-2} k_\perp. \quad (5.21)$$

Then we perform the k_+ integration using Cauchy's residue theorem. The integration over the perpendicular components then reduces to a massive tadpole integral and the remaining dk_- integration reads:

$$\begin{aligned} \mathcal{F}_c^{(1)} &= -2 e^{\varepsilon\gamma_E} \Gamma(\varepsilon) \left(\frac{\mu^2}{m^2}\right)^\varepsilon \int_0^Q \frac{dk_-}{k_-} \left(\frac{\nu}{k_-}\right)^\delta \left(\frac{Q-k_-}{Q}\right)^{1-\varepsilon} \\ &= -2 e^{\varepsilon\gamma_E} \Gamma(\varepsilon) \left(\frac{\mu^2}{m^2}\right)^\varepsilon \left(\frac{\nu}{Q}\right)^\delta \frac{\Gamma(-\delta)\Gamma(2-\varepsilon)}{\Gamma(2-\delta-\varepsilon)} \\ &\simeq \left(\frac{\mu^2}{m^2}\right)^\varepsilon \left(\frac{\nu}{Q}\right)^\delta \left[\frac{2}{\delta\varepsilon} + \frac{2}{\varepsilon} + 2 - \frac{\pi^2}{3} + \mathcal{O}(\delta, \varepsilon) \right] \equiv \mathcal{F}_c^{(1)}(L_{\mu,m}, L_{\nu,Q}). \end{aligned} \quad (5.22)$$

The pole in δ arises from $k_- \rightarrow 0$ for fixed $k_\perp^\mu \sim \lambda Q$. In other words the endpoint divergence comes from the limit where the collinear region starts to overlap with the anti-collinear region. The result for $\mathcal{F}_c^{(1)}$ depends on the natural scales in the collinear region only. The virtuality of collinear propagators is soft, $\mu_s \sim m$. Since we used $(\nu/k_-)^\delta$ as a regulator, and $k_- \sim Q$ is the large component of the loop momentum, we have $\nu_c \sim Q$ for the typical rapidity scale in the collinear region. Thus, although we would naively interpret the collinear region as a low-energy matrix element, through the anomalous behaviour in form of the pole in δ it still depends on the large scale Q .

Before investigating the anti-collinear region, we make several remarks about the regularisation prescription that we use:

- We have to introduce the regulator already by modifying the unexpanded integrand. There, as well as in the hard region, we can trivially take the limit $\delta \rightarrow 0$. We can thus reproduce the correct result of the full integral by introducing the new regulator only in the subset of the regions where it is required to give the integrals a meaning.
- With our regulator choice the expansions in δ and ε commute in the collinear region. This is in general not the case as we will see below. Since we did not regularise the hard region, we should expand in δ first and subsequently, if required, expand in ε .
- The physical problem is completely symmetric in $n \leftrightarrow \bar{n}$. Naively one would expect the collinear and the anti-collinear region to give identical results. However, the regulator $(\nu/k_-)^\delta$ breaks this symmetry. Introducing another regulator, e.g. $(\nu/k_0)^\delta$, restores this symmetry, but then the three regions (hard, collinear and anti-collinear) are no longer sufficient to reproduce the full result. We briefly discuss this issue below.

- We should keep in mind that introducing a regulator by simply raising the power of certain propagators is highly dangerous in a gauge theory because it potentially violates gauge invariance. Furthermore, it is not clear how the regularised integral can be interpreted as a matrix element of an operator in the effective theory. We mention below how this can be cured for the Sudakov form factor.

Anti-collinear region: $k^\mu \sim (\lambda^2, \lambda, 1) Q$ with virtuality $\sqrt{k^2} \sim \lambda Q$.

In the anti-collinear region the fermion propagator on the collinear side has hard virtuality and similar simplifications as in the collinear sector arise. We again end up with the eikonal propagator

$$\frac{\gamma^\beta (-\not{k} + \not{p}_c)}{(k - p_c)^2 + i\varepsilon} \rightarrow \frac{n^\beta}{-k_+ + i\varepsilon}, \quad (5.23)$$

and find for the leading power integral

$$\begin{aligned} & \langle f(p_c) | J^\mu(x) | f(p_{\bar{c}}) \rangle \Big|_{\mathcal{O}(\alpha), 1\text{PI}, \text{anti-coll.}} \\ & \simeq -g^2 \int \frac{d^d k}{(2\pi)^d} \left(\frac{\nu}{k_-} \right)^\delta \frac{\bar{u}_f(p_c) \gamma^\mu (-\not{k} + \not{p}_{\bar{c}}) \gamma^\alpha u_f(p_{\bar{c}})}{[(k - p_{\bar{c}})^2 + i\varepsilon]} \frac{n^\beta}{k_+ - i\varepsilon} \frac{-i g_{\alpha\beta}}{k^2 - m^2 + i\varepsilon} \\ & \simeq +2ig^2 \bar{u}_f(p_c) \gamma_\perp^\mu u_f(p_{\bar{c}}) \int \frac{d^d k}{(2\pi)^d} \left(\frac{\nu}{k_-} \right)^\delta \frac{Q - k_+}{[k^2 - m^2 + i\varepsilon][(k - p_{\bar{c}})^2 + i\varepsilon][k_+ - i\varepsilon]}. \end{aligned} \quad (5.24)$$

With our regulator choice we would like to perform the k_+ integration with contour methods again. This can be done, but one has to be very careful since, when closing the contour, the contribution from the arc does not vanish due to the additional k_+ in the numerator. One can circumvent this problem e.g. by a slight misalignment of the external momentum $p_{\bar{c}}$ with respect to the reference vector \bar{n} , $p_{\bar{c}} \not\parallel \bar{n}$ (but $p_{\bar{c}}^2 = 0$ still holds), and take the limit $p_{\bar{c}}^\mu = Q/2 \bar{n}^\mu$ after the integral has been performed. However, we choose to use Cauchy's theorem for the variable k_- . Then we have to specify a $\pm i\varepsilon$ prescription in our regulator in order to treat the branch-cut consistently. Considering Eq. (5.19), the natural choice would be $\nu^\delta/k_-^\delta \rightarrow \nu^\delta/(k_- - i\varepsilon)^\delta$.

Evaluating the regulator at the corresponding poles inevitably links the $d^{d-2}k_\perp$ integration with δ . With $x \equiv \vec{k}_\perp^2 = -k_\perp^2 > 0$ and $\hat{k}_+ \equiv k_+/Q$ we find for the integral in the anti-collinear region

$$\mathcal{F}_{\bar{c}}^{(1)} = - \frac{2 e^{\varepsilon\gamma_E}}{\Gamma(1-\varepsilon)} \left(\frac{\mu^2}{m^2} \right)^\varepsilon \left(\frac{\nu Q}{m^2} \right)^\delta \int_0^1 d\hat{k}_+ \frac{1 - \hat{k}_+}{\hat{k}_+^{1-\delta}} \int_0^\infty dx \frac{x^{-\varepsilon} (1+x)^{-\delta}}{x+1-\hat{k}_+}. \quad (5.25)$$

Note that the expansions in δ and ε no longer commute. As argued above, we should perform the δ expansion first. The pole in δ now comes from the limit $k_+ \rightarrow 0$ (or $k_- \rightarrow \infty$) for fixed $k_\perp^\mu \sim \lambda Q$, in line with our observation in the collinear region that rapidity divergences arise when propagators start to overlap. We can isolate the pole in

δ using a standard plus-distribution:

$$\begin{aligned}
 & \int_0^1 d\hat{k}_+ \frac{1 - \hat{k}_+}{\hat{k}_+^{1-\delta}} \int_0^\infty dx \frac{x^{-\varepsilon} (1+x)^{-\delta}}{x+1-\hat{k}_+} \\
 & \simeq \int_0^1 \frac{d\hat{k}_+}{\hat{k}_+^{1-\delta}} \int_0^\infty dx x^{-\varepsilon} (1+x)^{-1-\delta} + \int_0^1 \frac{d\hat{k}_+}{\hat{k}_+} \int_0^\infty dx x^{-\varepsilon} \left(\frac{1 - \hat{k}_+}{x+1-\hat{k}_+} - \frac{1}{x+1} \right) + \mathcal{O}(\delta) \\
 & = \frac{1}{\delta} \frac{\Gamma(1-\varepsilon)\Gamma(\delta+\varepsilon)}{\Gamma(1+\delta)} - \Gamma(\varepsilon)\Gamma(1-\varepsilon)H_{1-\varepsilon} + \mathcal{O}(\delta), \tag{5.26}
 \end{aligned}$$

where $H_x = \psi(x+1) + \gamma_E$ (with the digamma function $\psi(x) = \frac{d}{dx} \log \Gamma(x)$) is the analytic continuation of the harmonic numbers. Since $\Gamma(\delta+\varepsilon) \simeq 1/\varepsilon - \delta/\varepsilon^2 + \mathcal{O}(\delta^2, \varepsilon^0)$, the expansion in δ in the second term generates an additional double pole in ε that cancels with the one found in the hard region. We note that this double pole comes from the endpoint region and only occurs in the region with the ‘‘asymmetric’’ regulator. The contribution to the form factor from the anti-collinear region reads:

$$\begin{aligned}
 \mathcal{F}_{\bar{c}}^{(1)} & = \left(\frac{\mu^2}{m^2} \right)^\varepsilon \left(\frac{\nu Q}{m^2} \right)^\delta \left[-\frac{2}{\delta\varepsilon} + \frac{2}{\varepsilon^2} + \frac{2}{\varepsilon} + 2 - \frac{\pi^2}{2} + \mathcal{O}(\delta, \varepsilon) \right] \\
 & \equiv \mathcal{F}_{\bar{c}}^{(1)}(L_{\mu, m}, L_{\nu Q, m^2}). \tag{5.27}
 \end{aligned}$$

The virtuality of this region is again soft. However, k_- is now the small component of the loop momentum, $k_- \sim \lambda^2 Q^2$, and the natural value for the rapidity scale ν would be $\nu_{\bar{c}} \sim m^2/Q \sim \lambda^2 Q$.

After summing up all three regions we get the result

$$\mathcal{F}_h^{(1)} + \mathcal{F}_c^{(1)} + \mathcal{F}_{\bar{c}}^{(1)} = +\frac{1}{\varepsilon} + 2 \log \frac{\mu}{m} - 4 - \frac{2\pi^2}{3} - 6 \log \frac{m}{Q} - 4 \log^2 \frac{m}{Q} + \mathcal{O}(\varepsilon). \tag{5.28}$$

The fermion self-energy diagrams live on the individual collinear legs. Hence, one would naturally include one factor of $\sqrt{Z_2}$ in each region. In order to ensure Eq. (5.9), we thus rewrite $\mathcal{F}_c^{(1)} \rightarrow \mathcal{F}_c^{(1)} + \frac{1}{2}\delta Z_2$ and $\mathcal{F}_{\bar{c}}^{(1)} \rightarrow \mathcal{F}_{\bar{c}}^{(1)} + \frac{1}{2}\delta Z_2$, with the wave-function renormalisation factor Z_2 given in Eq. (5.7) and $\delta Z_2 = Z_2 - 1 \simeq \frac{\alpha(\mu)}{4\pi} \left(\frac{\mu^2}{m^2} \right)^\varepsilon \left(-\frac{1}{\varepsilon} + \frac{1}{2} \right)$. With this replacement we find indeed the correct leading-power result for the form factor given in the second line of Eq. (5.8), in agreement with our assumption that only the examined three regions contribute. In particular, the large logarithms of λ are generated through the following steps. The cancellation of poles in δ and ε results in the cancellation of the artificial scales ν and μ between the various regions, which only know their natural scales. For dimensional reasons, this cancellation generates large logarithms of ratios of virtualities and rapidities (in this case of λ).

Soft region: $k^\mu \sim (\lambda, \lambda, \lambda) Q$ with virtuality $\sqrt{k^2} \sim \lambda Q$.

Although we already reproduced the correct result, let us nevertheless study the integral in the soft region, which lies between the two collinear regions on the same invariant

mass hyperbola:

$$\begin{aligned} & \langle f(p_c) | J^\mu(x) | f(p_{\bar{c}}) \rangle \Big|_{\mathcal{O}(\alpha), 1\text{PI}, \text{soft}} \\ & \simeq g^2 \bar{u}_f(p_c) \gamma_\perp^\mu u_f(p_{\bar{c}}) \int \frac{d^d k}{(2\pi)^d} \left(\frac{\nu}{k_-} \right)^\delta \frac{n^\beta}{k_+ - i\varepsilon} \frac{\bar{n}^\alpha}{k_- - i\varepsilon} \frac{-i g_{\alpha\beta}}{k^2 - m^2 + i\varepsilon}. \end{aligned} \quad (5.29)$$

Here both fermion propagators can be replaced by their eikonal limit. The integrand corresponds to the overlap region between the two collinear regions. That means, we take the integrand in the collinear region and expand it according to the scaling in the anti-collinear region afterwards (or vice versa).

Again the integral can be performed most easily using Cauchy's theorem in the variable k_+ . With our regularisation prescription we find

$$\begin{aligned} \mathcal{F}_s^{(1)} &= -2\Gamma(\varepsilon) e^{\varepsilon\gamma_E} \left(\frac{\mu^2}{m^2} \right)^\varepsilon \int_0^\infty \frac{dk_-}{k_-} \left(\frac{\nu}{k_-} \right)^\delta \\ &\simeq -2\Gamma(\varepsilon) e^{\varepsilon\gamma_E} \left(\frac{\mu^2}{m^2} \right)^\varepsilon \left(\frac{\nu}{\Lambda_{\text{cut}}} \right)^\delta \left(\frac{1}{\delta_{\text{UV}}} - \frac{1}{\delta_{\text{IR}}} \right) = 0 \quad (\text{scaleless}), \end{aligned} \quad (5.30)$$

where we introduced an artificial cut-off scale Λ_{cut} in the k_- integration. We find that the soft region is indeed scaleless, which confirms the assumption that overlap contributions are not present in Eq. (5.9). However, note that the information about the poles in δ that appear in the two collinear regions is also contained in the soft region integral. In other words, the poles in δ cancel between the collinear region (from $k_- \rightarrow 0$) and the soft region in the limit $k_- \rightarrow \infty$, as well as between the anti-collinear region (from $k_- \rightarrow \infty$) and the soft region in the limit $k_- \rightarrow 0$ separately.

Lastly, let us study the various contributions using the regulator $\nu^\delta/(2k_0 - i\varepsilon)^\delta$, with $2k_0 = k_+ + k_-$. We indicate the contributions from the various regions using this prescription with a tilde. The hard region is not affected by the regulator and thus $\tilde{\mathcal{F}}_h^{(1)} = \mathcal{F}_h^{(1)}$. As mentioned earlier, this regulator must be expanded in the different regions as well and preserves the symmetry in $n \leftrightarrow \bar{n}$. We thus find exactly the same result $\tilde{\mathcal{F}}_{\bar{c}}^{(1)} = \tilde{\mathcal{F}}_c^{(1)} = \mathcal{F}_c^{(1)}$ from Eq. (5.22) for the two collinear contributions. We can only obtain the correct result for the full form factor if another region is present; the soft region. We now find (with the usual notation $\tilde{\mu}^{2\varepsilon} = \frac{e^{\varepsilon\gamma_E}}{(4\pi)^\varepsilon} \mu^{2\varepsilon}$)

$$\begin{aligned} \tilde{\mathcal{F}}_s^{(1)} &= -32 i\pi^2 \tilde{\mu}^{2\varepsilon} \int \frac{d^d k}{(2\pi)^d} \left(\frac{\nu}{k_+ + k_- - i\varepsilon} \right)^\delta \frac{1}{k_+ - i\varepsilon} \frac{1}{k_- - i\varepsilon} \frac{1}{k^2 - m^2 + i\varepsilon} \\ &= -2 e^{\varepsilon\gamma_E} \left(\frac{\mu^2}{m^2} \right)^\varepsilon \left(\frac{\nu}{m} \right)^\delta \frac{\Gamma(\delta/2) \Gamma(\delta/2 + \varepsilon)}{\Gamma(1 + \delta)} \\ &\simeq \left(\frac{\mu^2}{m^2} \right)^\varepsilon \left(\frac{\nu}{m} \right)^\delta \left[-\frac{4}{\delta\varepsilon} + \frac{2}{\varepsilon^2} - \frac{\pi^2}{6} \right] \equiv \tilde{\mathcal{F}}_s^{(1)}(L_{\mu,m}, L_{\nu,m}). \end{aligned} \quad (5.31)$$

Using for example Cauchy's theorem in k_- , the poles in δ come again from $k_+ \rightarrow 0$ (overlap with the collinear region) and $k_+ \rightarrow \infty$ (overlap with the anti-collinear region) and the double pole in ε again comes from the expansion in δ . The difficulties with the

asymmetric regulator in the anti-collinear region (see Eqs. (5.26) and (5.27)) now have been shifted completely to the soft region. The leading power form factor is now given by

$$\mathcal{F}^{(1)}(Q^2) = \tilde{\mathcal{F}}_h^{(1)} + \tilde{\mathcal{F}}_c^{(1)} + \tilde{\mathcal{F}}_{\bar{c}}^{(1)} + \tilde{\mathcal{F}}_s^{(1)} = \mathcal{F}_h^{(1)} + 2\mathcal{F}_c^{(1)} + \tilde{\mathcal{F}}_s^{(1)}. \quad (5.32)$$

The implications of this ambiguity on the factorisation of the form factor will be discussed briefly towards the end of this chapter, and again in a different context in Chapter 8.

5.3 Soft-Collinear Effective Theory

The method of regions provides a useful tool for calculating loop integrals in a power expansion in a small parameter. Simplifications arise in the individual regions and the integrals can be computed with much less effort than the full integral. However, the strength of the method is not only on a purely calculational level. One can also construct the expansion at the Lagrangian level. *Soft-Collinear Effective Theory* [67, 89–94] is the effective field theory designed for high-energy processes involving energetic particles. The Feynman rules reproduce the integrals that we found in the low-energy regions, whereas the hard region arises as a matching coefficient. Furthermore, SCET allows us to resum large logarithms to all orders in perturbation theory. A pedagogical introduction to SCET can be found in [87]. In some parts of this section we follow the notation and arguments of this article.³

In this section we focus on the effective-field-theory description of the massive on-shell Sudakov form factor at leading power. This is a typical example for a so-called SCET_{II} problem. The similarities and differences with respect to endpoint divergences between the two versions SCET_I and SCET_{II} will be discussed in greater detail in Section 6.1. The starting point is the splitting of all fields in the Lagrangian Eq. (5.1) into a sum of fields with definite momentum scaling (with restricted spatial variations in position space). We aim at integrating out hard fluctuations that appear as Wilson coefficients multiplying effective low-energy operators. Hence, the modes that live in the EFT are collinear, anti-collinear and soft modes:

$$\begin{aligned} \psi(x) &\rightarrow \psi_c(x) + \psi_{\bar{c}}(x) + \psi_s(x), \\ A^\mu(x) &\rightarrow A_c^\mu(x) + A_{\bar{c}}^\mu(x) + A_s^\mu(x). \end{aligned} \quad (5.33)$$

Moreover, we distinguish between different components of the spinor fields by introducing

$$\psi_{c,\bar{c}} \equiv \xi_{c,\bar{c}} + \eta_{c,\bar{c}}, \quad (5.34)$$

with

$$\xi_c = P_+ \psi_c, \eta_c = P_- \psi_c \quad \text{and} \quad \xi_{\bar{c}} = P_- \psi_{\bar{c}}, \eta_{\bar{c}} = P_+ \psi_{\bar{c}}. \quad (5.35)$$

Here $P_+ = \frac{\not{n}\not{\bar{n}}}{4}$ and $P_- = 1 - P_+ = \frac{\not{\bar{n}}\not{n}}{4}$ are projectors, i.e. they fulfil $P_+^2 = P_+$, $P_-^2 = P_-$ and $P_+P_- = P_-P_+ = 0$. This implies that $\not{n}\xi_c = \not{\bar{n}}\eta_c = \not{\bar{n}}\xi_{\bar{c}} = \not{n}\eta_{\bar{c}} = 0$.

³Note that, since we discuss a different introductory example, our definition of the soft mode does not coincide with the one in [87].

The scaling of the various fields in λ is determined by the Fourier transform of the two-point function. The gauge fields scale like their momenta (e.g. the components of A_c^μ scale like the components of a collinear momentum, $A_c^\mu \sim (1, \lambda, \lambda^2) Q$) and the fermionic fields scale as follows:

$$\psi_s \sim \lambda^{3/2} \quad \text{and} \quad \xi_{c,\bar{c}} \sim \lambda \quad \text{and} \quad \eta_{c,\bar{c}} \sim \lambda^2. \quad (5.36)$$

The leading-power effective Lagrangian – here denoted with a superscript (0) – in the massive $U(1)$ model can be decomposed as

$$\mathcal{L}_{\text{SCET, toy}}^{(0)} = \mathcal{L}_s^{(0)} + \mathcal{L}_c^{(0)} + \mathcal{L}_{\bar{c}}^{(0)} + \mathcal{L}_{\text{int}}^{(0)}, \quad (5.37)$$

where $\mathcal{L}_{s,c,\bar{c}}^{(0)}$ are Lagrangians of the individual sectors and $\mathcal{L}_{\text{int}}^{(0)}$ are potential interaction terms between soft, collinear and anti-collinear modes. The only piece of the effective Lagrangian, which is at first sight different from the corresponding QCD terms, is the collinear (and anti-collinear) fermion Lagrangian \mathcal{L}_{ψ_c} , which after the decomposition Eq. (5.34) reads

$$\mathcal{L}_{\psi_c} = \bar{\psi}_c i \not{D}_c \psi_c = \bar{\xi}_c \frac{\not{n}}{2} i n \cdot D_c \xi_c + \bar{\xi}_c i \not{D}_{c,\perp} \eta_c + \bar{\eta}_c i \not{D}_{c,\perp} \xi_c + \bar{\eta}_c \frac{\not{\bar{n}}}{2} i \bar{n} \cdot D_c \eta_c, \quad (5.38)$$

with $i D_c^\mu = i \partial^\mu + g A_c^\mu$. Since \mathcal{L}_{ψ_c} is quadratic in the suppressed η_c components, they can be integrated out exactly from the path integral. (One can show that the resulting determinant is independent of the gauge field and has therefore no physical consequences [87].) This can be achieved by employing the equations of motion and expressing the η_c through the ξ_c components, which yields:

$$\mathcal{L}_{\psi_c} = \bar{\xi}_c \frac{\not{n}}{2} i n \cdot D_c \xi_c + \bar{\xi}_c i \not{D}_{c,\perp} \frac{1}{i \bar{n} \cdot D_c} i \not{D}_{c,\perp} \frac{\not{\bar{n}}}{2} \xi_c. \quad (5.39)$$

Note that both terms scale as $\sim \lambda^4$ and give a leading power contribution to the action, $\int d^4x \mathcal{L}_{\psi_c} \sim \lambda^0$. The gauge-boson piece in the collinear Lagrangian is simply a copy of the corresponding terms in the full Lagrangian with the replacement $A^\mu \rightarrow A_c^\mu$. The same is true for all terms in $\mathcal{L}_s^{(0)}$ (with $\psi \rightarrow \psi_s$ and $A^\mu \rightarrow A_s^\mu$). The anti-collinear Lagrangian $\mathcal{L}_{\bar{c}}^{(0)}$ can be obtained from $\mathcal{L}_c^{(0)}$ by interchanging $n \leftrightarrow \bar{n}$.

Any interaction between different modes in the effective theory would put the particles far off-shell and generate a momentum configuration that is not part of the low-energy theory. Hence, interaction terms of the kind $\psi_c \not{A}_{\bar{c}} \psi_c$ are forbidden by momentum conservation. Moreover, at leading power in λ all modes decouple completely (cf. [54, 94]). In other words, interaction terms between modes in the EFT are power-suppressed, $\mathcal{L}_{\text{int}}^{(0)} \sim \mathcal{O}(\lambda)$, and the leading power Lagrangian simply reads:

$$\mathcal{L}_{\text{SCET, toy}}^{(0)} = \mathcal{L}_s^{(0)} + \mathcal{L}_c^{(0)} + \mathcal{L}_{\bar{c}}^{(0)}, \quad (5.40)$$

with

$$\begin{aligned} \mathcal{L}_s^{(0)} &= \bar{\psi}_s i \not{D}_s \psi_s - \frac{1}{4} F_{s,\mu\nu} F_s^{\mu\nu} + \frac{m^2}{2} A_{s,\mu} A_s^\mu, \\ \mathcal{L}_c^{(0)} &= \mathcal{L}_{\psi_c} - \frac{1}{4} F_{c,\mu\nu} F_c^{\mu\nu} + \frac{m^2}{2} A_{c,\mu} A_c^\mu, \\ \mathcal{L}_{\bar{c}}^{(0)} &= \mathcal{L}_{\psi_{\bar{c}}} - \frac{1}{4} F_{\bar{c},\mu\nu} F_{\bar{c}}^{\mu\nu} + \frac{m^2}{2} A_{\bar{c},\mu} A_{\bar{c}}^\mu. \end{aligned} \quad (5.41)$$

Furthermore, in the absence of sources that create collinear particles, the collinear fermion Lagrangian is related to the full fermion Lagrangian through a Lorentz boost, and is thus nothing but a complicated rewriting in terms of the two-component spinors ξ_c . As a consequence, the collinear fermion Lagrangian – as all the other terms in $\mathcal{L}^{(0)}$ which are just copies of the full-theory Lagrangian – is exact to all orders in λ and does not require renormalisation [67].

The non-existence of interactions at leading power has profound consequences for physical observables and is the basis for deriving factorisation theorems. The non-trivial aspect is the matching of the external current onto the effective theory. In contrast to the terms in the Lagrangian, the expression of the external current in the effective theory does receive matching corrections. In general, we obtain the matching of a current onto the effective theory by writing down all possible operators with proper quantum numbers, each of which multiplied by a Wilson coefficient. In SCET, even at leading power, we have to include

- an infinite number of operators including arbitrarily high derivatives in the direction of the large momentum component (e.g. $\bar{n} \cdot \partial \xi_c \sim \lambda^0 \xi_c$), as well as
- an infinite number of terms comprised of an arbitrarily large number of gauge-field operators (e.g. $\bar{n} \cdot A_c \sim \lambda^0$).

The most general way to incorporate the first point is to allow for *non-local* operators. Field operators in SCET are smeared along the light-cone direction corresponding to the large momentum component, e.g. $\xi_c(x) \rightarrow \xi_c(x + t\bar{n})$. The matching relation is therefore in general a *convolution* of a hard (t -dependent) function with non-local operators. For the discussion of the second point let us assume for a moment that we work in an $SU(N)$ gauge theory (like QCD). Although the Lagrangian Eq. (5.1) has no gauge symmetry, the operators in the effective theory nevertheless share the structure that is dictated by gauge invariance. Just as the spatial variations of the fields in the effective theory are restricted, one has to ensure that the gauge transformations respect this scaling as well. The effective theory must be separately invariant under collinear, anti-collinear and soft gauge transformations. Since all modes decouple, the individual transformations take the standard form. For example, collinear fields transform under collinear gauge transformations as

$$\xi_c \rightarrow V_c \xi_c, \quad A_c^\mu \rightarrow V_c A_c^\mu V_c^\dagger + \frac{i}{g} V_c [\partial^\mu, V_c^\dagger], \quad (5.42)$$

where $V_c(x) = \exp(if_c^a(x)t^a)$, with the $SU(N)$ generators t^a in the fundamental representation and a function $f_c^a(x)$ with collinear scaling, $\partial^\mu f_c^a(x) \sim (1, \lambda, \lambda^2) f_c^a(x)$. The transformation of collinear fields under soft or anti-collinear gauge transformations is trivial.

A product of fields at different spacetime points is only gauge invariant if the fields are connected by *Wilson lines*: the bilinear

$$\bar{\xi}_c(x + s\bar{n})[x + s\bar{n}, x]\xi_c(x) \quad (5.43)$$

with

$$[x + s\bar{n}, x] \equiv \mathbf{P} \exp \left[ig \int_0^s ds' \bar{n} \cdot A_c(x + s'\bar{n}) \right] \quad (5.44)$$

is gauge invariant, since the Wilson line transforms under gauge transformations as

$$[x + s\bar{n}, x] \rightarrow V_c(x + s\bar{n}) [x + s\bar{n}, x] V_c^\dagger(x). \quad (5.45)$$

The \mathbf{P} -symbol in Eq. (5.44) denotes the path ordering of colour matrices in a non-abelian gauge-theory. In SCET it is convenient to work with Wilson lines that go to infinity,

$$\begin{aligned} W_c(x) &\equiv \mathbf{P} \exp \left[ig \int_{-\infty}^0 ds \bar{n} \cdot A_c(x + s\bar{n}) \right], \\ W_c(x) &\rightarrow V_c(x) W_c(x) \quad (\text{gauge transformation}). \end{aligned} \quad (5.46)$$

This definition allows us to construct gauge-invariant building blocks that greatly simplify the construction of operators in the effective theory:⁴

$$\chi_c(x) \equiv W_c^\dagger(x) \xi_c(x), \quad \text{and} \quad \bar{\chi}_c(x) \equiv \bar{\xi}_c(x) W_c(x). \quad (5.47)$$

A Wilson line along a finite segment is then given by

$$[x + s\bar{n}, x] = W_c(x + s\bar{n}) W_c^\dagger(x), \quad (5.48)$$

and the bilinear can be expressed through gauge-invariant building blocks via

$$\bar{\xi}_c(x + s\bar{n}) [x + s\bar{n}, x] \xi_c(x) = \bar{\chi}_c(x + s\bar{n}) \chi_c(x). \quad (5.49)$$

We should consider the following different types of Wilson lines for the discussion of the Sudakov form factor, which are associated to the various low-energy degrees of freedom:

$$\begin{aligned} W_c(x) &= \mathbf{P} \exp \left[ig \int_{-\infty}^0 ds \bar{n} \cdot A_c(x + s\bar{n}) \right] && (\text{collinear}), \\ W_{\bar{c}}(x) &= \mathbf{P} \exp \left[ig \int_{-\infty}^0 ds n \cdot A_{\bar{c}}(x + sn) \right] && (\text{anti-collinear}), \\ S_n(x) &= \mathbf{P} \exp \left[ig \int_{-\infty}^0 ds n \cdot A_s(x + sn) \right] && (\text{soft in } n\text{-direction}), \\ S_{\bar{n}}(x) &= \mathbf{P} \exp \left[ig \int_{-\infty}^0 ds \bar{n} \cdot A_s(x + s\bar{n}) \right] && (\text{soft in } \bar{n}\text{-direction}). \end{aligned} \quad (5.50)$$

Note that the soft mode has no preferred light-cone direction and thus both Wilson lines $S_n(x)$ and $S_{\bar{n}}(x)$ appear in the matching relation. Analogously to Eq. (5.47), we define gauge-invariant building blocks in the anti-collinear sector using the Wilson line $W_{\bar{c}}(x)$.

⁴One can as well define gauge-invariant building blocks for the gauge fields A^μ . However, they are not necessary for the discussion of the Sudakov form factor and will be introduced first in Section 6.3.

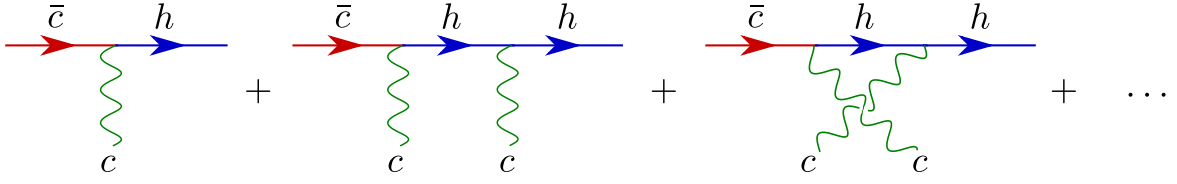


Figure 5.4: Sub-diagrams contributing to the Wilson line W_c up to $\mathcal{O}(g^2)$. At leading power an arbitrary number of $\bar{n} \cdot A_c$ gluons can be attached to the anti-collinear leg. The diagrams are to be understood as part of a multi-loop integral contributing to the Sudakov form factor, i.e. only the anti-collinear line represents an external leg.

Figure 5.4 shows the diagrammatical interpretation of a Wilson line. Replacing the fermion propagators with hard virtuality by their eikonal limit, the sub-diagrams contribute to the integrand (in the abelian theory) as a factor

$$\begin{aligned} & \frac{g \bar{n}^{\mu_1}}{k_{1,-}} + \frac{g^2 \bar{n}^{\mu_1} \bar{n}^{\mu_1}}{k_{2,-}(k_{1,-} + k_{2,-})} + \frac{g^2 \bar{n}^{\mu_1} \bar{n}^{\mu_1}}{k_{1,-}(k_{1,-} + k_{2,-})} \\ &= \frac{g \bar{n}^{\mu_1}}{k_{1,-} - i\varepsilon} + \frac{g \bar{n}^{\mu_1}}{k_{1,-} - i\varepsilon} \frac{g \bar{n}^{\mu_2}}{k_{2,-} - i\varepsilon}, \end{aligned} \quad (5.51)$$

where $k_{1,2}$ are the gauge-boson momenta and the $-i\varepsilon$ prescriptions have been omitted in the first line. Given that the argument of the exponential function in the definition of the Wilson lines is related to an inverse derivative via

$$\frac{i}{in \cdot \partial + i\varepsilon} \phi(x) = \int_{-\infty}^0 ds \phi(x + sn), \quad (5.52)$$

Eq. (5.51) exactly corresponds to the Feynman rules generated by Wilson lines (they can be found e.g. in appendix E in [87]). Note that in a non-abelian theory the path ordering reproduces the correct structure of the amplitude in colour space.

Finally, we give the matching relation of the vector current J^μ onto the effective theory. In accordance with the arguments given so far one finds a convolution of a hard function with (anti-)collinear non-local gauge-invariant building blocks of the form:⁵

$$\begin{aligned} J^\mu(x=0) &= \bar{\psi} \gamma^\mu \psi(0) \\ &\rightarrow S_n^\dagger(0) S_{\bar{n}}(0) \int ds \int dt C_V(\varepsilon; s, t) \bar{\chi}_c(s\bar{n}) \gamma_\perp^\mu \chi_{\bar{c}}(tn) + \mathcal{O}(\lambda). \end{aligned} \quad (5.53)$$

The Fourier transform of the hard coefficient function $C_V(\varepsilon; s, t)$ corresponds to hard-region integrals (the one loop expression has been calculated in Eq. (5.18)). Note that for $x \neq 0$ one needs to *multipole expand* the fields in products of different modes in order to construct a consistent power expansion [93]. This reflects the fact that momentum conservation at a vertex can be violated by a small amount.

⁵After a decoupling transformation and multipole expansion one obtains the same matching relation in SCET_I. The difference between SCET_I and SCET_{II} is described in Section 6.1.

Another symmetry of SCET that helps constructing operators in the effective theory is *reparametrisation invariance* (RPI). RPI arises because we introduced two reference vectors n and \bar{n} , whose choice is not unique. As a remnant of Lorentz symmetry, there is a set of transformations acting on n and \bar{n} under which the effective theory is invariant. Relevant for leading-power discussions is the RPI transformation of type three (RPI_{III}), which corresponds to a rescaling of the reference vectors, i.e. a boost along the z -axis: $n \rightarrow \hat{n} = a \cdot n$ and $\bar{n} \rightarrow \hat{\bar{n}} = a^{-1} \cdot \bar{n}$, with $a \sim \lambda^0$. Then the relations $\hat{n}^2 = \hat{\bar{n}}^2 = 0$ and $\hat{n} \cdot \hat{\bar{n}} = 2$ are still fulfilled. RPI_I and RPI_{II} transformations describe a small rotation of the reference vectors and become relevant for the investigation of power corrections. Details are not relevant for the remainder of this thesis and we again refer to [87].

We should now ask the question whether the matching relation (5.53) remains true in the presence of analytic regularisation. In fact, the ad-hoc analytic regulator that we introduced in the one-loop calculation spoils all the symmetries that underly the matching relation. Raising powers of certain propagators in loop integrals spoils the exponentiation of eikonal propagators to Wilson lines and therefore (in a gauge theory) spoils the gauge invariance of individual sectors. Only after adding up all contributions overall gauge invariance is restored. Fortunately, at least in covariant gauges, gauge invariance in each individual sector can be restored. This has been argued in [95] by implementing a regulator in the exponent of the Wilson line, thus preserving (non-abelian) exponentiation. To discuss this in depth requires to introduce concepts that go beyond the objective of this thesis. For more details we refer to [95] and [87]. At one-loop level, however, our ad-hoc regulator is sufficient to treat endpoint divergences consistently. Note that in case of the Sudakov form factor all rapidity divergences come from Wilson-line propagators, which does not necessarily remain true for more complicated observables. Boost invariance, on the other hand, must be broken in the individual sectors as soon as we encounter endpoint divergences. Modes with equal virtuality can be interchanged by a Lorentz boost and dimensional regularisation is not sufficient to distinguish between these modes. Analytic regularisation must differentiate between the relative rapidities of the collinear and the anti-collinear mode and boost invariance is restored only after summing up all sectors.

5.4 Factorisation and Resummation

We now investigate the Sudakov form factor in the effective theory and derive a leading-power factorisation theorem. Taking the desired matrix element of the matching relation Eq. (5.53) yields

$$\begin{aligned}
 & \langle f(p_c) | J^\mu(0) | f(p_{\bar{c}}) \rangle \\
 & \rightarrow (\gamma_\perp^\mu)_{\alpha\beta} \langle 0 | S_n^\dagger(0) S_{\bar{n}}(0) | 0 \rangle \int ds \int dt C_V(\varepsilon; s, t) \langle f(p_c) | \bar{\chi}_c^\alpha(s\bar{n}) | 0 \rangle \langle 0 | \chi_{\bar{c}}^\beta(tn) | f(p_{\bar{c}}) \rangle \\
 & = (\gamma_\perp^\mu)_{\alpha\beta} \tilde{C}_V(\varepsilon, Q^2) \langle 0 | S_n^\dagger S_{\bar{n}} | 0 \rangle \langle f(p_c) | \bar{\chi}_c^\alpha | 0 \rangle \langle 0 | \chi_{\bar{c}}^\beta | f(p_{\bar{c}}) \rangle. \tag{5.54}
 \end{aligned}$$

Here we used spacetime translations to get rid of the convolution integrals. In the last line all fields live at the spacetime point $x = 0$. The Fourier transform of the hard

matching coefficient is given by

$$\tilde{C}_V(\varepsilon, Q^2 = p_{c-} p_{\bar{c}+}) = \int ds \int dt C_V(\varepsilon; s, t) e^{isp_{c-}} e^{-itp_{\bar{c}+}}. \quad (5.55)$$

Note that we are still dealing with bare quantities and the renormalisation will be undertaken later in this section.

When introducing the rapidity regulator in the variable k_- , we found that the soft region gives a scaleless contribution at one loop. Assuming that this is true to all orders, we can set $\langle 0 | S_n^\dagger S_{\bar{n}} | 0 \rangle \equiv 1$. Separating the Dirac structure in Eq. (5.54) via $\langle f(p_c) | \bar{\chi}_c^\alpha | 0 \rangle \equiv \bar{u}_f^\alpha(p_c) J_c$ (and similarly for $c \leftrightarrow \bar{c}$), with a collinear function J_c , we find the *naive factorisation formula* for the form factor $\mathcal{F}(Q^2)$ at leading power in λ :

$$\mathcal{F}(Q^2) = \tilde{C}_V(\varepsilon, Q^2) J_c(\delta, L_{\nu, Q}; \varepsilon, m^2) J_{\bar{c}}(\delta, L_{\nu, Q, m^2}; \varepsilon, m^2). \quad (5.56)$$

We call this equation a “naive” factorisation formula because it still depends on the artificial rapidity regulator ν . We achieved a factorisation of the form factor into a product of a hard matching coefficient and two collinear functions. In the one-loop perturbative expansion these functions correspond to the various regions that have been computed in Section 5.2.

Since the physical form factor $\mathcal{F}(Q^2)$ is independent of the artificial scale ν , the following differential equation needs to be fulfilled:

$$\frac{d}{d \log \nu} \left[J_c(\delta, L_{\nu, Q}; \varepsilon, m^2) J_{\bar{c}}(\delta, L_{\nu, Q, m^2}; \varepsilon, m^2) \right] = 0. \quad (5.57)$$

One can show in various ways that the solution to this equation is a simple exponential (cf. [83, 96]). For example, if we expand around $\delta \rightarrow 0$, we can write the two collinear functions as a Taylor series in their logarithms in ν as follows:

$$J_c = \sum_{n=0}^{\infty} J_c^{(n)} \log^n \frac{\nu}{Q} \quad \text{and} \quad J_{\bar{c}} = \sum_{m=0}^{\infty} J_{\bar{c}}^{(m)} \log^m \frac{\nu Q}{m^2}, \quad (5.58)$$

where we omitted the arguments for readability, $J_{c, \bar{c}}^{(n)} = J_{c, \bar{c}}^{(n)}(\delta; \varepsilon, m^2)$. Then Eq. (5.57) leads to the following recursion relation

$$n \frac{J_c^{(n)}}{J_c^{(n-1)}} + m \frac{J_{\bar{c}}^{(m)}}{J_{\bar{c}}^{(m-1)}} = 0, \quad \forall n, m \geq 1. \quad (5.59)$$

Note that we did not perform a perturbative expansion in α . The integers n and m can be chosen independently and the system can be solved by fixing three coefficients, e.g. $J_c^{(0)}$, $J_{\bar{c}}^{(0)}$ and $J_c^{(1)}$:

$$J_c = J_c^{(0)} \left(\frac{\nu}{Q} \right)^{J_c^{(1)}/J_c^{(0)}}, \quad \text{and} \quad J_{\bar{c}} = J_{\bar{c}}^{(0)} \left(\frac{\nu Q}{m^2} \right)^{-J_{\bar{c}}^{(1)}/J_{\bar{c}}^{(0)}}, \quad (5.60)$$

so that

$$J_c J_{\bar{c}} = J_c^{(0)} J_{\bar{c}}^{(0)} \left(\frac{Q^2}{m^2} \right)^{-J_{\bar{c}}^{(1)}/J_c^{(0)}}. \quad (5.61)$$

The regulator δ must drop out as well, which means it has to cancel in the exponent $J_c^{(1)}(\delta)/J_c^{(0)}(\delta)$ and the prefactor $J_c^{(0)}(\delta) J_{\bar{c}}^{(0)}(\delta)$ separately. Conventionally, these quantities are called the *collinear anomaly* F [96],

$$\frac{J_c^{(1)}(\delta; \varepsilon, m^2)}{J_c^{(0)}(\delta; \varepsilon, m^2)} \equiv F(\varepsilon, m^2), \quad (5.62)$$

and the *remainder function* R ,

$$J_c^{(0)}(\delta; \varepsilon, m^2) J_{\bar{c}}^{(0)}(\delta; \varepsilon, m^2) \equiv R(\varepsilon, m^2). \quad (5.63)$$

Given the explicit calculation from Section 5.2, we find

$$\begin{aligned} F(\varepsilon, m^2) &= \frac{\alpha(\mu)}{4\pi} \left[\frac{2}{\varepsilon} + 4 \log \frac{\mu}{m} \right] + \mathcal{O}(\alpha^2), \\ R(\varepsilon, m^2) &= 1 + \frac{\alpha(\mu)}{4\pi} \left[\frac{2}{\varepsilon^2} + \frac{4}{\varepsilon} \log \frac{\mu}{m} + 4 \log^2 \frac{\mu}{m} + \frac{4}{\varepsilon} + 8 \log \frac{\mu}{m} + 4 - \frac{5\pi^2}{6} \right] + \mathcal{O}(\alpha^2). \end{aligned} \quad (5.64)$$

The factorisation formula for $\mathcal{F}(Q^2)$ now takes the form:

$$\mathcal{F}(Q^2) = \tilde{C}_V(\varepsilon, Q^2) R(\varepsilon, m^2) \left(\frac{Q^2}{m^2} \right)^{-F(\varepsilon, m^2)}. \quad (5.65)$$

Note that this result does not change when we use a different regularisation prescription implying a soft region that might not be scaleless. In that case the soft region contributes to the low-energy functions R and F . The differential equation (5.57) can also be interpreted as a renormalisation group equation in ν . By solving this equation we effectively reorganised the perturbative expansion and achieved a resummation of large logarithms that arise from the large rapidity separation between the two collinear modes. On the other hand, the low-energy modes are no longer factorised. We rather combined modes with equal virtuality $\mu_s \sim m$ into the anomaly exponent and the remainder function.

Resummation by RG evolution: The functions \tilde{C}_V , R and F in Eq. (5.65) still contain large logarithms for any fixed value of μ . A resummation of these large logarithms can be achieved by standard renormalisation group evolution.

We introduce a multiplicative Z -factor for the hard matching coefficient that absorbs all divergences in ε :

$$\tilde{C}_V(Q^2, \mu) = Z_h^{-1}(\varepsilon, Q^2, \mu) \tilde{C}_V^{\text{bare}}(\varepsilon, Q^2), \quad (5.66)$$

with

$$Z_h(\varepsilon, Q^2, \mu) = 1 + \frac{\alpha(\mu)}{4\pi} \left(-\frac{2}{\varepsilon^2} - \frac{2}{\varepsilon} \log \frac{\mu^2}{Q^2} - \frac{3}{\varepsilon} \right) + \mathcal{O}(\alpha^2). \quad (5.67)$$

The renormalised matching coefficient reads

$$\tilde{C}_V(Q^2, \mu) = 1 + \frac{\alpha(\mu)}{4\pi} \left(-\log^2 \frac{\mu^2}{Q^2} - 3 \log \frac{\mu^2}{Q^2} + \frac{\pi^2}{6} - 8 \right) + \mathcal{O}(\alpha^2), \quad (5.68)$$

and obeys the following renormalisation group equation (RGE) to all orders in perturbation theory:

$$\begin{aligned} \frac{d\tilde{C}_V(Q^2, \mu)}{d \log \mu} &= -\frac{d \log Z_h(\varepsilon, Q^2, \mu)}{d \log \mu} \tilde{C}_V(Q^2, \mu) \\ &= \left(-\gamma_{\text{cusp}}(\alpha) \log \frac{\mu^2}{Q^2} + \gamma_V(\alpha) \right) \tilde{C}_V(Q^2, \mu). \end{aligned} \quad (5.69)$$

The explicit dependence of the anomalous dimension on $\log \mu$ is characteristic for quantities involving Sudakov double logarithms. Here γ_{cusp} is the universal *cusp anomalous dimension* that describes the renormalisation of Wilson lines with a cusp [97–99]. At one-loop accuracy the two terms in the anomalous dimension are given by

$$\gamma_{\text{cusp}}(\alpha) = 4 \frac{\alpha(\mu)}{4\pi} + \mathcal{O}(\alpha^2) \quad \text{and} \quad \gamma_V(\alpha) = -6 \frac{\alpha(\mu)}{4\pi} + \mathcal{O}(\alpha^2). \quad (5.70)$$

Similarly one can show that the remainder function R obeys an analogous RGE,

$$\frac{dR(m^2, \mu)}{d \log \mu} = \left(\gamma_{\text{cusp}}(\alpha) \log \frac{\mu^2}{m^2} - \gamma_V(\alpha) \right) R(m^2, \mu), \quad (5.71)$$

whereas the equation that governs the running in μ of the anomaly coefficient F looks quite simple (for more details see Appendix B.2):

$$\frac{dF(m^2, \mu)}{d \log \mu} = \gamma_{\text{cusp}}(\alpha). \quad (5.72)$$

Using Eqs. (5.69), (5.71) and (5.72), it is now easy to verify that the physical form factor is independent of μ :

$$\frac{d \log \mathcal{F}(Q^2)}{d \log \mu} = \frac{d}{d \log \mu} \left(\log \tilde{C}_V(Q^2, \mu) + \log R(m^2, \mu) - \log \frac{Q^2}{m^2} F(m^2, \mu) \right) = 0. \quad (5.73)$$

The solutions of the various RGEs can be written as:

$$\begin{aligned} \tilde{C}_V(Q^2, \mu) &= e^{2S(\mu_h, \mu) - A_{\gamma_V}(\mu_h, \mu)} \left(\frac{Q^2}{\mu_h^2} \right)^{-A_{\gamma_{\text{cusp}}}(\mu_h, \mu)} \tilde{C}_V(Q^2, \mu_h), \\ R(m^2, \mu) &= e^{-2S(\mu_s, \mu) + A_{\gamma_V}(\mu_s, \mu)} \left(\frac{\mu_s^2}{m^2} \right)^{-A_{\gamma_{\text{cusp}}}(\mu_s, \mu)} R(m^2, \mu_s), \\ F(m^2, \mu) &= F(m^2, \mu_s) - A_{\gamma_{\text{cusp}}}(\mu_s, \mu). \end{aligned} \quad (5.74)$$

Here we adopt the notation of [87] for the various evolution kernels:

$$\begin{aligned} S(\mu_1, \mu_2) &= -\int_{\alpha(\mu_1)}^{\alpha(\mu_2)} d\alpha \frac{\gamma_{\text{cusp}}(\alpha)}{\beta(\alpha)} \int_{\alpha(\mu_1)}^{\alpha} \frac{d\alpha'}{\beta(\alpha')}, \\ A_{\gamma_i}(\mu_1, \mu_2) &= -\int_{\alpha(\mu_1)}^{\alpha(\mu_2)} d\alpha \frac{\gamma_i(\alpha)}{\beta(\alpha)}, \quad (i = V, \text{cusp}). \end{aligned} \quad (5.75)$$

The functions \tilde{C}_V , R and F are evaluated in the vicinity of their natural scales and do no longer contain large logarithms, which are resummed by the evolution kernels. With $d \log \mu = d\alpha/\beta(\alpha)$ one can easily verify the following useful identities:

$$\begin{aligned} \frac{d}{d \log \mu} S(\tilde{\mu}, \mu) &= -\gamma_{\text{cusp}}(\alpha(\mu)) \log \frac{\mu}{\tilde{\mu}}, \\ \frac{d}{d \log \mu} A_{\gamma_i}(\tilde{\mu}, \mu) &= -\gamma_i(\alpha(\mu)), \end{aligned} \quad (5.76)$$

and

$$\begin{aligned} S(\mu_1, \mu_2) + S(\mu_2, \mu_3) &= S(\mu_1, \mu_3) + A_{\gamma_{\text{cusp}}}(\mu_2, \mu_3) \log \frac{\mu_1}{\mu_2}, \\ A_{\gamma_i}(\mu_1, \mu_2) + A_{\gamma_i}(\mu_2, \mu_3) &= A_{\gamma_i}(\mu_1, \mu_3). \end{aligned} \quad (5.77)$$

More details and explicit expressions for the evolution kernels can be found in Appendix B.1.

Putting everything together, we obtain the final μ -independent result for the resummed form factor:

$$\begin{aligned} &\mathcal{F}^{\text{res.}}(Q^2) \\ &= \tilde{C}_V(Q^2, \mu_h) R(m^2, \mu_s) \left(\frac{Q^2}{m^2} \right)^{-F(m^2, \mu_s)} e^{2S(\mu_h, \mu_s) - A_{\gamma_V}(\mu_h, \mu_s)} \left(\frac{Q^2}{\mu_h^2} \right)^{-A_{\gamma_{\text{cusp}}}(\mu_h, \mu_s)}. \end{aligned} \quad (5.78)$$

With the expressions given in Eq. (B.3), we can re-expand this result in fixed-order perturbation theory. Setting $\mu_h = Q$ and $\mu_s = m$ to their natural values, we indeed find the correct fixed-order one-loop result given in the second line of Eq. (5.8).

In general, large logarithms of the following form are resummed by the evolution kernels:

$$\frac{1}{\alpha} g_1(\alpha L) + g_2(\alpha L) + \alpha g_3(\alpha L) + \mathcal{O}(\alpha^2), \quad (5.79)$$

with $\alpha = \alpha(\mu_h)$ and L being a large logarithm, thus $\alpha L \sim \mathcal{O}(1)$. The approximation where only the first term $\sim g_1$ is kept is called resummation of leading logarithms (LL), or leading logarithmic approximation. Including contributions $\sim g_2$ is called next-to-leading logarithmic (NLL) approximation, etc. Investigating the expressions of the evolution kernels given in Eq. (B.2), we find that in the Sudakov form factor only $S(\mu_h, \mu_s)$ contributes to LL order. Evaluating the hard matching coefficient C_V as well as the remainder function R at tree-level, the Sudakov form factor at LL approximation is then simply given by the exponential Sudakov factor, $\mathcal{F}^{\text{res.}}(Q^2) \simeq e^{2S(\mu_h, \mu_s)}$ (where for consistency we should also drop the subleading terms in $S(\mu_h, \mu_s)$).

The rapidity renormalisation group: In the preceding discussion, we argued that the rapidity scale ν has to drop out in the product of the two collinear functions. Solving the resultant differential equation leads to an exponentiation of a subset of large logarithms. Thereafter, we discussed standard RG evolution to resum the remaining large logarithms in μ and finally obtained the result Eq. (5.78). Chiu, Jain, Neill and Rothstein proposed

an alternative strategy to deal with endpoint divergences; the *rapidity renormalisation group* (RRG) [95]. Within this approach all divergences in δ and ε are treated in a common Z -factor leading to evolution equations in μ and ν . Using the RRG, we obtain an expression for the resummed form factor that is equivalent to Eq. (5.78).

Let us recapitulate the naive factorisation formula Eq. (5.56). Now we would like to consider the two collinear functions as bare quantities that are μ and ν independent:

$$\begin{aligned} J_c(\delta, L_{\nu, Q}; \varepsilon, m^2) &\rightarrow J_c(\delta, Q; \varepsilon, m^2), \\ J_{\bar{c}}(\delta, L_{\nu, Q, m^2}; \varepsilon, m^2) &\rightarrow J_{\bar{c}}(\delta, m^2/Q; \varepsilon, m^2). \end{aligned} \quad (5.80)$$

To this end, just like in dimensional regularisation where $\alpha(\mu) \mu^{2\varepsilon} \sim \alpha_0$, we introduce a bare dimensionful “coupling” parameter w_0 for each power of $1/k_-^2$:

$$w_0 = w(\nu) \nu^\delta, \quad \text{with} \quad \frac{dw(\nu)}{d \log \nu} = -\delta w(\nu). \quad (5.81)$$

In contrast to $\frac{d\alpha(\mu)}{d \log \mu} = -2\varepsilon\alpha + \mathcal{O}(\alpha^2)$, the above relation is exact. The renormalised parameter $w(\nu)$ does not absorb any divergences, $Z_w \equiv 1$, and hence, the “ β -function” vanishes (for $\delta \rightarrow 0$). In fact, $w(\nu)$ has no physical meaning and is only a book-keeping parameter that eventually will be sent to $w(\nu) \rightarrow 1$ after the RGEs have been derived.

We now study the rapidity renormalisation group evolution of the various objects in the naive factorisation formula. The hard matching coefficient does not suffer from endpoint divergences and therefore has no evolution in ν . The μ -evolution is still given by Eq. (5.74). For the two collinear functions we write

$$\begin{aligned} J_c(Q, \nu; m^2, \mu) &= Z_c^{-1}(\delta, Q, \nu; \varepsilon, m^2, \mu) \sqrt{Z_2(\varepsilon, m^2)} J_c^{\text{bare}}(\delta, Q; \varepsilon, m^2), \\ J_{\bar{c}}(m^2/Q, \nu; m^2, \mu) &= Z_{\bar{c}}^{-1}(\delta, m^2/Q, \nu; \varepsilon, m^2, \mu) \sqrt{Z_2(\varepsilon, m^2)} J_{\bar{c}}^{\text{bare}}(\delta, m^2/Q; \varepsilon, m^2), \end{aligned} \quad (5.82)$$

with the wave-function renormalisation factor Z_2 given in Eq. (5.7). In addition to ε and μ , the Z -factors now depend on δ and ν as well. At leading non-trivial order in the perturbative expansion we find:

$$\begin{aligned} Z_c &= 1 + \frac{\alpha(\mu) w(\nu)}{4\pi} \left[\frac{2}{\delta\varepsilon} + \frac{4}{\delta} \log \frac{\mu}{m} + \frac{2}{\varepsilon} \log \frac{\nu}{Q} + \frac{3}{2\varepsilon} \right], \\ Z_{\bar{c}} &= 1 + \frac{\alpha(\mu) w(\nu)}{4\pi} \left[-\frac{2}{\delta\varepsilon} - \frac{4}{\delta} \log \frac{\mu}{m} - \frac{2}{\varepsilon} \log \frac{\nu Q}{m^2} + \frac{2}{\varepsilon^2} + \frac{4}{\varepsilon} \log \frac{\mu}{m} + \frac{3}{2\varepsilon} \right], \end{aligned} \quad (5.83)$$

for the Z -factors, and

$$\begin{aligned} J_c(Q, \nu; m^2, \mu) &= 1 + \frac{\alpha(\mu) w(\nu)}{4\pi} \left[4 \log \frac{\mu}{m} \log \frac{\nu}{Q} + 3 \log \frac{\mu}{m} + \frac{9}{4} - \frac{\pi^2}{3} \right], \\ J_{\bar{c}}(m^2/Q, \nu; m^2, \mu) &= 1 + \frac{\alpha(\mu) w(\nu)}{4\pi} \left[-4 \log \frac{\mu}{m} \log \frac{\nu Q}{m^2} + 4 \log^2 \frac{\mu}{m} + 3 \log \frac{\mu}{m} + \frac{9}{4} - \frac{\pi^2}{2} \right], \end{aligned} \quad (5.84)$$

for the renormalised collinear functions. The latter now obey RGEs in μ and ν :

$$\frac{dJ_{c, \bar{c}}}{d \log \{\mu, \nu\}} = -\gamma_{c, \bar{c}}^{\{\mu, \nu\}} J_{c, \bar{c}}. \quad (5.85)$$

We find for the anomalous dimensions in μ :

$$\begin{aligned}\gamma_c^{\{\mu\}} &= -\gamma_{\text{cusp}}(\alpha) \log \frac{\nu}{Q} + \frac{\gamma_V(\alpha)}{2}, \\ \gamma_{\bar{c}}^{\{\mu\}} &= -\gamma_{\text{cusp}}(\alpha) \log \frac{\mu^2}{m^2} + \gamma_{\text{cusp}}(\alpha) \log \frac{\nu Q}{m^2} + \frac{\gamma_V(\alpha)}{2},\end{aligned}\quad (5.86)$$

which ensures the μ -independence of the form factor, $\gamma_c^{\{\mu\}} + \gamma_{\bar{c}}^{\{\mu\}} + \gamma_h^{\{\mu\}} = 0$, where $\gamma_h^{\{\mu\}}$ can be read off from Eq. (5.69). Demanding that all functions under consideration are smooth enough, so that

$$\left[\frac{d}{d \log \nu}, \frac{d}{d \log \mu} \right] = 0, \quad (5.87)$$

imposes the following condition on the anomalous dimensions:

$$\mp \gamma_{\text{cusp}} = \frac{d\gamma_{c,\bar{c}}^{\{\mu\}}}{d \log \nu} = \frac{d\gamma_{c,\bar{c}}^{\{\nu\}}}{d \log \mu}, \quad (5.88)$$

where the minus sign is true for γ_c and the plus sign for $\gamma_{\bar{c}}$. Integration gives (use Eq. (5.76)):

$$\gamma_c^{\{\nu\}} = -\gamma_{\bar{c}}^{\{\nu\}} = A_{\gamma_{\text{cusp}}}(\mu_s, \mu) - F(\mu_s), \quad (5.89)$$

where at this point $F(\mu_s)$ is an integration constant that lives at the soft scale μ_s and is to be determined from the fixed-order calculation. (Note that the one-loop result for F gives zero at $\mu_s = m$.) Note that in the previous step we already performed a resummation of potentially large logarithms $\alpha^i(\mu) \log^j \frac{\mu}{m}$ (with $j \leq i$) to determine the all-order structure of the RGE. A detailed discussion of this peculiarity can be found in [95].

The evolution in ν is governed by simple RGEs that have the following solutions:

$$\begin{aligned}J_c(Q, \nu; m^2, \mu) &= \left(\frac{\nu}{\nu_c} \right)^{-A_{\gamma_{\text{cusp}}}(\mu_s, \mu) + F(\mu_s)} J_c(Q, \nu_c; m^2, \mu), \\ J_{\bar{c}}(m^2/Q, \nu; m^2, \mu) &= \left(\frac{\nu}{\nu_{\bar{c}}} \right)^{A_{\gamma_{\text{cusp}}}(\mu_s, \mu) - F(\mu_s)} J_{\bar{c}}(m^2/Q, \nu_{\bar{c}}; m^2, \mu).\end{aligned}\quad (5.90)$$

Here $\nu_c \sim Q$ and $\nu_{\bar{c}} \sim m^2/Q$ are the natural rapidity scales of the collinear and the anti-collinear region (when we use $1/k_-^\delta$ as an analytic regulator), so that $J_c(Q, \nu_c; m^2, \mu)$ and $J_{\bar{c}}(m^2/Q, \nu_{\bar{c}}; m^2, \mu)$ do not contain any large logarithms in ν . The solutions of the RGEs in μ read:

$$\begin{aligned}J_c(Q, \nu; m^2, \mu) &= \exp \left(\frac{1}{2} A_{\gamma_V}(\mu_s, \mu) - A_{\gamma_{\text{cusp}}}(\mu_s, \mu) \log \frac{\nu}{Q} \right) J_c(Q, \nu; m^2, \mu_s), \\ J_{\bar{c}}(m^2/Q, \nu; m^2, \mu) &= \exp \left(\frac{1}{2} A_{\gamma_V}(\mu_s, \mu) + A_{\gamma_{\text{cusp}}}(\mu_s, \mu) \log \frac{\nu Q}{m^2} \right) \\ &\quad \times \exp \left(-2 S(\mu_s, \mu) - A_{\gamma_{\text{cusp}}}(\mu_s, \mu) \log \frac{\mu_s^2}{m^2} \right) J_{\bar{c}}(m^2/Q, \nu; m^2, \mu_s).\end{aligned}\quad (5.91)$$

Since the evolutions in μ and ν commute as long as we use the resummed anomalous dimensions Eq. (5.89), we can for example take Eq. (5.90) to run the functions to their natural scales in ν , and subsequently use Eq. (5.91) to perform the running in μ .

Finally, we find the following expression for the resummed form factor:

$$\begin{aligned} \mathcal{F}^{\text{res.}}(Q^2) &= \tilde{C}_V(Q^2, \mu_h) J_c(Q, \nu_c; m^2, \mu_s) J_{\bar{c}}(m^2/Q, \nu_{\bar{c}}; m^2, \mu_s) \left(\frac{\nu_c}{\nu_{\bar{c}}}\right)^{-F(\mu_s)} \\ &\times e^{2S(\mu_h, \mu_s) - A_{\gamma_V}(\mu_h, \mu_s)} \left(\frac{Q^2}{\mu_h^2}\right)^{-A_{\gamma_{\text{cusp}}}(\mu_h, \mu_s)}, \end{aligned} \quad (5.92)$$

which is to be compared with the result in Eq. (5.78), derived from the collinear anomaly argument. The hard matching coefficient \tilde{C}_V as well as the evolution kernels in μ are exactly the same in both results. The difference is that the remaining pieces now depend on the choice of the scales ν_c and $\nu_{\bar{c}}$, whereas these were exactly fixed at their natural values in the previous treatment. However, setting $\nu_c = Q$ and $\nu_{\bar{c}} = m^2/Q$, we find a one-to-one correspondence between the two results. The integration constant that appeared in Eq. (5.89) is exactly the anomaly exponent, which justifies our label $F(\mu_s)$, and the remainder function R is the product of the two renormalised collinear functions, evaluated at their natural scales. In the RRG formalism, the variation in $\nu_{c,\bar{c}}$ is tantamount to shuffling subleading logarithms in or out of the collinear functions $J_{c,\bar{c}} = J_{c,\bar{c}}(\nu_{c,\bar{c}})$. Hence, a variation in the residual scale dependence (in μ and ν) can be used to estimate the theoretical uncertainty.

In conclusion, we found that both languages of the collinear anomaly on the one hand and the rapidity renormalisation group on the other hand give identical results when the rapidity scales are set to their natural values. For more complicated observables, however, the RRG treatment is more transparent. We will thus use this language in the following chapter.

Chapter 6

Factorisation of Heavy-to-Light Form Factors at Large Recoil

This chapter is dedicated to derive the naive factorisation formula for the soft $B \rightarrow \pi$ form factor ξ_π . Similar to the discussion of the Sudakov form factor, “naive” refers to a factorised expression that still suffers from endpoint divergences. After a short discussion about the relevant QCD modes in the problem, we investigate the matching onto the effective theory SCET_{II}. In particular, we calculate the tree-level hard-collinear matching coefficients as well as a subset of one-loop corrections relevant for the resummation of leading logarithms in the model that will be discussed in Chapter 7. To this end, we have to consider non-zero quark masses. This complicates the factorisation structure compared to the massless case that already has been discussed in the literature [100,101]. However, all results presented in this section are model independent.

6.1 Preliminary Discussion

We consider charmless semileptonic $B \rightarrow \pi \ell \nu$ transitions in the kinematic region where the pion and the lepton pair recoil against each other with large energies of the order of the B -meson mass, $E_\pi \lesssim M_B/2 \sim \mathcal{O}(M_B)$ in the B -meson rest frame. In this situation we expect HQET and SCET to be the proper EFTs of QCD that allow us to expand the form factors in the small ratios Λ/M_B and Λ/E_π . We define the expansion parameter λ through $\lambda^2 = \Lambda/M_B$.¹

The construction of the desired effective theory goes mainly along the same lines as discussed in Section 5.3. As a starting point let us review the relevant modes that contribute to the form factors at leading power. Without loss of generality we consider the decay in the B -meson rest frame and choose the (positive) z -axis along the flight direction of the light energetic meson. The reference vectors n and \bar{n} are then defined as in Eq. (5.10). The relevant scales are:

- In the presence of the heavy b quark a perturbative *hard* mode with the scaling $(1, 1, 1) M_B$ and virtuality $\mu_h \sim M_B \gg \Lambda$ contributes.

¹In [54] it has been argued that power corrections to heavy-to-light form factors contribute at $\mathcal{O}(\lambda^2)$ and not at $\mathcal{O}(\lambda)$.

	Sudakov form factor ($\lambda = m/Q$)	Heavy-to-light form factors ($\lambda^2 = \Lambda/M_B$)
hard	$(1, 1, 1) Q$	$(1, 1, 1) M_B$
hard-collinear	–	$(1, \lambda, \lambda^2) M_B$
collinear	$(1, \lambda, \lambda^2) Q$	$(1, \lambda^2, \lambda^4) M_B$
soft	$(\lambda, \lambda, \lambda) Q$	$(\lambda^2, \lambda^2, \lambda^2) M_B$
anti-collinear	$(\lambda^2, \lambda, 1) Q$	–

Table 6.1: Scaling of the various modes and their terminology in the Sudakov problem and for heavy-to-light transitions.

- In the B -meson rest frame the light partons fluctuate isotropically with typical energies of order Λ . Hence, we define a non-perturbative *soft* mode with the scaling $(\lambda^2, \lambda^2, \lambda^2) M_B$ and virtuality $\mu_s \sim \lambda^2 M_B$.
- The partons of the energetic final-state meson are boosted and have large energies of $\mathcal{O}(M_B)$ in the n -direction. Since the virtuality of the partons is again $\mu_s \sim \lambda^2 M_B$, the non-perturbative *collinear* mode scales as $(1, \lambda^2, \lambda^4) M_B$.
- Momenta exchanged between soft and collinear partons have *hard-collinear* scaling $(1, \lambda, \lambda^2) M_B$. Their virtuality $\mu_{hc} \sim \lambda M_B = \sqrt{\Lambda M_B} \lesssim 2 \text{ GeV} \gg \Lambda$ is still considered to be in the perturbative regime.

All modes that contribute to heavy-to-light form factors as well as to the Sudakov form factor are summarised in Table 6.1.

Due to the perturbativity of the hard and the hard-collinear mode we aim at an effective theory comprising soft and collinear modes only, both of which have equal invariant mass. The matching of the form factors onto the effective theory can be achieved in two steps. First, we integrate out hard modes and match onto an intermediate effective theory with soft, collinear and hard-collinear modes, called SCET_I. Second, hard-collinear modes are integrated out and the form factors are matched onto the final effective theory with soft and collinear modes only; SCET_{II} (see also Fig. 6.1).

We are not aiming at a detailed discussion of SCET_I at this point. A main difference between the two versions of SCET is that even the leading-power SCET_I Lagrangian contains interaction terms, since soft particles can couple to hard-collinear particles without carrying them off-shell. The relevant leading-power SCET_{II} Lagrangian [54], however, is very similar to what has been discussed in Section 5.3, Eqs. (5.39) and (5.41). We have

$$\mathcal{L}_{\text{SCET}_{\text{II}}}^{(0)} = \mathcal{L}_s + \mathcal{L}_c, \quad (6.1)$$

with

$$\begin{aligned}\mathcal{L}_s &= -\frac{1}{2} \text{tr} (G_{\mu\nu,s} G_s^{\mu\nu}) + \bar{q}_s (i\not{D}_s - m) q_s + \mathcal{L}_{\text{HQET}}, \\ \mathcal{L}_c &= -\frac{1}{2} \text{tr} (G_{\mu\nu,c} G_c^{\mu\nu}) + \bar{\xi}_c \left(in \cdot D_c + (i\not{D}_{c,\perp} - m) \frac{1}{i\bar{n} \cdot D_c} (i\not{D}_{c,\perp} + m) \right) \not{n} \xi_c.\end{aligned}\quad (6.2)$$

Here $m \sim \lambda^2 M_B$ is a (small) fermion mass and $\mathcal{L}_{\text{HQET}} = \bar{h}_v i v \cdot D_s h_v$ is the leading-power HQET Lagrangian (see example 2 in Section 1.2). The four-velocity of the B meson can be expressed through the light-cone vectors via $v^\mu = \frac{1}{2}(n^\mu + \bar{n}^\mu) = (1, 0, 0, 0)$. Furthermore, $G_{\mu\nu} = G_{\mu\nu}^A t^A = \frac{i}{g_s} [D_\mu, D_\nu]$ is the usual field-strength tensor of QCD with the covariant derivative $iD_\mu = i\partial_\mu + g_s A_\mu = i\partial_\mu + g_s A_\mu^A t^A$, which are both simply copied onto the soft and the collinear sector.

By momentum conservation, insertions of soft-collinear interaction terms from the subleading SCET_{II} Lagrangian have vanishing hadronic $\langle \text{light-meson} | \dots | B \rangle$ matrix elements. Hence, all soft-collinear interactions relevant to heavy-to-light form factors originate only from the effective currents. The matching of the external currents onto SCET_{II} has been worked out for tree-level hard-collinear exchanges in [54, 100]. This study reveals that the leading contribution with non-vanishing $\langle \pi | J_{\text{eff}} | B \rangle$ matrix element arises for $J_{\text{eff}} \sim \lambda^8 M_B^3$. Thus, taking into account the scaling of the external states, $|B\rangle \sim \lambda^{-3}/M_B$ and $|P\rangle \sim \lambda^{-2}/M_B$, heavy-to-light form factors at large recoil scale like

$$\langle \pi | J_{\text{eff}} | B \rangle \sim \lambda^3 M_B = M_B \left(\frac{\Lambda}{M_B} \right)^{3/2}. \quad (6.3)$$

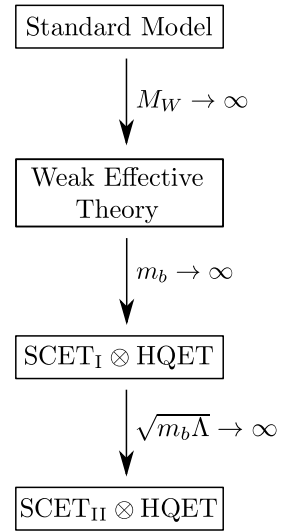


Figure 6.1: Scales relevant to heavy-to-light transitions and the respective EFT pattern.

Endpoint divergences in SCET_I vs. SCET_{II}: Before we investigate the factorisation of heavy-to-light form factors let us shortly discuss in which theories endpoint divergences can emerge. They are defined as divergences that arise from momentum regions where the ratio k_+/k_- (or k_-/k_+) diverges but the invariant mass k^2 is fixed. As rapidity divergences do not appear in the full theory they can be considered as an artefact of factorisation and have to cancel between the various EFT modes that lie on the same invariant-mass hyperbola [95]. Moreover, they are neither of UV nor of IR origin, since they always arise from a limit where e.g. $k_+ \rightarrow \infty$ with fixed invariant mass k^2 , which implies that at the same time $k_- \rightarrow 0$. Rapidity divergences rather arise when different modes start to overlap. Nevertheless, the large relative boost between the modes generates large logarithms which require resummation.

By definition, rapidity divergences can only arise in an effective theory with at least two modes with equal virtuality. In the Sudakov form factor they arise from a cross-talk

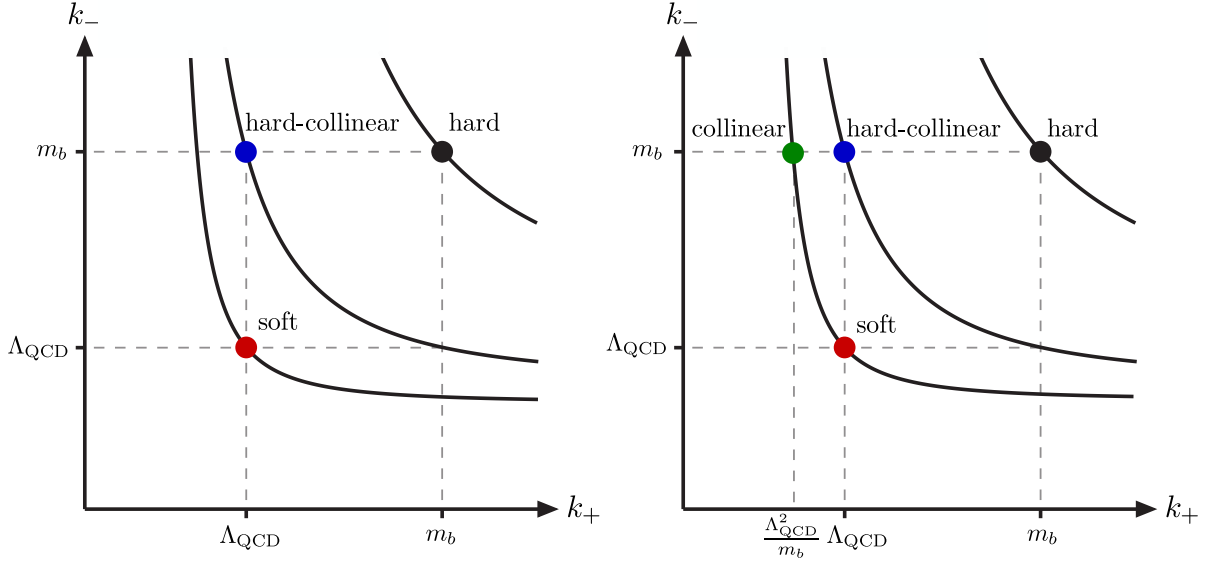


Figure 6.2: Modes that live in SCET_I and SCET_{II}. Only in SCET_{II} two modes live on the same invariant-mass hyperbola whose overlap give rise to endpoint divergences.

of the collinear and the anti-collinear region and in heavy-to-light transitions they arise from the cross-talk of the collinear and the soft mode. However, this means that they can only appear in SCET_{II} but not in SCET_I. Figure 6.2 shows a schematic comparison of the modes in both theories. In flavour-physics applications, SCET_I is the proper effective theory that describes inclusive heavy-to-light transitions like $B \rightarrow X_u \ell \bar{\nu}_\ell$ in the endpoint region. The inclusive system is largely boosted but has hard-collinear virtuality, $\mu_{hc} \sim \lambda M_B$, and thus has no overlap with the soft region. In fact, in SCET_I all divergences are regularised in d dimensions and matrix elements do not suffer from endpoint divergences.

6.2 (Incomplete) Factorisation Formula

The hadronic matrix elements in $B \rightarrow \pi$ transitions are parametrised in terms of three form factors, which can be defined through the following Lorentz decomposition:

$$\begin{aligned} \langle \pi(p) | \bar{q} \gamma^\mu b | \bar{B}(p_B) \rangle &= F_+(q^2) (p_B^\mu + p^\mu) + F_-(q^2) q^\mu, \\ \langle \pi(p) | \bar{q} \sigma^{\mu\nu} q_\nu b | \bar{B}(p_B) \rangle &= \frac{i F_T(q^2)}{M_B + m_\pi} [q^2 (p_B^\mu + p^\mu) - (M_B^2 - m_\pi^2) q^\mu]. \end{aligned} \quad (6.4)$$

Here $q = p_B - p$ is the momentum transfer which is related to the pion energy E_π (in the B -meson rest frame) via $q^2 = M_B^2 + m_\pi^2 - 2M_B E_\pi$. Details on how to project onto the various form factors can be found in Appendix C.1.

We now briefly review the two QCD \rightarrow SCET_I \rightarrow SCET_{II} matching steps, that lead to the factorisation formula in Eq. (1.14). Upon integrating out the hard modes, the

three form factors $F_{+,-,\perp}$ can be factorised in SCET_I according to

$$F_i(q^2) \simeq H_i(q^2) \xi_\pi(q^2) + \int_0^1 d\tau C_i(q^2; \tau) \Xi_\pi(\tau; q^2), \quad i \in \{+, -, \perp\}. \quad (6.5)$$

Here $H_i(q^2)$ and $C_i(q^2; \tau)$ are hard matching functions and the two still process dependent leading-power SCET_I form factors Ξ_π and ξ_π are defined as $\langle \pi | \dots | B \rangle$ matrix elements of two distinct (so-called A-type and B-type) SCET_I operators:

$$\begin{aligned} J_A &= (\bar{\xi}_{hc} W_{hc}) h_v, \\ J_B &= (\bar{\xi}_{hc} W_{hc}) (W_{hc}^\dagger i \not{D}_{hc,\perp} W_{hc}) h_v. \end{aligned} \quad (6.6)$$

In particular, the soft-overlap form factor ξ_π is defined as

$$2E_\pi \xi_\pi(q^2) = \langle \pi(p) | (\bar{\xi}_{hc} W_{hc}) h_v | \bar{B}(v) \rangle, \quad (6.7)$$

where all fields live at the spacetime point $x = 0$, $2E_\pi \simeq \bar{n} \cdot p$ is (twice) the energy of the final-state pion and $|\bar{B}(v)\rangle$ is a B -meson state in HQET. (For the exact definition of Ξ_π see for example [102].) Note that this definition is in agreement with the one given in Eq. (2.11) (for $\Gamma_X = \mathbb{1}$). Whereas the current J_B is power suppressed compared to J_A , the hadronic matrix elements of J_A and J_B are of the same order in λ . The number of independent hadronic parameters is reduced from three in the full theory to two, which can be used to construct relations among the three form factors in the large-recoil limit. The spin-dependent information is completely encoded in the perturbative functions H_i and C_i .

The QCD \rightarrow SCET_I matching of the external currents has been performed in [90, 103] up to one-loop order. For our purpose we only quote the tree-level contributions as well as the leading poles of the one-loop corrections (of the bare quantities) for the A -type operator (see also [100]):

$$\begin{aligned} \bar{q} \gamma^\mu b &\rightarrow \left(1 - \frac{\alpha_s C_F}{4\pi} \left(\frac{\mu^2}{\mu_h^2} \right)^\varepsilon \frac{1}{\varepsilon^2} \right) n^\mu J_A, \\ \bar{q} i \sigma^{\mu\nu} q_\nu b &\rightarrow \left(1 - \frac{\alpha_s C_F}{4\pi} \left(\frac{\mu^2}{\mu_h^2} \right)^\varepsilon \frac{1}{\varepsilon^2} \right) (M_B v^\mu - (M_B - E_\pi) n^\mu) J_A, \end{aligned} \quad (6.8)$$

where $\mu_h \sim M_B \sim E_\pi$ is a typical hard scale. After some algebra this can be translated to the hard functions $H_i(q^2)$ (see also Appendix C.1):

$$H_i(q^2) = \left(1 - \frac{\alpha_s C_F}{4\pi} \left(\frac{\mu^2}{\mu_h^2} \right)^\varepsilon \frac{1}{\varepsilon^2} \right) \times \begin{cases} +1 & (i = +) \\ -1 & (i = -) \\ 1 + m_\pi/M_B & (i = T) \end{cases}. \quad (6.9)$$

Here the power-suppressed ratio m_π/M_B arises as a kinematical factor from the definition of the form factor $F_T(q^2)$ in Eq. (6.4).

The second term in Eq. (6.5) can be factorised further by integrating out hard-collinear modes, i.e. matching onto SCET_{II}:

$$\Xi_\pi(\tau; q^2) = \int_0^\infty d\omega \int_0^1 du \phi_B^+(\omega) J^{(B \rightarrow \pi)}(\tau; u, \omega; q^2) \phi_\pi(u). \quad (6.10)$$

We identify

$$T_i^{(B \rightarrow \pi)}(u, w; q^2) = \int_0^1 d\tau C_i(q^2; \tau) J^{(B \rightarrow \pi)}(\tau; u, \omega; q^2), \quad (6.11)$$

and find

$$F_i(q^2) \simeq H_i(q^2) \xi_\pi(q^2) + \int_0^\infty d\omega \int_0^1 du \phi_B^+(\omega) T_i^{(B \rightarrow \pi)}(u, \omega; q^2) \phi_\pi(u). \quad (6.12)$$

Here $T_i^{(B \rightarrow \pi)}(u, \omega; q^2)$ is a process-dependent, but perturbatively calculable scattering kernel that contains hard and hard-collinear momentum fluctuations. It depends on appropriate light-cone projections of soft and collinear partonic momenta and is known up to one-loop order [53, 102]. The kernel is to be convoluted with leading-twist light-cone distribution amplitudes of the B -meson, $\phi_B^+(\omega)$, and the pion, $\phi_\pi(u)$. The LCDAs are defined through matrix elements of purely soft or collinear operators and are thus process independent; more details will be given in Section 6.4.

Equation (6.12) has even stronger phenomenological consequences than Eq. (6.5), which already have been sketched in the introduction in Section 1.3. Nevertheless, Eq. (6.12) has its limitations since ξ_π is still a process dependent object. Therefore the applications are restricted to relate the various form factors for a given final-state meson only.

An all-order proof of the factorisation formula Eq. (6.12) is given in [54]. Given the operator definition of the soft form factor ξ_π in Eq. (6.7), the crucial point is that the convolution integrals in the second term always exist. We thus call this term the “factorisable” contribution to the form factors, in which large logarithms can be resummed using standard RGE running of the LCDAs [30–32, 104] and the scattering kernel [103]. Whereas the matrix element of the B -type current J_B can be factorised in SCET_{II}, the non-factorisable soft-overlap function ξ_π is still defined in SCET_I. Integrating out hard-collinear modes yields endpoint-divergent convolution integrals, which were first observed in 2000 by Beneke and Feldmann [53]. Since then it is an unsolved problem how, or if, these contributions can be factorised further. The collinear anomaly and the rapidity RGE, that we exemplified with the Sudakov form factor, have been successfully applied to various (perturbative) collider physics observables; see for example [82, 83, 95, 96, 105–110]. The main objective of this thesis is the attempt to apply these new methods to heavy-to-light form factors in a perturbative toy model.

6.3 Matching the A -Type Current onto SCET_{II}

As we did in the investigation of the Sudakov form factor we start with the derivation of the naive factorisation formula by simply assuming that the occurring convolution integrals are somehow analytically regularised. The various steps that lead to this result are presented in the following.

6.3.1 Operator Basis

For vanishing masses of the light quarks the matching of the time-ordered product $i \int d^4x T\{J_A(0), \mathcal{L}_{\text{SCET}_I}(x)\}$ onto four-quark operators in SCET_{II} has been performed at leading order in [100]. For pseudoscalar final states the following operator basis has been proposed:

$$\begin{aligned}
 \mathcal{O}_1 &= g_s^2 \left[\bar{\chi}(0) \frac{\not{n}}{2} \gamma_5 \chi(s\bar{n}) \right] \left[\bar{Q}_s(\tau n) \frac{\not{n}}{4} \gamma_5 \mathcal{H}_v(0) \right], \\
 \mathcal{O}_2 &= g_s^2 \left[\bar{\chi}(0) \frac{\not{n}}{2} \gamma_5 i \not{\phi}_\perp \chi(s\bar{n}) \right] \left[\bar{Q}_s(\tau n) \frac{\not{n}}{2} \gamma_5 \mathcal{H}_v(0) \right], \\
 \mathcal{O}_3 &= g_s^2 \left[\bar{\chi}(0) \frac{\not{n}}{2} \gamma_5 \mathcal{A}_{c,\perp}(r\bar{n}) \chi(s\bar{n}) \right] \left[\bar{Q}_s(\tau n) \frac{\not{n}}{2} \gamma_5 \mathcal{H}_v(0) \right], \\
 \mathcal{O}_4 &= g_s^2 \left[\bar{\chi}(0) \frac{\not{n}}{2} \gamma_5 \chi(s\bar{n}) \right] \left[\bar{Q}_s(\tau n) \mathcal{A}_{s,\perp}(\sigma n) \frac{\not{n}}{2} \gamma_5 \mathcal{H}_v(0) \right],
 \end{aligned} \tag{6.13}$$

where the gauge-invariant building blocks are defined as

$$\chi = W_c^\dagger \xi_c, \quad \mathcal{A}_{c,\perp} = W_c^\dagger (iD_{c,\perp} W_c), \tag{6.14}$$

for collinear fields and

$$\mathcal{Q}_s = S_n^\dagger \psi_s, \quad \mathcal{H}_v = S_n^\dagger h_v, \quad \mathcal{A}_{s,\perp} = S_n^\dagger (iD_{s,\perp} S_n), \tag{6.15}$$

for soft fields. The Wilson lines W_c and S_n are as defined in Eq. (5.50). From the gauge transformation of the covariant derivative, $D^\mu \rightarrow V_i D^\mu V_i^\dagger$ (with $i = s, c$), and of the Wilson line, Eq. (5.46), it is easy to see that the \mathcal{A}_i^μ fields serve as gauge-invariant building blocks for the gauge fields. The operator basis in Eq. (6.13) shows that even at leading power ξ_π involves 3-particle distribution amplitudes which arise from the matrix elements of \mathcal{O}_{2-4} . We adopt the convention of [100], where the factor g_s^2 is defined as part of the operators rather than the Wilson coefficients since it already arises in tree-level matching.

In the non-relativistic perturbative toy model that we aim to investigate, we have to take into account light-quark masses. In this scenario, we find that one additional operator \mathcal{O}_m is present, which we define as

$$\mathcal{O}_m = g_s^2 \left[\bar{\chi}(0) \frac{\not{n}}{2} \gamma_5 \chi(s\bar{n}) \right] \left[\bar{Q}_s(tn) \frac{\not{n}}{2} \gamma_5 \mathcal{H}_v(0) \right]. \tag{6.16}$$

Naively one might think that including a small mass $m \sim \lambda^2 m_b$ should not affect the hard-collinear function. However, whereas a mass can be neglected in propagator denominators, it can nevertheless appear in the numerator structure consistent with the power counting.

6.3.2 Tree-Level Matching

The coefficient functions D_i of the operators \mathcal{O}_i are defined through the matching relation Eq. (6.62). At LO they can be extracted from the tree-level diagrams in Figs. 6.3 and 6.4.

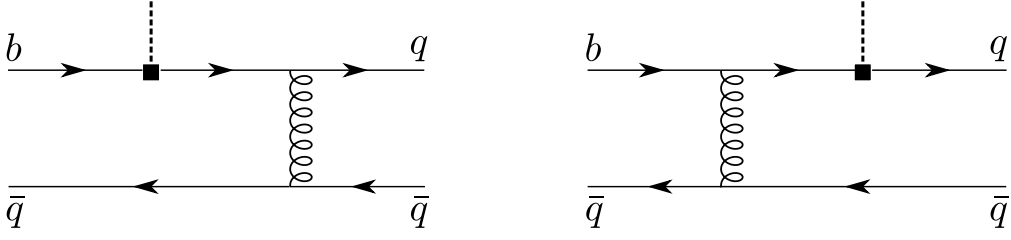


Figure 6.3: Tree-level diagrams with a two-particle initial and final state that contribute to the matching onto the SCET_{II} operators $\mathcal{O}_{m,1-4}$. The gluon that is exchanged between the spectator quark and one of the upper quark lines has hard-collinear virtuality.

For vanishing light-quark masses, D_{1-4} are given in [100], whereas D_m is not given in the literature. We work in Feynman gauge and follow the same strategy as in [100] to compute the D_i for massive quarks.

Considering the two diagrams in Fig. 6.3, we define the kinematics of the partonic process as follows. The momentum of the heavy b -quark is $p_b^\mu = m_b v^\mu$, with $v^\mu = \frac{1}{2}(n^\mu + \bar{n}^\mu)$, up to a small residual momentum of $\mathcal{O}(\Lambda)$ that we can neglect. The momentum l^μ of the soft spectator quark in the B meson has the light-cone decomposition

$$l^\mu = \frac{\omega}{2} \bar{n}^\mu + l_\perp^\mu + \frac{\bar{\omega}}{2} n^\mu, \quad (6.17)$$

whereas the momenta of the collinear quarks in the final state meson are decomposed as

$$p_q^\mu = u E_\pi n^\mu + p_\perp^\mu + \frac{m_q^2 - p_\perp^2}{4u E_\pi} \bar{n}^\mu \quad \text{and} \quad p_{\bar{q}}^\mu = \bar{u} E_\pi n^\mu - p_\perp^\mu + \frac{m_{\bar{q}}^2 - p_\perp^2}{4\bar{u} E_\pi} \bar{n}^\mu. \quad (6.18)$$

Here the label q refers to the quark that is produced in the weak vertex (which we call “active quark”) and \bar{q} to the spectator quark that is converted to a collinear quark by a hard-collinear interaction. We can choose the perpendicular components in this way because our choice of the reference frame is such, that the light meson flies exactly along the z -axis, $p \simeq p_q + p_{\bar{q}}$.

The partonic amplitude of the two tree-level diagrams in Fig. 6.3 reads at leading power

$$A_{\text{part.}} = -g_s^2 \left(\gamma_\mu \frac{E_\pi \not{n} - \not{l} + m_q}{4E_\pi^2 \bar{u} \omega^2} \Gamma + \Gamma \frac{m_b(1 + \psi) - \bar{u} E_\pi \not{n}}{4m_b E_\pi^2 \bar{u}^2 \omega} \gamma_\mu \right) t_a * \gamma^\mu t_a, \quad (6.19)$$

where the $*$ operator means that the terms must be sandwiched between the on-shell spinors of the respective quarks, and Γ is the Dirac structure of the flavour-changing current. As in [100], we match $A_{\text{part.}}$ onto the SCET_{II} operators directly without going through the intermediate SCET_I theory. In order to separate the factorisable from the non-factorisable part, it is sufficient to replace the Dirac structure Γ with the Dirac structure of the A -type current, $\Gamma \rightarrow \frac{\not{n} \not{n}}{4}$, and project onto the $\bar{n} \cdot A_{hc}$ polarisation state for each gluon that is attached to the heavy b -quark line.

At this point, the only difference to the massless case is the factor m_q that arises in the numerator of the first diagram. At first sight, this contribution seems to be of

subleading power. However, the superficially leading-power contribution $\sim \gamma_\mu E_\pi \not{p} \Gamma * \gamma^\mu$ projects onto the subleading η_c components of the on-shell spinors of the collinear quarks, and hence, all terms in Eq. (6.19) contribute at the same power. The subleading η_c components can be related to the leading ξ_c components by means of the equations of motion. In momentum space we find

$$\begin{aligned} \bar{u}(p_q) (\not{p}_q - m_q) = 0 &\Rightarrow \bar{u}(p_q) \not{p} = \bar{u}(p_q) \frac{\not{p}_\perp \not{p}}{4} \frac{m_q - \not{p}_\perp}{u E_\pi} + \dots, \\ (\not{p}_{\bar{q}} + m_{\bar{q}}) v(p_{\bar{q}}) = 0 &\Rightarrow \not{p} v(p_{\bar{q}}) = \frac{\not{p}_\perp - m_{\bar{q}}}{\bar{u} E_\pi} \frac{\not{p} \not{p}}{4} v(p_{\bar{q}}) + \dots, \end{aligned} \quad (6.20)$$

where the ellipses stand for power-suppressed contributions and the projections on the right-hand side match onto the leading ξ_c spinor components. The contributions involving the perpendicular momentum component \not{p}_\perp match onto the operator \mathcal{O}_2 . Note that when applying the equations of motion we also need to take into account contributions with additional gluon fields which originate from the covariant derivative. Thus, the diagrams in Fig. 6.3 also give a contribution to the operators $\mathcal{O}_{3,4}$.

After expressing the amplitude through the ξ_c projections, we perform a Fierz transformation in the 2×2 collinear subspace by defining a basis $\Gamma^{(n)}$ and a dual basis $\Gamma_{(n)}$ in Dirac-space,

$$\Gamma^{(n)} = \left\{ \frac{\not{p}}{2}, \frac{\not{p}}{2} \gamma_5, \frac{\not{p}}{2} \gamma_\perp^\alpha \right\} \quad \text{and} \quad \Gamma_{(n)} = \left\{ \frac{\not{p}}{2}, \gamma_5 \frac{\not{p}}{2}, \gamma_{\perp, \alpha} \frac{\not{p}}{2} \right\}. \quad (6.21)$$

This basis is orthonormal with respect to the scalar product $\frac{1}{2} \text{tr}[\Gamma^{(n)} \Gamma_{(m)}] = \delta_m^n$ and allows us to rewrite

$$\begin{aligned} 2 [\bar{u}_\xi M u_h] [\bar{v}_s N v_\xi] &= [\bar{u}_\xi \frac{\not{p}}{2} v_\xi] [\bar{v}_s N \frac{\not{p}}{2} M u_h] + [\bar{u}_\xi \frac{\not{p}}{2} \gamma_5 v_\xi] [\bar{v}_s N \gamma_5 \frac{\not{p}}{2} M u_h] \\ &\quad + [\bar{u}_\xi \frac{\not{p}}{2} \gamma_{\perp, \alpha} v_\xi] [\bar{v}_s N \gamma_{\perp, \alpha} \frac{\not{p}}{2} M u_h] \end{aligned} \quad (6.22)$$

for arbitrary matrices M and N . Here \bar{u}_ξ and v_ξ are abbreviations for the leading projections of the collinear on-shell spinors, v_s denotes the spinor of the soft spectator quark and u_h the leading spinor-components of the heavy b -quark, respectively. Furthermore, the identities

$$\gamma_\perp^\mu \gamma_5 \not{p} = -i \varepsilon_\perp^{\mu\nu} \gamma_{\perp, \nu} \not{p} \quad \text{and} \quad \gamma_\perp^\mu \gamma_\perp^\nu \not{p} = (g_\perp^{\mu\nu} + i \varepsilon_\perp^{\mu\nu} \gamma_5) \not{p} \quad (6.23)$$

are helpful to simplify the Dirac structure. Here the metric tensor and the totally antisymmetric tensor in the collinear subspace are defined as $g_\perp^{\mu\nu} \equiv g^{\mu\nu} - \frac{1}{2}(n^\mu \bar{n}^\nu + n^\nu \bar{n}^\mu)$ and $\varepsilon_\perp^{\mu\nu} \equiv \frac{1}{2} \varepsilon^{\mu\nu\alpha\beta} \bar{n}_\alpha n_\beta$. We use the convention $\varepsilon^{0123} = +1$ which differs from the one used in [100] (they use $\varepsilon_{0123} = +1 = -\varepsilon^{0123}$). This results in a different sign in front of the $\varepsilon_\perp^{\mu\nu}$ terms in (6.23).

After dropping operators with quantum numbers that do not match $B \rightarrow \pi$ matrix elements, the amplitude $A_{\text{part.}}$ is now expressed as momentum-space Wilson coefficients multiplied with tree-level contractions of the SCET_{II} operators defined in Eq. (6.13). We

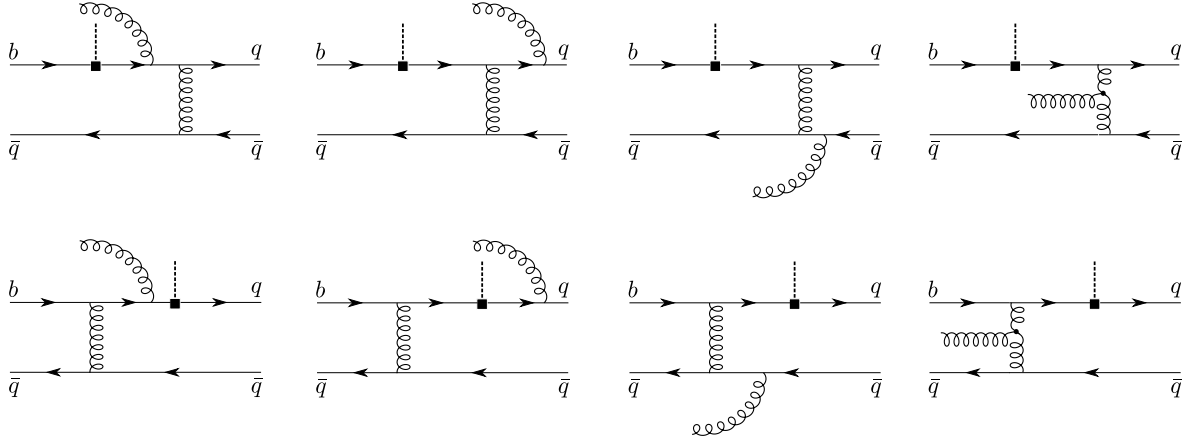


Figure 6.4: Tree-level diagrams with an extra soft gluon that contribute to the matching coefficient D_4 . Mirror-image diagrams with an extra collinear gluon contribute to D_3 .

finally project onto colour-singlet states ($t_a * t_a \rightarrow C_F/N_C$) and include a minus sign from the interchange of fermionic field operators in the Fierz relation. The momentum-space coefficient functions corresponding to two-valence-quark Fock states of the initial and the final-state meson can now be read off as

$$D_1 = -\frac{C_F}{N_C} \frac{1 + \bar{u}}{4E_\pi^2 \bar{u}^2 \omega} \quad \text{and} \quad D_2 = -\frac{C_F}{N_C} \frac{1}{4E_\pi^2 u \bar{u}^2 \omega^2}, \quad (6.24)$$

in agreement with the literature and

$$D_m = +\frac{C_F}{N_C} \frac{1}{4E_\pi^2 \bar{u} \omega^2} \left(m_q \frac{\bar{u}}{u} + m_{\bar{q}} \frac{u}{\bar{u}} \right), \quad (6.25)$$

for the coefficient function of the additional operator \mathcal{O}_m . The contributions to D_m arise from the explicit mass term in the numerator of the light-quark propagator and by applying the equations of motion for the on-shell spinors.

We proceed similarly for the matching coefficients D_3 and D_4 of operators with an additional soft (collinear) gluon in the initial (final) state by evaluating the tree-level diagrams in Fig. 6.4. We call the light-cone projection of the soft gluon momentum $\xi = n \cdot l_g$,² and decompose the momenta of collinear partons as $p_q^\mu \simeq \alpha_q E_\pi n^\mu$, $p_g^\mu \simeq \alpha_g E_\pi n^\mu$ and $p_{\bar{q}}^\mu \simeq \alpha_{\bar{q}} E_\pi n^\mu$, with $\alpha_q + \alpha_g + \alpha_{\bar{q}} = 1$. Note that at leading power only transverse polarisations of the external gluon fields must be kept. The computation is in principle straightforward. The only additional subtlety that one has to take care of is the contribution that arises from the diagrams in Fig. 6.3 when applying the equations of motion to the soft and collinear on-shell spinors. For example, these contributions amount to attaching a soft gluon to the soft spectator quark line, and can be extracted by a simple replacement $\omega \rightarrow \omega + \xi$ in the contributions where the equation of motion has been

²The light-cone projection $\xi = n \cdot l_g$ is not to be confused with the leading components of the collinear spinor ξ_c .

applied to \bar{v}_s . The coefficient functions of the 3-particle operators read

$$\begin{aligned}
 D_3 &= \frac{1}{8E_\pi^2(\alpha_{\bar{q}} + \alpha_g)^2\omega^2} \left[-4\frac{C_F}{N_C} + \frac{\alpha_{\bar{q}} + \alpha_g}{\alpha_{\bar{q}}} \frac{C_A}{N_C} - \frac{2C_F}{N_C} \frac{(\alpha_{\bar{q}} + \alpha_g)^2}{\alpha_{\bar{q}}(\alpha_q + \alpha_g)} \right], \\
 D_4 &= \frac{-1}{8E_\pi^2\bar{u}^2(\omega + \xi)^2} \left[\left(\frac{2C_F\bar{u} - C_A}{N_C} \right) \frac{\xi}{\omega} + \frac{2C_F - C_A}{N_C} \right], \tag{6.26}
 \end{aligned}$$

in agreement with [100]. Hence, we showed that a small fermion mass contributes to \mathcal{O}_m only and does not alter the Wilson coefficients of the remaining operators.

6.3.3 Leading Poles in One-Loop Corrections to $D_{m,1}$

As a next step, we compute the $1/\varepsilon^2$ poles of the one-loop corrections to the (bare) coefficient functions D_m and D_1 , which is a necessary input to resum leading logarithms in the non-relativistic perturbative model. We will discuss our model in detail below, but it is easy to understand that the matrix elements of the operators $\mathcal{O}_{2,3,4}$ are suppressed by one power of α_s compared to those of \mathcal{O}_m and \mathcal{O}_1 . To first approximation in the non-relativistic expansion, the mesons are built from two on-shell massive quarks in the static limit. Any deviation from this configuration requires at least one relativistic gluon exchange. Hence, matrix elements of the operators with an additional gluon field, \mathcal{O}_3 and \mathcal{O}_4 , are $\mathcal{O}(\alpha_s)$ suppressed. Moreover, the momenta of the massive on-shell partons are exactly aligned to the respective meson momenta and hence have vanishing perpendicular components. Therefore also the matrix element of \mathcal{O}_2 vanishes at $\mathcal{O}(\alpha_s^0)$.

All one-loop diagrams that contribute to the matching are given in Fig. 6.5. We work again in Feynman gauge and compute the full QCD diagrams in the hard-collinear region instead of using SCET_I Feynman rules. Our strategy for the computation of the double poles is as follows. We first introduce Feynman parameters and after a shift perform the integration over the loop momentum. The resulting parameter integrals contain overlapping divergences which can be separated using one or more sector decomposition steps [111]. We then extract the double pole in ε from the parameter integrals and after that manipulate the Dirac structure in the same way as we did in the tree-level calculation: we first perform the power expansion and express the amplitude through the leading ξ_c projections and afterwards perform the Fierz transformation in the collinear subspace.

Note that the Fierz relation is only valid in $d = 4$ dimensions. For a consistent treatment of the full one-loop hard-collinear function in d dimensions one must take into account evanescent operators, which is related to the treatment of γ_5 in d dimensions. This is similar to what has been done in the derivation of the one-loop hard-collinear function for the factorisable contribution in [102]. However, this issue does not affect the leading poles in ε and can be ignored in our approximation. We can use the same procedure as in the tree-level calculation and work in naive dimensional regularisation with anticommuting γ_5 .

Let us exemplify our strategy with the diagram in Fig. 6.6. The external kinematics is as in the tree-level calculation. We define the loop momentum k^μ as the momentum that flows through the spectator-quark propagator (from left to right), and evaluate the

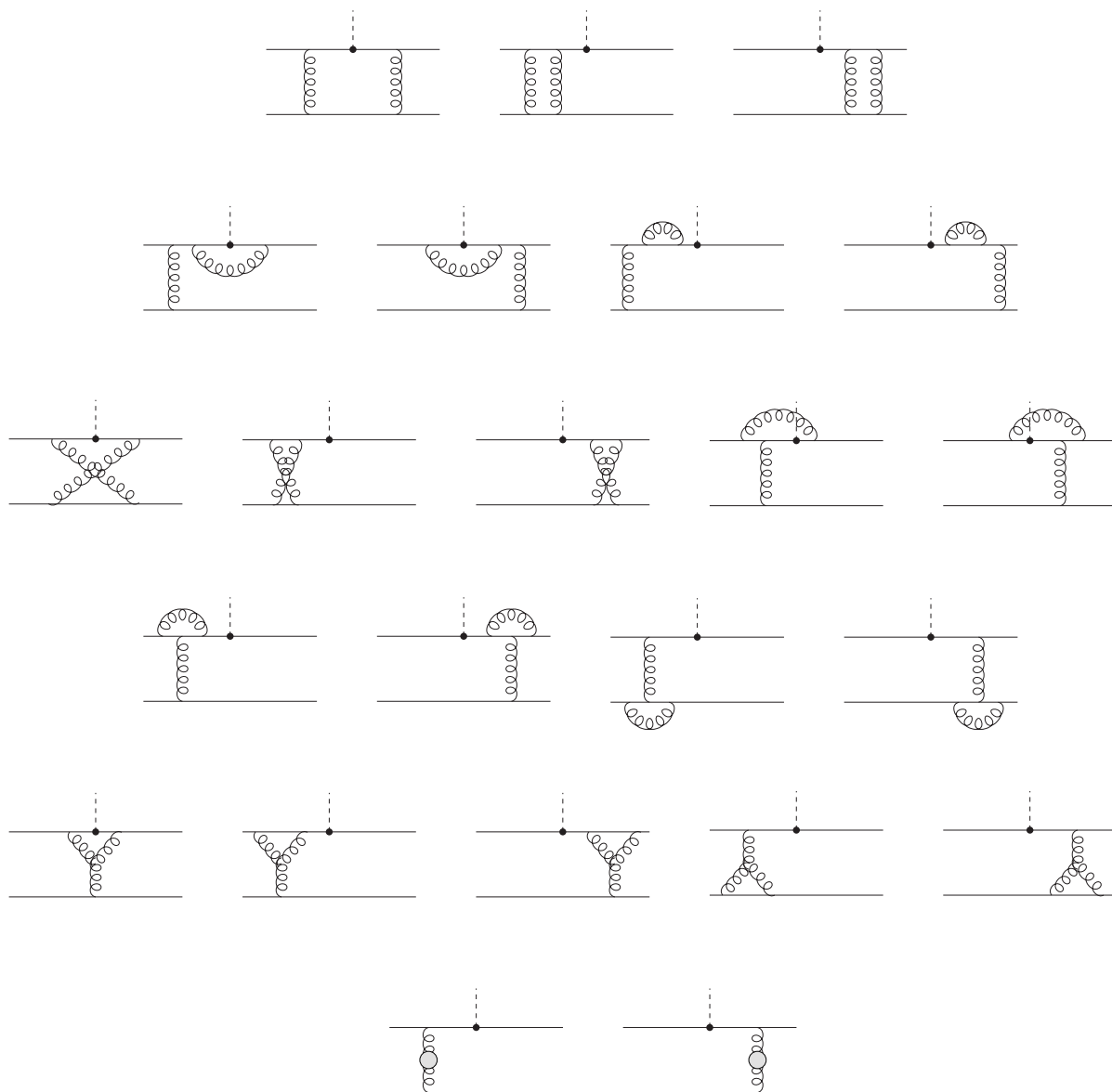


Figure 6.5: One-Loop diagrams with a two-particle initial and final state that contribute to the matching onto the SCET_{II} operators $\mathcal{O}_{m,1-4}$ (adapted from [112]). Note that some diagrams have a scaleless hard-collinear region and that additional diagrams are present for flavour-singlet final states, which we do not include in our calculation.

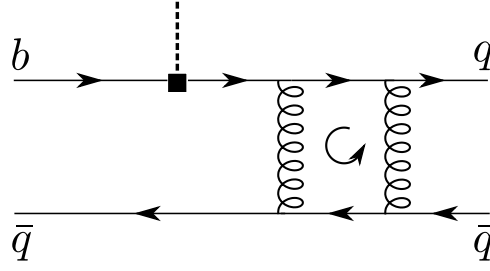


Figure 6.6: Example diagram that contributes to the one-loop correction of $D_{m,1}$.

integral in the hard-collinear region, $k \sim (1, \lambda, \lambda^2)M_B$. The unexpanded amplitude of the diagram reads

$$iA = \frac{ig_s^4 \tilde{\mu}^{4\epsilon} t_a t_b * t_b t_a}{(p-l)^2} \int \frac{d^d k}{(2\pi)^d} \frac{[\bar{v}_s(l)\gamma^\mu(-\not{k} + m_{\bar{q}})\gamma^\nu v_c(p_2)]}{[k^2 - m_{\bar{q}}^2] [(k-p)^2 - m_{\bar{q}}^2] [(k-l)^2] [(k-p_2)^2]} [\bar{u}_c(p_1)\gamma_\nu(\not{p} - \not{k} + m_q)\gamma_\mu(\not{p} - \not{l} + m_q)\Gamma u_h(p_b)], \quad (6.27)$$

with the proper $+i\epsilon$ prescriptions in each propagator denominator. Next we introduce Feynman parameters to combine the four denominators, shift the loop momentum and perform the $d^d k$ integration with the standard formulas for massive tadpole integrals. This yields

$$iA = \frac{g_s^4 \tilde{\mu}^{4\epsilon} t_a t_b * t_b t_a}{(4\pi)^{d/2} 2E_\pi \omega} \frac{\Gamma(1+\epsilon)}{2} \int_0^1 dx \int_0^{1-x} dy \int_0^{1-x-y} dz \left\{ (2+2\epsilon)\Delta^{(hc)}(x, y, z; \omega, \bar{u})^{-2-\epsilon} [\bar{v}_s\gamma^\mu(-x\not{p} - y\not{p}_2 - z\not{l} + m_{\bar{q}})\gamma^\nu v_c] [\bar{u}_c\gamma_\nu(\bar{x}\not{p} - y\not{p}_2 - z\not{l} + m_q)\gamma_\mu(\not{p} - \not{l} + m_q)\Gamma u_h] - \Delta^{(hc)}(x, y, z; \omega, \bar{u})^{-1-\epsilon} [\bar{v}_s\gamma^\mu\gamma^\alpha\gamma^\nu v_c] [\bar{u}_c\gamma_\nu\gamma_\alpha\gamma_\mu(\not{p} - \not{l} + m_q)\Gamma u_h] \right\}, \quad (6.28)$$

where we have omitted the momenta of the on-shell spinors for readability. Adopting hard-collinear power counting gives $\Delta^{(hc)}(x, y, z; \omega, \bar{u}) = 2E_\pi\omega z(x + \bar{u}y)$. Before dealing with the Dirac structure let us investigate the parameter integrals, which have the generic form

$$I^{(a,b,c;n)} = \int_0^1 dx \int_0^{1-x} dy \int_0^{1-x-y} dz \frac{x^a y^b z^c}{\Delta^{(hc)}(x, y, z; \omega, \bar{u})^{n+\epsilon}}, \quad (6.29)$$

with $a, b, c \geq 0$ and $n = 1, 2$. Poles in ϵ emerge in the limit $z \rightarrow 0$ as well as $x + \bar{u}y \rightarrow 0$, which for generic \bar{u} means that simultaneously $x \rightarrow 0$ and $y \rightarrow 0$. The pole from this *overlapping divergence* can be isolated by performing a sector decomposition step. (See for example [113] for a review about the sector decomposition method.) After rescaling $y = (1-x)t$ we integrate over the two dimensional unit cube with an overlapping divergence at $(x, t) = (0, 0)$. We subdivide the square according to

$$\int_0^1 dx \int_0^1 dt = \int_0^1 dx \int_0^x dt + \int_0^1 dt \int_0^t dx \quad (6.30)$$

into two triangles, which we each map again onto unit squares by a simple rescaling. Performing the z -integration explicitly and relabeling the integration variables gives

$$I^{(a,b,c;n)} = \frac{1}{(2E_\pi\omega)^{n+\varepsilon}} \frac{1}{1+c-n-\varepsilon} \int_0^1 dx \int_0^1 dr x^{1+a+b-n-\varepsilon} \times \left\{ \frac{\bar{x}^{2+b+c-n-\varepsilon} r^b (1-xr)^{1+c-n-\varepsilon}}{(1+\bar{u}\bar{x}r)^{n+\varepsilon}} + \frac{\bar{x}^{1+c-n-\varepsilon} r^a (1-xr)^{2+b+c-n-\varepsilon}}{(r+\bar{u}(1-rx))^{n+\varepsilon}} \right\}, \quad (6.31)$$

which at first sight looks cumbersome, but has the advantage that the poles in ε are now isolated and can be extracted by expanding in plus-distributions. Analysing the integrand reveals that a double pole can only arise in the case $(a, b, c) = (0, 0, 1)$ and for $n = 2$:

$$\begin{aligned} I^{(0,0,1;2)} &= \frac{-1}{\varepsilon} \frac{1}{(2E_\pi\omega)^{2+\varepsilon}} \int_0^1 dx \int_0^1 dr x^{-1-\varepsilon} \left\{ \frac{\bar{x}^{1-\varepsilon} (1-xr)^{-\varepsilon}}{(1+\bar{u}\bar{x}r)^{2+\varepsilon}} + \frac{\bar{x}^{-\varepsilon} (1-xr)^{1-\varepsilon}}{(r+\bar{u}(1-rx))^{2+\varepsilon}} \right\} \\ &= \frac{1}{\varepsilon^2} \frac{1}{(2E_\pi\omega)^{2+\varepsilon}} \int_0^1 dr \left\{ \frac{1}{(1+\bar{u}r)^{2+\varepsilon}} + \frac{1}{(r+\bar{u})^{2+\varepsilon}} \right\} + \mathcal{O}(1/\varepsilon) \\ &= \frac{1}{\varepsilon^2} \frac{1}{(2E_\pi\omega)^{2+\varepsilon}} \frac{1+\bar{u}^{-\varepsilon} - (1+\bar{u})^{-\varepsilon}}{(1+\varepsilon)\bar{u}} + \mathcal{O}(1/\varepsilon) \\ &= \frac{1}{\varepsilon^2} \frac{1}{\bar{u} (2E_\pi\omega)^2} + \mathcal{O}(1/\varepsilon), \end{aligned} \quad (6.32)$$

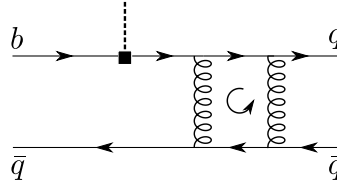
where from the first to the second line we made the pole from $x \rightarrow 0$ explicit by substituting $x^{-1-\varepsilon} \rightarrow -\delta(x)/\varepsilon + \mathcal{O}(\varepsilon^0)$. Plugging this back into the amplitude of our example diagram yields

$$\begin{aligned} iA &= \frac{\alpha_s(\mu)}{4\pi} \frac{1}{\varepsilon^2} \frac{-g_s^2 t_a t_b * t_b t_a}{\bar{u} (2E_\pi\omega)^3} \left\{ [\bar{v}_s \gamma^\mu \not{l} \gamma^\nu v_c] [\bar{u}_c \gamma_\nu (\not{p} + m_q) \gamma_\mu (\not{p} - \not{l} + m_q) \Gamma u_h] \right. \\ &\quad \left. + m_{\bar{q}} [\bar{v}_s \gamma^\mu \gamma^\nu v_c] [\bar{u}_c \gamma_\nu \not{l} \gamma_\mu (\not{p} - \not{l} + m_q) \Gamma u_h] \right\} + \mathcal{O}(1/\varepsilon). \end{aligned} \quad (6.33)$$

Now we start manipulating the Dirac structure as it has been explained above. After projecting onto colour singlet states ($t_a t_b * t_b t_a \rightarrow C_F^2/N_C$) and dropping operators with quantum numbers that do not match $B \rightarrow \pi$ transitions, the amplitude is now cast into the following form

$$iA \sim \frac{\alpha_s(\mu)}{4\pi} \frac{1}{\varepsilon^2} \frac{C_F^2/N_C}{2\omega^2 \bar{u} E_\pi^2} \left(m_q \frac{\bar{u}}{u} + m_{\bar{q}} \frac{1+\bar{u}}{\bar{u}} \right) g_s^2 \left[\bar{u}_c \frac{\not{h}}{2} \gamma_5 v_c \right] \left[\bar{v}_s \frac{\not{h}}{2} \gamma_5 u_h \right]. \quad (6.34)$$

The Dirac structure (including the factor of g_s^2) is the tree-level matrix element of \mathcal{O}_m . Hence, we can read off the contributions of the diagram under consideration to the hard-collinear functions $D_{m,1}$:



$$\begin{aligned}
 D_m &: \frac{\alpha_s(\mu) C_F C_F}{4\pi N_C} \frac{1}{\varepsilon^2} \frac{1}{2\omega^2 \bar{u} E_\pi^2} \left(m_q \frac{\bar{u}}{u} + m_{\bar{q}} \frac{1 + \bar{u}}{\bar{u}} \right), \\
 D_1 &: 0.
 \end{aligned} \tag{6.35}$$

The results for the remaining diagrams in Fig. 6.5 are summarised in Appendix C.2. After summing up all diagrams we find a very simple result for the double pole in the one-loop correction to the matching coefficient D_1 :

$$D_1 = -\frac{C_F}{N_C} \frac{1 + \bar{u}}{4E_\pi^2 \bar{u}^2 \omega} \left[1 + \frac{\alpha_s(\mu) C_F}{\pi} \frac{1}{\varepsilon^2} \right] + \mathcal{O}(\alpha_s/\varepsilon, \alpha_s^2). \tag{6.36}$$

Whereas the ω -dependence is fixed on dimensional grounds, it is non-trivial that we exactly reproduce the functional behaviour in \bar{u} of the tree-level result. The correction to D_m looks more complicated and new structures arise (we again abbreviate $C_{FA} \equiv \frac{C_A}{2} - C_F$):

$$\begin{aligned}
 D_m &= +\frac{C_F}{N_C} \frac{1}{4E_\pi^2 \bar{u} \omega^2} \left\{ \left(m_q \frac{\bar{u}}{u} + m_{\bar{q}} \frac{u}{\bar{u}} \right) \left[1 + \frac{\alpha_s(\mu) C_F}{\pi} \frac{1}{\varepsilon^2} \right] + \frac{\alpha_s(\mu)}{\pi} \frac{1}{\varepsilon^2} m_{\bar{q}} \left(C_F - \frac{C_{FA}}{2\bar{u}} \right) \right\} \\
 &+ \mathcal{O}(\alpha_s/\varepsilon, \alpha_s^2).
 \end{aligned} \tag{6.37}$$

Let us conclude this section with a comment on endpoint divergences in the presence of hard-collinear loops. Again, dimensionality dictates that each hard-collinear loop in a generic diagram with a two-particle initial state comes with a factor $\mu^{2\varepsilon}/(\omega E_\pi)^\varepsilon$, which could regularise potential endpoint divergences from $\omega \rightarrow 0$ dimensionally.³ This argument cannot be used for the dimensionless momentum fractions u and \bar{u} . Nevertheless, the functional behaviour in Eq. (6.32) is such, that an endpoint-sensitive moment is regularised in d dimensions for $\bar{u} \rightarrow 0$. This must be the case since the method of regions works separately for individual diagrams as long as one works in one and the same gauge in every region. Consider a two-loop ladder-type diagram, where an additional gluon is exchanged between the spectator quark and the “active” quark line, in the mixed (soft, hard-collinear) and (hard-collinear, collinear) regions. Naive factorisation tells us that we should interpret these diagrams as convolutions of one-loop (soft or collinear) LCDAs with a one-loop hard-collinear scattering kernel. We found that the one-loop kernel regularises the (soft, hard-collinear) region. The endpoint finiteness of the full integral then guarantees, that the hard-collinear kernel must also regularise the (hard-collinear, collinear) region. Note that this argument is no longer true as soon as we consider corrections to the operators $\mathcal{O}_{3,4}$ since an additional dimensionful parameter ξ is present. In fact, in this case endpoint divergences occur that require additional (analytic) regularisation.

³The natural hard-collinear scale would be for example $\left(\frac{\mu^2}{2\omega\bar{u}E_\pi}\right)^\varepsilon$ up to parametrically small logarithms that are generated through the expansion in ε .

6.4 Light-Cone Distribution Amplitudes

The operators \mathcal{O}_i are products of non-local soft and collinear currents. Since interactions are power-suppressed in SCET_{II}, the hadronic matrix elements factorise into meson-vacuum matrix elements, $\langle \pi | \mathcal{O}_i | \bar{B} \rangle \sim \langle \pi | \bar{\chi} \dots \chi | 0 \rangle \times \langle 0 | \bar{\mathcal{Q}}_s \dots \mathcal{H}_v | \bar{B} \rangle$, which define the light-cone distribution amplitudes. In this section we summarise their definitions, the translation of the occurring matrix elements into LCDAs, their equations of motion as well as their asymptotic behaviour for heavy and light pseudoscalar mesons.

6.4.1 Heavy Mesons

We define the 2-particle LCDAs of a heavy pseudoscalar B meson through the decomposition of the HQET coordinate space matrix element [114]

$$\langle 0 | \bar{q}^\beta(z)[z, 0]h_v^\alpha(0) | \bar{B}(v) \rangle = -\frac{i\tilde{f}_B M_B}{4} \left[P_v \left(2\tilde{\Phi}_B^+(t, z^2) + \frac{\tilde{\Phi}_B^-(t, z^2) - \tilde{\Phi}_B^+(t, z^2)}{t} \not{z} \right) \gamma_5 \right]^{\alpha\beta}, \quad (6.38)$$

in the light-like limit, $z^2 \rightarrow 0$. Here $\tilde{f}_B(\mu)$ is the B -meson decay constant in HQET and $t \equiv v \cdot z$. Adopting the power counting induced by the convolution with a generic hard-collinear scattering kernel, $\bar{n} \cdot z \gg z_\perp \gg n \cdot z$, we can further expand

$$\begin{aligned} & 2\tilde{\Phi}_B^+(t, z^2) + \frac{\tilde{\Phi}_B^-(t, z^2) - \tilde{\Phi}_B^+(t, z^2)}{t} \not{z} \\ & \simeq \tilde{\phi}_B^+(\tau) \not{n} + \tilde{\phi}_B^-(\tau) \not{l} + \frac{\tilde{\phi}_B^-(\tau) - \tilde{\phi}_B^+(\tau)}{\tau} \not{z}_\perp + \mathcal{O}(n \cdot z, z_\perp^2), \end{aligned} \quad (6.39)$$

with $\tilde{\phi}_B^\pm(t) \equiv \tilde{\Phi}_B^\pm(t, z^2 = 0)$ and $\tau \equiv \frac{\bar{n} \cdot z}{2}$ is the Fourier-conjugated variable to $\omega = n \cdot l$. Here we used that the terms in Eq. (6.39) are multiplied with the heavy-quark projector $P_v = \frac{1+\not{v}}{2}$ from the left.⁴ The momentum-space LCDAs are then defined via the Fourier transform

$$\tilde{\phi}_B^\pm(\tau) = \int_0^\infty d\omega e^{-i\omega\tau} \phi_B^\pm(\omega), \quad \phi_B^\pm(\omega) = \int \frac{d\tau}{2\pi} e^{i\omega\tau} \tilde{\phi}_B^\pm(\tau). \quad (6.40)$$

The hadronic matrix elements of the 2-particle currents in the \mathcal{O}_i can be read off as

$$\langle 0 | \bar{\mathcal{Q}}_s(\tau n) \frac{\not{n}}{2} \gamma_5 \mathcal{H}_v(0) | \bar{B}(v) \rangle = \frac{i\tilde{f}_B M_B}{2} \tilde{\phi}_B^+(\tau), \quad (6.41)$$

and

$$\langle 0 | \bar{\mathcal{Q}}_s(\tau n) \frac{\not{l} \not{n}}{4} \gamma_5 \mathcal{H}_v(0) | \bar{B}(v) \rangle = -\frac{i\tilde{f}_B M_B}{2} \tilde{\phi}_B^-(\tau). \quad (6.42)$$

⁴Note that the expansion Eq. (6.39) is only true in the frame where $v^\mu = \frac{n^\mu + \bar{n}^\mu}{2}$.

We define the 3-particle LCDAs of the B meson in position space following [114, 115]:

$$z_\nu \langle 0 | \bar{q}^\beta(z) [z, uz] g_s G^{\mu\nu}(uz) [uz, 0] h_v^\alpha(0) | \bar{B}(v) \rangle = \frac{\tilde{f}_B M_B}{2} \left[P_v \left\{ (v^\mu \not{z} - t\gamma^\mu) \left(\tilde{\Psi}_A(t, u) \right) - \tilde{\Psi}_V(t, u) \right) - i\sigma^{\mu\nu} z_\nu \tilde{\Psi}_V(t, u) - z^\mu \tilde{X}_A(t, u) + \frac{z^\mu \not{z}}{t} \tilde{Y}_A(t, u) \right\} \gamma_5 \right]^{\alpha\beta}. \quad (6.43)$$

The operator on the left-hand side of this equation is a gauge singlet and can most easily be treated in soft light-cone gauge, $n \cdot A_s = 0$, which makes all soft Wilson lines trivial, $S_n \equiv 1$. After multiplying Eq. (6.43) with $(\gamma_{\mu\perp} \frac{\not{n}}{2} \gamma_5)_{\beta\alpha}$, evaluating the trace in d dimensions and performing the light-cone expansion $z^\mu \simeq \tau n^\mu$, we find for the soft matrix element that arises from \mathcal{O}_4 :

$$\begin{aligned} & \langle 0 | \bar{Q}_s(\tau n) \mathcal{A}_{s,\perp}(u\tau n) \frac{\not{n}}{2} \gamma_5 \mathcal{H}_v(0) | \bar{B}(v) \rangle \\ &= (d-2) \frac{i\tilde{f}_B M_B}{2} \int_0^\infty d\omega \int_0^\infty d\xi e^{-i\omega\tau} e^{-i\xi(u\tau)} \frac{\Psi_A(\omega, \xi) - \Psi_V(\omega, \xi)}{\xi}. \end{aligned} \quad (6.44)$$

Note that gauge invariance is restored by utilising gauge-invariant building blocks. Here $\omega = n \cdot l_q$ is the Fourier-conjugated variable to τ and $\xi = n \cdot l_g$ is the Fourier-conjugated variable to $(u\tau)$ ($u\tau \equiv \sigma$ in the definition of \mathcal{O}_4):

$$\tilde{\Psi}_{V,A}(\tau, u) = \int_0^\infty d\omega \int_0^\infty d\xi e^{-i\omega\tau} e^{-i\xi(u\tau)} \Psi_{V,A}(\omega, \xi). \quad (6.45)$$

The factor $1/\xi$ in Eq. (6.44) originates from the contraction of the field-strength tensor with a reference vector, $n_\nu G^{\mu\nu}(uz) \sim (n \cdot \partial) A^\mu(uz)$, which after Fourier transform and light-cone expansion corresponds to $(-i\xi \tilde{A}^\mu(\bar{n} \xi/2))$.

Asymptotic behaviour for small ω : Whether or not the various moments appearing in the naive factorisation formula are well-defined depends decisively on the asymptotic behaviour of the LCDAs for $\omega \rightarrow 0$. Investigating their renormalisation group evolution reveals this information. The evolution of the LCDA $\phi_B^+(\omega, \mu)$ is governed by the Lange-Neubert kernel [104] whose analytic solution is known [116]. Independent of the form of the LCDA at a scale μ_0 , the evolution $\mu_0 \rightarrow \mu$ generates a linear behaviour for small ω . Thus, the first inverse moment $\lambda_B^{-1}(\mu)$ is a well-defined quantity, whereas the second inverse moment is ill-defined as $\omega \rightarrow 0$. Similarly, one can study the endpoint behaviour of the LCDAs ϕ_B^- and $\Psi_{A-V} \equiv \Psi_A - \Psi_V$. For vanishing spectator-quark mass one finds (see e.g. [117]):

$$\phi_B^+(\omega; \mu) \sim \omega, \quad \phi_B^-(\omega; \mu) \sim \text{const.}, \quad \Psi_{A-V}(\omega, \xi; \mu) \sim \omega \xi^2. \quad (6.46)$$

Note that the asymptotic behaviour is also determined by the conformal spins of the respective fields defining the LCDAs [118]. This implies that the first inverse moment

of ϕ_B^- is endpoint divergent, whereas a convolution of the 3-particle LCDA Ψ_{A-V} with a scattering-kernel that behaves like $\omega^{-1}\xi^{-2}$ (compare to D_4) for small ω would be endpoint finite.

The asymptotic behaviour of ϕ_B^+ remains the same if one includes a non-zero spectator-quark mass $m_{\bar{q}}$ in the theory. However, the mass causes a mixing of ϕ_B^+ into ϕ_B^- under renormalisation group evolution, which could in principle alter that $\phi_B^- \sim \text{const.}$ for $\omega \rightarrow 0$. This has been observed in [119], but the authors have not studied the implications of this mixing to the solution of the corresponding RGE. However, the equations of motion (see below) show that due to the non-zero spectator-quark mass, the endpoint behaviour of Ψ_{A-V} is indeed altered and the $\langle \omega^{-1}\xi^{-2} \rangle_{A-V}$ moment also becomes endpoint divergent.

To summarise, for a non-zero spectator-quark mass we encounter three endpoint-divergent moments: the second inverse moment of ϕ_B^+ , the first inverse moment of ϕ_B^- , and the 3-particle LCDA Ψ_{A-V} convoluted with a scattering-kernel that behaves as $\sim \frac{1}{\omega}$ for $\omega \rightarrow 0$. Note that the endpoint behaviour discussed above refers to the *renormalised* LCDAs. It is not clear how (or if) the renormalised LCDAs are related to the objects in endpoint-divergent moments, which somehow need to be regularised. Furthermore, at higher-orders in the perturbative expansion and before expanding in ε , the bare LCDAs develop a logarithmic behaviour for $\omega \rightarrow 0$, e.g. $\phi_B^{+, (n)}(\omega) \sim \omega \log^{n-1} \omega / m_{\bar{q}}$, which generate higher poles in δ in an endpoint-divergent moment.

Equations of motion: Equations of motion of the quark fields result in relations among the non-local operators that can in turn be translated into relations between the three distribution amplitudes ϕ_B^+ , ϕ_B^- and Ψ_{A-V} . For non-zero spectator-quark mass, the LCDAs obey [119]:

$$\begin{aligned} \omega \phi_B^-(\omega) - m_{\bar{q}} \phi_B^+(\omega) + \frac{d-2}{2} \int_0^\omega d\eta [\phi_B^+(\eta) - \phi_B^-(\eta)] \\ = (d-2) \int_0^\omega d\eta \int_{\omega-\eta}^\infty \frac{d\xi}{\xi} \frac{\partial}{\partial \xi} \Psi_{A-V}(\eta, \xi). \end{aligned} \quad (6.47)$$

We prefer to use the following equivalent representation:

$$\begin{aligned} \omega \phi_B^-(\omega) - m_{\bar{q}} \phi_B^+(\omega) + \frac{d-2}{2} \int_0^\omega d\eta [\phi_B^+(\eta) - \phi_B^-(\eta)] \\ = - (d-2) \int_0^\infty d\tilde{\omega} \int_0^\infty d\tilde{\xi} \frac{\Psi_{A-V}(\tilde{\omega}, \tilde{\xi})}{\tilde{\xi}} \left\{ \delta(\omega - (\tilde{\omega} + \tilde{\xi})) + \frac{\theta(\omega - (\tilde{\omega} + \tilde{\xi})) - \theta(\omega - \tilde{\omega})}{\tilde{\xi}} \right\}, \end{aligned} \quad (6.48)$$

from which it is easier to derive relations among moments of the LCDAs. For example, taking the second inverse moment in ω yields (in $d = 4 - 2\varepsilon$ dimensions)

$$(d-2) \int_0^\infty d\omega \int_0^\infty d\xi \frac{\Psi_{A-V}(\omega, \xi)}{\omega(\omega + \xi)^2} = \int_0^\infty \frac{d\omega}{\omega} \left((1 - \varepsilon) \phi_B^+(\omega) - \frac{m_{\bar{q}}}{\omega} \phi_B^+(\omega) + \varepsilon \phi_B^-(\omega) \right). \quad (6.49)$$

A word of caution is necessary, since this would only be true if the moments were well-defined. We can not guarantee that analytic regularisation preserves the relation quoted above. Nevertheless, as we will see, using Eq. (6.49) to simplify the naive factorisation formula for ξ_π at least does not affect the leading poles in δ and still allows us to consistently extract the leading large logarithms.

6.4.2 Light Mesons

For light mesons we adopt the following definitions of 2-particle LCDAs of twist-2 and twist-3 [68, 120]:

$$\begin{aligned} \langle \pi(p) | \bar{q}_1(y)[y, x] \gamma_\mu \gamma_5 q_2(x) | 0 \rangle &= -i f_\pi P_\mu \int_0^1 du e^{i(up \cdot y + \bar{u}p \cdot x)} \phi_\pi(u), \\ \langle \pi(p) | \bar{q}_1(y)[y, x] i \gamma_5 q_2(x) | 0 \rangle &= f_\pi \mu_\pi \int_0^1 du e^{i(up \cdot y + \bar{u}p \cdot x)} \phi_P(u), \\ \langle \pi(p) | \bar{q}_1(y)[y, x] \sigma_{\mu\nu} \gamma_5 q_2(x) | 0 \rangle &= i f_\pi \tilde{\mu}_\pi (p_\mu z_\nu - p_\nu z_\mu) \int_0^1 du e^{i(up \cdot y + \bar{u}p \cdot x)} \frac{\phi_\sigma(u)}{2d-2}. \end{aligned} \quad (6.50)$$

Here $z_\mu = y_\mu - x_\mu$ and $P_\mu = p_\mu - m_\pi^2 / (2p \cdot z) z_\mu$ are two light-like vectors,⁵ and u ($\bar{u} = 1 - u$) denotes the momentum fraction associated with the q_1 (q_2) quark field. $\phi_\pi(u)$ is the leading-twist LCDA (twist-2), while $\phi_P(u)$ and $\phi_\sigma(u)$ are of subleading twist (twist-3). Furthermore, f_π is the pion decay constant. The ‘‘chirally enhanced’’ constant μ_π is given by $\mu_\pi = \frac{m_\pi^2}{m_q + m_{\bar{q}}}$ and $\tilde{\mu}_\pi$ by Eq. (6.59). All LCDAs are normalised to one, so that the prefactors in Eq. (6.50) are defined through the local limit $x \rightarrow y$,

After performing the light-cone expansion we find

$$\langle \pi(p) | \bar{\chi}(0) \frac{\not{n}}{2} \gamma_5 \chi(s\bar{n}) | 0 \rangle = -i f_\pi E_\pi \int_0^1 du e^{i2E_\pi s \bar{u}} \phi_\pi(u), \quad (6.51)$$

where $2E_\pi \simeq \bar{n} \cdot p$ is (twice) the energy of the pion. Note that in case of massive final-state mesons the momentum p^μ is not exactly aligned with the light-cone vector n^μ .

We define the 3-particle LCDA of the pion as [68, 120]

$$\begin{aligned} &\langle \pi(p) | \bar{q}_1(0)[0, vx] g_s G_{\alpha\beta}(vx) \sigma_{\mu\nu} \gamma_5 [vx, x] q_2(x) | 0 \rangle \\ &= i f_{3\pi} [P_\alpha P_\mu g_{\nu\beta}^\perp - P_\alpha P_\nu g_{\mu\beta}^\perp - P_\beta P_\mu g_{\nu\alpha}^\perp + P_\beta P_\nu g_{\mu\alpha}^\perp] \int \mathcal{D}\alpha e^{ip \cdot x (\alpha_{\bar{q}} + v\alpha_g)} \phi_{3\pi}(\alpha_{\bar{q}}, \alpha_q, \alpha_g). \end{aligned} \quad (6.52)$$

Here, α_i denotes the momentum fractions of the ‘‘active’’ quark (α_q), the spectator quark ($\alpha_{\bar{q}}$) and the gluon (α_g), respectively, and the integration measure is defined as

$$\int \mathcal{D}\alpha \equiv \int_0^1 d\alpha_{\bar{q}} \int_0^1 d\alpha_q \int_0^1 d\alpha_g \delta(1 - \alpha_{\bar{q}} - \alpha_q - \alpha_g). \quad (6.53)$$

⁵Note that our notation for the light-like vector P^μ and the meson momentum p^μ differs from [120].

Similar to what has been done in the soft sector, we multiply Eq. (6.52) with $\frac{\bar{n}^\nu \bar{n}^\beta}{4} g_\perp^{\mu\alpha}$, use collinear light-cone gauge, $\bar{n} \cdot A_c = 0$, and restore gauge invariance by using gauge-invariant building blocks after we arrive at the desired expression. We find for the matrix element that arises from \mathcal{O}_3 ($sv \equiv r$ in the definition of \mathcal{O}_3):

$$\langle \pi(p) | \bar{\chi}(0) \frac{\not{n}}{2} \gamma_5 \mathcal{A}_{c,\perp}(vs\bar{n}) \chi(s\bar{n}) | 0 \rangle = (d-2) i E_\pi f_{3\pi} \int \mathcal{D}\alpha e^{i2E_\pi(\alpha_{\bar{q}}s + \alpha_g sv)} \frac{\phi_{3\pi}(\alpha_{\bar{q}}, \alpha_q, \alpha_g)}{\alpha_g}. \quad (6.54)$$

Again, the factor $1/\alpha_g$ is due to the contraction $\bar{n}^\beta G_{\alpha\beta}(vx) \sim (\bar{n} \cdot \partial) A_c^\mu(vx)$, which after Fourier transform and light-cone expansion gives $(2iE_\pi \alpha_g) \tilde{A}_c^\mu(\alpha_g n)$.

Finding an expression for the matrix element of the current $\bar{\chi}(0) \frac{\not{n}}{2} \gamma_5 i \not{\phi}_\perp \chi(s\bar{n})$ requires some work. The derivation makes use of the equations of motion (see below) and can be found in Appendix C.3. We choose to work with the following representation

$$\begin{aligned} & \langle \pi(p) | \bar{\chi}(0) \frac{\not{n}}{2} \gamma_5 i \not{\phi}_\perp \chi(s\bar{n}) | 0 \rangle \\ &= i E_\pi (d-2) \int_0^1 du e^{i2E_\pi s \bar{u}} \left\{ \frac{f_\pi \tilde{\mu}_\pi \phi_\sigma(u)}{2d-2} + f_{3\pi} \int \mathcal{D}\alpha \frac{\phi_{3\pi}(\{\alpha_i\})}{\alpha_g^2} \left(\theta(\alpha_q - u) - \theta(\bar{u} - \alpha_{\bar{q}}) \right) \right\}, \end{aligned} \quad (6.55)$$

which has the advantage that no spurious endpoint divergences from $u \rightarrow 0$ arise in the naive factorisation formula that cancel within the collinear sector.

Asymptotic behaviour for small \bar{u} : The renormalisation of the leading-twist LCDA $\phi_\pi(u; \mu)$ is governed by the ERBL evolution kernel (Efremov, Radyushkin, Brodsky, Lepage [30–32]) and the corresponding RGE can be diagonalised by expanding $\phi_\pi(u; \mu)$ in Gegenbauer polynomials. The endpoint behaviour for small \bar{u} is then determined by the leading term in this expansion, which reads $\phi_\pi(u; \mu) \sim 6u\bar{u}$. Similarly, the LCDAs of subleading twist can be investigated (for a summary see e.g. [120]) and for massless partons one finds

$$\phi_\pi(u; \mu) \sim \phi_\sigma(u; \mu) \sim 6u\bar{u}, \quad \phi_P(u; \mu) \sim 1, \quad \phi_{3\pi}(\{\alpha_i\}; \mu) \sim 360 \frac{f_{3\pi}}{f_\pi \mu_\pi} \alpha_q \alpha_{\bar{q}} \alpha_g^2, \quad (6.56)$$

which would imply three endpoint-divergent moments that arise in the naive factorisation formula: the second inverse moment of ϕ_π and ϕ_σ , as well as the first inverse moment of ϕ_P .⁶ The 3-particle LCDA $\phi_{3\pi}$ convoluted with a kernel $\sim 1/\alpha_{\bar{q}}$ (for $\alpha_{\bar{q}} \rightarrow 0$) would be endpoint finite.

Similar to what we observed for heavy mesons, the equations of motion imply that in the presence of parton masses the endpoint behaviour of $\phi_{3\pi}$ is different. In that case the occurring inverse moments for a scattering kernel $\sim 1/\alpha_{\bar{q}}$ become endpoint divergent.

⁶Note that an inverse moment of the linear combination $\phi_P(u) + \frac{\phi'_\sigma(u)}{6} \sim 2\bar{u}$ would be endpoint finite.

Equations of motion: Again, the equations of motion of the quark fields lead to relations among the non-local collinear currents that are given in [120]. After taking the hadronic matrix elements thereof, we find the following relations among the LCDAs:

$$\begin{aligned} \frac{f_\pi \tilde{\mu}_\pi \phi'_\sigma(u)}{2d-2} + (2u-1) f_\pi \mu_\pi \phi_P(u) + (m_{\bar{q}} - m_q) f_\pi \phi_\pi(u) \\ = - (d-2) f_{3\pi} \int \mathcal{D}\alpha \frac{\phi_{3\pi}(\{\alpha_i\})}{\alpha_g} (\delta(\alpha_q - u) - \delta(\alpha_{\bar{q}} - \bar{u})) , \end{aligned} \quad (6.57)$$

and

$$\begin{aligned} \frac{f_\pi \tilde{\mu}_\pi}{2d-2} \left((2u-1) \phi'_\sigma(u) - 2(d-2) \phi_\sigma(u) \right) + f_\pi \mu_\pi \phi_P(u) - (m_q + m_{\bar{q}}) f_\pi \phi_\pi(u) \\ = (d-2) f_{3\pi} \int \mathcal{D}\alpha \frac{\phi_{3\pi}(\{\alpha_i\})}{\alpha_g} \left(\delta(\alpha_q - u) + \delta(\alpha_{\bar{q}} - \bar{u}) + \frac{2}{\alpha_g} \left[\theta(\alpha_q - u) - \theta(\bar{u} - \alpha_{\bar{q}}) \right] \right) . \end{aligned} \quad (6.58)$$

Integration of equations (6.57) and (6.58) yields

$$\int_0^1 du u \phi_P(u) = \frac{1}{2} + \frac{m_q - m_{\bar{q}}}{2\mu_\pi} \quad \text{and} \quad \tilde{\mu}_\pi = \mu_\pi - (m_q + m_{\bar{q}}) , \quad (6.59)$$

in agreement with [119].

We extract relations between inverse moments by multiplying the first equation with $(u\bar{u})^{-1}$, which leads to

$$\begin{aligned} f_\pi \int_0^1 du \left(\mu_\pi \phi_P(u) \frac{u - \bar{u}}{u\bar{u}} + \frac{\tilde{\mu}_\pi}{2d-2} \frac{\phi'_\sigma(u)}{u\bar{u}} + (m_{\bar{q}} - m_q) \frac{\phi_\pi(u)}{u\bar{u}} \right) \\ = (d-2) f_{3\pi} \int \mathcal{D}\alpha \frac{\phi_{3\pi}(\{\alpha_i\})}{\alpha_g} \left(\frac{1}{\alpha_{\bar{q}}(\alpha_g + \alpha_q)} - \frac{1}{\alpha_q(\alpha_g + \alpha_{\bar{q}})} \right) . \end{aligned} \quad (6.60)$$

Furthermore, the difference of both equations multiplied with \bar{u}^{-2} leads to

$$\begin{aligned} f_\pi \int_0^1 du \left(\frac{d-3}{2d-2} \tilde{\mu}_\pi \frac{\phi'_\sigma(u)}{\bar{u}} + \mu_\pi \frac{\phi_P(u)}{\bar{u}} - m_{\bar{q}} \frac{\phi_\pi(u)}{\bar{u}^2} \right) \\ = - (d-2) f_{3\pi} \int \mathcal{D}\alpha \frac{\phi_{3\pi}(\{\alpha_i\})}{\alpha_g} \left(\frac{1}{\alpha_{\bar{q}}(\alpha_g + \alpha_{\bar{q}})} - \frac{1}{(\alpha_g + \alpha_{\bar{q}})^2} \right) . \end{aligned} \quad (6.61)$$

Here we used integration by parts, $\langle \bar{u}^{-2} \rangle_\sigma = -\langle \bar{u}^{-1} \rangle_{\sigma'}$, which is only justified when the convolution integral is somehow regularised. Again, we do not know if one can implement an analytic regulator in a way that preserves the equations of motion. This is a crucial point that definitely needs to be clarified for a consistent treatment of endpoint divergences. Regardless of that, it again does not affect the leading poles in δ .

6.5 Naive Factorisation Formula for ξ_π

We now have everything at hand to write down a naive factorisation formula for ξ_π in SCET_{II}:

$$\begin{aligned}
 2E_\pi \xi_\pi(E_\pi) &= \sum_{i=m,1,2} \int ds d\tau \tilde{D}_i(s, \tau; E_\pi) \langle \pi(p) | \mathcal{O}_i | \bar{B}(v) \rangle(s, \tau) \\
 &\quad + \int dr ds d\tau \tilde{D}_3(r, s, \tau; E_\pi) \langle \pi(p) | \mathcal{O}_3 | \bar{B}(v) \rangle(r, s, \tau) \\
 &\quad + \int ds d\tau d\sigma \tilde{D}_4(s, \tau, \sigma; E_\pi) \langle \pi(p) | \mathcal{O}_4 | \bar{B}(v) \rangle(s, \tau, \sigma). \quad (6.62)
 \end{aligned}$$

Note that the factor $2E_\pi$ comes from the definition of ξ_π in Eq. (6.7). This can be converted into an expression in momentum space using the Fourier transformed coefficient functions

$$D_i(\omega, \bar{u}; E_\pi) = \int ds e^{i2E_\pi s \bar{u}} \int dt e^{-i\omega\tau} \tilde{D}_i(s, \tau; E_\pi), \quad \text{for } i = m, 1, 2, \quad (6.63)$$

of operators corresponding to 2-particle Fock-states and

$$D_3(\omega, \alpha_{\bar{q}}, \alpha_g; E_\pi) = \int dr ds e^{i2E_\pi(s\alpha_{\bar{q}}+r\alpha_g)} \int dt e^{-i\omega\tau} \tilde{D}_3(r, s, \tau; E_\pi), \quad (6.64)$$

$$D_4(\omega, \xi, \bar{u}; E_\pi) = \int ds e^{i2E_\pi s \bar{u}} \int d\tau d\sigma e^{-i(\omega\tau+\xi\sigma)} \tilde{D}_4(s, \tau, \sigma; E_\pi), \quad (6.65)$$

of operators corresponding to 3-particle Fock-states. The factorisation formula then takes the form of a convolution of the various B -meson and pion LCDAs with the momentum-space hard-collinear coefficient functions $D_{m,1-4}$.

The contributions of the individual operators $\mathcal{O}_{m,1-4}$ are summarised in Appendix C.4. With the abbreviation

$$\xi_0 \equiv \frac{\alpha_s \pi^2 f_\pi \tilde{f}_B M_B}{4\pi N_C E_\pi^2} \quad (6.66)$$

we find for tree-level hard-collinear exchanges (which we denote by ξ_π^{hc0}) the following expression:

$$\begin{aligned}
 \frac{\xi_\pi^{\text{hc0}}(E_\pi)}{\xi_0} &= C_F \int_0^\infty d\omega \int_0^1 du \left[\frac{\phi_B^-(\omega)}{\omega} \frac{1+\bar{u}}{\bar{u}^2} \phi_\pi(u) + \frac{\phi_B^+(\omega)}{\omega} \frac{u}{\bar{u}^2} \phi_\pi(u) \right. \\
 &\quad \left. + \frac{\phi_B^+(\omega)}{\omega^2} \left(-\frac{m_q \bar{u} + 2m_{\bar{q}}}{\bar{u}^2} \phi_\pi(u) + 3 \frac{\mu_\pi \phi_P(u)}{\bar{u}} + \frac{(d-3) \tilde{\mu}_\pi \phi'_\sigma(u)}{2d-2} \frac{1}{\bar{u}} \right) \right] \\
 &\quad - (d-2) C_{FA} \frac{f_{3\pi}}{f_\pi} \int_0^\infty d\omega \frac{\phi_B^+(\omega)}{\omega^2} \int \mathcal{D}\alpha \frac{\phi_{3\pi}(\{\alpha_i\})}{\alpha_g \alpha_{\bar{q}} (\alpha_g + \alpha_{\bar{q}})} \\
 &\quad + (d-2) C_{FA} \int_0^\infty d\omega \int_0^\infty d\xi \frac{\Psi_{A-V}(\omega, \xi)}{\omega \xi (\omega + \xi)} \int_0^1 du \frac{\phi_\pi(u)}{\bar{u}^2}. \quad (6.67)
 \end{aligned}$$

Furthermore, considering the specific subset of one-loop corrections to the hard-collinear functions, we find

$$\begin{aligned} \frac{\xi^{\text{hcl}}(E_\pi)}{\xi_0} \subset & \frac{\alpha_s(\mu)C_F}{\pi} \frac{1}{\varepsilon^2} \int_0^\infty d\omega \int_0^1 du \left\{ C_F \frac{\phi_B^-(\omega)}{\omega} \frac{1+\bar{u}}{\bar{u}^2} \phi_\pi(u) \right. \\ & \left. + \frac{\phi_B^+(\omega)}{\omega^2} \phi_\pi(u) \left[C_F \frac{m_q}{u} + \left(C_F - \frac{C_{FA}}{2} \right) \frac{m_{\bar{q}}}{\bar{u}^2} \right] \right\}. \end{aligned} \quad (6.68)$$

The analysis of the asymptotic behaviour of the various LCDAs showed that endpoint divergences in the factorisation of heavy-to-light form factors show up as ill-defined convolution integrals. This has to be contrasted with the Sudakov form factor, where Wilson lines in purely collinear operators render their matrix elements divergent. Here the situation is more complicated since endpoint divergences arise due to the interplay of low-energy modes with the hard-collinear sector. Moreover, as the calculation in the next chapter shows, soft or collinear Wilson-line gluons do not seem to play a special role and endpoint divergences in loop diagrams arise for all polarisations of virtual gluons.

We compare our result with the literature. Beneke and Feldmann calculated the tree-level spectator-scattering contributions to the $B \rightarrow \pi$ form factor in [53] for massless light-quarks. Their result for the form factor F_+ is the following:

$$\begin{aligned} F_+^{(\text{BF})} = & \frac{\alpha_s C_F}{4\pi} \frac{\pi^2 \tilde{f}_B \tilde{f}_\pi M_B}{N_C E_\pi^2} \int_0^1 du \int_0^\infty d\omega \left\{ \frac{4E_\pi - M_B}{M_B} \frac{\phi_\pi(u)}{\bar{u}} \frac{\phi_B^+(\omega)}{\omega} \right. \\ & \left. + \frac{1+\bar{u}}{\bar{u}^2} \phi_\pi(u) \frac{\phi_B^-(\omega)}{\omega} + \frac{\mu_\pi}{2E_\pi} \left[\frac{(\phi_P(u) - \phi'_\sigma(u)/6)}{\bar{u}^2} \frac{\phi_B^+(\omega)}{\omega} + 4E_\pi \frac{\phi_P(u)}{\bar{u}} \frac{\phi_B^+(\omega)}{\omega^2} \right] \right\}, \end{aligned} \quad (6.69)$$

where only the three terms in the second line are spin-symmetric. Moreover, the authors work in the Wandzura-Wilczek approximation, which leads to the following explicit solutions for the pion LCDAs: $\phi_P(u) = 1$ and $\phi_\sigma(u) = 6u\bar{u}$ (see also the discussion in Subsection 2.2.2). Dropping the quark masses m_q and $m_{\bar{q}}$ and adopting the Wandzura-Wilczek approximation, only the operators \mathcal{O}_1 and \mathcal{O}_2 contribute and Eq. (6.67) reduces in $d = 4$ dimensions to

$$\xi_\pi^{\text{hc0}}(E_\pi) \simeq \frac{\alpha_s C_F}{4\pi} \frac{\pi^2 \tilde{f}_B \tilde{f}_\pi M_B}{N_C E_\pi^2} \int_0^\infty d\omega \int_0^1 du \left\{ \frac{\phi_B^-(\omega)}{\omega} \frac{1+\bar{u}}{\bar{u}^2} \phi_\pi(u) + \frac{\phi_B^+(\omega)}{\omega^2} 2\mu_\pi \frac{\phi_P(u)}{\bar{u}} \right\}. \quad (6.70)$$

Note that, since $\phi_P(u)$ and $\phi_\sigma(u)$ are completely determined, we should not use integration by parts for ill-defined moments in any step to arrive at this expression. We interpret the mismatch of this result and the second line of Eq. (6.69) as follows. The authors of [53] claim, that all three spin-symmetric terms are of the same power in Λ/M_B if one introduces a cut-off regulator $\bar{u} \gtrsim \Lambda/M_B$ to regularise the endpoint divergences. However, in the context of the method of regions one should rather expand the *integrand* consistently. Using analytic regularisation, the third term in Eq. (6.69) is formally an endpoint divergent term of subleading power.

To conclude this chapter let us briefly recapitulate the status in the theoretical description of heavy-to-light form factors compared to the Sudakov form factor. We have derived naive factorisation formulas for fixed-order scattering kernels on a rigorous field theoretical basis by performing a matching calculation onto four-quark operators in SCET_{II}. The hadronic matrix elements of the effective operators are parametrised in terms of light-cone distributions amplitudes, which are convoluted with respective momentum-space Wilson coefficients. By investigating the asymptotic endpoint behaviour of the various LCDAs we identified ill-defined moments in the soft and the collinear sector, which require further regularisation. Equations (6.67) and (6.68) thus correspond to the naive factorisation formula for the Sudakov form factor given in Eq. (5.56). The main difference between the two observables is that rapidity divergences in the factorisation of heavy-to-light form factors arise due to an ill-defined convolution of well-defined objects, whereas in the Sudakov form factor the perturbative expansion of collinear matrix elements give rise to ill-defined loop integrals. Proceeding along the lines of Chapter 5, we would next apply the collinear anomaly argument or derive and solve rapidity RGEs to resum large logarithms. However, due to the different factorisation structure this is a highly non-trivial task. To approach this goal, we investigate the form factors in a non-relativistic setup in the next chapter. In this approximation the ill-defined moments can be calculated perturbatively and similarities and differences with respect to the Sudakov form factor can be studied.

Chapter 7

Heavy-to-Light Form Factors for Non-Relativistic Bound States

In this chapter we investigate heavy-to-light transitions at large hadronic recoil in a perturbative setup [119]. To this end, we consider the decay $\bar{B}_c \rightarrow \eta_c \ell \nu_\ell$ in the non-relativistic limit. On the one hand, the bottom quark is assumed to be much heavier than the charm quark, $m_b \gg m_c$. On the other hand, if even the charm-quark is considered heavy, the hadronic states can be approximated as non-relativistic (NR) bound states of two heavy quarks in the static limit. The relativistic QCD dynamics is then calculable in perturbation theory and by employing the method of regions the factorisation properties of the form factors can be studied. As in the case of the Sudakov form factor endpoint divergences in this setup arise as ill-defined loop integrals. We show that the resummation of leading rapidity logarithms can be achieved by solving rapidity RG equations for inverse moments. Together with the evolution of the hard and the hard-collinear functions, we derive a resummed expression for the product $H_i \xi_\pi$ in the leading logarithmic approximation.

7.1 Setup

We use the setup described in [112, 119] which we briefly summarise in this section. Non-relativistic QCD (NRQCD) [121–127] is an effective field theory designed to describe bound states of two heavy quarks. In the heavy-quark limit, their relative velocity is small, $w \ll 1$, such that the system becomes non-relativistic to first approximation. A factorisation of scales can then be achieved through an expansion in w . Within NRQCD, wave functions for NR bound states can be obtained from the resummation of so-called potential gluon exchanges, see Fig. 7.1. To first approximation, the \bar{B}_c meson is built of a bottom quark with mass m_b and momentum $p_b^\mu = m_b v^\mu$, and a spectator antiquark with mass $m_{\bar{q}}$ and momentum $l^\mu = m_{\bar{q}} v^\mu$. Both partons move with the same four-velocity as the heavy meson, $v^\mu = \frac{n^\mu + \bar{n}^\mu}{2}$. Based on equations of motion for the field operators and quantum numbers of the pseudoscalar \bar{B}_c meson, its spinor degrees of freedom are incorporated in the Dirac projector $\mathcal{P}_H = \frac{1}{2}(1 + \not{v})\gamma_5$.

Similarly, a pseudoscalar η_c meson is a bound state of an “active” quark with momentum $p_q^\mu = m_q v'^\mu$ and a spectator antiquark with $p_{\bar{q}}^\mu = m_{\bar{q}} v'^\mu$, where v'^μ is the four-velocity of the η_c meson, with $v'^2 = 1$. Its Dirac projector is given by $\mathcal{P}_L = \frac{1}{2}(1 - \not{v}')\gamma_5$. Note that $m_{\bar{q}} = m_q \equiv m_c$ for the η_c meson. However, since this setup only serves as a toy model to

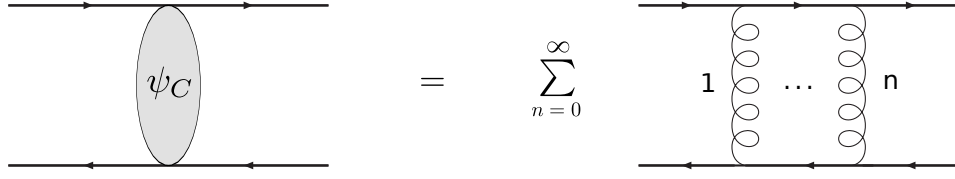


Figure 7.1: Resummation of potential gluons into a NR Coulomb wave-function. The figure is taken from [119].

investigate the QCD dynamics, we distinguish the masses of the “active” quark m_q and the spectator quark $m_{\bar{q}}$, with $m_q \sim m_{\bar{q}} \sim \lambda^2 m_b$. We stress that this does not correspond to a physical process, but it allows us to reveal more structures in the perturbative results. Moreover, we introduce the mass ratios $u_0 \equiv m_q/m_\eta$ and $\bar{u}_0 \equiv m_{\bar{q}}/m_\eta = 1 - u_0$ with $u_0 = \bar{u}_0 = \frac{1}{2}$ in the realistic case.

If we identify the mass of the energetic final-state meson with the hadronic scale, $m_\eta \simeq m_q + m_{\bar{q}} \sim \lambda^2 M_B$, the QCD dynamics is at leading power described by the modes in Table 6.1. In the limit $m_c \rightarrow \infty$, however, the charm-quark mass defines another hard scale in the context of NRQCD. At leading power in Λ/m_c , fluctuations associated with m_c are decoupled and relativistic corrections to the NR wave functions can be calculated in a perturbative expansion in $\alpha_s(m_c)$. In summary, the scales relevant to this process are

$$\mu_h \sim m_b \gg \mu_{hc} \sim \sqrt{m_b m_c} \gg \mu_{s,c} \sim m_c \gg \mu_{\text{NR}} \sim m_c w, \quad (7.1)$$

where μ_{NR} is the virtuality of potential gluons in NRQCD. Since all masses are much larger than the hadronic scale, $m_{b,c} \gg \Lambda$, the relativistic dynamics in this setup is accessible in perturbation theory.

For large recoil energies with $M_B^2 - q^2 \sim \mathcal{O}(M_B^2)$, soft and collinear degrees of freedom are separated through a large Lorentz boost

$$\gamma \equiv v \cdot v' \simeq \frac{M_B^2 - q^2}{4M_B m_\eta} \sim \mathcal{O}(M_B/m_\eta) \sim \mathcal{O}(1/\lambda^2), \quad (7.2)$$

which implies $E = \gamma m_\eta \sim \mathcal{O}(M_B)$ for the energy E of the η_c meson (in the \bar{B}_c -meson rest frame). Up to power corrections we can express the four-velocity v'^μ of the energetic η_c meson as

$$v'^\mu = \gamma n^\mu + \frac{\bar{n}^\mu}{4\gamma}, \quad (7.3)$$

such that $p_{\eta,q,\bar{q}}^\mu \sim (1, 0, \lambda^4) M_B$ have collinear scaling.

7.2 Non-Factorisable Double Logarithms at One-Loop

We compute leading large logarithms in the non-factorisable contribution to the $\bar{B}_c \rightarrow \eta_c$ form factors at one-loop order. We derive all results from the naive SCET_{II} factorisation formulas Eqs. (6.67) and (6.68). Large logarithms in the factorisable contribution are

not investigated, since their resummation is well understood. Comparing leading-power QCD results with the expressions resulting from Eqs. (6.67) and (6.68) gives a non-trivial cross-check of the naive factorisation formulas that we derived in the previous chapter. To this end, we start with the calculation of the endpoint-finite tree-level expression for ξ_π .

7.2.1 ξ_π at Tree-Level

Converting the soft spectator quark of the \bar{B}_c meson into a highly energetic parton requires at least one hard-collinear gluon exchange. At leading order in the perturbative expansion, the form factors can be calculated from the two tree-level diagrams in Fig. 6.3. At leading power we find the results:

$$\frac{s}{s + \bar{u}_0} F_+^{(0)} = -F_-^{(0)} = F_T^{(0)} = \frac{\xi_0 C_F}{m_\eta} \frac{2}{\bar{u}_0^3}, \quad (7.4)$$

with $s = M_B/(2E)$. Note that we use the superscript (0) for leading-order results, although they are accompanied by one factor of α_s . The constant ξ_0 is as defined in Eq. (6.66) with appropriate decay constants $f_B^{(\text{NR})}$ and $f_\eta^{(\text{NR})}$ defined in the NR limit.¹

In complete analogy to the calculation of the one-loop hard-collinear functions in Section 6.3.3, the non-factorisable (spin-symmetric) contribution to the form factors is characterised by the Dirac-structure $\Gamma \rightarrow \frac{\not{\eta}\not{\eta}}{4}$ in the flavour-changing current and by a longitudinally polarised gluon attached to the b -quark line. Consequently, the remaining terms belong to the factorisable contribution for which we find

$$\frac{s}{2-s} F_+^{(0), \text{fac.}} = F_-^{(0), \text{fac.}} = -F_T^{(0), \text{fac.}} = \frac{\xi_0 C_F}{m_\eta} \frac{1}{\bar{u}_0^2}. \quad (7.5)$$

This result can be reproduced from the second term in the factorisation formula Eq. (6.12), by employing the tree-level hard and hard-collinear matching coefficients [102, 112]:

$$\frac{C_+^{(0)}(\tau)}{s-2} = -\frac{C_-^{(0)}(\tau)}{s} = \frac{C_T^{(0)}(\tau)}{s} = 1, \quad (7.6)$$

and

$$J^{(0)}(\tau; u, \omega) = -\frac{\pi \alpha_s C_F \tilde{f}_B f_\eta}{N_C} \frac{\delta(\tau - \bar{u})}{2\bar{u}E\omega}. \quad (7.7)$$

Furthermore, at LO the LCDAs merely project the momentum fraction u and the light-cone component ω onto their respective values for the on-shell partons. We thus have $\phi_B^+(\omega) \simeq \delta(\omega - m_{\bar{q}})$ for the \bar{B}_c -meson LCDA and $\phi_\eta(u) \simeq \delta(u - u_0)$ for the leading-twist LCDA of the η_c meson.

¹The LO decay constants in the NR limit coincide with the HQET (QCD) definition of \tilde{f}_B (f_η). One-loop corrections have been calculated in [119], but are not relevant in the LL approximation.

Using the tree-level hard matching coefficients H_i from Eq. (6.9), we can extract the soft form factor $\xi_\eta(E)$ from the full QCD calculation as well:

$$\xi_\eta^{(0)}(E) = \frac{\xi_0 C_F}{m_\eta} \frac{2 + \bar{u}_0}{\bar{u}_0^3}. \quad (7.8)$$

This result can be reproduced from the naive factorisation formula Eq. (6.67), which is a first non-trivial cross-check of our calculation. The NR wave-functions have been calculated in [119] up to $\mathcal{O}(\alpha_s)$ and are collected in Appendix D.1. As one can see from these expressions, we can neglect contributions from 3-particle wave-functions as well as the subleading-twist LCDA $\phi_\sigma(u)$ at LO. The latter one is accompanied by the α_s suppressed prefactor $\tilde{\mu}_\eta$. Furthermore, the ‘‘chirally enhanced’’ prefactor is given by $\mu_\eta \simeq m_q + m_{\bar{q}}$ and all remaining LCDAs are simple delta distributions.

7.2.2 Cancellation of Double Poles at One-Loop Order

While investigating the Sudakov form factor, we observed that the double logarithm at one-loop order is generated through a cancellation of double poles of the form $\sim \frac{1}{\delta\varepsilon}$ and $\sim \frac{1}{\varepsilon^2}$. Similar poles emerge in the one-loop calculation of heavy-to-light form factors. However, the situation here is more complicated since first, the rapidity divergences only arise through the convolution integrals and second, more scales are present in the problem. In the following, we again choose $\nu^\delta/(k_- - i\varepsilon)^\delta$ as an (still ad-hoc) analytic regulator. Poles in δ then cancel between the soft and the collinear region of all one-loop diagrams, and the ‘‘asymmetric’’ regulator in the soft region gives a double pole in ε from the expansion in δ . Furthermore, the hard-collinear region receives double poles in ε which have been calculated in Section 6.3.3, and also the hard region has a double pole in ε which is given by Eq. (6.9). Additionally, due to the presence of a HQT field, the soft region receives another double pole in ε . The latter two are treated in the standard Sudakov-like RG evolution. In the following, we will compute the various contributions and explicitly show the cancellation of poles in the sum of all four regions.

Endpoint divergences first arise at one-loop order in the perturbative expansion from the diagrams in Fig. 6.5 in the soft or the collinear region. Among all diagrams only those with exactly one spectator-quark propagator, which can overlap between the soft and the collinear region, receive endpoint-divergent contributions that require additional regularisation (at least in Feynman gauge). That is, the three box-type diagrams in the first row, the three non-planar diagrams in the third row, and the last two diagrams with a non-abelian vertex in the fifth row.

Contrariwise, the last two diagrams in the fourth row could potentially receive endpoint-sensitive contributions that are regularised in d dimensions. This is true in general when the overlapping propagator is massless (see discussion in [88]). In a nutshell, the reason for this is the following. Endpoint divergences arise when the overlapping propagator goes on-shell. Picking up the residue e.g. in k_+ amounts to the replacement

$$k_+ \rightarrow \frac{m^2 - k_\perp^2}{k_-}, \quad \text{or} \quad k_+ \rightarrow -\frac{k_\perp^2}{k_-}, \quad (7.9)$$

in the massive and the massless case, respectively. After performing the perpendicular $d^{d-2}k_\perp$ integrations, the k_- integral gets an additional power of k_-^ε in the massless case, which regularises potential endpoint divergences dimensionally. In the presence of a mass this is in general not true. In the soft region, for example, the diagrams under consideration should be interpreted as a convolution of a 3-particle \bar{B}_c -meson LCDA with a tree-level hard-collinear kernel. If we define the loop-momentum k as the momentum carried by the (overlapping) gluon propagator, we have $k_+ \equiv \xi$. However, although the argument from above is true for the corresponding scalar integral, the only occurring 3-particle LCDA vanishes quadratically for small ξ (see Appendix D.1 for the full expression). Endpoint-sensitive contributions from $\xi \rightarrow 0$ are thus not present in the factorisation of ξ_η .

We perform the calculation of the diagrams that do receive poles in δ using Cauchy's theorem in the k_+ variable. Since we are only interested in endpoint contributions, there is no need to separate the factorisable from the non-factorisable terms. In the sum of all diagrams we find the following result for the double poles in the collinear region:

$$\xi_\eta^{(c)}(E) = \frac{\xi_0 C_F \alpha_s(\mu)}{m_\eta 4\pi} \left(-\frac{1}{\delta\varepsilon}\right) \left(\frac{\mu^2}{m_q^2}\right)^\varepsilon \left(\frac{\nu}{2\gamma m_{\bar{q}}}\right)^\delta \left(6C_F \frac{1+\bar{u}_0}{\bar{u}_0^3} - \frac{C_A}{\bar{u}_0^3}\right) + \mathcal{O}(\varepsilon/\delta, \delta^0/\varepsilon). \quad (7.10)$$

Note that the poles in δ do not receive $\mathcal{O}(\varepsilon^0)$ contributions. Similarly, we find for the endpoint contributions in the soft sector

$$\xi_\eta^{(s)}(E) \simeq \frac{\xi_0 C_F \alpha_s(\mu)}{m_\eta 4\pi} \left(\frac{1}{\delta\varepsilon} - \frac{1}{\varepsilon^2}\right) \left(\frac{\mu^2}{m_q^2}\right)^\varepsilon \left(\frac{\nu}{m_{\bar{q}}}\right)^\delta \left(6C_F \frac{1+\bar{u}_0}{\bar{u}_0^3} - \frac{C_A}{\bar{u}_0^3}\right) + \mathcal{O}(\varepsilon/\delta, \delta^0/\varepsilon), \quad (7.11)$$

such that the sum of both regions is finite for $\delta \rightarrow 0$. Note again that analysing the polarisation of the virtual gluons showed that longitudinally as well as transversely polarised gluons give rise to poles in δ . In contrast to the Sudakov form factor, the regulator can thus not be implemented in the exponent of Wilson lines in soft or collinear operators.

In the following, we will first verify the results in Eqs. (7.10) and (7.11) using the naive factorisation formula Eq. (6.67). Afterwards, we derive the remaining double poles in ε from the factorised expression.

Collinear region The result in Eq. (7.10) can be reproduced from the naive factorisation formula by evaluating the collinear matrix elements at $\mathcal{O}(\alpha_s)$ and the soft matrix elements at tree-level. Most of the occurring LCDAs in the non-relativistic setup have been calculated in [119] up to $\mathcal{O}(\alpha_s)$, see Appendix D.1. An expression for the 3-particle LCDA $\phi_{3\pi}$ is not provided in the literature, but the occurring moments can be expressed through moments of 2-particle LCDAs and an endpoint-finite moment of $\phi_{3\pi}$ by means of the equation of motion in Eq. (6.61). Dropping endpoint-finite moments in the collinear

sector,² Eq. (6.67) then reduces to

$$\frac{\xi_\eta^{(c)}(E)}{\xi_0} \simeq \frac{1}{m_{\bar{q}}} \int_0^1 du \left[-C_{FA} \frac{\phi_\eta(u)}{\bar{u}^2} + \left(2C_F + \frac{C_A}{2} \right) \frac{\mu_\eta}{m_{\bar{q}}} \frac{\phi_P(u)}{\bar{u}} + \frac{C_A}{2} \frac{\tilde{\mu}_\eta}{6m_{\bar{q}}} \frac{\phi'_\sigma(u)}{\bar{u}} \right]. \quad (7.13)$$

At one-loop order our choice of the analytic regulator, ν^δ/k_-^δ , amounts to an additional factor of $\nu^\delta/(2E\bar{u})^\delta$ in moments of collinear 2-particle LCDAs. Hence, we can compute the regularised moments with the expressions given in the literature. We find the following results for the leading poles:

$$\begin{aligned} \int_0^1 du \frac{\phi_\eta^{(1)}(u)}{\bar{u}^2} \left(\frac{\nu}{2E\bar{u}} \right)^\delta &\simeq \frac{\alpha_s(\mu)C_F}{4\pi} \left(-\frac{2}{\delta\varepsilon} \right) \left(\frac{\mu^2}{m_{\bar{q}}^2} \right)^\varepsilon \left(\frac{\nu}{2\gamma m_{\bar{q}}} \right)^\delta \frac{1+\bar{u}_0}{\bar{u}_0^2}, \\ \int_0^1 du \frac{\mu_\eta^{(0)} \phi_P^{(1)}(u)}{\bar{u}} \left(\frac{\nu}{2E\bar{u}} \right)^\delta &\simeq \frac{\alpha_s(\mu)C_F}{4\pi} m_\eta \left(-\frac{2}{\delta\varepsilon} \right) \left(\frac{\mu^2}{m_{\bar{q}}^2} \right)^\varepsilon \left(\frac{\nu}{2\gamma m_{\bar{q}}} \right)^\delta \frac{1+\bar{u}_0}{\bar{u}_0}, \\ \int_0^1 du \frac{\tilde{\mu}_\eta^{(1)}}{6} \frac{\phi'_\sigma^{(0)}(u)}{\bar{u}} \left(\frac{\nu}{2E\bar{u}} \right)^\delta &\simeq \frac{\alpha_s(\mu)C_F}{4\pi} m_\eta \left(+\frac{2}{\delta\varepsilon} \right) \left(\frac{\mu^2}{m_{\bar{q}}^2} \right)^\varepsilon \left(\frac{\nu}{2\gamma m_{\bar{q}}} \right)^\delta \frac{1}{\bar{u}_0}. \end{aligned} \quad (7.14)$$

Note that we showed by explicit calculation of the endpoint-divergent moments of $\phi_{3\pi}$ from the perturbative expansion of the matrix element Eq. (6.54), that the equations of motion hold in this approximation. Plugging the above results back into Eq. (7.13) reproduces the result from the diagrammatic calculation in Eq. (7.10).

Soft region I: endpoint contribution Analogously, neglecting endpoint-finite soft moments and evaluating collinear LCDAs at tree-level, the poles in δ arising in the soft region can be extracted from

$$\frac{\xi_\eta^{(s)}(E)}{\xi_0} \simeq \int_0^\infty d\omega \left[\frac{\phi_B^-(\omega)}{\omega} C_F \frac{1+\bar{u}_0}{\bar{u}_0^2} + m_{\bar{q}} \frac{\phi_B^+(\omega)}{\omega^2} \left(\frac{C_F}{\bar{u}_0} - \frac{C_{FA}}{\bar{u}_0^2} \right) \right]. \quad (7.15)$$

Here we again used the equation of motion Eq. (6.49) to substitute moments of the 3-particle LCDA Ψ_{A-V} through moments of 2-particle LCDAs.³ In the soft sector the regulator ν^δ/k_+^δ would correspond to a factor of ν^δ/ω^δ in one-loop moments of $\phi_B^\pm(\omega)$.

²Endpoint divergences arise from $\bar{u} \rightarrow 0$ or $\alpha_{\bar{q}} \rightarrow 0$. The only endpoint-finite moments that appear in this calculation are

$$\int_0^1 du \frac{\phi_\pi(u)}{\bar{u}} \quad \text{and} \quad \int \mathcal{D}\alpha \frac{\phi_{3\pi}(\{\alpha_i\})}{\alpha_g(\alpha_g + \alpha_{\bar{q}})^2}. \quad (7.12)$$

³Endpoint divergences in the soft sector arise from $\omega \rightarrow 0$. We use $\frac{1}{\omega\xi(\omega+\xi)} = \frac{1}{\omega(\omega+\xi)^2} + \frac{1}{\xi(\omega+\xi)^2}$ and drop the endpoint-finite moments

$$\int_0^\infty d\omega \frac{\phi_B^+(\omega)}{\omega} \quad \text{and} \quad \int_0^\infty d\omega \int_0^\infty d\xi \frac{\Psi_{A-V}(\omega, \xi)}{\xi(\omega + \xi)^2}. \quad (7.16)$$

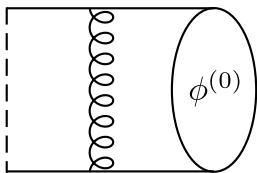


Figure 7.2: Relativistic correction to the LCDAs ϕ_B^\pm that gives rise to a pole in δ in endpoint-divergent moments (adapted from [119]). The dashed line indicates the Wilson line in the definition of the LCDAs (which is trivial for $n \cdot A_s = 0$).

Raising the power of k_- , however, results in an intrinsic dependence of the LCDAs on the analytic regulator. We thus should not use the expressions for the soft LCDAs given in the literature and rather repeat their derivation in the presence of analytic regularisation. We stress that these objects are no longer defined through the usual hadronic matrix elements of soft operators, and that their relation to the actual LCDAs is not clear to us. Instead of calculating distribution-valued LCDAs, we choose to perform the calculation at the level of the inverse moments. This has the advantage that we can directly extract the poles in δ from loop integrals. Moreover, we work in light-cone gauge, $n \cdot A_s = 0$, which implies the Feynman rule for the gluon propagator

$$\frac{-i}{k^2 + i\varepsilon} \left(g_{\mu\nu} - \frac{n^\mu k^\nu + n^\nu k^\mu}{n \cdot k} \right). \quad (7.17)$$

In this gauge only the one diagram shown in Fig. 7.2 gives a $1/\delta$ contribution to endpoint-divergent moments at one-loop order. We find for the two relevant 2-particle moments in the soft sector:

$$\begin{aligned} 2m_{\bar{q}} \int_0^\infty \frac{d\omega}{\omega^2} \phi_B^{+, (1)}(\omega; \delta) &\simeq \int_0^\infty \frac{d\omega}{\omega} \phi_B^{-, (1)}(\omega; \delta) \\ &\simeq \frac{\alpha_s(\mu) C_F}{4\pi} \frac{1}{m_{\bar{q}}} \left(\frac{\mu^2}{m_{\bar{q}}^2} \right)^\varepsilon \left(\frac{\nu}{m_{\bar{q}}} \right)^\delta \left(\frac{4}{\delta\varepsilon} - \frac{4}{\varepsilon^2} \right). \end{aligned} \quad (7.18)$$

Again, we have checked that this is in agreement with the constraint from the equation of motion Eq. (6.49). Plugging this result back into Eq. (7.15) gives the the one-loop expression in the soft region given in Eq. (7.11).

To summarise, we reproduced the results obtained in full QCD at tree-level and for the endpoint contributions at one-loop order in the soft and the collinear region. This is a non-trivial cross-check for the validity of the naive factorisation formula Eq. (6.67). In the following, we thus use the factorised expression to derive the remaining divergences. They arise in the hard-collinear and the hard region as well as due to the cusp in the soft sector. The cancellation of poles then serves as another cross-check.

Soft region II: cusp contribution In contrast to the Sudakov form factor, there is an additional source of double poles in ε in the soft region that is completely independent of the endpoint. These poles rather arise due to the cusp between two Wilson-lines and are treated in the standard renormalisation of the B -meson LCDAs. The HQET field

h_v can be described by a Wilson line in the v^μ direction multiplied with a sterile field. This Wilson line forms a cusp with the usual soft Wilson line in the n^μ direction in the definition of the SCET_{II} operators. The corresponding anomalous dimension is thus proportional to γ_{cusp} and the RG evolution resums large double-logarithms associated with double-poles in ε [104]. This source of double logarithms is only present in the soft region since the collinear SCET_{II} operators do not involve a HQET field. The corresponding contribution to ξ_η can be calculated using the one-loop \bar{B}_c -meson LCDAs given in Appendix D.1, and evaluating the collinear LCDAs at tree-level. The result is proportional to the tree-level soft form factor. We find:

$$\frac{\xi_\eta^{(s),\text{cusp}}(E)}{\xi_\eta^{(0)}(E)} \simeq -\frac{\alpha_s(\mu)C_F}{4\pi} \frac{1}{\varepsilon^2} \left(\frac{\mu^2}{m_q^2}\right)^\varepsilon. \quad (7.19)$$

Hard and hard-collinear region The remaining two contributions come from the hard-collinear and the hard region. In the former we take Eq. (6.68) evaluated with tree-level soft and collinear wave-functions, which yields (up to parametrically small logarithms)

$$\xi_\eta^{(hc)}(E) \simeq \frac{\xi_0 C_F}{m_\eta} \frac{\alpha_s(\mu)}{\pi} \frac{1}{\varepsilon^2} \left(\frac{\mu^2}{2\gamma m_q^2}\right)^\varepsilon \left(2C_F \frac{1+\bar{u}_0}{\bar{u}_0^3} - \frac{C_{FA}}{2} \frac{1}{\bar{u}_0^3}\right). \quad (7.20)$$

Together with the hard function in Eq. (6.9), which contributes e.g. to F_+ as

$$H_+^{(1)}(E) \xi_\eta^{(0)}(E) \simeq -\frac{\alpha_s(\mu)C_F}{4\pi} \left(\frac{\mu^2}{m_b^2}\right)^\varepsilon \frac{\xi_\eta^{(0)}(E)}{\varepsilon^2}, \quad (7.21)$$

we can now explicitly check the cancellation of all double-poles and compute the double-logarithm in the non-factorisable contribution to the form factors at one-loop order. The sum of collinear, soft, hard-collinear and hard region yields up to single-logarithms:

$$F_+^{(1),\text{non-fac.}} \simeq H_+^{(0)} \xi_\eta^{(1)} + H_+^{(1)} \xi_\eta^{(0)} \simeq \frac{\xi_0 C_F}{m_\eta} \frac{\alpha_s(\mu)}{4\pi} \left(\frac{2C_F}{\bar{u}_0^2} - \frac{C_{FA}}{\bar{u}_0^3}\right) \log(2\gamma)^2. \quad (7.22)$$

We notice that the argument of the logarithm is the large Lorentz boost between the rest frames of the \bar{B}_c and the η_c meson. This result shows that the double logarithms are not incorporated in a simple Sudakov factor e^{2S} that multiplies the tree-level result. We will see that this is due to a mixing between the various matrix elements of $\mathcal{O}_{m,1-4}$ under (rapidity) renormalisation group evolution.

7.3 Resummation of Leading Logarithms

We now aim at a resummation of all leading logarithms in the NR setup. Therefore, we first derive recursion relations for endpoint-divergent moments and, at least in the soft sector, solve them explicitly. The solutions resum leading endpoint singularities $\sim \left(\frac{\alpha_s}{\delta\varepsilon}\right)^n$ to all orders in α_s . Subsequently, we interpret these relations as the computation of usual Z -factors and derive analytical solutions to the corresponding rapidity RGEs in the LL

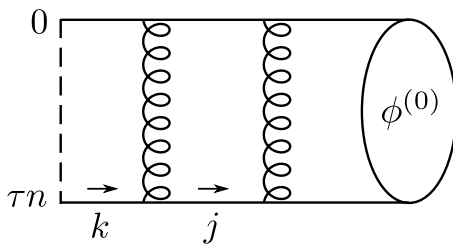


Figure 7.3: Example diagram for a two-loop relativistic correction to the 2-particle \bar{B}_c -meson LCDAs, whose contribution to endpoint-sensitive moments receives a double pole in δ . Recall that the heavy-quark field lives at spacetime point 0 and the spectator-quark field at τn . The dashed line indicates the Wilson line which extends from 0 to τn .

approximation. We find that both solutions are in agreement. Since endpoint divergences arise only at the level of inverse moments, we investigate their evolution instead of discussing the usual evolution of the LCDAs. Finally, we include the evolution of the hard function and the hard-collinear scattering kernel and give a resummed expression for the product $H_i \xi_\eta$ in the LL approximation.

7.3.1 Recursion Relations for Inverse Moments

In the previous section we showed the cancellation of poles of the form $\frac{\alpha_s}{\delta\varepsilon}$ at one-loop order between the soft and the collinear region. The sum of Eqs. (7.10) and (7.11) gives

$$\xi_\eta^{(c)} + \xi_\eta^{(s)} \simeq \frac{\xi_0 C_F \alpha_s(\mu)}{m_\eta} \frac{1}{4\pi} \left(\frac{\mu^2}{m_q^2} \right)^\varepsilon \frac{1}{\varepsilon} \left[6C_F \frac{1 + \bar{u}_0}{\bar{u}_0^3} - \frac{C_A}{\bar{u}_0^3} \right] \log^2(2\gamma). \quad (7.23)$$

In Appendix D.2 we extend this calculation to two loops and show that the leading poles $\sim \left(\frac{\alpha_s}{\delta\varepsilon} \right)^2$ cancel in the sum of the double-soft, the double-collinear and the mixed soft-collinear region. Here we find

$$\begin{aligned} & \xi_\eta^{(s-s)} + \xi_\eta^{(c-c)} + \xi_\eta^{(s-c)} \\ & \simeq \frac{\xi_0 C_F}{m_\eta} \left(\frac{\alpha_s(\mu)}{4\pi} \right)^2 \left(\frac{\mu^2}{m_q^2} \right)^{2\varepsilon} \frac{2}{\varepsilon^2} \left[4C_F^2 \frac{1 + \bar{u}_0}{\bar{u}_0^3} - \frac{C_A C_F}{2} \frac{2 + \bar{u}_0}{\bar{u}_0^3} \right] \log^2(2\gamma). \end{aligned} \quad (7.24)$$

We will now show the cancellation of these singularities to all orders in α_s and derive a resummed expression for the resulting large logarithms. Since hard-collinear loops do not cause poles in δ , it is sufficient to study tree-level hard-collinear exchanges that are captured in the naive factorisation formula Eq. (6.67). While investigating the Sudakov form factor we found that the considered poles cause the logarithms that exponentiate with the collinear anomaly. However, the expression that we derive for ξ_η has a more complicated structure than a simple exponential.

The main observation that leads to the resummation is that the leading poles in δ in inverse moments show a recursive behaviour. Consider for example the contribution of the two-loop ladder-type diagram in Fig. 7.3 to an endpoint-divergent soft moment. We regularise the integral by raising the power of the $\bar{n} \cdot k_i$ component of both loop momenta

by δ , i.e. we write a factor of ν^δ/k_-^δ and a factor of ν^δ/j_-^δ in the integrand. Here k^μ is the loop momentum assigned to the spectator-quark propagator that is attached to the spacetime point τn (so $k_+ = \omega$) and j^μ is the loop momentum assigned to the neighbouring spectator-quark propagator. Furthermore, we work in light-cone gauge, $n \cdot A_s = 0$. When performing the k_- and j_- integrations with contour methods, the double pole in δ comes from the region where first the limit $k_+ \rightarrow 0$ and then $j_+ \rightarrow 0$ is taken. As shown in Appendix D.2, instead of investigating the pole structure of all propagators, in the approximation under consideration we obtain the same result Eq. (D.23) by considering the integrations successively. That is, we perform the k_- integration with contour methods, separate the pole in δ in the k_+ integration and repeat the same steps for the $d^d j$ integral thereafter.

This can be generalised to arbitrarily many loops. An n -loop diagram that generates a pole $\sim \left(\frac{\alpha_s}{\delta\varepsilon}\right)^n$ must contain n spectator-quark propagators and each loop integration must account for one factor of $\frac{\alpha_s}{\delta\varepsilon}$. We now note that the endpoint contribution of the first integration (with the spectator-quark propagator that sits next to τn) is proportional to an inverse moment of an LCDA at $\mathcal{O}(\alpha_s^{n-1})$. This gives the desired recursion relations that will be discussed below in Eq. (7.25). Here we find a mixing between moments associated with different currents, a mixing of 2-particle and 3-particle LCDAs, and also a mixing between endpoint-divergent and endpoint-finite moments.

Figure 7.4 shows all diagrams that contribute to these recurrence relations. In the sum we find the following expressions for the 2-particle endpoint-divergent soft moments:

$$\begin{aligned} \int_0^\infty \frac{d\omega}{\omega^2} \phi_B^{+, (n)}(\omega; \delta) &\simeq \frac{\alpha_s(\mu)}{4\pi} 2C_F \left(\frac{\mu^2}{m_q^2}\right)^\varepsilon \left(\frac{1}{\delta\varepsilon} - \frac{1}{\varepsilon^2}\right) \int_0^\infty \frac{d\omega}{\omega^2} \left(\frac{\nu\omega}{m_q^2}\right)^\delta \phi_B^{+, (n-1)}(\omega; \delta), \\ \int_0^\infty \frac{d\omega}{\omega} \phi_B^{-, (n)}(\omega; \delta) &\simeq \frac{\alpha_s(\mu)}{4\pi} \left(\frac{\mu^2}{m_q^2}\right)^\varepsilon \left(\frac{1}{\delta\varepsilon} - \frac{1}{\varepsilon^2}\right) \left\{ \right. \\ & 2C_F \int_0^\infty d\omega \left(\frac{\nu\omega}{m_q^2}\right)^\delta \left(\frac{\phi_B^{-, (n-1)}(\omega; \delta)}{\omega} + m_{\bar{q}} \frac{\phi_B^{+, (n-1)}(\omega; \delta)}{\omega^2} \right) \\ & \left. + (d-2) \int_0^\infty d\omega \int_0^\infty d\xi \left(\frac{\nu\omega}{m_q^2}\right)^\delta \frac{\Psi_{A-V}^{(n-1)}(\omega, \xi; \delta)}{(\omega + \xi)^2} \left(\frac{C_A}{\omega} - \frac{2C_{FA}}{\xi} \left[1 - 2 \left(\frac{\xi}{\omega}\right)^\delta \right] \right) \right\}. \end{aligned} \quad (7.25)$$

Several comments about this result are in order.

- In the momentum-space calculation contributions involving the perpendicular component l_\perp^μ of the spectator-quark momentum arise. Analogously to what has been done in the collinear sector in Appendix C.3, the corresponding position-space matrix element can be related to ϕ_B^\pm and Ψ_{A-V} via the equation of motion for the soft spectator-quark field, which translates into:

$$\begin{aligned} \int \frac{d\tau}{2\pi} e^{i\omega\tau} \langle 0 | \bar{Q}_s(\tau n) i \overleftarrow{\not{\partial}}_\perp \not{n} \gamma_5 \mathcal{H}(0) | \bar{B}(v) \rangle &= \frac{i \tilde{f}_B M_B}{2} \left(\right. \\ & \left. \omega \phi_B^-(\omega) - m_{\bar{q}} \phi_B^+(\omega) + (d-2) \int_0^\infty d\tilde{\omega} \int_0^\infty d\tilde{\xi} \frac{\tilde{\Psi}_{A-V}(\tilde{\omega}, \tilde{\xi})}{\tilde{\xi}} \delta(\tilde{\omega} + \tilde{\xi} - \omega) \right). \end{aligned} \quad (7.26)$$

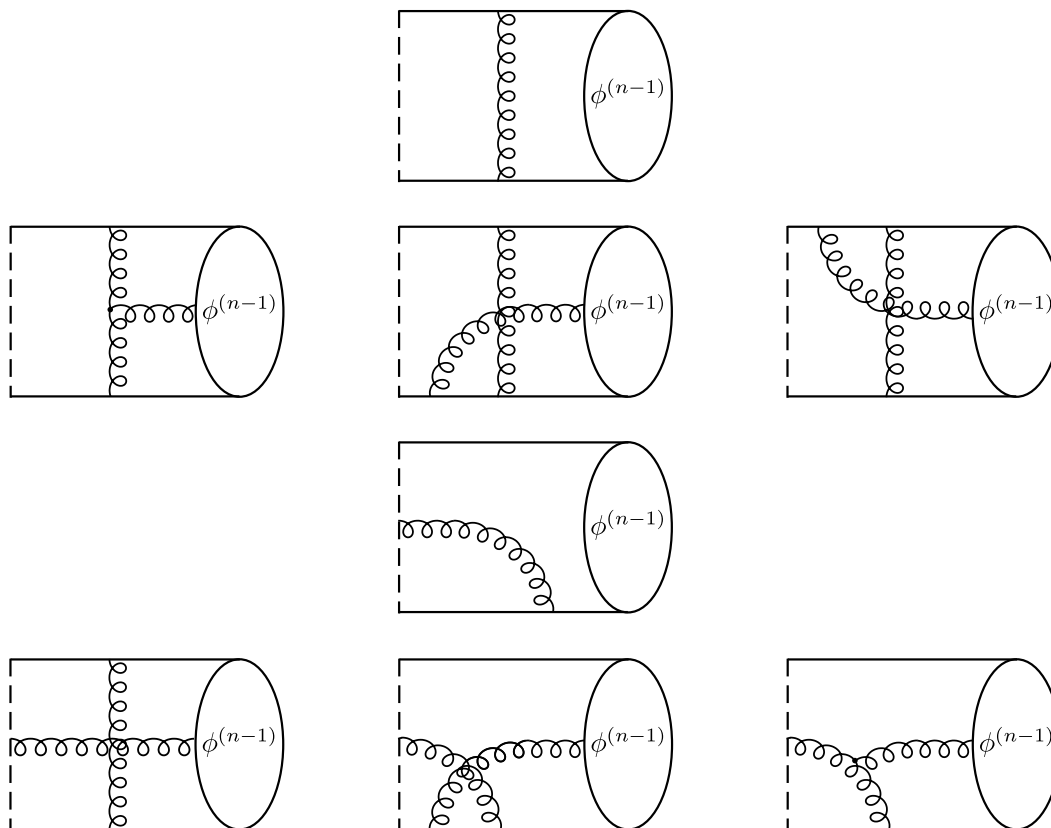


Figure 7.4: Diagrams that determine the recursion relation of endpoint-sensitive moments. The first row contributes to the mixing of moments of 2-particle LCDAs into (different) moments of 2-particle LCDAs. The second row determines the $2 \rightarrow 3$ mixing, the third row the $3 \rightarrow 2$ mixing and the fourth row the $3 \rightarrow 3$ mixing. Note that gluons attached to $\phi^{(n-1)}$ as well as gluons coming from the operator (dashed line) have perpendicular polarisation and are thus not associated with Wilson lines. As an example, the leading poles in δ of the two-loop ladder-type diagram in Fig. 7.3 are given by a successive integration of two times the first diagram; the contribution of the non-abelian diagram in Fig. D.1 by integrating the loops of the second and then the fifth diagram.

- In addition to the δ -dependence of the LCDAs on the right-hand side, the performed longitudinal k_+ integration gives an additional factor of $\left(\frac{\nu\omega}{m_q^2}\right)^\delta$ (or $\left(\frac{\nu\xi}{m_q^2}\right)^\delta$). We cannot expand and truncate in δ at this point because the factor serves as a regulator for the remaining integrals. As a consequence, for each $n \cdot k_i$ integration the power of the regulator for the remaining integrals is increased by δ . Hence, the leading poles in δ of an endpoint-sensitive moment at $\mathcal{O}(\alpha_s^n)$ have the form $\sim \frac{1}{\delta} \cdot \frac{1}{2\delta} \dots \frac{1}{n\delta} = \frac{\delta^{-n}}{n!}$, which already shows their exponential structure.
- We observe that the second inverse moment of ϕ_B^+ does not mix into other moments. Hence, the leading pole in δ simply exponentiates. In general, however, we find a mixing into endpoint-divergent and endpoint-finite moments.
- We explicitly checked that the endpoint-divergent moment of Ψ_{A-V} is consistent with the constraint from the equation of motion Eq. (6.49) in the desired approximation. Thus, we do not show the respective result here. On the one hand this is a useful cross-check of our calculation. On the other hand it shows that the equations of motion for the LCDAs in the presence of analytic regularisation can be used to resum the leading poles in δ . Note that the previous bullet point implies that all diagrams contributing to $3 \rightarrow 3$ mixing (fourth row in Fig. 7.4) are endpoint finite. This is confirmed by the calculation.
- Using Eq. (7.25) we can reproduce the leading endpoint contributions of the moments at one-loop (given in Eq. (7.18)) and at two-loop order (Eq. (D.24)).

We proceed with the analogous relations for endpoint-divergent moments in the collinear sector. Using the linear combinations $m_\eta \phi_{P\pm\sigma'}(u) \equiv \mu_\eta \phi_P(u) \pm \frac{\bar{\mu}_\eta}{2d-2} \phi'_\sigma(u)$ simplifies the expressions to some extent. We obtain:

$$\begin{aligned}
 \int_0^1 \frac{du}{\bar{u}^2} \phi_\eta^{(n)}(u; \delta) &\simeq \frac{\alpha_s(\mu)}{4\pi} 2C_F \left(\frac{\mu^2}{m_q^2}\right)^\varepsilon \left(-\frac{1}{\delta\varepsilon}\right) \int_0^1 du \left(\frac{\nu}{2\bar{u}E}\right)^\delta \frac{1+\bar{u}}{\bar{u}^2} \phi_\eta^{(n-1)}(u; \delta), \\
 \int_0^1 \frac{du}{\bar{u}} \phi_{P-\sigma'}^{(n)}(u; \delta) &\simeq \frac{\alpha_s(\mu)}{4\pi} \left(\frac{\mu^2}{m_q^2}\right)^\varepsilon \left(-\frac{1}{\delta\varepsilon}\right) \left\{ \right. \\
 &\quad \left. 2C_F \int_0^1 du \left(\frac{\nu}{2\bar{u}E}\right)^\delta \left(\frac{\phi_{P-\sigma'}^{(n-1)}(u; \delta)}{\bar{u}} + \phi_\eta^{(n-1)}(u; \delta) \left[\frac{2+\bar{u}}{\bar{u}^2} \bar{u}_0 - \frac{1}{\bar{u}} \right] \right) \right. \\
 &\quad \left. - \frac{f_{3\eta}}{m_\eta f_\eta} (d-2) \int \mathcal{D}\alpha \left(\frac{\nu}{2\alpha_{\bar{q}}E}\right)^\delta \frac{\phi_{3\eta}(\{\alpha_i\})}{(\alpha_g + \alpha_{\bar{q}})^2} \left(\frac{2C_F + C_A}{\alpha_{\bar{q}}} - \frac{2C_{FA}}{\alpha_g} \left[1 - 2 \left(\frac{\alpha_{\bar{q}}}{\alpha_g}\right)^\delta \right] \right) \right\}, \\
 \int_0^1 \frac{du}{\bar{u}} \phi_{P+\sigma'}^{(n)}(u; \delta) &\simeq \frac{\alpha_s(\mu)}{4\pi} 2C_F \left(\frac{\mu^2}{m_q^2}\right)^\varepsilon \left(-\frac{1}{\delta\varepsilon}\right) \bar{u}_0 \int_0^1 \frac{du}{\bar{u}} \left(\frac{\nu}{2\bar{u}E}\right)^\delta \phi_\eta^{(n-1)}(u; \delta).
 \end{aligned} \tag{7.27}$$

All comments that we made above remain true for these results.

Usually one would interpret the above expressions as Z -factors in one-loop corrections to the moments. However, we are not allowed to expand and truncate in δ as long as the convolution integral itself requires regularisation. Thus, we first study the explicit solutions of the recursion relations. We shift their derivation to Appendix D.3 and only show the results here. Furthermore, we only consider the relevant soft moments. For the second inverse moment of ϕ_B^+ we find a simple exponential (we ignore the double-pole in ε for the moment):

$$\int_0^\infty \frac{d\omega}{\omega^2} \phi_B^+(\omega; \delta) \simeq \int_0^\infty \frac{d\omega}{\omega^2} \phi_B^{+, (0)}(\omega) \exp \left\{ \frac{F_{\text{div.}}^{(1)}}{\delta} \left(\frac{\nu\omega}{m_q^2} \right)^\delta \right\}, \quad (7.28)$$

where we identify the divergent contribution of the one-loop anomaly as

$$F_{\text{div.}}^{(1)} = \frac{\alpha_s(\mu)}{4\pi} \left(\frac{\mu^2}{m_q^2} \right)^\varepsilon \frac{2C_F}{\varepsilon}, \quad (7.29)$$

which is (up to a colour factor C_F) exactly the same anomaly coefficient as in the Sudakov form factor, see Eq. (5.64). The exponentiation happens already in the integration variable ω and the resummed expression is to be convoluted with the tree-level LCDA in the LL approximation. Since this convolution is always well-defined, the right-hand side of Eq. (7.28) can be expanded in δ . Note, however, that we do not have to perform this convolution in order to show the cancellation of the leading poles in ξ_η . The first inverse moment of ϕ_B^- has a more complicated structure. Neglecting contributions that are of subleading logarithmic order in the non-relativistic setup we find:

$$\begin{aligned} \int_0^\infty \frac{d\omega}{\omega} \phi_B^-(\omega; \delta) \simeq \int_0^\infty d\omega \left\{ \frac{\phi_B^{-, (0)}(\omega)}{\omega} \exp \mathcal{E} \right. \\ \left. - m_{\bar{q}} \frac{C_{FA}}{C_F} \frac{\phi_B^{+, (0)}(\omega)}{\omega^2} \mathcal{E} \exp \mathcal{E} + \frac{C_A}{2C_F} \frac{\phi_B^{+, (0)}(\omega)}{\omega} (\exp \mathcal{E} - 1) \right\}, \end{aligned} \quad (7.30)$$

with the abbreviation for the factors that go in the exponent:

$$\mathcal{E} \equiv \frac{F_{\text{div.}}^{(1)}}{\delta} \left(\frac{\nu\omega}{m_q^2} \right)^\delta = \frac{\alpha_s(\mu)}{4\pi} \left(\frac{\mu^2}{m_q^2} \right)^\varepsilon \frac{2C_F}{\delta\varepsilon} \left(\frac{\nu\omega}{m_q^2} \right)^\delta. \quad (7.31)$$

The various structures in this result arise due to mixing. In particular, the second term arises due to a mixing into a different endpoint-divergent moment,⁴ whereas the last term comes from a mixing into an endpoint-finite moment. Note that both contributions in the second line are of $\mathcal{O}(\alpha_s)$ and thus, in the fixed-order expansion, the colour factor C_F in the denominator always gets cancelled by a C_F from the anomaly.

We can construct similar solutions in the collinear sector and show that the poles in δ cancel in ξ_η to all orders. However, we postpone this to the next subsection. First, we notice that the leading-twist LCDA of the η_c -meson convoluted with the kernel $\frac{1+\bar{u}}{\bar{u}^2}$

⁴Similar structures with an explicit logarithm, which does not exponentiate, were also found in a subleading-power resummation in [128].

exponentiates in a similar way as the second inverse moment of ϕ_B^+ . Thus, in a hypothetical contribution of a product of these two moments the leading poles in δ would drop out to all orders in α_s :

$$\begin{aligned} & \int_0^\infty d\omega \frac{\phi_B^+(\omega; \delta)}{\omega^2} \int_0^1 du \phi_\eta(u; \delta) \frac{1 + \bar{u}}{\bar{u}^2} \\ & \simeq \int_0^\infty d\omega \frac{\phi_B^{+, (0)}(\omega)}{\omega^2} \int_0^1 du \phi_\eta^{(0)}(u) \frac{1 + \bar{u}}{\bar{u}^2} \left(\frac{2\bar{u}E\omega}{m_q^2} \right)^{F_{\text{div.}}^{(1)}} = \frac{1}{m_q^2} \frac{1 + \bar{u}_0}{\bar{u}_0^2} (2\gamma)^{F_{\text{div.}}^{(1)}}. \end{aligned} \quad (7.32)$$

The observed exponentiation in this simple product is determined by the collinear anomaly argument, i.e. that the ν -dependence must drop out between the two moments. However, whereas in the Sudakov form factor the large ratio Q^2/m^2 comes with the exponent $-F$, the large boost (2γ) in ξ_η exponentiates with $+F$. As a consequence, this leads to an enhancement of ξ_η instead of the usual Sudakov suppression, which slightly overcompensates the suppression from the hard matching coefficient. This will be shown numerically towards the end of this chapter.

7.3.2 Rapidity Renormalisation Group Treatment of Inverse Moments

So far we were cautious in treating the recursive expressions in the standard renormalisation procedure. Nevertheless, we will now derive and solve rapidity RGEs for the inverse moments. This is justified only in the LL approximation by the following argument. In the soft region, for example, we can rewrite the logarithm generated by the expansion of the factor $\frac{1}{\delta} \left(\frac{\nu\omega}{m_q^2} \right)^\delta$ in δ via

$$\log \frac{\nu\omega}{m_q^2} = \log \frac{\nu}{\nu_s} + \log \frac{\omega\nu_s}{m_q^2}, \quad (7.33)$$

with a soft rapidity scale $\nu_s \sim m_{\bar{q}}$. Even in divergent moments the second logarithm is parametrically small and can be dropped in the LL approximation.⁵ Then the right-hand side of the recursion relations can be interpreted as (matrix-valued) Z -factors *multiplying* (a vector of) renormalised moments. This allows us to treat the inverse moments in the standard rapidity RG approach. The solutions of the corresponding RGEs confirm the solutions of the recursion relations given in Eqs. (7.28) and (7.30), when the renormalised LCDAs evaluated at their typical rapidity scales are identified with the tree-level expressions. We will now derive these solutions for soft and collinear moments and eventually check the ν -independence of the soft form factor ξ_η . Since the evolution in μ and ν is path independent, we can investigate the μ evolution thereafter. Here we use an analogous replacement of logarithms in the renormalisation of the hard-collinear function.

⁵The dependence on the explicit kinematic variables arising in the logarithms feed into subleading logarithms only. This can be seen e.g. in the solutions that we derived for the hard and the remainder function in the Sudakov form factor Eq. (5.74). Another example would be the endpoint-finite first inverse moment $\lambda_B^{-1}(\mu)$, which in general mixes into logarithmic moments, see e.g. [114]. The LL solution however is simply $\lambda_B^{-1}(\mu) = e^{S(\mu_s, \mu)} \lambda_B^{-1}(\mu_s)$ (see also Eq. (7.58)), so this mixing is again a subleading effect.

The analytic regulator is intrinsically part of the (bare) distribution amplitudes. Correspondingly, the renormalised objects now depend on the scales μ and ν . We stress again that their general relation to the actual LCDAs defined as hadronic matrix elements of non-local operators remains unclear at this point. We nevertheless denote them by the same symbol but indicate their ν -dependence as an explicit argument such that it is always clear to which object we refer. In endpoint-finite moments, such as the first inverse moment of $\phi_B^+(\omega; \mu)$, the ν -dependence of the LCDA can be dropped.

Before deriving the RGEs, we rewrite the naive factorisation formula for tree-level hard-collinear exchanges Eq. (6.67) in a slightly different form. To this end, we define the following vector in the soft sector

$$\vec{M}(\omega; \varepsilon, \delta) = \left(\frac{m_{\bar{q}}^2}{\omega^2} \phi_B^+(\omega; \varepsilon, \delta), \frac{m_{\bar{q}}}{\omega} \phi_B^-(\omega; \varepsilon, \delta), \frac{m_{\bar{q}}}{\omega} \phi_B^+(\omega; \varepsilon) \right), \quad (7.34)$$

where we introduced factors of $m_{\bar{q}}$ to keep the dimension in all entries homogeneous, and similarly in the collinear sector

$$\vec{N}(u; \varepsilon, \delta) = \left(\frac{1 + \bar{u}}{\bar{u}^2} \phi_\eta(u; \varepsilon, \delta), \frac{\phi_{P-\sigma'}(u; \varepsilon, \delta)}{\bar{u}}, \frac{\phi_{P+\sigma'}(u; \varepsilon, \delta)}{\bar{u}}, \frac{\phi_\eta(u; \varepsilon)}{\bar{u}} \right). \quad (7.35)$$

Employing the equations of motion to replace endpoint-divergent moments of 3-particle LCDAs and dropping terms that are not relevant for the resummation of leading logarithms,⁶ the soft form factor can then be written as the bilinear form

$$\xi_\eta^{\text{hc0}} = \frac{\xi_0 C_F}{m_\eta} \int_0^\infty d\omega \int_0^1 du \vec{M}^T \cdot J^{(0)} \cdot \vec{N}, \quad (7.36)$$

with $J^{(0)}$ being a matrix whose entries are functions of colour factors and mass ratios only:

$$J^{(0)} = \frac{1}{\bar{u}_0} \begin{pmatrix} -\frac{C_A}{C_F} & \frac{1}{\bar{u}_0} & \frac{2C_F + C_A}{2C_F \bar{u}_0} & \frac{C_A \bar{u}_0 - C_F u_0}{C_F \bar{u}_0} \\ 1 & 0 & 0 & 0 \\ \frac{C_A}{2C_F} & 0 & 0 & -\frac{2C_F + C_A}{2C_F} \end{pmatrix}. \quad (7.37)$$

For the resummation of all leading logarithms we should also take into account the hard function as well as the subset of one-loop hard-collinear corrections calculated in the previous chapter. We would like to cast the latter one into a similar bilinear form as Eq. (7.36). Here the additional endpoint-finite moment $\langle u^{-1} \rangle_\eta$ of the leading-twist LCDA ϕ_η arises in Eq. (6.68), which we should add to the vector \vec{N} . It is then straightforward to construct a matrix $J^{(1)}$ incorporating the one-loop hard-collinear effects. However, in their calculation we assumed that Ψ_{A-V} , $\phi_{3\eta}$ and $\tilde{\mu}_\eta$ are $\mathcal{O}(\alpha_s)$ suppressed. Similar to the Wandzura-Wilczek approximation, the equations of motion for the collinear LCDAs can be solved explicitly in this limit leading to the tree-level delta-distributions for ϕ_η and ϕ_P . This allows us to relate the new moment to the ones already contained in \vec{N} and

⁶That is, endpoint-finite moments of 3-particle LCDAs can be neglected since they do neither cause leading poles in δ nor in ε and their tree-level matrix element is zero.

we can rewrite the double-poles in ε of the hard-collinear corrections as a matrix-valued Z -factor multiplying $J^{(0)}$:

$$J^{(1)}(\omega, u; \varepsilon) \Big|_{1/\varepsilon^2} = Z_J^{(1)}(\omega, u; \varepsilon, \mu) \cdot J^{(0)}. \quad (7.38)$$

With the explicit expression for $Z_J^{(1)}$ that will be given below, we then reproduce the poles in the one-loop hard-collinear region Eq. (7.20), when we evaluate

$$\xi_\eta^{(hc)} = \frac{\xi_0 C_F}{m_\eta} \int_0^\infty d\omega \int_0^1 du (\vec{M}^T)^{(0)} \cdot J^{(1)} \cdot \vec{N}^{(0)} \quad (7.39)$$

with tree-level LCDAs. In order to show that $H_i \xi_\pi$ is μ independent we thus have to use tree-level expressions for the LCDAs. Recall that this is not necessary to verify the ν -independence of ξ_π .

We now write the μ and ν -independent product $H_i \xi_\eta$ expressed through renormalised quantities as

$$H_+(\mu) \xi_\eta(\mu) = H_+(\mu) \frac{\xi_0 C_F}{m_\eta} \int_0^\infty d\omega \int_0^1 du \vec{M}^T(\omega; \mu, \nu) \cdot J(\omega, u; \mu) \cdot \vec{N}(u; \mu, \nu). \quad (7.40)$$

Note that the collinear moments depend on μ only since their evolution in ν is governed by $A_{\gamma_{\text{cusp}}}(\mu_s, \mu)$. Similar to the discussion around Eq. (7.33), in the LL approximation we can replace logarithms in the hard-collinear region via

$$\log \frac{\mu^2}{2\bar{u}E\omega} = \log \frac{\mu^2}{\mu_{hc}^2} + \log \frac{\mu_{hc}^2}{2\bar{u}E\omega}. \quad (7.41)$$

Here μ_{hc} is a typical hard-collinear scale, $\mu_{hc} \sim \sqrt{m_{\bar{q}} E}$. The second logarithm is again parametrically small and can be dropped, which removes the dependence on ω and u in the matrix J : $J(\omega, u; \mu) \xrightarrow{\text{LL}} J(\mu)$.

Rapidity renormalisation group equations: In the following we summarise the one-loop Z -factors and the resulting RGEs for all quantities arising in the factorisation formula. The Z -factor for the hard function is given in Eq. (6.9). From the recursion relations Eqs. (7.25) and (7.27) we read off the matrix-valued Z -factors for the soft and collinear moments as

$$\begin{aligned} Z_M &= 1 + \frac{\alpha_s(\mu) C_F}{4\pi} \left\{ \left[\frac{2}{\delta\varepsilon} + \frac{2}{\varepsilon} \log \frac{\nu}{\nu_s} + \frac{4}{\delta} \log \frac{\mu}{\mu_s} \right] \cdot B + \left[-\frac{1}{\varepsilon^2} - \frac{2}{\varepsilon} \log \frac{\mu}{\mu_s} \right] \cdot (\mathbb{1} + 2B) \right\}, \\ Z_N &= 1 + \frac{\alpha_s(\mu) C_F}{4\pi} \left[-\frac{2}{\delta\varepsilon} - \frac{2}{\varepsilon} \log \frac{\nu}{\nu_c} - \frac{4}{\delta} \log \frac{\mu}{\mu_s} \right] \cdot C, \end{aligned} \quad (7.42)$$

with $\mu_s \sim \nu_s \sim m_{\bar{q}}$ and $\nu_c \sim E$. Here the matrix B incorporates the mixing among the soft moments,

$$B \equiv \begin{pmatrix} 1 & 0 & 0 \\ -\frac{C_{FA}}{C_F} & 1 & \frac{C_A}{2C_F} \\ 0 & 0 & 0 \end{pmatrix}, \quad (7.43)$$

whereas the part proportional to the unit matrix $\mathbb{1}$ in Z_M comes from the cusp contribution. The mixing among collinear moments is encoded in the matrix

$$C \equiv \begin{pmatrix} 1 & 0 & 0 & 0 \\ -\bar{u}_0 \frac{C_{FA}}{C_F} & 1 & 1 + \frac{C_A}{2C_F} & \bar{u}_0 \frac{C_A}{2C_F} - 1 \\ 0 & 0 & 0 & \bar{u}_0 \\ 0 & 0 & 0 & 0 \end{pmatrix}. \quad (7.44)$$

Finally, the Z -factor for the hard-collinear matrix J is given by

$$Z_J = 1 + \frac{\alpha_s(\mu)C_F}{4\pi} \left[\frac{2}{\varepsilon^2} + \frac{4}{\varepsilon} \log \frac{\mu}{\mu_{hc}} \right] (\mathbb{1} + B^T). \quad (7.45)$$

This result shows the hybrid role of the hard-collinear function. On the one hand the term proportional to the unit matrix in $J(\mu)$ cancels the μ -dependence from the standard evolution of the hard function and of the cusp contribution in the soft sector. On the other hand the term proportional to the matrix B cancels the μ -dependence originating from the endpoint contributions.

These Z -factors determine the rapidity RGEs in the scales ν and μ whose solutions resum large logarithms in the LL approximation. Assuming that all double logarithms renormalise with γ_{cusp} , we find the following evolution equations in ν for the soft and collinear moments:

$$\frac{d}{d \log \nu} \int_0^\infty d\omega \vec{M}(\omega; \mu, \nu) = -A_{\gamma_{\text{cusp}}}(\mu_s, \mu) \int_0^\infty d\omega B \cdot \vec{M}(\omega; \mu, \nu), \quad (7.46)$$

and

$$\frac{d}{d \log \nu} \int_0^1 du \vec{N}(u; \mu, \nu) = +A_{\gamma_{\text{cusp}}}(\mu_s, \mu) \int_0^1 du C \cdot \vec{N}(u; \mu, \nu). \quad (7.47)$$

Note that in QCD the one-loop expression of γ_{cusp} gets an additional colour factor C_F compared to the expression in the non-abelian $U(1)$ -model (see Appendix B.1). The evolution in μ is governed by the equations (remember that $\gamma_{\text{cusp}} \equiv \gamma_{\text{cusp}}(\alpha_s(\mu))$):

$$\begin{aligned} \frac{d}{d \log \mu} \int_0^\infty d\omega \vec{M}(\omega; \mu, \nu) &= -\gamma_{\text{cusp}} \int_0^\infty d\omega \left[-\log \frac{\nu}{\nu_s} B + \log \frac{\mu}{\mu_s} (\mathbb{1} + 2B) \right] \cdot \vec{M}(\omega; \mu, \nu), \\ \frac{d}{d \log \mu} \int_0^1 du \vec{N}(u; \mu, \nu) &= -\gamma_{\text{cusp}} \int_0^1 du \log \frac{\nu}{\nu_c} C \cdot \vec{N}(u; \mu, \nu). \end{aligned} \quad (7.48)$$

For the hard and the hard-collinear function we find (with a typical hard scale $\mu_h \sim m_b$):

$$\begin{aligned} \frac{d}{d \log \mu} H_i(\mu) &= -\gamma_{\text{cusp}} \log \frac{\mu}{\mu_h} H_i(\mu), \quad (i = +, -, T), \\ \frac{d}{d \log \mu} J(\mu) &= 2\gamma_{\text{cusp}} \log \frac{\mu}{\mu_{hc}} (\mathbb{1} + B^T) \cdot J(\mu). \end{aligned} \quad (7.49)$$

With the help of this set of equations it is easy to check that the product $H_i(\mu) \xi_\eta(\mu)$ is ν and μ independent in the LL approximation. This means that $\frac{d}{d \log \mu} H_i(\mu) \xi_\eta(\mu)$ is not identical to zero, but the resulting logarithms combine to a parametrically small logarithm that we should drop. In particular, we adopt the scaling $\mu_{hc} \sim \sqrt{\mu_h \mu_s}$ for typical hard-collinear virtualities as well as $\nu_s \sim \mu_s$ and $\nu_c \sim \mu_h$ for soft and collinear rapidities. To guarantee the ν -independence of ξ_η we need to demand that

$$J(\mu) \cdot C - B^T \cdot J(\mu) = 0, \quad (7.50)$$

which is confirmed using the explicit solution for $J(\mu)$ given in Eq. (7.62).

Since the evolutions in ν and μ commute we can perform the running in ν first and afterwards solve simpler RGEs in μ for objects evaluated at their natural rapidity scales. In particular, the evolution in μ simplifies for the soft moments $\vec{M}(\omega; \mu, \nu_s)$, and becomes trivial for the collinear moments $\vec{N}(u; \mu, \nu_c)$. Note that this changes for a different choice of the analytic regulator.

Evolution in ν : The resummation of rapidity logarithms generated through a cancellation of the poles in δ can be achieved by an evolution in the scale ν . Equation (7.46) contains the trivial solution for the ν -independent (endpoint finite) first inverse moment of the LCDA ϕ_B^+ . The solution for the second inverse moment of ϕ_B^+ gives a simple exponential:

$$\int_0^\infty d\omega \frac{\phi_B^+(\omega; \nu)}{\omega^2} = \int_0^\infty d\omega \frac{\phi_B^+(\omega; \nu_s)}{\omega^2} \left(\frac{\nu}{\nu_s} \right)^{-A}, \quad (7.51)$$

with $A \equiv A_{\gamma_{\text{cusp}}}(\mu_s, \mu)$. This is consistent with the solution Eq. (7.28) of the recursion relation if we set $\phi_B^+(\omega; \nu_s)$ to the tree-level expression, identify the natural rapidity scale as $\nu_s = m_q^2/\omega$ and replace the evolution kernel with $A \rightarrow -F_{\text{div.}}^{(1)}$. The RGE for the first inverse moment of ϕ_B^- can be solved using variation of constants. We find:

$$\begin{aligned} \int_0^\infty d\omega \frac{\phi_B^-(\omega; \nu)}{\omega} &= \int_0^\infty d\omega \left\{ \frac{\phi_B^-(\omega; \nu_s)}{\omega} \left(\frac{\nu}{\nu_s} \right)^{-A} + \frac{C_A}{2C_F} \frac{\phi_B^+(\omega)}{\omega} \left[\left(\frac{\nu}{\nu_s} \right)^{-A} - 1 \right] \right. \\ &\quad \left. + m_q \frac{C_{FA}}{C_F} \frac{\phi_B^+(\omega; \nu_s)}{\omega^2} A \left(\frac{\nu}{\nu_s} \right)^{-A} \log \frac{\nu}{\nu_s} \right\}, \end{aligned} \quad (7.52)$$

which again has the same structure as the solution given in Eq. (7.30).

Analogously, in the collinear sector the endpoint-finite first inverse moment of the leading-twist LCDA ϕ_η is ν -independent. The sum of the first and the second inverse moment of ϕ_η exponentiates,

$$\int_0^1 du \phi_\eta(u; \nu) \frac{1 + \bar{u}}{\bar{u}^2} = \int_0^1 du \phi_\eta(u; \nu_c) \frac{1 + \bar{u}}{\bar{u}^2} \left(\frac{\nu}{\nu_c} \right)^A, \quad (7.53)$$

and a somewhat more interesting structure appears for the inverse moment of the linear combination of twist-3, $\phi_{P+\sigma'}$:

$$\int_0^1 du \frac{\phi_{P+\sigma'}(u; \nu)}{\bar{u}} = \int_0^1 du \frac{\phi_{P+\sigma'}(u; \nu_c)}{\bar{u}} + \bar{u}_0 A \int_0^1 du \frac{\phi_\eta(u)}{\bar{u}} \log \frac{\nu}{\nu_c}. \quad (7.54)$$

The difference of the two LCDAs of twist-3, $\phi_{P-\sigma'}$, has a more complicated solution:

$$\begin{aligned} \int_0^1 du \frac{\phi_{P-\sigma'}(u; \nu)}{\bar{u}} &= \int_0^1 du \left\{ \frac{\phi_{P-\sigma'}(u; \nu_c)}{\bar{u}} \left(\frac{\nu}{\nu_c} \right)^A \right. \\ &\quad - \frac{C_{FA}}{C_F} A \bar{u}_0 \phi_\eta(u; \nu_c) \frac{1+\bar{u}}{\bar{u}^2} \left(\frac{\nu}{\nu_c} \right)^A \log \frac{\nu}{\nu_c} + \frac{2C_F + C_A}{2C_F} \frac{\phi_{P+\sigma'}(u; \nu_c)}{\bar{u}} \left[\left(\frac{\nu}{\nu_c} \right)^A - 1 \right] \\ &\quad \left. + \frac{\phi_\eta(u)}{\bar{u}} \left(\frac{\bar{u}_0 C_A - u_0 C_F}{C_F} \left[\left(\frac{\nu}{\nu_c} \right)^A - 1 \right] - \frac{2C_F + C_A}{2C_F} A \bar{u}_0 \log \frac{\nu}{\nu_c} \right) \right\}. \end{aligned} \quad (7.55)$$

Using these results we find the following expression for the partially resummed soft form factor ξ_η^{hc0} :

$$\begin{aligned} \xi_\eta^{\text{hc0}}(\mu)|_{\nu\text{-evolved}} &\simeq \xi_0 C_F \int_0^\infty d\omega \int_0^1 du \left\{ \frac{\phi_B^-(\omega; \mu, \nu_s)}{\omega} \phi_\eta(u; \nu_c) \frac{1+\bar{u}}{\bar{u}^2} \left(\frac{\nu_c}{\nu_s} \right)^{-A} \right. \\ &\quad + \frac{\phi_B^+(\omega; \mu)}{\omega} \left(\frac{C_A}{2C_F} \phi_\eta(u; \nu_c) \frac{1+\bar{u}}{\bar{u}^2} \left(\frac{\nu_c}{\nu_s} \right)^{-A} - \frac{2C_F + C_A}{2C_F} \frac{\phi_\eta(u)}{\bar{u}} \right) \\ &\quad + m_{\bar{q}} \frac{\phi_B^+(\omega; \mu, \nu_s)}{\omega^2} \left(\frac{\nu_c}{\nu_s} \right)^{-A} \left(-\phi_\eta(u; \nu_c) \frac{1+\bar{u}}{\bar{u}^2} \left[\frac{C_A}{C_F} - \frac{C_{FA}}{C_F} A \log \frac{\nu_c}{\nu_s} \right] \right. \\ &\quad \left. + \frac{\phi_\eta(u)}{\bar{u}} \left[\frac{C_A}{C_F} - \frac{u_0}{\bar{u}_0} \right] + \frac{\phi_{P-\sigma'}(u; \nu_c)}{\bar{u}_0 \bar{u}} + \frac{2C_F + C_A}{2C_F} \frac{\phi_{P+\sigma'}(u; \nu_c)}{\bar{u}_0 \bar{u}} \right) \right\}. \end{aligned} \quad (7.56)$$

Note again that the cancellation of ν at no point requires that we use the explicit tree-level LCDAs in the non-relativistic setup. Nevertheless, in the LL approximation it is sufficient to identify the (partially) renormalised LCDAs with the tree-level delta-distributions. Performing the convolutions then gives

$$\begin{aligned} \xi_\eta^{\text{hc0}}(\mu)|_{\nu\text{-evolved}} &\simeq \frac{\xi_0 C_F}{m_\eta \bar{u}_0^2} \left\{ \frac{2+\bar{u}_0}{\bar{u}_0} + \left[2 \frac{1+\bar{u}_0}{\bar{u}_0} + \frac{C_A}{2C_F} \right] \left((2\gamma)^{-A} - 1 \right) \right. \\ &\quad \left. + \frac{C_{FA}}{C_F} \frac{1+\bar{u}_0}{\bar{u}_0} A \log(2\gamma) (2\gamma)^{-A} \right\}. \end{aligned} \quad (7.57)$$

Here the first term corresponds to the tree-level result and the other two terms are $\mathcal{O}(\alpha_s)$ suppressed. Replacing $A \rightarrow -F_{\text{div}}^{(1)}$ and performing the fixed-order expansion up to $\mathcal{O}(\alpha_s^2)$ reproduces the results of the explicit one-loop calculation in Eq. (7.23) and two-loop calculation in Eq. (7.24).

Lastly, we remark that the same structure of the partially resummed soft form factor can be obtained by just requiring that ξ_η is independent of ν (we investigate a somewhat simpler example in Appendix D.4). Thus, the rapidity RG, the collinear anomaly argument and the explicit solution of the recursion relations all give equivalent results.

Combined evolution in ν and μ : We now present the solutions to the RGEs for the soft, the collinear, the hard and the hard-collinear functions in μ . As explained above, all collinear moments evaluated at $\nu = \nu_c$ are μ -independent in the LL approximation. The endpoint-finite first inverse moment of ϕ_B^+ evolves with the usual Sudakov factor:

$$\int_0^\infty \frac{d\omega}{\omega} \phi_B^+(\omega; \mu) = e^{S(\mu_s, \mu)} \int_0^\infty \frac{d\omega}{\omega} \phi_B^+(\omega; \mu_s). \quad (7.58)$$

Due to the ‘‘asymmetric’’ analytic regulator, the second inverse moment of ϕ_B^+ gets an additional Sudakov factor $\exp\{2S(\mu_s, \mu)\}$ from the endpoint contribution:

$$\int_0^\infty \frac{d\omega}{\omega^2} \phi_B^+(\omega; \mu, \nu_s) = e^{3S(\mu_s, \mu)} \int_0^\infty \frac{d\omega}{\omega^2} \phi_B^+(\omega; \mu_s, \nu_s). \quad (7.59)$$

For the first inverse moment of ϕ_B^- we observe very similar structures as in the ν -evolution:

$$\begin{aligned} \int_0^\infty \frac{d\omega}{\omega} \phi_B^-(\omega; \mu, \nu_s) &= e^{S(\mu_s, \mu)} \int_0^\infty \frac{d\omega}{\omega} \left\{ \frac{\phi_B^-(\omega; \mu_s, \nu_s)}{\omega} e^{2S(\mu_s, \mu)} \right. \\ &\left. + \frac{C_A}{2C_F} \frac{\phi_B^+(\omega; \mu_s)}{\omega} (e^{2S(\mu_s, \mu)} - 1) - 2m_{\bar{q}} \frac{C_{FA}}{C_F} \frac{\phi_B^+(\omega; \mu_s, \nu_s)}{\omega^2} S(\mu_s, \mu) e^{2S(\mu_s, \mu)} \right\}. \end{aligned} \quad (7.60)$$

Lastly, the evolution of the hard function is simply given by

$$H_i(\mu) = e^{S(\mu_h, \mu)} H_i(\mu_h), \quad (i = +, -, T), \quad (7.61)$$

and the evolution of the hard-collinear matrix reads

$$J(\mu) = e^{-4S(\mu_{hc}, \mu)} \begin{pmatrix} 1 & \frac{2C_{FA}}{C_F} S(\mu_{hc}, \mu) & 0 \\ 0 & 1 & 0 \\ 0 & \frac{C_A}{2C_F} (1 - e^{2S(\mu_{hc}, \mu)}) & e^{2S(\mu_{hc}, \mu)} \end{pmatrix} \cdot J(\mu_{hc}). \quad (7.62)$$

For the resummation of all leading logarithms we run the quantities in Eq. (7.40) to their natural rapidities and virtualities and evaluate all LCDAs at tree-level. To simplify the resummed expression we make use of the identities in Eq. (5.77). We then find the result:⁷

$$\begin{aligned} H_+(\mu) \xi_\eta(\mu) \Big|_{\text{LL}} &= \frac{\xi_0 C_F}{m_\eta} e^{S(\mu_h, \mu_s) - 4S(\mu_{hc}, \mu_s)} \left\{ \frac{2 + \bar{u}_0}{\bar{u}_0^3} + \frac{2C_{FA}}{C_F} \frac{1 + \bar{u}_0}{\bar{u}_0^3} S(\mu_{hc}, \mu_s) \right. \\ &\left. + \frac{2C_F + C_A}{2C_F} \frac{1}{\bar{u}_0^2} (1 - e^{2S(\mu_{hc}, \mu_s)}) \right\}. \end{aligned} \quad (7.63)$$

The first term is the tree-level result multiplied with two different Sudakov factors. One resums large double logarithms of ratios of the hard and the soft scale, and one of

⁷Note that the scale dependence of ξ_0 , which is defined as a function of the HQET decay constant $\tilde{f}_B(\mu)$ and the coupling $\alpha_s(\mu)$, is irrelevant for the resummation of leading logarithms.

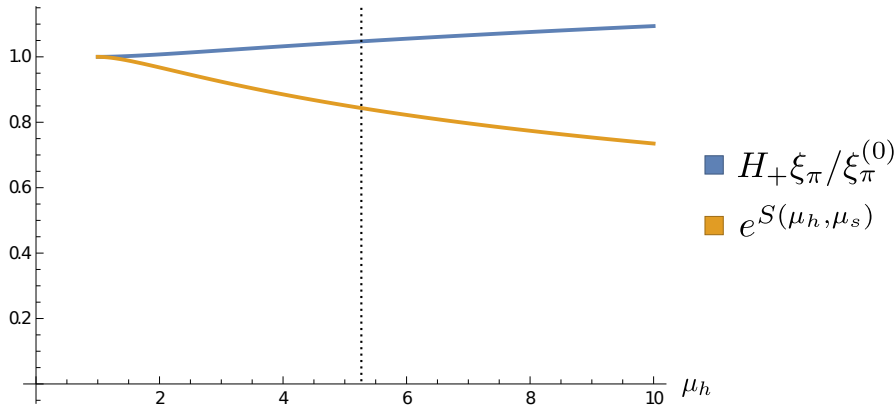


Figure 7.5: The blue curve shows the result Eq. (7.63) for the resummed non-factorisable contribution to the form factors, normalised to the tree-level expression, as a function of the hard scale μ_h for fixed $\mu_s = 1$ GeV. The orange curve shows the usual Sudakov evolution kernel. Furthermore, the dotted line indicates the value of the B -meson mass: $M_B \simeq 5.3$ GeV. In this analysis we set $\mu_{hc} \rightarrow \sqrt{\mu_h \mu_s}$. Further numerical inputs are: $n_f = 5$ (number of active flavours), $M_Z \simeq 91.2$ GeV and $\alpha_s(M_Z) \simeq 0.12$.

ratios of the hard-collinear and the soft scale, respectively. Note that in the one-loop fixed-order expansion of the linear combination $S(\mu_h, \mu_s) - 4S(\mu_{hc}, \mu_s)$ the large double logarithm drops out for $\mu_{hc} \sim \sqrt{\mu_h \mu_s}$. The other terms show similar structures as already observed in the evolution of the individual objects.⁸ Fixed-order expansion of the whole expression up to $\mathcal{O}(\alpha_s)$ reproduces the tree-level result as well as the one-loop result derived in Eq. (7.22).

Figure 7.5 shows the resummed expression (7.63) as a function of the hard scale μ_h . Interestingly, the resummation rather results in a slight enhancement instead of the usual Sudakov suppression. Considering the evolution of the hard function H_i in Eq. (7.61), this means that the soft form factor ξ_π must be exponentially enhanced in the limit $m_b \rightarrow \infty$. In particular, the suppression associated with the hard scale is overcompensated by an enhancement associated with the intermediate hard-collinear scale, such that the linear combination $S(\mu_h, \mu_s) - 4S(\mu_{hc}, \mu_s)$ has only a very weak dependence on μ_h . This result implies that the non-factorisable contribution to the form factors is numerically of the same size as the factorisable terms, thus, contradicting the assumption that underlies the so-called perturbative QCD (pQCD) approach [129, 130].

⁸In the second term in the braces we could replace $S(\mu_{hc}, \mu_s)$ with its explicit one-loop double-logarithmic contribution in the LL approximation.

Chapter 8

Beyond the Resummation of Leading Logarithms

Many simplifications arise in the LL approximation that allow us to perform a resummation of logarithms using rapidity RG equations for inverse moments. Nevertheless, a resummation beyond this approximation and the objective of understanding a complete factorisation of modes has not yet been accomplished. We identify the following main obstacles in reaching this goal:

- In contrast to the Sudakov form factor, endpoint divergences in heavy-to-light form factors arise in the convolution of separately well-defined soft or collinear LCDAs with hard-collinear scattering kernels. Understanding the interplay between the different modes in their convolution, and in particular the role of the hard-collinear dynamics, seems to be the technical hurdle to reveal the factorisation of heavy-to-light form factors at large recoil.
- Since endpoint divergences do not seem to be associated with Wilson-line gluons, a consistent implementation of an analytic regulator at the operator level is unknown to us. The relation between the LCDAs and the regularised objects in ill-defined convolution integrals remains unclear.
- The collinear anomaly tells us that the rapidity logarithms exponentiate and the relevant low-energy quantities are the anomaly coefficient F and a remainder function R . A treatment along these lines is somehow against the spirit of factorisation since non-perturbative objects are expected to be process-independent. We are not aware of an operator definition of neither R nor F , which is necessary for realistic B -meson decays.
- Similar to the soft mode in the Sudakov problem, a “soft-collinear” mode with the scaling $(\lambda, \lambda^2, \lambda^3)M_B$ contributes to heavy-to-light form factors in the NR setup if we choose a symmetric regulator for the rapidity divergences. The role of this mode in a non-perturbative treatment needs to be investigated.

In the following we first address the last point and investigate how the factorisation is modified when a new low-energy mode is included in the theory. Afterwards we tackle the technical problem that endpoint divergences arise in convolutions of well-defined objects with the help of scalar toy integrals. This discussion touches the first three points.

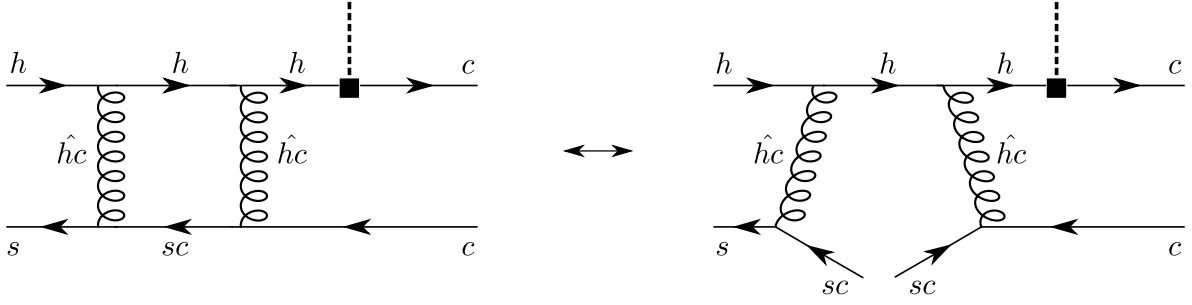


Figure 8.1: An example diagram which exhibits a pole in δ in the soft, the collinear and the soft-collinear region (left diagram). The contribution from the soft-collinear region can be obtained in an effective theory with soft, collinear and soft-collinear modes. The relevant diagram that contributes to the matching is shown on the right.

8.1 The Soft-Collinear Mode

When calculating the various regions that contribute to the one-loop Sudakov form factor in Section 5.2, we found that the endpoint contributions are regulator dependent, i.e. they can not be unambiguously assigned to individual regions. In particular, the soft region gives scaleless integrals when k_+ or k_- is raised to the power of δ but not when we choose e.g. k_0^δ as an analytic regulator. In the latter case the soft and the two collinear regions suffer from rapidity divergences which cancel in their sum.

In this section we illustrate how the factorisation of heavy-to-light form factors changes when the corresponding mode – which we call the “soft-collinear” (sc) mode – is included in the theory. To this end, we investigate the endpoint contribution of the one-loop diagram in Fig. 8.1 as an example. We define a soft-collinear momentum with the scaling $(\lambda, \lambda^2, \lambda^3)M_B$, which has soft virtuality $\mu_{sc} \sim \mu_s \sim \lambda^2 M_B$. A momentum transfer between soft-collinear and soft or collinear particles corresponds to a perturbative mode, which we label \hat{hc} , with virtuality $\mu_{\hat{hc}} \sim \lambda^{3/2} M_B$. At leading power, the soft-collinear mode decouples from the other low-energy modes and the relevant SCET_{II} Lagrangian can be obtained by adding a corresponding contribution \mathcal{L}_{sc} to Eq. (6.1).¹

Using the regulator ν^δ/k_-^δ , the left diagram in Fig. 8.1 is scaleless and the pole in δ cancels in the sum of the soft and the collinear region. In the soft region, for example, we find (in Feynman gauge)

$$iA|_{\text{soft}} = \frac{\xi_0 C_F}{m_\eta} \frac{\alpha_s(\mu)}{4\pi} \frac{2C_F}{\bar{u}_0^3} \frac{1}{\delta\varepsilon} \left(\frac{\mu^2}{m_q^2}\right)^\varepsilon \left(\frac{\nu}{m_{\bar{q}}}\right)^\delta + \mathcal{O}(\delta^0). \quad (8.1)$$

As argued in Section 5.2, the soft-collinear region contains the information about the pole in δ encoded in a scaleless integral. We now aim at reproducing this contribution in an effective theory of soft, collinear and soft-collinear modes. To this end we calculate the tree-level matching onto six-quark operators in the effective theory from the right

¹A similar idea has been proposed in [100]. Motivated by investigating a toy integral with off-shell external legs, the authors considered a “soft-collinear messenger” mode with the scaling $(\lambda^2, \lambda^3, \lambda^4)M_B$. In our setup this mode does not contribute since its virtuality $\mu_{\text{mess.}} \sim \lambda^3 M_B$ lies even below the quark mass $m \sim \lambda^2 M_B$ and thus the corresponding integrals are scaleless.

diagram in Fig. 8.1. This can be done in complete analogy to what has been presented in Section 6.3. However, due to the six external legs, performing the Fierz transformations is more complicated. The above diagram matches onto a single operator whose matrix element is parametrised by the leading-twist LCDA of the η_c meson, the subleading-twist 2-particle LCDA of the \bar{B}_c meson and a soft-collinear wave function, defined as the Fourier transform of the vacuum matrix element

$$\langle 0 | \mathcal{T} \{ \bar{\theta}_{sc}(\sigma n) (S_n^{(sc)} W_{\bar{n}}^{(sc)}) (0) \frac{\not{n}}{2} \theta_{sc}(r\bar{n}) \} | 0 \rangle. \quad (8.2)$$

Here θ_{sc} is the large component of a soft-collinear spinor-field, dressed with appropriate Wilson lines to ensure the gauge invariance, and $S_n^{(sc)}$ and $W_{\bar{n}}^{(sc)}$ are additional soft-collinear Wilson lines in the n and the \bar{n} direction, respectively. The corresponding matching coefficient reads

$$D_{sc} = -\frac{C_F^2}{N_C} \frac{1}{4E_\pi^2 \bar{u}^2 \omega \tilde{l}_- \tilde{p}_+}, \quad (8.3)$$

where, in addition to ω and $\bar{u}E_\pi$, the light-cone projections \tilde{l}_- and \tilde{p}_+ of the external soft-collinear momenta emerge at leading power.

In the non-relativistic setup we can calculate the new hadronic function perturbatively. Employing LO wave-functions, the soft and collinear moments are well-defined, but the inverse moment of the soft-collinear wave function is endpoint divergent. Without going into the details, using the regulator ν^δ/k_-^δ we find the result

$$iA|_{(sc)} = \frac{\xi_0 C_F}{m_\eta} \frac{\alpha_s(\mu)}{4\pi} \frac{2C_F}{\bar{u}_0^3} \frac{1}{\varepsilon} \left(\frac{\mu^2}{m_q^2} \right)^\varepsilon \left(\frac{\nu}{\tilde{\Lambda}} \right)^\delta \left(\frac{1}{\delta_{UV}} - \frac{1}{\delta_{IR}} \right), \quad (8.4)$$

with an artificial cut-off scale $\tilde{\Lambda}$. This reproduces the sc-region integral which indeed contains the information about the pole in Eq. (8.1) encoded in a scaleless integral. Note again that with a different regulator this contribution is not necessarily scaleless. From other diagrams in the matching also different Dirac structures between the soft-collinear fields emerge. In particular, also subleading spinor-components arise, which, similar to the collinear sector, can be related to the leading spinor-components via the equations of motion.

In addition to endpoint-divergent soft and collinear moments, in the presence of a soft-collinear mode, the factorisation formula of heavy-to-light form factors now contains also endpoint-divergent soft-collinear moments. Thus, although the information about the endpoint contributions is encoded in these vacuum matrix elements, simply including this new mode to the theory does not seem to solve the problem of endpoint divergences.

8.2 Endpoint Re-Factorisation

In this section we address the technical problem that endpoint divergences in heavy-to-light form factors arise in convolutions of separately well-defined objects. We conjecture a factorisation formula for the small- ω behaviour of the bare LCDAs which can be used

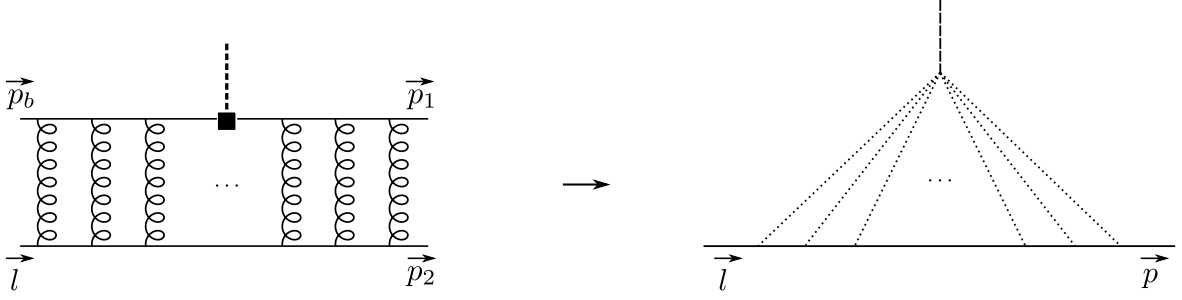


Figure 8.2: Scalar toy integrals that correspond to arbitrary many ladder-type gluon emissions from an effective vertex arising when the heavy quark and the active quark line are shrunk to a point. Solid lines represent massive and dotted lines massless propagators.

to define endpoint-subtracted LCDAs with well-defined inverse moments. The cancellation of endpoint divergences then happens at the level of ill-defined inverse moments of vacuum matrix elements similar to Eq. (8.2). We discuss this idea by means of unphysical and artificially constructed scalar toy integrals in $d = 4 - 2\varepsilon$ dimensions and stress that the diagrams do not result from a well-defined perturbative expansion. They should rather be viewed as a subset of master integrals contributing to heavy-to-light form factors in the NR setup. Nevertheless, they show the same factorisation structure that we aim to investigate. The terminology (factorisation, LCDAs, etc.) that we continue to use in this section should thus not be taken too literally.

Rapidity logarithms arise since the spectator-quark propagator can overlap between the soft and the collinear region. In Section 7.3 we found that ladder-type diagrams determine the exponentiation of the leading poles in δ in the second inverse moment of ϕ_B^+ . We thus study corresponding scalar integrals where the heavy quark as well as the quark produced in the weak vertex are shrunk to a point, see Fig. 8.2. We define a toy observable $\mathcal{I} = \mathcal{I}(m^2, p \cdot l)$ as

$$\mathcal{I} = \mathcal{I}^{(0)} + \frac{\alpha}{4\pi} \mathcal{I}^{(1)} + \left(\frac{\alpha}{4\pi}\right)^2 \mathcal{I}^{(2)} + \dots, \quad (8.5)$$

with a dimensionless coupling α and the n -loop integrals $\mathcal{I}^{(n)}$ defined through the diagrams in Fig. 8.2 with $n + 1$ massless lines. We consider massive on-shell external legs with a soft particle with momentum l in the initial state and a collinear particle with momentum p in the final state. In particular, similar to heavy-to-light form factors, the LO contribution $\mathcal{I}^{(0)}$ is determined by one tree-level exchange of a hard-collinear gluon. Furthermore, we choose a frame where the perpendicular components of the external momenta vanish, such that

$$\text{soft:} \quad l^\mu = \frac{l_-}{2} n^\mu + \frac{l_+}{2} \bar{n}^\mu, \quad \text{with} \quad l^2 = l_+ l_- = m^2, \quad (8.6)$$

and

$$\text{collinear:} \quad p^\mu = \frac{p_-}{2} n^\mu + \frac{p_+}{2} \bar{n}^\mu, \quad \text{with} \quad p^2 = p_+ p_- = m^2. \quad (8.7)$$

At leading power in the small ratio $\lambda^2 \equiv \frac{m^2}{2p \cdot l}$, the integrals receive contributions from soft, collinear and hard-collinear regions when we raise k_- to a non-integer power δ . In analogy to ξ_π we thus conjecture the following leading-power naive factorisation formula for \mathcal{I} :

$$\mathcal{I} \simeq \int_0^\infty d\omega \int_0^\infty d\sigma \phi_s(\omega; \delta) \phi_c(\sigma; \delta) J(\omega\sigma). \quad (8.8)$$

Here the ‘‘LCDAs’’ have support $\omega \in [0, l_+]$ and $\sigma \in [0, p_-]$, respectively:

$$\phi_s(\omega) = \delta(\omega - l_+) + \frac{\theta(l_+ - \omega)}{l_+} f_s(\omega), \quad (8.9)$$

and

$$\phi_c(\sigma) = \delta(\sigma - p_-) + \frac{\theta(p_- - \sigma)}{p_-} g_c(\sigma). \quad (8.10)$$

The functions f_s and g_c have a perturbative expansion starting at $\mathcal{O}(\alpha)$.

In the following we verify this naive factorisation formula up to one-loop order. Furthermore, we investigate the bare LCDAs at two-loops which leads to the observation that the endpoint behaviour of the LCDAs factorise in a similar way as \mathcal{I} .

\mathcal{I} at tree-level: The tree-level diagram is given by the massless propagator

$$\mathcal{I}^{(0)} \equiv \frac{1}{(p-l)^2} = -\frac{1}{2p \cdot l} + \mathcal{O}\left(\frac{m^2}{2p \cdot l}\right), \quad (8.11)$$

where we can further expand $2p \cdot l \simeq p_- l_+$. This defines the LO hard-collinear kernel

$$J^{(0)}(\omega\sigma) = -\frac{1}{\omega\sigma}. \quad (8.12)$$

Similar to heavy and light mesons in the NR setup, the tree-level LCDAs are given by the delta distributions

$$\phi_s^{(0)}(\omega) = \delta(\omega - l_+) \quad \text{and} \quad \phi_c^{(0)}(\sigma) = \delta(\sigma - p_-), \quad (8.13)$$

such that the leading-power contribution to $\mathcal{I}^{(0)}$ can be reproduced via Eq. (8.8).

\mathcal{I} at one-loop order: We define the one-loop integral $\mathcal{I}^{(1)}$ as

$$\mathcal{I}^{(1)} \equiv \int \frac{[dk]}{[k^2 - m^2 + i\varepsilon] [(k-l)^2 + i\varepsilon] [(k-p)^2 + i\varepsilon]}, \quad (8.14)$$

with the integration measure

$$[dk] \equiv \mu^{2\varepsilon} \frac{\Gamma(1-\varepsilon)}{i\pi^{d/2}} d^d k = \mu^{2\varepsilon} \frac{\Gamma(1-\varepsilon)}{2i\pi^{d/2}} dk_+ dk_- d^{d-2} k_\perp. \quad (8.15)$$

Since the mass m serves as an IR regulator $\mathcal{I}^{(1)}$ is finite in $d = 4$ dimensions. We find for the leading-power contribution:

$$\mathcal{I}^{(1)} = -\frac{1}{p_- l_+} \left(\frac{1}{2} \log^2 \frac{p_- l_+}{m^2} + \frac{2\pi^2}{3} + \mathcal{O}\left(\varepsilon, \frac{m^2}{p_- l_+}\right) \right). \quad (8.16)$$

In the rest frame of the soft particle we have $l_+ = m$ and $p_- = 2\gamma m$, such that the argument of the large logarithm is again the large boost 2γ between the soft and the collinear particle.

The integral $\mathcal{I}^{(1)}$ receives leading-power contributions from the soft, the collinear and the hard-collinear momentum region. In the latter one we find

$$\mathcal{I}^{(hc)} = -\frac{1}{p_- l_+} \left(\frac{\mu^2}{p_- l_+} \right)^\varepsilon \frac{1}{\varepsilon^2} + \mathcal{O}(\varepsilon), \quad (8.17)$$

which defines the one-loop contribution to the hard-collinear kernel:

$$J^{(1)}(\omega\sigma) = -\frac{1}{\omega\sigma} \left(\frac{\mu^2}{\omega\sigma} \right)^\varepsilon \frac{1}{\varepsilon^2} + \mathcal{O}(\varepsilon). \quad (8.18)$$

Regulating endpoint divergences with ν^δ/k_-^δ , we find in the collinear region

$$\mathcal{I}^{(c)} = \frac{1}{p_- l_+} \left(\frac{\mu^2}{m^2} \right)^\varepsilon \left(\frac{\nu}{p_-} \right)^\delta \left[\frac{1}{\delta\varepsilon} - \frac{\pi^2}{3} \right] + \mathcal{O}(\delta, \varepsilon), \quad (8.19)$$

and in the soft region

$$\mathcal{I}^{(s)} = \frac{1}{p_- l_+} \left(\frac{\mu^2}{m^2} \right)^\varepsilon \left(\frac{\nu l_+}{m^2} \right)^\delta \left[-\frac{1}{\delta\varepsilon} + \frac{1}{\varepsilon^2} - \frac{\pi^2}{3} \right] + \mathcal{O}(\delta, \varepsilon), \quad (8.20)$$

such that in the sum of the three regions we obtain the leading-power result for $\mathcal{I}^{(1)}$ in Eq. (8.16).

In complete analogy to the definition of the LCDAs in the NR model we define the one-loop ‘‘LCDAs’’ in this setup as

$$\phi_c^{(1)}(\sigma) = \int [dk] \frac{\delta(k_- - \sigma)}{[(k - p)^2 + i\varepsilon][k^2 - m^2 + i\varepsilon]}, \quad (8.21)$$

and

$$\phi_s^{(1)}(\omega) = \int [dk] \frac{\delta(k_+ - \omega)}{[(k - l)^2 + i\varepsilon][k^2 - m^2 + i\varepsilon]}. \quad (8.22)$$

Including their dependence on the regulator δ , we then find for the bare and unexpanded one-loop expressions:

$$\begin{aligned} f_s^{(1)}(\omega; \delta) &= \left(\frac{\nu\omega}{m^2} \right)^\delta \left(\frac{\mu^2}{m^2} \right)^\varepsilon \frac{\Gamma(\delta + \varepsilon)\Gamma(1 - \varepsilon)}{\Gamma(1 + \delta)} {}_2F_1(1, \delta + \varepsilon; 1 + \delta; 1 - (1 - \omega/l_+)^2), \\ g_c^{(1)}(\sigma; \delta) &= \left(\frac{\mu^2}{m^2} \right)^\varepsilon \left(\frac{\nu}{\sigma} \right)^\delta \frac{\pi}{\sin(\pi\varepsilon)} \left(\frac{p_- - \sigma}{p_-} \right)^{-2\varepsilon}. \end{aligned} \quad (8.23)$$

With these functions we can reproduce the results of the various regions in Eqs. (8.17), (8.19) and (8.20), using our ‘‘factorisation assumption.’’

Two-loop LCDA and endpoint re-factorisation: We define the soft LCDA at two-loop order as the integral

$$\phi_s^{(2)}(\omega) = \int [dk][dj] \frac{\delta(j_+ - \omega)}{[(k-l)^2 + i\varepsilon][k^2 - m^2 + i\varepsilon][(k-j)^2 + i\varepsilon][j^2 - m^2 + i\varepsilon]}, \quad (8.24)$$

which, for $\delta = 0$, has the analytic solution (we abbreviate $\hat{\omega} = \omega/l_+$):

$$\begin{aligned} f_s^{(2)}(\omega) = & \left(\frac{\mu^2}{m^2}\right)^{2\varepsilon} \frac{\pi^2}{\sin^2(\pi\varepsilon)} (1 - \hat{\omega})^{-4\varepsilon} \left\{ \right. \\ & \frac{\Gamma^2(1 - 2\varepsilon)}{\Gamma(2 - 4\varepsilon)} (1 - \hat{\omega}) \hat{\omega}^{-1+2\varepsilon} {}_2F_1(1 - 2\varepsilon, 1 - 2\varepsilon; 2 - 4\varepsilon; 1 - 1/\hat{\omega}) \\ & + \frac{\pi}{\sin(2\pi\varepsilon)} (1 - \hat{\omega})^{-1} [2\varepsilon \hat{\omega} {}_2F_1(1 - 2\varepsilon, 1 - 2\varepsilon; 2; \hat{\omega}) - {}_2F_1(1 - 2\varepsilon, -2\varepsilon; 1; \hat{\omega})] \\ & \left. - \frac{2^{-1+4\varepsilon} \Gamma(\varepsilon + \frac{1}{2}) \Gamma(-\varepsilon)}{\Gamma(1 + \varepsilon) \Gamma(1/2 - \varepsilon)} \hat{\omega}^\varepsilon {}_3F_2(\{1, 1 - \varepsilon, 1 - \varepsilon\}, \{1 + \varepsilon, 1 + \varepsilon\}, \hat{\omega}) \right\}, \quad (8.25) \end{aligned}$$

where ${}_pF_q$ is the generalised hypergeometric function. We now want to analyse the behaviour of this function for small ω , which, in inverse moments, causes rapidity divergences. The hypergeometric functions in the second and the third line are normalised to one for $\omega \rightarrow 0$. The first hypergeometric function, however, has a logarithmic behaviour as $\omega \rightarrow 0$. We find:

$$\begin{aligned} f_s^{(2)}(\omega) \simeq & - \left(\frac{\mu^2}{m^2}\right)^{2\varepsilon} \frac{\pi^2}{\sin^2(\pi\varepsilon)} \left\{ \log \hat{\omega} + 2H_{-2\varepsilon} + \frac{\pi}{\sin(2\pi\varepsilon)} + \hat{\omega}^\varepsilon \frac{2^{-1+4\varepsilon} \Gamma(\varepsilon + \frac{1}{2}) \Gamma(-\varepsilon)}{\Gamma(1 + \varepsilon) \Gamma(1/2 - \varepsilon)} \right\} \\ & + \mathcal{O}(\hat{\omega}). \quad (8.26) \end{aligned}$$

The logarithmic contribution is, after employing analytical regularisation, accountable for the double pole in δ of the two-loop integral $\mathcal{I}^{(2)}$ in the double soft region. The ω -independent term generates a single pole in δ whereas the term proportional to ω^ε has a well-defined convolution with the tree-level hard-collinear kernel $J^{(0)}$ in d dimensions. Surprisingly, we find that $\phi^{(2)}$ convoluted with $J^{(1)}$, i.e. the three-loop integral in the (s, s, hc) region, requires again analytic regularisation and receives a single pole in δ . Note that, for $\delta = 0$, the result for $g_c^{(2)}(\sigma)$ can be obtained from Eq. (8.25) by replacing $\omega \rightarrow \sigma$ and $l_+ \rightarrow p_-$.

We expect a similar endpoint behaviour for the bare LCDAs in the NR model. The result in Eq. (8.26) shows that neither the LCDAs nor the hard-collinear kernel J can be expanded in plus-distributions to separate endpoint divergences. This is the main problem that prevents us from defining renormalised objects beyond the LL approximation.

Although the LCDAs are defined by soft or collinear matrix elements, the result Eq. (8.26) indicates that their asymptotic behaviour receives again contributions from various regions. Consider for example the two-loop ladder-type diagram in Fig. 8.3 in the soft sector. For unnaturally small ω the loop momentum k becomes collinear and at leading power in ω/l_+ the $d^d j$ integral has again a soft, a collinear and a hard-collinear

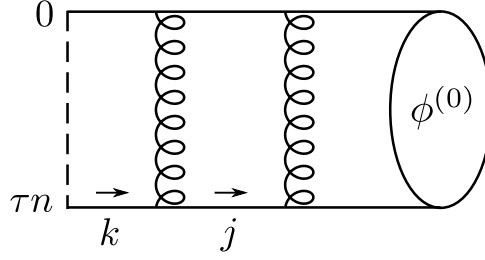


Figure 8.3: Two-loop ladder-type contribution to soft or collinear 2-particle LCDAs in the NR setup.

contribution.² We thus conjecture the following “factorisation formula” for the asymptotic endpoint behaviour of ϕ_s :

$$\phi_s(\omega \simeq 0; \delta) = \int_{\mathbb{R}} dk_- \int_0^\infty d\tilde{\omega} \phi_s(\tilde{\omega}; \delta) J(\tilde{\omega}k_-) \psi(\omega, k_-; \delta) + \mathcal{O}(\omega). \quad (8.27)$$

On the right-hand side, ϕ_s is again the soft LCDA which gets convoluted with the hard-scattering kernel J .³ We interpret the new function ψ as a vacuum matrix element of a non-local operator of collinear fields. For $\delta = 0$ it depends on the product ωk_- only. Equation (8.27) is the main result of this section, which we verified up to two-loop order.

At LO, ψ is defined as the loop integral

$$\psi^{(1)}(\omega\sigma) = \int [dk] \frac{\delta(k_- - \sigma) \delta(k_+ - \omega)}{[k^2 - m^2 + i\varepsilon]}, \quad (8.28)$$

and at NLO as

$$\psi^{(2)}(\omega\sigma) = \int [dk][dj] \frac{\delta(k_- - \sigma) \delta(j_+ - \omega)}{[k^2 - m^2 + i\varepsilon] [(k-j)^2 + i\varepsilon] [j^2 - m^2 + i\varepsilon]}. \quad (8.29)$$

Note that ψ has no tree-level contribution since rapidity divergences first arise at one-loop order. With these definitions we can indeed reproduce the correct endpoint behaviour of ϕ_s . For example, the two-loop result in Eq. (8.26) is determined by

$$\phi_s^{(2)}(\omega \simeq 0; \delta) = \int_{\mathbb{R}} dk_- \int_0^\infty d\tilde{\omega} \left\{ \phi_s^{(1)} J^{(0)} \psi^{(1)} + \phi_s^{(0)} J^{(1)} \psi^{(1)} + \phi_s^{(0)} J^{(0)} \psi^{(2)} \right\}. \quad (8.30)$$

The first term contains an endpoint divergent one-loop moment of the soft LCDA which receives a pole in δ from $\omega \rightarrow 0$. The k_- integral over $\psi^{(1)}$ is well-defined. However, the k_- integral over $\psi^{(2)}$ in the last term receives a pole in δ from $k_+ \rightarrow \infty$, which cancels the pole from the first term and generates the $\log \omega/l_+$ contribution observed in Eq. (8.26). Since the LCDA is a well-defined object, poles in δ must cancel between endpoint-divergent moments of ϕ_s and ψ to all orders. Furthermore, in the second term we perform a convolution with the one-loop hard scattering kernel $J^{(1)}$ which for

²Adopting soft-collinear scaling for k gives a scaleless hard-collinear region and does not reproduce the full result in Eq. (8.26).

³Note that the same hard-collinear kernel J as in Eq. (8.8) arises only due to our symmetric setup.

dimensional reasons generates the term $\sim \omega^\varepsilon$ in Eq. (8.26). Note that, since we integrate k_- over \mathbb{R} , the $i\varepsilon$ prescription in the hard-collinear kernel must be kept.

In the remainder of this section we investigate implications of the endpoint factorisation formula Eq. (8.27) on the factorisation of \mathcal{I} . We first note that with our regularisation prescription overlapping regions give scaleless integrals. To separate the endpoint contribution from ϕ_s we may introduce a hard cut-off, similar to the Heaviside step function $\theta(l_+ - \omega)$ that defines the support of ϕ_s . An ‘‘endpoint subtracted’’ LCDA $\tilde{\phi}_s$, which vanishes linearly in ω to all orders, can then be defined through the following convolution

$$\tilde{\phi}_s(\omega, \omega_{\text{cut}}) = \int_0^\infty d\tilde{\omega} \phi_s(\tilde{\omega}; \delta) \left\{ \delta(\omega - \tilde{\omega}) - \theta(\omega_{\text{cut}} - \omega) \int_{\mathbb{R}} dk_- J(\tilde{\omega}k_-) \psi(k_-, \omega; \delta) \right\}. \quad (8.31)$$

This function has well-defined inverse moments and the dependence on the regulator δ can be dropped. Inverting this relation results in an infinite sum of convolutions of the form:

$$\begin{aligned} \phi_s(\omega; \delta) = & \int_0^\infty d\tilde{\omega} \tilde{\phi}_s(\tilde{\omega}, \omega_{\text{cut}}) \left\{ \delta(\omega - \tilde{\omega}) + \int_{\mathbb{R}} dk_- \left[J(\tilde{\omega}k_-) \psi(k_-, \omega; \delta, \omega_{\text{cut}}) \right. \right. \\ & \left. \left. + \int_{\mathbb{R}} d\hat{k}_- \int_0^\infty d\hat{\omega} J(\tilde{\omega}\hat{k}_-) \psi(\hat{k}_-, \hat{\omega}; \delta, \omega_{\text{cut}}) J(\hat{\omega}k_-) \psi(k_-, \omega; \delta, \omega_{\text{cut}}) + \dots \right] \right\}, \end{aligned} \quad (8.32)$$

where all ψ 's have support between 0 and ω_{cut} , i.e. the Heaviside step function is assumed implicitly. The information about the endpoint is now completely encoded in convolutions of vacuum matrix elements with scattering kernels, which indicates that endpoint divergences are indeed universal. Moreover, it is sufficient to implement the analytic regulator on ψ . The structure on the right-hand side of the above equation seems to be quite complicated. This may be due to the hard cut-off that we introduced. It remains to be investigated if defining an endpoint-subtracted LCDA in a more clever way simplifies this structure.

Employing the same idea on the collinear side as well, we can rewrite the naive factorisation formula for \mathcal{I} as

$$\begin{aligned} \mathcal{I} &= \int_0^\infty d\omega \int_0^\infty d\sigma \phi_s(\omega; \delta) \phi_c(\sigma; \delta) J(\omega\sigma) \\ &= \int_0^\infty d\omega \int_0^\infty d\sigma \tilde{\phi}_s(\omega, \omega_{\text{cut}}) \tilde{\phi}_c(\sigma, \sigma_{\text{cut}}) \tilde{J}(\omega\sigma; \omega_{\text{cut}}, \sigma_{\text{cut}}), \end{aligned} \quad (8.33)$$

with well-defined convolution integrals in ω and σ . We have effectively shifted the endpoint of the LCDAs into a modified scattering kernel \tilde{J} by imposing a hard cut-off. The individual LCDAs can now be expanded in ε but depend on the artificial cut-off scales. However, the latter are not accountable for large logarithms if we choose values around $\omega_{\text{cut}} \sim l_+$ and $\sigma_{\text{cut}} \sim p_-$. The modified scattering kernel \tilde{J} has again a rather complicated

structure:

$$\begin{aligned}
 \tilde{J}(\omega\sigma; \omega_{\text{cut}}, \sigma_{\text{cut}}) &= J(\omega\sigma) + \int_0^\infty d\tilde{\sigma} \int_{\mathbb{R}} dk_+ J(\omega\tilde{\sigma})\psi(\tilde{\sigma}, k_+; \delta, \sigma_{\text{cut}})J(k_+\sigma) \\
 &\quad + \int_0^\infty d\tilde{\omega} \int_{\mathbb{R}} dk_- J(\omega k_-)\psi(\tilde{\omega}, k_-; \delta, \omega_{\text{cut}})J(\tilde{\omega}\sigma) \\
 &\quad + J * \psi * J * \psi * J + \dots,
 \end{aligned} \tag{8.34}$$

where the $*$ operator in the last line stands for the convolution integrals. Nevertheless, all rapidity divergences must cancel in \tilde{J} . We stress again that $\psi(\omega k_-)$ is defined on $\omega \in [0, \omega_{\text{cut}}]$, whereas $\psi(k_+\sigma)$ is defined on $\sigma \in [0, \sigma_{\text{cut}}]$.

Re-factorisation at one-loop order: To conclude this section, we verify Eq. (8.33) at one-loop order. At tree-level, the modified objects coincide with the tree-level expressions for the LCDAs, $\tilde{\phi}_{s,c}^{(0)} = \phi_{s,c}^{(0)}$, and the scattering kernel, $\tilde{J}^{(0)} = J^{(0)}$. For the endpoint-subtracted LCDAs at one-loop order, we find (up to $\mathcal{O}(\varepsilon)$):

$$\begin{aligned}
 l_+ \tilde{\phi}_s^{(1)}(\omega, \omega_{\text{cut}}) &= \left(\frac{1}{\varepsilon} + \log \frac{\mu^2}{m^2} \right) [\theta(l_+ - \omega) - \theta(\omega_{\text{cut}} - \omega)] - 2\theta(l_+ - \omega) \log \left(\frac{l_+ - \omega}{l_+} \right), \\
 p_- \tilde{\phi}_c^{(1)}(\sigma, \sigma_{\text{cut}}) &= \left(\frac{1}{\varepsilon} + \log \frac{\mu^2}{m^2} \right) [\theta(p_- - \sigma) - \theta(\sigma_{\text{cut}} - \sigma)] - 2\theta(p_- - \sigma) \log \left(\frac{p_- - \sigma}{p_-} \right),
 \end{aligned} \tag{8.35}$$

whereas the modified scattering kernel reads

$$\begin{aligned}
 \tilde{J}^{(1)}(\omega\sigma; \omega_{\text{cut}}, \sigma_{\text{cut}}) &= J^{(1)}(\omega\sigma) \\
 &\quad + \frac{1}{\omega\sigma} \left\{ \int_0^\infty \frac{d\tilde{\sigma}}{\tilde{\sigma}} \int_{\mathbb{R}} \frac{dk_+}{k_+ - i\varepsilon} \psi^{(1)}(\tilde{\sigma}, k_+; \delta, \sigma_{\text{cut}}) + \int_0^\infty \frac{d\tilde{\omega}}{\tilde{\omega}} \int_{\mathbb{R}} \frac{dk_-}{k_- - i\varepsilon} \psi^{(1)}(\tilde{\omega}, k_-; \delta, \omega_{\text{cut}}) \right\} \\
 &= -\frac{1}{\omega\sigma} \left\{ \log \frac{\sigma_{\text{cut}}\omega_{\text{cut}}}{\sigma\omega} \left(\frac{1}{\varepsilon} + \log \frac{\mu^2}{m^2} \right) + \frac{1}{2} \log^2 \frac{\omega\sigma}{m^2} \right\}.
 \end{aligned} \tag{8.36}$$

Here the two integrals in the second line are identical for $\delta = 0$ but regularised in a different variable. Thus, the poles in δ cancel in the sum of both. Furthermore, the double pole in ε cancels between $J^{(1)}$ and the integral that is regularised with the asymmetric regulator. When performing the convolution integrals in Eq. (8.27) the cut-off scales drop out and we indeed obtain the correct leading-power one-loop result given in Eq. (8.16).

Although the individual quantities are quite complicated, we showed that the naive factorisation formula can be rewritten in a form where the convolution integrals in ω and σ are well-defined. Endpoint divergences then cancel between inverse moments of vacuum matrix elements which indicates their universality. Additionally, it follows that it is sufficient to implement the analytic regulator on the ψ functions. Whether or not one can understand a resummation of all large logarithms along the lines of what has been presented in this section requires further investigation.

Chapter 9

Summary

We conclude this part with a brief summary of the achievements that we made in improving the factorisation of heavy-to-light form factors. For this purpose, we briefly revisit the various steps that led to the resummed expression in Eq. (7.63).

We first performed the matching of the SCET_I A -type current onto four-quark operators in SCET_{II}. We showed that all quark-mass contributions are captured in the Wilson coefficient of one additional operator, whose hadronic matrix element is expressed in terms of the leading-twist LCDAs ϕ_B^+ and ϕ_π . Assuming that endpoint-divergent moments are somehow regularised, we derived a naive factorisation formula which expresses the soft form factor ξ_π as a convolution of soft and collinear 2-particle and 3-particle LCDAs of twist-2 and twist-3 with a scattering kernel determined by hard-collinear fluctuations.

To gain a better understanding of the ill-defined convolution integrals, we investigated the soft form factor in a non-relativistic setup in which all quark masses are large enough to allow for a perturbative treatment of the relativistic QCD dynamics. Within this setup, we first performed multiple checks of the factorisation formula by a comparison with several leading-power QCD expressions. We then derived the leading logarithmic contribution of the product $H_i \xi_\pi$ at one-loop order, which arises from a non-trivial cancellation of rapidity divergences in the soft and the collinear region as well as additional poles in the hard, the hard-collinear and the soft sector.

The leading rapidity divergences in endpoint-divergent inverse moments show a recursive behaviour resulting in an exponentiation similar to the collinear functions in the Sudakov form factor. Since these poles arise in convolutions rather than matrix elements in individual sectors, a treatment within the framework of the rapidity RG is more involved. Nevertheless, after a subtle rewriting of logarithms, we were able to derive rapidity RGEs for inverse moments whose solutions resum the leading logarithmic contributions. Together with the evolution of the hard and the hard-collinear function, we derived a resummed expression for the product of the hard function and the soft form factor in the LL approximation, which only involves the usual Sudakov evolution kernel $S(\mu_1, \mu_2)$. However, due to a mixing among the various moments and due to the multiple scales in the problem, the structure of the result is more complicated compared to the simple exponential that resums leading logarithms in the Sudakov form factor. This leads to the important observation that, numerically, the interplay between different Sudakov factors leads to a slight enhancement instead of a suppression for large scale separations.

Lastly, we investigated two ideas with the objective of understanding a factorisation and resummation beyond the leading logarithmic approximation. We first studied how the factorisation is modified when a soft-collinear mode is present in the theory. However, it seems that including this mode does not render the occurring moments well-defined, and it does not solve the problem. Moreover, in addition to endpoint-divergent soft and collinear moments, also endpoint-divergent moments of soft-collinear vacuum matrix elements arise. Secondly, we showed by means of toy integrals that the endpoint behaviour of the (bare) LCDAs can be reproduced through a factorisation formula that involves new objects, which we interpret as vacuum matrix elements of non-local operators. Employing a hard cut-off, we showed that this can be used to construct modified LCDAs with well-defined inverse moments, and furthermore, that rapidity divergences cancel already at the level of inverse moments of hadronic objects that are independent of the external states. Since this idea has not been elaborated in the realistic scenario so far, the interpretation of our results and their applications for the resummation of subleading logarithms is yet to be worked out.

Conclusion and Outlook

Chapter 10

Conclusion and Outlook

Exclusive charmless B -meson decays offer the possibility for a precise determination of some of the flavour parameters of the SM, and furthermore, are excellent probes of new physics. The theoretical description of these decays is, however, challenging. Based on first principles, the QCD factorisation approach represents a model-independent framework that allows to separate perturbative from non-perturbative effects through a power expansion in Λ/m_b .

In this thesis, new applications and technical developments of the QCD factorisation approach were presented. In the first project we investigated semileptonic multi-body $B \rightarrow \pi\pi\ell\nu$ decays, which will become accessible in future Belle II analyses and allow for an independent determination of the CKM-matrix element $|V_{ub}|$. We derived a novel factorisation formula for the dipion form factors in the limit of large dipion invariant mass. Although the decay rate, in the considered phase-space region, is too small to be measured with reasonable precision, our results can be used to interpolate between different phase-space regions using proper form factor parametrisations.

In the main part of this thesis we addressed the problem of a complete factorisation of scales in $B \rightarrow \pi$ form factors, or, equivalently, understanding the correct treatment of endpoint divergences. A solution to this long-standing problem would have implications for a large class of observables in exclusive charmless B decays, and furthermore, would be a breakthrough on the conceptual level. Investigating the form factors for non-relativistic bound states allows for a perturbative expansion of the hadronic quantities. Within this setup, we found that in the leading logarithmic approximation the factorisation can still be formulated with inverse moments of light-cone distribution amplitudes. We presented the first resummation of rapidity logarithms in the context of exclusive B -meson decays using the language of the rapidity renormalisation group. Phenomenologically important, our result showed that – even in the limit $m_b \rightarrow \infty$ – the non-factorisable contribution to the form factors receives no Sudakov suppression and is thus numerically of the same size as the factorisable terms.

With the currently running LHCb experiment at CERN in Switzerland and the upcoming Belle II experiment at KEK in Japan, B physics has a promising and fruitful future over the next years or decades. The theoretical challenge will be to match the precision of future measurements. The results derived in this thesis provide useful conceptual and phenomenological insights that can help to finally understand power corrections in the framework of QCDF, thus, pushing this field to the precision frontier.

Appendix

Appendix A

Details on $B \rightarrow \pi\pi$ Form Factors at Large Dipion Invariant Masses

A.1 Definition of Dipion Form Factors

We follow the conventions in [63] and define vector and axial-vector form factors for $b \rightarrow u$ currents in the SM as

$$\langle \pi^+(k_1)\pi^-(k_2)|\bar{\psi}_u\gamma^\mu\psi_b|B^-(p)\rangle = iF_\perp \frac{1}{\sqrt{k^2}} q_\perp^\mu, \quad (\text{A.1})$$

and

$$-\langle \pi^+(k_1)\pi^-(k_2)|\bar{\psi}_u\gamma^\mu\gamma_5\psi_b|B^-(p)\rangle = F_t \frac{q^\mu}{\sqrt{q^2}} + F_0 \frac{2\sqrt{q^2}}{\sqrt{\lambda}} k_{(0)}^\mu + F_\parallel \frac{1}{\sqrt{k^2}} \bar{k}_\parallel^\mu, \quad (\text{A.2})$$

where

$$\begin{aligned} k_{(0)}^\mu &= k^\mu - \frac{k \cdot q}{q^2} q^\mu, \\ \bar{k}_\parallel^\mu &= \bar{k}^\mu - \frac{4(k \cdot q)(q \cdot \bar{k})}{\lambda} k^\mu + \frac{4k^2(q \cdot \bar{k})}{\lambda} q^\mu, \\ q_\perp^\mu &= 2\epsilon^{\mu\alpha\beta\gamma} \frac{q_\alpha k_\beta \bar{k}_\gamma}{\sqrt{\lambda}}. \end{aligned} \quad (\text{A.3})$$

Here our convention for the Levi-Cevitá tensor is related to the definition of the Dirac matrix γ_5 via

$$\text{tr}[\gamma_5 \gamma^\mu \gamma^\nu \gamma^\rho \gamma^\sigma] = -4i \epsilon^{\mu\nu\rho\sigma}. \quad (\text{A.4})$$

In terms of the so-defined ‘‘helicity form factors’’, one obtains simple expressions for the differential decay width and the angular observables, and simple relations between form factors in HQET or SCET, which has also been emphasised for other decay modes [59, 131–134]. To extract the individual form factors, the above relations can be simply

inverted,

$$\begin{aligned}
 F_{\perp}(k^2, q^2, q \cdot \bar{k}) &= -\frac{i\sqrt{k^2}}{q_{\perp}^2} \langle \pi^+ \pi^- | \bar{\psi}_u \not{q}_{\perp} \psi_b | B^- \rangle, \\
 F_{\parallel}(k^2, q^2, q \cdot \bar{k}) &= -\frac{\sqrt{k^2}}{\bar{k}_{\parallel}^2} \langle \pi^+ \pi^- | \bar{\psi}_u \not{\bar{k}}_{\parallel} \gamma_5 \psi_b | B^- \rangle, \\
 F_0(k^2, q^2, q \cdot \bar{k}) &= -\frac{\sqrt{\lambda}}{2\sqrt{q^2} k_{(0)}^2} \langle \pi^+ \pi^- | \bar{\psi}_u \not{k}_{(0)} \gamma_5 \psi_b | B^- \rangle, \\
 F_t(k^2, q^2, q \cdot \bar{k}) &= -\frac{1}{\sqrt{q^2}} \langle \pi^+ \pi^- | \bar{\psi}_u \not{q} \gamma_5 \psi_b | B^- \rangle,
 \end{aligned} \tag{A.5}$$

where

$$q_{\perp}^2 = \bar{k}_{\parallel}^2 = -\frac{k^2(4E_1E_2 - k^2)}{(E_1 + E_2)^2 - k^2}, \quad k_{(0)}^2 = -\frac{M_B^2((E_1 + E_2)^2 - k^2)}{q^2}. \tag{A.6}$$

These form factors can be further expanded in terms of partial waves (see e.g. [63]), using

$$\begin{aligned}
 F_{\perp, \parallel}^{(\ell)} &= -\int_{-1}^{+1} dz \frac{\sqrt{2\ell+1}}{2} F_{\perp, \parallel}(z) p_{\ell}^1(z) \sqrt{1-z^2}, \\
 F_{0,t}^{(\ell)} &= +\int_{-1}^{+1} dz \frac{\sqrt{2\ell+1}}{2} F_{0,t}(z) p_{\ell}^0(z),
 \end{aligned} \tag{A.7}$$

where $p_{\ell}^m(z)$ denote the symmetrised associated Legendre polynomials,

$$p_{\ell}^m(z) \equiv \sqrt{\frac{(\ell-m)!}{(\ell+m)!}} P_{\ell}^m(z), \tag{A.8}$$

which fulfil the orthogonality relations

$$\int_{-1}^{+1} dz p_{\ell}^m(z) p_k^m(z) = \frac{2}{2\ell+1} \delta_{\ell k}, \tag{A.9}$$

with $z \equiv \cos \theta_{\pi} = \frac{2q \cdot \bar{k}}{\sqrt{\lambda}}$. Note that in our convention the form factors turn out to be purely imaginary at leading order.

A.2 Twist-3 Contributions to the Kernel T^{I}

Since subleading-twist effects are sensitive to the perpendicular component of the collinear parton momenta, a comment is in order about the definition of the transverse plane related to the underlying light-cone expansion for the positively charged pion state: As can be seen from the explicit structure of the leading order diagrams leading to (2.16), the gluon propagator associated with the separation of the quark fields in the $|\pi^+\rangle$ state involves the large momenta $(p_b - q)^\mu \simeq (k_1^\mu + k_2^\mu)$ and k_1^μ . The transverse momenta in the light-cone expansion for the π^+ matrix elements are therefore to be chosen as transverse to both pion momenta, k_1 and k_2 . The parton momenta in the two-particle Fock state are then expanded as

$$\begin{aligned} \text{up-quark in } \pi^+ : & \quad k_{q1}^\mu \simeq uk_1^\mu + k_\perp^\mu, \\ \text{anti-down-quark in } \pi^+ : & \quad k_{\bar{q}1}^\mu \simeq \bar{u}k_1^\mu - k_\perp^\mu, \quad \text{with } k_{1,2} \cdot k_\perp \equiv 0, \end{aligned}$$

with $|k_\perp|$ scaling as a hadronic momentum of order Λ . The corresponding twist-3 momentum-space projector can then be written as (see also [53])

$$\mathcal{M}_{\pi^+}^{(3)}(u) = \frac{if_\pi\mu_\pi}{4} \frac{\mathbb{1}}{N_C} \gamma_5 \left\{ -\phi_p(u) + i\sigma_{\mu\nu} \frac{k_1^\mu k_2^\nu}{k_1 \cdot k_2} \frac{\phi'_\sigma(u)}{6} - i\sigma_{\mu\nu} \frac{\phi_\sigma(u)}{6} k_1^\mu \frac{\partial}{\partial k_{\perp\nu}} \right\} \Big|_{k_\perp \rightarrow 0}. \quad (\text{A.10})$$

Neglecting 3-particle contributions, the corresponding LCDAs are fixed by the equations of motion, see Eq. (2.26). The twist-3 analogue to (2.16) can then be derived from

$$\Gamma_X \rightarrow -\frac{\gamma_\alpha \mathcal{M}_{\pi^+}^{(3)}(u) \gamma^\alpha (\not{p}_b - \not{q}) \Gamma}{(p_b - q)^2 (p_b - q - uk_1)^2} - \frac{\gamma_\alpha \mathcal{M}_{\pi^+}^{(3)}(u) \Gamma (uk_1 + \not{k}_\perp + \not{q} + m_b) \gamma^\alpha}{[(uk_1 + q)^2 + 2k_\perp \cdot q - m_b^2] (p_b - q - uk_1)^2}. \quad (\text{A.11})$$

The corresponding contributions to the $B \rightarrow \pi\pi$ matrix elements can be written as

$$\begin{aligned} & \langle \pi^+(k_1)\pi^-(k_2) | \bar{\psi}_u \Gamma \psi_b | B^-(p) \rangle \Big|_{\text{twist-3, LO}} \\ &= \frac{2\pi f_\pi}{k^2} \xi_\pi(E_2; \mu) \int_0^1 du \left(\phi_p(u) T_\Gamma^{(\text{I,P})}(u, k^2, E_1, E_2) + \phi_\sigma(u) T_\Gamma^{(\text{I},\sigma)}(u, k^2, E_1, E_2) \right). \end{aligned} \quad (\text{A.12})$$

(Note that – from the approximate relations in (2.26) – there is an ambiguity in expressing $\phi'_\sigma(u)$ in terms of $\phi_\sigma(u)$ and $\phi_p(u)$.) The first term in (A.11) contributes

$$T_\Gamma^{(\text{I,P})} = i \frac{\alpha_s C_F}{N_C} \frac{2M_B \mu_\pi}{k^2} \frac{s_5}{\bar{u}}, \quad (\text{A.13})$$

whereas the second term in (A.11) contributes

$$\begin{aligned}
 T_{\Gamma}^{(I,\sigma)} = & i \frac{\alpha_s C_F}{N_C} \frac{M_B \mu_{\pi}}{3(\bar{u}(k^2 - 2M_B E_1) - 2M_B E_2)} \\
 & \times \left\{ \frac{1}{\bar{u}} \left[-s_2 - \frac{E_2}{M_B} s_4 + \frac{2E_2 M_B}{k^2} s_6 + \frac{s_7}{2} \right] \right. \\
 & \left. + \frac{1}{u} \left[-s_2 - \frac{E_2}{M_B} s_4 + \frac{2E_2 M_B}{k^2} s_6 + \frac{s_8}{2} \right] + \frac{2E_2 M_B}{k^2} \frac{s_5}{\bar{u}^2} \right\} \\
 & + i \frac{\alpha_s C_F}{N_C} \frac{2E_2 M_B^2 \mu_{\pi}}{3(\bar{u}(k^2 - 2M_B E_1) - 2M_B E_2)^2} \\
 & \times \left\{ \frac{1}{\bar{u}} \left[\frac{E_2}{M_B} s_3 - s_5 + \frac{s_7}{2} + \frac{(4E_1 E_2 - k^2) M_B}{2E_2 k^2} s_5 \right] \right. \\
 & \left. - \left[\frac{k^2}{2E_2 M_B} \left(s_1 - \frac{s_3}{2} \right) - \frac{E_1}{E_2} \frac{s_7}{2} \right] \right\}, \tag{A.14}
 \end{aligned}$$

where we have used the Wandzura-Wilczek approximation Eq. (2.26). Note that the potential endpoint divergence from the term $\phi_p(u)/\bar{u}$ in the limit $\bar{u} \rightarrow 0$ in (A.13) cancels with the last term in the first curly brackets in (A.14). This does not necessarily need to remain true after spectator-scattering corrections are taken into account, i.e. the contributions to the kernel T_{Γ}^{II} involving the twist-3 LCDAs of the positively charged pion can be expected to exhibit additional endpoint-divergent expressions, similar to what is observed in the QCDF approach to non-leptonic $B \rightarrow \pi\pi$ decays. In the approximation (2.26) the convolution integrals with respect to the quark momentum fraction u can be done explicitly, leading to

$$\begin{aligned}
 & \int_0^1 du \left(\phi_p(u) T_{\Gamma}^{(I,p)}(u, k^2, E_1, E_2) + \phi_{\sigma}(u) T_{\Gamma}^{(I,\sigma)}(u, k^2, E_1, E_2) \right) \\
 & \simeq \frac{2M_B \mu_{\pi}}{k^2} \left((1+L) s_5 - \frac{E_2}{E_1} L s_6 \right) \\
 & - \frac{2M_B \mu_{\pi} L}{k^2 - 2M_B E_1} \left(s_2 + \frac{E_2}{M_B} s_4 - \frac{E_2}{E_1} s_6 \right) \\
 & - \frac{2M_B \mu_{\pi}}{k^2 - 2M_B E_1} \left[1 + \frac{2M_B E_2}{k^2 - 2M_B E_1} L \right] \left(\frac{E_2}{M_B} s_3 - \frac{M_B}{2E_2} s_5 - \frac{s_8}{2} \right) \\
 & + \frac{2M_B k^2 \mu_{\pi}}{(k^2 - 2M_B E_1)^2} \left[1 + \left(\frac{2M_B E_2}{k^2 - 2M_B E_1} - \frac{1}{2} \right) L \right] (2s_1 - s_3 - s_7) \tag{A.15}
 \end{aligned}$$

with

$$L \equiv \log \left[\frac{2M_B E_1 + 2M_B E_2 - k^2}{2M_B E_2} \right] = \log \left[\frac{M_B^2 - q^2}{2M_B E_2} \right]. \tag{A.16}$$

Note that the twist-3 contributions to T_{Γ}^{I} now also involve the Dirac structures $s_{4,6,8}$, which did not appear in (2.23).

A.3 Detailed Calculation for the Kernel T^{II}

In the following we summarise the individual results for the spectator-scattering diagrams that contribute to the kernel T^{II} at leading order. We find it convenient to split the expressions into two terms: one representing the individual contributions to the sub-process $b \rightarrow d\pi^+g\ell^-\bar{\nu}_\ell$, and the other the hard-collinear interaction with the spectator quark, which induces the $B^- \rightarrow \pi^-$ transition, such that generically we have

$$\langle \pi\pi | \bar{\psi}_u \Gamma \psi_b | B \rangle \Big|_{\text{Diagram X}} = \text{tr} [A_X A^{\text{spec}}] , \quad (\text{A.17})$$

with

$$A^{\text{spec}} = -g_s T^B \frac{\mathcal{M}_{B\gamma\beta} \mathcal{M}_{\pi^-}}{(\ell - k_{\bar{q}2})^2} \simeq g_s T^B \frac{\mathcal{M}_{B\gamma\beta} \mathcal{M}_{\pi^-}}{2\bar{v}\omega E_2} . \quad (\text{A.18})$$

Here the trace runs over Dirac and colour indices and the integration over the (light-cone) momenta of the quarks is understood implicitly. The factor $(-i)$ from the hard-collinear gluon propagator (in Feynman gauge) and the minus sign from the trace over the closed fermion loop has been assigned to the spectator term. If we restrict ourselves to the leading-power contributions in the $1/m_b$ expansion, we can neglect the external transverse momenta in the *hard* sub-process. However, as is known and understood from the analogous case of $B \rightarrow \pi\ell\nu$ transitions [53, 54, 66], the impact of transverse momenta in the hard-collinear spectator scattering is more subtle, and as a consequence transverse momenta in the associated propagator numerators must not be neglected from the very beginning. The resulting contribution to the $B \rightarrow \pi\pi$ matrix element will be decomposed according to (2.28).

A.3.1 Recapitulation: the $B \rightarrow \pi$ Form Factor F_+

In this thesis, we will use a physical definition of the soft $B \rightarrow \pi$ form factor $\xi_\pi(E_2)$. To this end, we will identify it with the physical form factor $F_+((p-k_2)^2)$, where $(p-k_2)^2 = M_B^2 - 2M_B E_2$. The leading-power spectator-scattering contributions to F_+ have been calculated in [53] (for a definition of F_+ see Eq. (6.4)) and amount to

$$\begin{aligned} \xi_\pi^{(\text{HSA})}(E_2) &\equiv F_+^{(\text{HSA})}(E_2) \\ &= \frac{\alpha_s}{4\pi} \frac{\pi^2 f_B f_\pi M_B}{N_C E_2^2} \int_0^1 dv \int_0^\infty d\omega \left(g_+^{\text{finite}}(v, \omega, E_2) + g_+^{\text{endpoint}}(v, \omega, E_2) \right) , \end{aligned} \quad (\text{A.19})$$

with

$$g_+^{\text{finite}}(v, \omega, E_2) = C_F \frac{4E_2 - M_B}{M_B} \frac{\phi_\pi(v)}{\bar{v}} \frac{\phi_B^+(\omega)}{\omega} , \quad (\text{A.20})$$

and

$$\begin{aligned} g_+^{\text{endpoint}}(v, \omega, E_2) &= C_F \frac{(1+\bar{v})\phi_\pi(v)}{\bar{v}^2} \frac{\phi_B^-(\omega)}{\omega} + 2\mu_\pi \frac{\phi_p(v)}{\bar{v}} \frac{\phi_B^+(\omega)}{\omega^2} \\ &\quad + \frac{\mu_\pi}{2E_2} \left(\frac{\phi_p(v) - \phi'_\sigma(v)/6}{\bar{v}^2} \right) \frac{\phi_B^+(\omega)}{\omega} . \end{aligned} \quad (\text{A.21})$$

Here the scaling of the various moments (after some ad-hoc regularisation, $\bar{v} \gtrsim \frac{\Lambda}{M_B}$, $\omega \gtrsim \frac{\Lambda^2}{M_B}$) is to be understood as [53]

$$\begin{aligned} \left\langle \frac{\phi_\pi(v)}{\bar{v}} \right\rangle &\sim \mathcal{O}(1), \\ \left\langle \frac{\phi_p(v) + \phi'_\sigma(v)/6}{\bar{v}^2} \right\rangle &\sim \left\langle \frac{\phi_p(v)}{\bar{v}} \right\rangle \sim \left\langle \frac{\phi_\pi(v)}{\bar{v}^2} \right\rangle \sim \mathcal{O}\left(\ln \frac{\Lambda}{M_B}\right), \\ \left\langle \frac{\phi_p(v) - \phi'_\sigma(v)/6}{\bar{v}^2} \right\rangle &\sim \left\langle \frac{\phi_p(v)}{\bar{v}^2} \right\rangle \sim \mathcal{O}\left(\frac{M_B}{\Lambda}\right), \end{aligned} \quad (\text{A.22})$$

and

$$\left\langle \frac{\phi_B^+(\omega)}{\omega} \right\rangle = \mathcal{O}\left(\frac{1}{\Lambda}\right), \quad \left\langle \frac{\phi_B^+(\omega)}{\omega^2} \right\rangle \sim \mathcal{O}\left(\frac{1}{\Lambda^2} \ln \frac{\Lambda}{M_B}\right), \quad \left\langle \frac{\phi_B^-(\omega)}{\omega} \right\rangle = \mathcal{O}\left(\frac{1}{\Lambda} \ln \frac{\Lambda}{M_B}\right). \quad (\text{A.23})$$

Note that when utilising an analytic regularisation prescription, e.g. raising powers of certain propagators to a non-integer value, this scaling may change. In the following we have to show that the structures in g_+^{endpoint} are indeed universal and also appear in exactly the same form in the spectator-scattering contributions to the $B \rightarrow \pi\pi$ form factors at large k^2 , justifying the procedure employed around (2.18).

A.3.2 Expressions for $b \rightarrow d\pi^+ g\ell^- \bar{v}_\ell$ Amplitudes

In the following we collect the amplitudes A_X describing the $b \rightarrow d\pi^+ g\ell^- \bar{v}_\ell$ subprocess in (A.17) from the various diagrams, together with the approximations to be made in the large-recoil limit.

Diagrams (A1-A6)

$$\begin{aligned} A_1 &= 4\pi\alpha_s C_F g_s T^B \frac{\gamma^\alpha \mathcal{M}_{\pi^+}^{(2)} \gamma_\alpha (\not{k}_1 + \not{k}_{q_2}) \Gamma(\not{p} - \not{k}_{\bar{q}_2} + m_b) \gamma^\beta}{(k_1 + k_{q_2})^2 (k_{q_2} + k_{\bar{q}_1})^2 ((p_b - k_{\bar{q}_2})^2 - m_b^2)} \gamma^\beta \\ &\simeq -4\pi\alpha_s C_F g_s T^B \frac{\mathcal{M}_{\pi^+}^{(2)} \not{k}_2 \Gamma(\not{p} + M_B - \bar{v}\not{k}_2) \gamma^\beta}{\bar{u} v \bar{v} M_B E_2 (k^2)^2}, \end{aligned} \quad (\text{A.24})$$

$$\begin{aligned} A_2 &= 4\pi\alpha_s C_F g_s T^B \frac{\gamma^\beta (\not{k}_2 - \not{\ell}) \gamma^\alpha \mathcal{M}_{\pi^+}^{(2)} \gamma_\alpha (\not{k} - \not{\ell}) \Gamma}{(k_2 - \ell)^2 (k - \ell)^2 (k - \ell - k_{q_1})^2} \\ &\simeq -4\pi\alpha_s C_F g_s T^B \frac{\gamma^\beta (\not{k}_2 - \not{\ell}) \mathcal{M}_{\pi^+}^{(2)} \not{k}_2 \Gamma}{\bar{u} \omega E_2 (k^2)^2}, \end{aligned} \quad (\text{A.25})$$

$$\begin{aligned}
 A_3 &= -4\pi\alpha_s C_{FA} g_s T^B \frac{\gamma^\alpha \mathcal{M}_{\pi^+}^{(2)} \gamma^\beta (\not{k}_{q1} + \not{k}_{\bar{q}2} - \not{\ell}) \gamma_\alpha (\not{k} - \not{\ell}) \Gamma}{(k_{q1} + k_{\bar{q}2} - \ell)^2 ((k - \ell)^2) (k_{q1} + k_{q2})^2} \\
 &\simeq -4\pi\alpha_s C_{FA} g_s T^B \frac{\gamma^\alpha \mathcal{M}_{\pi^+}^{(2)} \gamma^\beta (u \not{k}_1 + \bar{v} \not{k}_2) \gamma_\alpha \not{k} \Gamma}{u \bar{u} v \bar{v} (k^2)^3}, \tag{A.26}
 \end{aligned}$$

$$\begin{aligned}
 A_4 &= -4\pi\alpha_s C_{FA} g_s T^B \frac{\gamma^\alpha (\not{l} - \not{k}_{\bar{q}1} - \not{k}_{\bar{q}2}) \gamma^\beta \mathcal{M}_{\pi^+}^{(2)} \gamma_\alpha (\not{k} - \not{\ell}) \Gamma}{(\ell - k_{\bar{q}1} - k_{\bar{q}2})^2 ((k - \ell)^2) (k_{\bar{q}1} + k_2 - \ell)^2} \\
 &\simeq 4\pi\alpha_s C_{FA} g_s T^B \frac{\gamma^\alpha (\bar{u} \not{k}_1 + \bar{v} \not{k}_2) \gamma^\beta \mathcal{M}_{\pi^+}^{(2)} \gamma_\alpha \not{k} \Gamma}{\bar{u}^2 \bar{v} (k^2)^3}, \tag{A.27}
 \end{aligned}$$

$$\begin{aligned}
 A_5 &= 4\pi\alpha_s C_F g_s T^B \frac{\gamma^\alpha \mathcal{M}_{\pi^+}^{(2)} \gamma_\alpha (\not{k}_1 + \not{k}_{q2}) \gamma^\beta (\not{k} - \not{\ell}) \Gamma}{(k_1 + k_{q2})^2 ((k - \ell)^2) (k_{q1} + k_{q2})^2} \\
 &\simeq 8\pi\alpha_s C_F g_s T^B \frac{\mathcal{M}_{\pi^+}^{(2)} \not{k}_2 \gamma^\beta \not{k} \Gamma}{\bar{u} v (k^2)^3}, \tag{A.28}
 \end{aligned}$$

$$\begin{aligned}
 A_6 &= 4\pi\alpha_s \frac{C_A}{2} g_s T^B \frac{\gamma_\alpha \mathcal{M}_{\pi^+}^{(2)} \gamma_\gamma (\not{k} - \not{\ell}) \Gamma}{(k - \ell)^2 (k_{\bar{q}1} + k_2 - \ell)^2 (k_{\bar{q}1} + k_{q2})^2} \\
 &\quad \times (g^{\alpha\beta} (k_{\bar{q}2} - k_{q2} - k_{\bar{q}1} - \ell)^\gamma + g^{\beta\gamma} (2\ell - k_{\bar{q}1} - k_2 - k_{\bar{q}2})^\alpha \\
 &\quad \quad + g^{\alpha\gamma} (2k_{\bar{q}1} + k_2 + k_{q2} - \ell)^\beta) \\
 &\simeq 2\pi\alpha_s C_A g_s T^B \frac{\gamma_\alpha \mathcal{M}_{\pi^+}^{(2)} \gamma_\gamma \not{k} \Gamma}{\bar{u}^2 v (k^2)^3} \\
 &\quad \times (g^{\alpha\beta} (\bar{v} - v) k_2^\gamma - g^{\beta\gamma} (1 + \bar{v}) k_2^\alpha + g^{\alpha\gamma} (2\bar{u} k_1 + (1 + v) k_2)^\beta). \tag{A.29}
 \end{aligned}$$

Diagrams (B1-B6)

$$\begin{aligned}
 B_1 &= 4\pi\alpha_s C_F g_s T^B \frac{\gamma^\alpha \mathcal{M}_{\pi^+}^{(2)} \Gamma (\not{p} - \not{k}_{\bar{q}1} - \not{k}_2 + m_b) \gamma_\alpha (\not{p} - \not{k}_{\bar{q}2} + m_b) \gamma^\beta}{((p - k_{\bar{q}1} - k_2)^2 - m_b^2) ((p - k_{\bar{q}2})^2 - m_b^2) (k_{\bar{q}1} + k_{q2})^2} \\
 &\simeq -4\pi\alpha_s C_F g_s T^B \frac{\gamma^\alpha \mathcal{M}_{\pi^+}^{(2)} \Gamma (\not{p} - \bar{u} \not{k}_1 - \not{k}_2 + M_B) \gamma_\alpha (\not{p} - \bar{v} \not{k}_2 + M_B) \gamma^\beta}{2\bar{u} v \bar{v} E_2 M_B k^2 (-2\bar{u} E_1 M_B - 2E_2 M_B + \bar{u} k^2)}, \tag{A.30}
 \end{aligned}$$

$$\begin{aligned}
 B_2 &= 4\pi\alpha_s C_F g_s T^B \frac{\gamma^\beta (\not{k}_2 - \not{l}) \gamma^\alpha \mathcal{M}_{\pi^+}^{(2)} \Gamma (\not{p} - \not{k}_{\bar{q}1} - \not{k}_2 - \not{l} + m_b) \gamma_\alpha}{(k_2 - \ell)^2 ((p - k_{\bar{q}1} - k_2 - \ell)^2 - m_b^2) (k_{\bar{q}1} + k_2 - \ell)^2} \\
 &\simeq -4\pi\alpha_s C_F g_s T^B \frac{\gamma^\beta (\not{k}_2 - \not{l}) \gamma^\alpha \mathcal{M}_{\pi^+}^{(2)} \Gamma (\not{p} - \bar{u} \not{k}_1 - \not{k}_2 + M_B) \gamma_\alpha}{2\bar{u} \omega E_2 k^2 (-2\bar{u} E_1 M_B - 2E_2 M_B + \bar{u} k^2)}, \tag{A.31}
 \end{aligned}$$

$$\begin{aligned}
 B_3 &= -4\pi\alpha_s C_{FA} g_s T^B \frac{\gamma^\alpha \mathcal{M}_{\pi^+}^{(2)} \gamma^\beta (\not{k}_{q_1} + \not{k}_{\bar{q}_2} - \not{\ell}) \Gamma(\not{p} - \not{k}_{\bar{q}_1} - \not{k}_{q_2} - \not{\ell} + m_b) \gamma_\alpha}{(k_{q_1} + k_{\bar{q}_2} - \ell)^2 ((p - k_{\bar{q}_1} - k_{q_2} - \ell)^2 - m_b^2) (k_{\bar{q}_1} + k_{q_2})^2} \\
 &\simeq -4\pi\alpha_s C_{FA} g_s T^B \frac{\gamma^\alpha \mathcal{M}_{\pi^+}^{(2)} \gamma^\beta (u \not{k}_1 + \bar{v} \not{k}_2) \Gamma(\not{p} - \bar{u} \not{k}_1 - v \not{k}_2 + M_B) \gamma_\alpha}{u \bar{u} v \bar{v} (k^2)^2 (-2\bar{u} E_1 M_B - 2v E_2 M_B + \bar{u} v k^2)}, \quad (\text{A.32})
 \end{aligned}$$

$$\begin{aligned}
 B_4 &= -4\pi\alpha_s C_{FA} g_s T^B \frac{\gamma^\alpha (-\not{k}_{\bar{q}_1} - \not{k}_{\bar{q}_2} + \not{\ell}) \gamma^\beta \mathcal{M}_{\pi^+}^{(2)} \Gamma(\not{p} - \not{k}_{\bar{q}_1} - \not{k}_2 + m_b) \gamma_\alpha}{(k_{\bar{q}_1} + k_{\bar{q}_2} - \ell)^2 ((p - k_{\bar{q}_1} - k_2)^2 - m_b^2) (k_{\bar{q}_1} + k_2 - \ell)^2} \\
 &\simeq -4\pi\alpha_s C_{FA} g_s T^B \frac{\gamma^\alpha (-\bar{u} \not{k}_1 - \bar{v} \not{k}_2) \gamma^\beta \mathcal{M}_{\pi^+}^{(2)} \Gamma(\not{p} - \bar{u} \not{k}_1 - \not{k}_2 + M_B) \gamma_\alpha}{\bar{u}^2 \bar{v} (k^2)^2 (-2\bar{u} E_1 M_B - 2E_2 M_B + \bar{u} k^2)}, \quad (\text{A.33})
 \end{aligned}$$

$$\begin{aligned}
 B_5 &= -4\pi\alpha_s C_{FA} g_s T^B \frac{\gamma^\alpha \mathcal{M}_{\pi^+}^{(2)} \Gamma(\not{p} - \not{k}_{\bar{q}_1} - \not{k}_2 + m_b) \gamma^\beta (\not{p} - \not{k}_{\bar{q}_1} - \not{k}_{q_2} - \not{\ell} + m_b) \gamma_\alpha}{((p - k_{\bar{q}_1} - k_2)^2 - m_b^2) ((p - k_{\bar{q}_1} - k_{q_2} - \ell)^2 - m_b^2) (k_{\bar{q}_1} + k_{q_2})^2} \\
 &\simeq -4\pi\alpha_s C_{FA} g_s T^B \\
 &\quad \times \frac{\gamma^\alpha \mathcal{M}_{\pi^+}^{(2)} \Gamma(\not{p} - \bar{u} \not{k}_1 - \not{k}_2 + M_B) \gamma^\beta (\not{p} - \bar{u} \not{k}_1 - v \not{k}_2 + M_B) \gamma_\alpha}{(-2\bar{u} M_B E_1 - 2M_B E_2 + \bar{u} k^2) (-2\bar{u} M_B E_1 - 2v M_B E_2 + \bar{u} v k^2) \bar{u} v k^2}, \quad (\text{A.34})
 \end{aligned}$$

$$\begin{aligned}
 B_6 &= 4\pi\alpha_s \frac{C_A}{2} g_s T^B \frac{\gamma_\alpha \mathcal{M}_{\pi^+}^{(2)} \Gamma(\not{p} - \not{k}_{\bar{q}_1} - \not{k}_2 + m_b) \gamma_\gamma}{((p - k_{\bar{q}_1} - k_2)^2 - m_b^2) (k_{\bar{q}_1} + k_2 - \ell)^2 (k_{\bar{q}_1} + k_{q_2})^2} \\
 &\quad \times (g^{\alpha\beta} (k_{\bar{q}_2} - k_{q_2} - k_{\bar{q}_1} - \ell)^\gamma + g^{\beta\gamma} (2\ell - k_{\bar{q}_1} - k_2 - k_{\bar{q}_2})^\alpha \\
 &\quad \quad + g^{\alpha\gamma} (2k_{\bar{q}_1} + k_2 + k_{q_2} - \ell)^\beta) \\
 &\simeq 2\pi\alpha_s C_A g_s T^B \frac{\gamma_\alpha \mathcal{M}_{\pi^+}^{(2)} \Gamma(\not{p} - \bar{u} \not{k}_1 - \not{k}_2 + M_B) \gamma_\gamma}{(-2\bar{u} E_1 M_B - 2E_2 M_B + \bar{u} k^2) \bar{u}^2 v (k^2)^2} \\
 &\quad \times (g^{\alpha\beta} ((\bar{v} - v) k_2 - \bar{u} k_1)^\gamma - g^{\beta\gamma} (1 + \bar{v}) k_2^\alpha + g^{\alpha\gamma} (2\bar{u} k_1 + v k_2)^\beta). \quad (\text{A.35})
 \end{aligned}$$

A.3.3 Contributions to $B \rightarrow \pi\pi$ Matrix Elements

In the following we collect the finite and endpoint-divergent contributions of the individual diagrams to the $B \rightarrow \pi\pi$ matrix elements as defined in Eq. (2.28). The contributions to the kernel T_Γ^{II} from the spectator scattering diagrams are expressed in terms of several functions of the momentum fractions \bar{u} and \bar{v} of the (anti-)quarks in the two pions, which are convoluted with the corresponding leading-twist LCDAs. We use again the same abbreviations for Dirac traces (2.19), kinematic invariants (2.29) and for colour factors (2.30). We also employ the equations of motion (2.31) to simplify the twist-3 contributions to the endpoint-divergent terms in the hard-scattering amplitudes.

Diagram (A1)

$$g_{(A1)}^{\text{finite}} = C_F \frac{E_2}{M_B} \frac{s_4}{\bar{u}} \frac{\phi_\pi(v)}{v\bar{v}} \frac{\phi_B^+(\omega)}{\omega} \quad (\text{A.36})$$

$$g_{(A1)}^{\text{endpoint}} = C_F \frac{S_A}{\bar{u}} \left(\frac{\phi_\pi(v)}{v\bar{v}^2} \frac{\phi_B^-(\omega)}{\omega} + \frac{\mu_\pi \phi_\sigma(v)}{6E_2 \bar{v}^3} \frac{\phi_B^+(\omega)}{\omega} \right) \quad (\text{A.37})$$

Diagram (A2)

$$g_{(A2)}^{\text{finite}} = C_F \left(\frac{2E_2 M_B}{k^2} \frac{s_6}{\bar{u}} - \frac{s_2}{\bar{u}} \right) \frac{\phi_\pi(v)}{\bar{v}} \frac{\phi_B^+(\omega)}{\omega}, \quad (\text{A.38})$$

$$g_{(A2)}^{\text{endpoint}} = C_F \frac{S_A}{\bar{u}} \left(\frac{\phi_\pi(v)}{\bar{v}} \frac{\phi_B^-(\omega)}{\omega} + 2\mu_\pi \frac{\phi_P(v)}{\bar{v}} \frac{\phi_B^+(\omega)}{\omega^2} \right). \quad (\text{A.39})$$

Diagrams (A3+A4)

$$g_{(A3+A4)}^{\text{finite}} = C_{FA} \left(\frac{2E_2 M_B}{k^2} \frac{s_6}{\bar{u}} - \frac{s_2}{\bar{u}} \right) \frac{\phi_\pi(v)}{v\bar{v}} \frac{\phi_B^+(\omega)}{\omega}, \quad (\text{A.40})$$

$$g_{(A3+A4)}^{\text{endpoint}} = -C_{FA} \left(\frac{2E_2 M_B}{k^2} \frac{s_5}{\bar{u}^2} \frac{\phi_\pi(v)}{\bar{v}} \frac{\phi_B^+(\omega)}{\omega} - \frac{S_A}{\bar{u}} \frac{\phi_\pi(v)}{v\bar{v}} \frac{\phi_B^-(\omega)}{\omega} \right). \quad (\text{A.41})$$

Diagram (A5)

$$g_{(A5)}^{\text{finite}} = C_F \frac{2E_2 M_B}{k^2} \frac{s_5}{\bar{u}} \frac{\phi_\pi(v)}{v\bar{v}} \frac{\phi_B^+(\omega)}{\omega}, \quad (\text{A.42})$$

$$g_{(A5)}^{\text{endpoint}} = 0. \quad (\text{A.43})$$

Diagram (A6)

$$g_{(A6)}^{\text{finite}} = C_A \left(\frac{s_2}{\bar{u}} - \frac{2E_2 M_B}{k^2} \frac{s_6}{\bar{u}} \right) \frac{\phi_\pi(v)}{2v\bar{v}} \frac{\phi_B^+(\omega)}{\omega}, \quad (\text{A.44})$$

$$g_{(A6)}^{\text{endpoint}} = C_A \left(\frac{2E_2 M_B}{k^2} \frac{s_5}{\bar{u}^2} \frac{(v-\bar{v})\phi_\pi(v)}{4v\bar{v}} \frac{\phi_B^+(\omega)}{\omega} - \frac{S_A}{\bar{u}} \frac{\phi_\pi(v)}{2v\bar{v}} \frac{\phi_B^-(\omega)}{\omega} \right). \quad (\text{A.45})$$

Diagram (B1)

$$g_{(B1)}^{\text{finite}} = C_F \frac{2E_2}{M_B} \frac{S_B^{(i)}(u)}{\bar{u}} \frac{\phi_\pi(v)}{v\bar{v}} \frac{\phi_B^+(\omega)}{\omega}, \quad (\text{A.46})$$

$$g_{(B1)}^{\text{endpoint}} = C_F \frac{S_B^{(i)}(u) + S_B^{(ii)}(u)}{\bar{u}} \left(\frac{\phi_\pi(v)}{v\bar{v}^2} \frac{\phi_B^-(\omega)}{\omega} + \frac{\mu_\pi \phi_\sigma(v)}{6E_2 \bar{v}^3} \frac{\phi_B^+(\omega)}{\omega} \right). \quad (\text{A.47})$$

Diagram (B2)

$$g_{(B2)}^{\text{finite}} = C_F \left(\left(\frac{2E_2}{M_B} - 1 \right) \frac{S_B^{(i)}(u)}{\bar{u}} + \frac{E_2 s_3}{M_B \bar{u}} \right) \frac{\phi_\pi(v)}{\bar{v}} \frac{\phi_B^+(\omega)}{\omega}, \quad (\text{A.48})$$

$$g_{(B2)}^{\text{endpoint}} = C_F \frac{S_B^{(i)}(u) + S_B^{(ii)}(u)}{\bar{u}} \left(\frac{\phi_\pi(v)}{\bar{v}} \frac{\phi_B^-(\omega)}{\omega} + 2\mu_\pi \frac{\phi_P(v)}{\bar{v}} \frac{\phi_B^+(\omega)}{\omega^2} \right). \quad (\text{A.49})$$

Diagrams (B3+B5)

$$g_{(B3+B5)}^{\text{finite}} = C_{FA} \left(-v_\perp^2 \frac{S_B^{(i)}(u)}{\bar{u}} \left(1 - \frac{2E_2 M_B}{\bar{u} v k^2 - 2\bar{u} E_1 M_B - 2v E_2 M_B} \right) + \frac{2E_2^2 s_3 - E_2 M_B (2s_5 - s_7)}{\bar{u} (\bar{u} v k^2 - 2\bar{u} E_1 M_B - 2v E_2 M_B)} \right) \frac{\phi_\pi(v)}{v\bar{v}} \frac{\phi_B^+(\omega)}{\omega}, \quad (\text{A.50})$$

$$g_{(B3+B5)}^{\text{endpoint}} = C_{FA} \left(\frac{S_B^{(i)}(u) + S_B^{(ii)}(u)}{\bar{u}} \frac{\phi_\pi(v)}{v\bar{v}^2} \frac{\phi_B^-(\omega)}{\omega} - v_\perp^2 \frac{S_B^{(i)}(u)}{\bar{u}} \frac{\phi_\pi(v)}{\bar{v}^2} \frac{\phi_B^+(\omega)}{\omega} + v_\perp^2 \frac{S_B^{(i)}(u)}{\bar{u}} \frac{\mu_\pi \phi_\sigma(v)}{6E_2 \bar{v}^3} \frac{\phi_B^-(\omega)}{\omega} - v_\perp^2 \frac{S_B^{(i)}(u) + S_B^{(ii)}(u)}{\bar{u}} \frac{\mu_\pi \phi_\sigma(v)}{6E_2 \bar{v}^3} \frac{\phi_B^+(\omega)}{\omega} \right). \quad (\text{A.51})$$

Diagram (B4)

$$g_{(B4)}^{\text{finite}} = C_{FA} \left(\frac{2E_2}{M_B} \left(\frac{2E_1 M_B}{k^2} - 1 \right) \frac{S_B^{(i)}(u)}{\bar{u}} - \frac{E_2 s_3}{M_B \bar{u}} \right) \frac{\phi_\pi(v)}{\bar{v}} \frac{\phi_B^+(\omega)}{\omega}, \quad (\text{A.52})$$

$$g_{(B4)}^{\text{endpoint}} = C_{FA} \left(\frac{2E_2 M_B s_5}{k^2} \frac{\phi_\pi(v)}{\bar{u}^2} \frac{\phi_B^+(\omega)}{\bar{v}} \frac{\phi_B^+(\omega)}{\omega} - \frac{S_B^{(i)}(u) + S_B^{(ii)}(u)}{\bar{u}} \frac{\phi_\pi(v)}{\bar{v}^2} \frac{\phi_B^-(\omega)}{\omega} + v_\perp^2 \frac{S_B^{(i)}(u)}{\bar{u}} \frac{\phi_\pi(v)}{\bar{v}^2} \frac{\phi_B^+(\omega)}{\omega} - v_\perp^2 \frac{S_B^{(i)}(u)}{\bar{u}} \frac{\mu_\pi \phi_\sigma(v)}{6E_2 \bar{v}^3} \frac{\phi_B^-(\omega)}{\omega} + v_\perp^2 \frac{S_B^{(i)}(u) + S_B^{(ii)}(u)}{\bar{u}} \frac{\mu_\pi \phi_\sigma(v)}{6E_2 \bar{v}^3} \frac{\phi_B^+(\omega)}{\omega} \right). \quad (\text{A.53})$$

Diagram (B6)

$$g_{(B6)}^{\text{finite}} = C_A \left(\frac{S_B^{(i)}(u)}{\bar{u}} \left(\left(1 - \frac{2E_2}{M_B} \right) \frac{\phi_\pi(v)}{2v} + v_\perp^2 \frac{\phi_\pi(v)}{2\bar{v}} \right) - \frac{E_2}{M_B} \frac{s_3}{\bar{u}} \frac{\phi_\pi(v)}{2v} \right) \frac{\phi_B^+(\omega)}{\omega}, \quad (\text{A.54})$$

$$g_{(B6)}^{\text{endpoint}} = C_A \left(\frac{2E_2 M_B}{k^2} \frac{s_5}{\bar{u}^2} \frac{(\bar{v} - v)}{4v\bar{v}} \frac{\phi_\pi(v)}{\omega} \frac{\phi_B^+(\omega)}{\omega} - \frac{S_B^{(i)}(u) + S_B^{(ii)}(u)}{\bar{u}} \frac{\phi_\pi(v)}{2v\bar{v}} \frac{\phi_B^-(\omega)}{\omega} \right). \quad (\text{A.55})$$

A.4 More on Kinematics

Expressing the pion energies $E_{1,2}$ in terms of the kinematic variables k^2 , q^2 and $\cos\theta$, one obtains

$$E_{1,2}(k^2, q^2, \cos\theta) = \frac{k^2 + M_B^2 - q^2 \pm \cos\theta \sqrt{\lambda(k^2, q^2)}}{4M_B}. \quad (\text{A.56})$$

Without loss of generality, we may assume that $\cos\theta \geq 0$, such that $E_2 < E_1$, and we thus have to determine the minimal value of E_2 for given phase-space constraints on $(k^2, q^2, \cos\theta)$,

$$E_{\min} = \min E_2(k^2, q^2, \cos\theta) \quad (\text{for } \cos\theta \geq 0). \quad (\text{A.57})$$

(For $\cos\theta \leq 0$, the same discussion goes through for E_1 .) Since E_2 is *decreasing* with $\cos\theta$, its minimal value (for fixed (k^2, q^2)) is obtained for the maximal value $\cos\theta|_{\max} \equiv 1/a$ with $a \geq 1$. Similarly, E_2 is *increasing* with k^2 , such that its minimal value is obtained for $k^2 = k_{\min}^2$. Concerning the q^2 -dependence (for fixed values $k^2 = k_{\min}^2$ and $\cos\theta = 1/a$), the situation is more involved. The function $E_2(q^2)$ exhibits a minimum at

$$q_{\star}^2 = M_B^2 + k_{\min}^2 - \frac{2aM_B \sqrt{k_{\min}^2}}{\sqrt{a^2 - 1}}. \quad (\text{A.58})$$

This always fulfils $q_{\star}^2 \leq q_{\max}^2 = (M_B - \sqrt{k_{\min}^2})^2$, which is the upper phase-space boundary for q^2 . However, the condition $q_{\star}^2 \geq 0$ yields a non-trivial relation between k_{\min}^2 and a :

$$\text{minimum at } q_{\star}^2 \geq 0 \quad \Leftrightarrow \quad k_{\min}^2 \leq \frac{a-1}{a+1} M_B^2. \quad (\text{A.59})$$

We thus have to consider two cases

- $q_{\star}^2 \geq 0$, with

$$\begin{aligned} E_{\min} &= E_2(k_{\min}^2, q_{\star}^2, 1/a) = \frac{\sqrt{a^2 - 1}}{2a} \sqrt{k_{\min}^2} \\ \Leftrightarrow k_{\min}^2 &= \frac{4a^2}{a^2 - 1} E_{\min}^2, \end{aligned} \quad (\text{A.60})$$

for which the relation (A.59) translates into (using $E_2 \leq M_B/2$)

$$E_{\min} < \frac{a-1}{a} \frac{M_B}{2}. \quad (\text{A.61})$$

- $q_{\star}^2 < 0$, with

$$\begin{aligned} E_{\min} &= E_2(k_{\min}^2, 0, 1/a) = \frac{(a+1)k^2 + (a-1)M_B^2}{4aM_B} \\ \Leftrightarrow k_{\min}^2 &= \frac{4aM_B E_{\min} - (a-1)M_B^2}{a+1} \end{aligned} \quad (\text{A.62})$$

for which the complement of the relation (A.59) now consistently translates into

$$E_{\min} > \frac{a-1}{a} \frac{M_B}{2}. \quad (\text{A.63})$$

Note that (A.62) always holds for $a = 1$, in which case the minimal value of E_2 is given at $q^2 = 0$, and $k_{\min}^2 = 2M_B E_{\min}$, as in scenarios A and B defined in the text. For a given value of E_{\min} , there is a critical value of the angular cut, $a_* = M_B/(M_B - 2E_{\min})$, above which (A.60) is to be used. In our scenario C we took $k_{\min}^2 = M_B^2/4$ and $a = 3$, for which one actually has $q_*^2 > 0$, and therefore the correct expression for k_{\min}^2 reads

$$\begin{aligned} k_{\min}^2 &= M_B^2/4, \quad |\cos \theta| \leq 1/3 \\ \Rightarrow E_{\min} &= \frac{\sqrt{a^2 - 1}}{2a} \sqrt{k_{\min}^2} = \frac{1}{3\sqrt{2}} M_B \simeq 1.24 \text{ GeV}. \end{aligned} \quad (\text{A.64})$$

(For the resulting value of E_{\min} one has $a_* \simeq 1.89$, and therefore $a > a_*$ in our scenario C.)

Appendix B

Details on the Sudakov Form Factor

B.1 Details on the RG Evolution Kernels

We summarise some details on the evolution kernels for the Sudakov form factor. With the expansions

$$\begin{aligned}\beta(\alpha) &= -2\alpha \left[\beta_0 \left(\frac{\alpha}{4\pi} \right) + \beta_1 \left(\frac{\alpha}{4\pi} \right)^2 + \mathcal{O}(\alpha^3) \right], \\ \gamma_{\text{cusp}}(\alpha) &= \gamma_{\text{cusp}}^{(0)} \left(\frac{\alpha}{4\pi} \right) + \gamma_{\text{cusp}}^{(1)} \left(\frac{\alpha}{4\pi} \right)^2 + \mathcal{O}(\alpha^3), \\ \gamma_V(\alpha) &= \gamma_V^{(0)} \left(\frac{\alpha}{4\pi} \right) + \gamma_V^{(1)} \left(\frac{\alpha}{4\pi} \right)^2 + \mathcal{O}(\alpha^3),\end{aligned}\tag{B.1}$$

one finds the following expressions for the functions $S(\mu_1, \mu_2)$ and $A_{\gamma_i}(\mu_1, \mu_2)$ (we abbreviate $r \equiv \alpha(\mu_2)/\alpha(\mu_1)$, see e.g. [87]):

$$\begin{aligned}A_{\gamma_V}(\mu_1, \mu_2) &= \frac{\gamma_V^{(0)}}{2\beta_0} \log r + \mathcal{O}(\alpha), \\ A_{\gamma_{\text{cusp}}}(\mu_1, \mu_2) &= \frac{\gamma_{\text{cusp}}^{(0)}}{2\beta_0} \log r + \mathcal{O}(\alpha), \\ S(\mu_1, \mu_2) &= \frac{\gamma_{\text{cusp}}^{(0)}}{4\beta_0^2} \left[\frac{4\pi}{\alpha(\mu_1)} \left(\frac{r-1}{r} - \log r \right) \right. \\ &\quad \left. + \left(\frac{\gamma_{\text{cusp}}^{(1)}}{\gamma_{\text{cusp}}^{(0)}} - \frac{\beta_1}{\beta_0} \right) (1-r + \log r) + \frac{\beta_1}{2\beta_0} \log^2 r \right] + \mathcal{O}(\alpha).\end{aligned}\tag{B.2}$$

Using the one-loop running coupling Eq. (1.3), we can re-expand these expressions in the coupling constant evaluated at a common scale, $\alpha(\mu_0)$:

$$\begin{aligned}A_{\gamma_{\text{cusp}}}(\mu_1, \mu_2) &\simeq \gamma_{\text{cusp}}^{(0)} \frac{\alpha(\mu_0)}{4\pi} \log \frac{\mu_1}{\mu_2} + \mathcal{O}(\alpha^2), \\ A_{\gamma_V}(\mu_1, \mu_2) &\simeq \gamma_V^{(0)} \frac{\alpha(\mu_0)}{4\pi} \log \frac{\mu_1}{\mu_2} + \mathcal{O}(\alpha^2), \\ S(\mu_1, \mu_2) &\simeq -\frac{\gamma_{\text{cusp}}^{(0)}}{2} \frac{\alpha(\mu_0)}{4\pi} \log^2 \frac{\mu_1}{\mu_2} + \mathcal{O}(\alpha^2).\end{aligned}\tag{B.3}$$

The one-loop coefficients are given by $\gamma_{\text{cusp}}^{(0)} = 4$ and $\gamma_V^{(0)} = -6$. We observe that $S(\mu_1, \mu_2)$ contains large double logarithms, whereas the $A_{\gamma_i}(\mu_1, \mu_2)$ only contain single logarithms.

B.2 Details on the Renormalisation of F and R

The RGE for the remainder function R takes a similar form as the one for the hard matching coefficient \tilde{C}_V . The wave-function renormalisation factor Z_2 already absorbs some of the UV-divergences. For the remaining divergences we introduce a Z -factor:

$$R(m^2, \mu) = Z_R^{-1}(\varepsilon, m^2, \mu) Z_2(\varepsilon, m^2) R^{\text{bare}}(\varepsilon, m^2), \quad (\text{B.4})$$

with

$$Z_R(\varepsilon, m^2, \mu) = 1 + \frac{\alpha(\mu)}{4\pi} \left(\frac{2}{\varepsilon^2} + \frac{4}{\varepsilon} \log \frac{\mu}{m} + \frac{3}{\varepsilon} \right) + \mathcal{O}(\alpha^2). \quad (\text{B.5})$$

The renormalised remainder function reads

$$R(m^2, \mu) = 1 + \frac{\alpha(\mu)}{4\pi} \left(4 \log^2 \frac{\mu}{m} + 6 \log \frac{\mu}{m} + \frac{9}{2} - \frac{5\pi^2}{6} \right), \quad (\text{B.6})$$

and obeys the following RGE to all orders in perturbation theory:

$$\frac{dR(m^2, \mu)}{d \log \mu} = \left(\gamma_{\text{cusp}}(\alpha) \log \frac{\mu^2}{m^2} - \gamma_V(\alpha) \right) R(m^2, \mu). \quad (\text{B.7})$$

The RGE for the anomaly coefficient F looks somewhat different. We write

$$F^{\text{bare}}(\varepsilon, m^2) = \frac{\alpha}{4\pi} \left[\frac{2}{\varepsilon} + 4 \log \frac{\mu}{m} \right] = \frac{\alpha}{4\pi} \frac{2}{\varepsilon} + F(m^2, \mu). \quad (\text{B.8})$$

The RGE for F is then simply

$$\frac{dF(m^2, \mu)}{d \log \mu} = \gamma_{\text{cusp}}(\alpha). \quad (\text{B.9})$$

Appendix C

Details on the Factorisation of Heavy-to-Light Form Factors

C.1 QCD \rightarrow SCET_I Matching of $B \rightarrow \pi$ Form Factors

We extract the LO hard functions H_i from the matching relations given in Eq. (6.8). We therefore define the following auxiliary vector

$$X^\mu = -\frac{q^2}{\lambda} \left(p_B^\mu + p^\mu - \frac{M_B^2 - m_\pi^2}{q^2} q^\mu \right), \quad (\text{C.1})$$

where

$$\lambda \equiv \lambda(M_B^2, m_\pi^2, q^2) = M_B^4 + m_\pi^4 + q^4 - 2M_B^2 m_\pi^2 - 2M_B^2 q^2 - 2m_\pi^2 q^2 \quad (\text{C.2})$$

is the Källén function. This vector fulfills

$$X^2 = -\frac{q^2}{\lambda}, \quad X \cdot (p_B - p) = 0, \quad X \cdot (p_B + p) = 1. \quad (\text{C.3})$$

With their definition given in Eq. (6.4), we can now project the hadronic matrix elements onto the various form factors via

$$\begin{aligned} F_+(q^2) &= X_\mu \langle \pi(p) | \bar{q} \gamma^\mu b | \bar{B}(p_B) \rangle, \\ F_-(q^2) &= \frac{q_\mu}{q^2} \langle \pi(p) | \bar{q} \gamma^\mu b | \bar{B}(p_B) \rangle - \frac{M_B^2 - m_\pi^2}{q^2} F_+, \\ F_T(q^2) &= -\frac{M_B + m_\pi}{q^2} X_\mu \langle \pi(p) | \bar{q} i \sigma^{\mu\nu} q_\nu b | \bar{B}(p_B) \rangle. \end{aligned} \quad (\text{C.4})$$

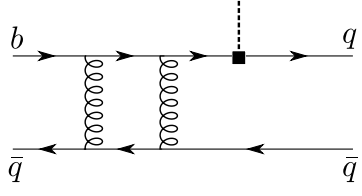
Using the definition of the soft-overlap form factor Eq. (6.7) and the QCD \rightarrow SCET_I matching relation Eq. (6.8), we find for the tree-level hard matching coefficients:

$$\begin{aligned} F_+(q^2) &= (n \cdot X) 2E_\pi \xi(q^2) = \xi(q^2), \\ F_-(q^2) &= \left(\frac{n \cdot q}{q^2} - \frac{M_B^2 - m_\pi^2}{q^2} (n \cdot X) \right) 2E_\pi \xi(q^2) = -\xi(q^2), \\ F_T(q^2) &= \frac{M_B + m_\pi}{M_B} \xi(q^2), \end{aligned} \quad (\text{C.5})$$

which is in agreement with [53], Eq. (22).

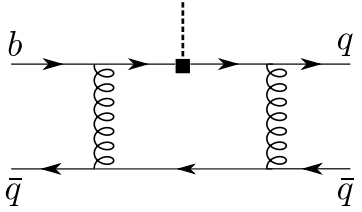
C.2 Details on the One-Loop Hard-Collinear Kernel

We collect the contributions of the individual diagrams to the one-loop hard-collinear functions D_m and D_1 . Diagrams that are not listed below have either a vanishing hard-collinear region or no double pole in ε (in Feynman gauge). The results are normalised according to $D_i = \frac{\alpha_s(\mu)}{4\pi} \frac{C_F}{N_C} \frac{1}{\varepsilon^2} \hat{D}_i$.



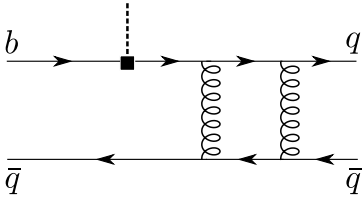
$$\hat{D}_m : 0$$

$$\hat{D}_1 : -\frac{C_F}{2\omega\bar{u}^2 E_\pi^2} \quad (\text{C.6})$$



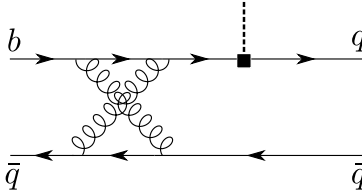
$$\hat{D}_m : 0$$

$$\hat{D}_1 : -\frac{C_F}{2\omega\bar{u} E_\pi^2} \quad (\text{C.7})$$



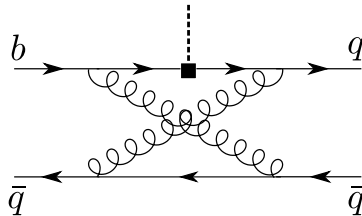
$$\hat{D}_m : \frac{C_F}{2\omega^2\bar{u} E_\pi^2} \left(m_q \frac{\bar{u}}{u} + m_{\bar{q}} \frac{1+\bar{u}}{\bar{u}} \right)$$

$$\hat{D}_1 : 0 \quad (\text{C.8})$$



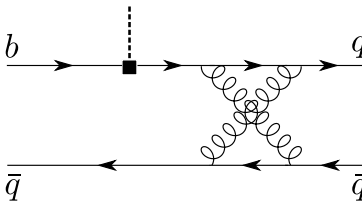
$$\hat{D}_m : 0$$

$$\hat{D}_1 : \frac{C_{FA}}{2\omega\bar{u}^2 E_\pi^2} \quad (\text{C.9})$$



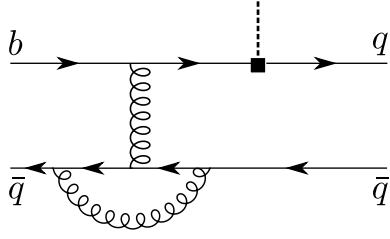
$$\hat{D}_m : -\frac{C_{FA}}{2\omega^2\bar{u} E_\pi^2} \left(m_q \frac{\bar{u}}{u} + m_{\bar{q}} \frac{1+u}{\bar{u}} \right)$$

$$\hat{D}_1 : C_{FA} \frac{1+\bar{u}}{2\omega\bar{u}^2 E_\pi^2} \quad (\text{C.10})$$



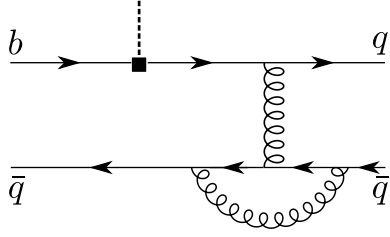
$$\hat{D}_m : -\frac{C_{FA}}{2\omega^2\bar{u} E_\pi^2} \left(m_q \frac{\bar{u}}{u} + m_{\bar{q}} \frac{u}{\bar{u}} \right)$$

$$\hat{D}_1 : \frac{C_{FA}}{2\omega\bar{u} E_\pi^2} \quad (\text{C.11})$$



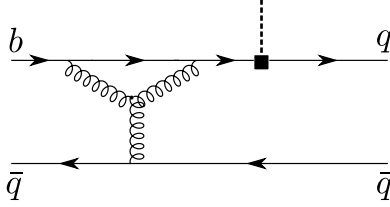
$$\hat{D}_m : 0$$

$$\hat{D}_1 : -\frac{C_{FA}}{2\omega\bar{u}^2 E_\pi^2} \quad (\text{C.12})$$



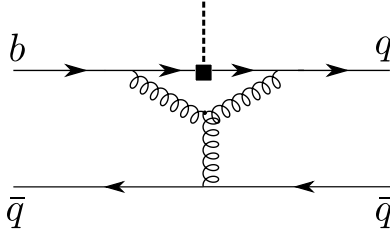
$$\hat{D}_m : \frac{C_{FA}}{2\omega^2\bar{u}E_\pi^2} \left(m_q \frac{\bar{u}}{u} + m_{\bar{q}} \frac{u}{\bar{u}} \right)$$

$$\hat{D}_1 : -\frac{C_{FA}}{2\omega\bar{u}E_\pi^2} \quad (\text{C.13})$$



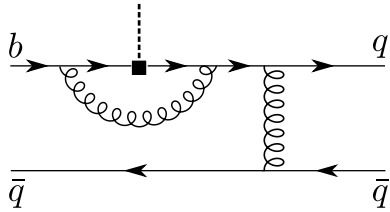
$$\hat{D}_m : 0$$

$$\hat{D}_1 : -\frac{C_A}{8\omega\bar{u}^2 E_\pi^2} \quad (\text{C.14})$$



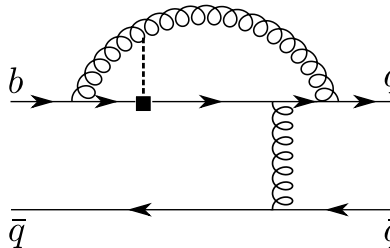
$$\hat{D}_m : 0$$

$$\hat{D}_1 : -\frac{C_A}{8\omega\bar{u}^2 E_\pi^2} \quad (\text{C.15})$$



$$\hat{D}_m : \frac{C_F}{2\omega^2\bar{u}E_\pi^2} \left(m_q \frac{\bar{u}}{u} + m_{\bar{q}} \frac{u}{\bar{u}} \right)$$

$$\hat{D}_1 : -\frac{C_F}{2\omega\bar{u}E_\pi^2} \quad (\text{C.16})$$



$$\hat{D}_m : \frac{C_{FA}}{2\omega^2\bar{u}E_\pi^2} \left(m_q \frac{\bar{u}}{u} + m_{\bar{q}} \frac{u}{\bar{u}} \right)$$

$$\hat{D}_1 : -\frac{C_{FA}}{2\omega\bar{u}E_\pi^2} \quad (\text{C.17})$$

C.3 Matrix Element of the Collinear Current $\bar{\chi} \frac{\not{n}}{2} \gamma_5 i \not{\phi}_\perp \chi$

In order to find an expression for the hadronic matrix element $\langle \pi(p) | \bar{\chi}(0) \frac{\not{n}}{2} \gamma_5 i \not{\phi}_\perp \chi(s\bar{n}) | 0 \rangle$ in terms of pion LCDAs, we make use of the Dirac equation for the spectator-quark field $q_2(x)$, $(i \not{\phi} + g_s \not{A}_c(x) - m_{\bar{q}}) q_2(x) = 0$, and the identity

$$1 = (-i) \frac{n^\alpha \bar{n}^\beta}{2} \sigma_{\alpha\beta} + 2 \frac{\not{n} \not{\bar{n}}}{4}. \quad (\text{C.18})$$

Moreover, we need the following identity for the covariant derivative acting on a collinear Wilson line:

$$W_c^\dagger i \bar{n} \cdot D_c W_c = i \bar{n} \cdot \partial. \quad (\text{C.19})$$

After some algebra we find the following operator relation:

$$\begin{aligned} \bar{q}_1(0)[0, x] \frac{\not{n}}{2} \gamma_5 i \not{\phi}_\perp q_2(x) &= \frac{\bar{n} \cdot \partial}{2} \bar{q}_1(0)[0, x] i \gamma_5 q_2(x) - \frac{n^\alpha \bar{n}^\beta}{2} \frac{\bar{n} \cdot \partial}{2} \bar{q}_1(0)[0, x] \sigma_{\alpha\beta} \gamma_5 q_2(x) \\ &\quad - \bar{q}_1(0)[0, x] \frac{\not{n}}{2} \gamma_5 g_s \not{A}_{c\perp}(x) q_2(x) + m_{\bar{q}} \bar{q}_1(0)[0, x] \frac{\not{n}}{2} \gamma_5 q_2(x), \end{aligned} \quad (\text{C.20})$$

from which the hadronic matrix element can be translated into LCDAs:

$$\begin{aligned} \langle \pi(p) | \bar{\chi}(0) \frac{\not{n}}{2} \gamma_5 i \not{\phi}_\perp \chi(s\bar{n}) | 0 \rangle &= i E_\pi f_\pi \int_0^1 du e^{i2E_\pi s \bar{u}} \left[\bar{u} \left(\mu_\pi \phi_P(u) - \frac{\tilde{\mu}_\pi \phi'_\sigma(u)}{2d-2} \right) - m_{\bar{q}} \phi_\pi(u) \right] \\ &\quad - (d-2) i E_\pi f_{3\pi} \int \mathcal{D}\alpha e^{is2E_\pi(\alpha_{\bar{q}} + \alpha_g)} \frac{\phi_{3\pi}(\{\alpha_i\})}{\alpha_g}. \end{aligned} \quad (\text{C.21})$$

The factor \bar{u} in the first line arises due to the $\bar{n} \cdot \partial$ derivative acting on the first two terms in Eq. (C.20).

In complete analogy we may just as well apply the Dirac equation to the quark field $\bar{q}_1(0)$, $\bar{q}_1(0)(-i \not{\phi} + g_s \not{A}_c(0) - m_q) = 0$, and find the operator identity

$$\begin{aligned} \bar{q}_1(0)[0, x] \frac{\not{n}}{2} \gamma_5 i \overleftarrow{\not{\phi}}_\perp q_2(x) &= - \frac{\bar{n} \cdot \partial_1}{2} \bar{q}_1(0)[0, x] i \gamma_5 q_2(x) - \frac{n^\alpha \bar{n}^\beta}{2} \frac{\bar{n} \cdot \partial_1}{2} \bar{q}_1(0)[0, x] \sigma_{\alpha\beta} \gamma_5 q_2(x) \\ &\quad + \bar{q}_1(0)[0, x] \frac{\not{n}}{2} \gamma_5 g_s \not{A}_{c\perp}(0) q_2(x) - m_q \bar{q}_1(0)[0, x] \frac{\not{n}}{2} \gamma_5 q_2(x), \end{aligned} \quad (\text{C.22})$$

where $\overleftarrow{\partial}$ and ∂_1 is the derivative acting on $\bar{q}_1(y)[y, *]$ before taking the limit $y \rightarrow 0$. This yields an equivalent representation of the desired matrix element:

$$\begin{aligned} \langle \pi(p) | \bar{\chi}(0) \frac{\not{n}}{2} \gamma_5 i \overleftarrow{\not{\phi}}_\perp \chi(s\bar{n}) | 0 \rangle &= i E_\pi f_\pi \int_0^1 du e^{i2E_\pi s \bar{u}} \left[u \left(-\mu_\pi \phi_P(u) - \frac{\tilde{\mu}_\pi \phi'_\sigma(u)}{2d-2} \right) + m_q \phi_\pi(u) \right] \\ &\quad + (d-2) i E_\pi f_{3\pi} \int \mathcal{D}\alpha e^{i2E_\pi s \alpha_{\bar{q}}} \frac{\phi_{3\pi}(\{\alpha_i\})}{\alpha_g}. \end{aligned} \quad (\text{C.23})$$

Utilising the equations of motion for the LCDAs in Eqs. (6.57) and (6.58), we can explicitly verify that

$$\langle \pi(p) | \bar{\chi}(0) \frac{\not{n}}{2} \gamma_5 (i \not{\phi}_\perp + i \overleftarrow{\not{\phi}}_\perp) \chi(s\bar{n}) | 0 \rangle = 0, \quad (\text{C.24})$$

which is a consequence of the vanishing perpendicular components of the pion momentum, $p_\perp^\mu \equiv 0$, in our reference frame. For our purposes it is suitable to use a symmetrised representation,

$$\begin{aligned} \langle \pi(p) | \bar{\chi}(0) \frac{\not{n}}{2} \gamma_5 i \not{\phi}_\perp \chi(s\bar{n}) | 0 \rangle &= \langle \pi(p) | \bar{\chi}(0) \frac{\not{n}}{2} \gamma_5 \frac{i \not{\phi}_\perp - i \overleftarrow{\not{\phi}}_\perp}{2} \chi(s\bar{n}) | 0 \rangle \\ &= \frac{i E_\pi f_\pi}{2} \int_0^1 du e^{i2E_\pi s \bar{u}} \left[\mu_\pi \phi_P(u) + (2u - 1) \frac{\tilde{\mu}_\pi \phi'_\sigma(u)}{2d - 2} - (m_q + m_{\bar{q}}) \phi_\pi(u) \right. \\ &\quad \left. - (d - 2) \frac{f_{3\pi}}{f_\pi} \int \mathcal{D}\alpha \frac{\phi_{3\pi}(\{\alpha_i\})}{\alpha_g} \left(\delta(\alpha_q - u) + \delta(\alpha_{\bar{q}} - \bar{u}) \right) \right], \quad (\text{C.25}) \end{aligned}$$

which can be cast into a somewhat simpler form by again using the equations of motion:

$$\begin{aligned} \langle \pi(p) | \bar{\chi}(0) \frac{\not{n}}{2} \gamma_5 i \not{\phi}_\perp \chi(s\bar{n}) | 0 \rangle &= i E_\pi (d - 2) \int_0^1 du e^{i2E_\pi s \bar{u}} \left[\frac{f_\pi \tilde{\mu}_\pi}{2d - 2} \phi_\sigma(u) + f_{3\pi} \int \mathcal{D}\alpha \frac{\phi_{3\pi}(\{\alpha_i\})}{\alpha_g^2} \left(\theta(\alpha_q - u) - \theta(\bar{u} - \alpha_{\bar{q}}) \right) \right]. \quad (\text{C.26}) \end{aligned}$$

C.4 Contributions of the Individual Operators to ξ_π

We list the contributions of the individual operators $\mathcal{O}_{m,1-4}$ to the naive factorisation of ξ_π for hard-collinear tree-level exchanges and the subset of one-loop corrections that we are interested in. In the expressions below, $\langle \dots \rangle_X$ means integration over all momentum fractions/projections weighted with the LCDA ϕ_X . Note that due to the equations of motion the explicit expressions are ambiguous.

Contribution of \mathcal{O}_m :

$$\begin{aligned} \xi_\pi|_{\mathcal{O}_m} \simeq & \xi_0 C_F \langle \omega^{-2} \rangle_+ \left\{ \left\langle m_q \frac{1}{u} + m_{\bar{q}} \frac{u}{\bar{u}^2} \right\rangle_\pi \left[1 + \frac{\alpha_s(\mu) C_F}{\pi} \frac{1}{\varepsilon^2} \right] \right. \\ & \left. + \frac{\alpha_s(\mu)}{\pi} \frac{1}{\varepsilon^2} m_{\bar{q}} \left\langle C_F \frac{1}{\bar{u}} - \frac{C_{FA}}{2} \frac{1}{\bar{u}^2} \right\rangle_\pi \right\} \end{aligned} \quad (\text{C.27})$$

Contribution of \mathcal{O}_1 :

$$\xi_\pi|_{\mathcal{O}_1} \simeq \xi_0 C_F \langle \omega^{-1} \rangle_- \left\langle \frac{1 + \bar{u}}{\bar{u}^2} \right\rangle_\pi \left[1 + \frac{\alpha_s(\mu) C_F}{\pi} \frac{1}{\varepsilon^2} \right] \quad (\text{C.28})$$

Contribution of \mathcal{O}_2 :

$$\begin{aligned} \xi_\pi|_{\mathcal{O}_2} \simeq & \xi_0 C_F \langle \omega^{-2} \rangle_+ \\ & \times \left[(d-2) \frac{f_{3\pi}}{f_\pi} \langle \alpha_g^{-1} \alpha_q^{-1} (\alpha_g + \alpha_{\bar{q}})^{-2} \rangle_3 + \mu_\pi \left\langle \frac{1}{u\bar{u}} \right\rangle_p - \frac{\tilde{\mu}_\pi}{2d-2} \left\langle \frac{1}{u\bar{u}} \right\rangle_{\sigma'} - m_{\bar{q}} \left\langle \frac{1}{u\bar{u}^2} \right\rangle_\pi \right] \end{aligned} \quad (\text{C.29})$$

Contribution of \mathcal{O}_3 :

$$\begin{aligned} \xi_\pi|_{\mathcal{O}_3} \simeq & (d-2) \frac{\xi_0 f_{3\pi}}{f_\pi} \langle \omega^{-2} \rangle_+ \\ & \times \left[2C_F \langle \alpha_g^{-1} (\alpha_g + \alpha_{\bar{q}})^{-2} \rangle_3 + C_F \langle \alpha_g^{-1} \alpha_{\bar{q}}^{-1} (\alpha_g + \alpha_g)^{-1} \rangle_3 - \frac{C_A}{2} \langle \alpha_g^{-1} \alpha_{\bar{q}}^{-1} (\alpha_g + \alpha_{\bar{q}})^{-1} \rangle_3 \right] \end{aligned} \quad (\text{C.30})$$

Contribution of \mathcal{O}_4 :

$$\begin{aligned} \xi_\pi|_{\mathcal{O}_4} \simeq & -(d-2) \xi_0 \\ & \times \left[\langle \omega^{-1} (\omega + \xi)^{-2} \rangle_{A-V} \left(C_F \langle \bar{u}^{-1} \rangle_\pi - \frac{C_A}{2} \langle \bar{u}^{-2} \rangle_\pi \right) - C_{FA} \langle \xi^{-1} (\omega + \xi)^{-2} \rangle_{A-V} \langle \bar{u}^{-2} \rangle_\pi \right] \end{aligned} \quad (\text{C.31})$$

Appendix D

Details on Heavy-to-Light Form Factors for NR Bound States

D.1 LCDAs for Non-Relativistic Bound States

We collect the results up to $\mathcal{O}(\alpha_s)$ for the LCDAs of non-relativistic bound states that have been calculated in [119].

D.1.1 Tree-Level

The tree-level results for all non-vanishing LCDAs are simple delta distributions that project onto the respective light-cone components of the on-shell quarks:

$$\phi_B^+(\omega) \simeq \phi_B^-(\omega) \simeq \delta(\omega - m_{\bar{q}}), \quad (\text{D.1})$$

for the \bar{B}_c meson and

$$\phi_\eta(u) \simeq \phi_P(u) \simeq \delta(u - u_0), \quad (\text{D.2})$$

for the η_c meson. The 3-particle LCDAs Ψ_{A-V} and $\phi_{3\eta}$ require an additional soft or collinear gluon exchange and are suppressed by one power of α_s .

The prefactors that come with the subleading-twist LCDAs of the η_c meson are given by

$$\mu_\eta \simeq m_\eta \quad \text{and} \quad \tilde{\mu}_\eta \simeq \mathcal{O}(\alpha_s). \quad (\text{D.3})$$

Note that the suppression of $\tilde{\mu}_\eta$ and $\phi_{3\eta}$ confirms our statement that the matrix element of the operator \mathcal{O}_2 is zero at tree-level (compare to Eq. (6.55)).

D.1.2 One-Loop Corrections

Heavy \bar{B}_c meson: The (bare) one-loop correction to the LCDA $\phi_B^+(\omega)$ reads

$$\begin{aligned} \phi_B^{+,(1)}(\omega; \mu)|_{\text{div.}} &= \delta(\omega - m_{\bar{q}}) \left[-\frac{1}{\varepsilon^2} + \frac{1}{\varepsilon} \left(1 - \log \frac{\mu^2}{m_{\bar{q}}^2} \right) \right] \\ &+ \frac{2\omega}{\varepsilon} \left[\frac{\theta(m_{\bar{q}} - \omega)}{m_{\bar{q}}(m_{\bar{q}} - \omega)} + \frac{\theta(\omega - m_{\bar{q}})}{\omega(\omega - m_{\bar{q}})} \right]_+, \end{aligned} \quad (\text{D.4})$$

for the divergent terms as $\varepsilon \rightarrow 0$, and

$$\begin{aligned} \frac{\phi_B^{+, (1)}(\omega; \mu)}{\omega} &= -\frac{\delta(\omega - m_{\bar{q}})}{m_{\bar{q}}} \left(\frac{1}{2} \log^2 \frac{\mu^2}{m_{\bar{q}}^2} - \log \frac{\mu^2}{m_{\bar{q}}^2} + \frac{3\pi^2}{4} + 2 \right) + \frac{4\theta(\omega - 2m_{\bar{q}})}{(\omega - m_{\bar{q}})^2} \\ &+ 2 \left[\left(\log \frac{\mu^2}{(\omega - m_{\bar{q}})^2} - 1 \right) \left(\frac{\theta(m_{\bar{q}} - \omega)}{m_{\bar{q}}(m_{\bar{q}} - \omega)} + \frac{\theta(\omega - m_{\bar{q}})}{\omega(\omega - m_{\bar{q}})} \right) \right]_+ \\ &+ 4 \left[\frac{\theta(2m_{\bar{q}} - \omega)}{(\omega - m_{\bar{q}})^2} \right]_{++}, \end{aligned} \quad (\text{D.5})$$

for the finite contributions. Similarly the result for $\phi_B^-(\omega)$ is split into the divergent piece

$$\begin{aligned} \phi_B^{-, (1)}(\omega; \mu)|_{\text{div.}} &= \delta(\omega - m_{\bar{q}}) \left[-\frac{1}{\varepsilon^2} - \frac{1}{\varepsilon} \left(1 + \log \frac{\mu^2}{m_{\bar{q}}^2} \right) \right] + \frac{2}{\varepsilon} \frac{\theta(m_{\bar{q}} - \omega)}{m_{\bar{q}}} \\ &+ \frac{2\omega}{\varepsilon} \left[\frac{\theta(\omega - m_{\bar{q}})}{\omega(\omega - m_{\bar{q}})} \right]_+ + \frac{2}{\varepsilon} \left[\frac{\theta(m_{\bar{q}} - \omega)}{(m_{\bar{q}} - \omega)} \right]_+, \end{aligned} \quad (\text{D.6})$$

and the finite piece

$$\begin{aligned} \phi_B^{-, (1)}(\omega; \mu) &= -\delta(\omega - m_{\bar{q}}) \left(\frac{1}{2} \log^2 \frac{\mu^2}{m_{\bar{q}}^2} + \log \frac{\mu^2}{m_{\bar{q}}^2} + \frac{3\pi^2}{4} + 6 \right) + \frac{4m_{\bar{q}}\theta(\omega - 2m_{\bar{q}})}{(\omega - m_{\bar{q}})^2} \\ &+ 2 \left(\log \frac{\mu^2}{(\omega - m_{\bar{q}})^2} - 1 \right) \frac{\theta(m_{\bar{q}} - \omega)}{m_{\bar{q}}} + 4m_{\bar{q}} \left[\frac{\theta(2m_{\bar{q}} - \omega)}{(\omega - m_{\bar{q}})^2} \right]_{++} \\ &+ 2\omega \left[\left(\log \frac{\mu^2}{(\omega - m_{\bar{q}})^2} - 1 \right) \frac{\theta(\omega - m_{\bar{q}})}{\omega(\omega - m_{\bar{q}})} \right]_+ \\ &+ 2 \left[\left(\log \frac{\mu^2}{(\omega - m_{\bar{q}})^2} - 1 \right) \frac{\theta(m_{\bar{q}} - \omega)}{m_{\bar{q}} - \omega} \right]_+. \end{aligned} \quad (\text{D.7})$$

The leading contribution to the 3-particle LCDA $\Psi_{A-V}(\omega, \xi)$ is given by

$$\Psi_{A-V}^{(1)}(\omega, \xi) = -\frac{\alpha_s(\mu)C_F}{4\pi} \frac{\delta(\omega - m_{\bar{q}} + \xi)}{m_{\bar{q}}} \left(\frac{1}{\varepsilon} + \log \frac{\mu^2}{\xi^2} + 1 \right) \xi^2 \theta(m_{\bar{q}} - \xi). \quad (\text{D.8})$$

Here the plus-distributions are defined as

$$\begin{aligned} \int_0^\infty d\omega \{ \dots \}_+ f(\omega) &\equiv \int_0^\infty d\omega \{ \dots \} (f(\omega) - f(m_{\bar{q}})), \\ \int_0^\infty d\omega \{ \dots \}_{++} f(\omega) &\equiv \int_0^\infty d\omega \{ \dots \} (f(\omega) - f(m_{\bar{q}}) - f'(m_{\bar{q}})(\omega - m_{\bar{q}})). \end{aligned} \quad (\text{D.9})$$

Light η_c meson: The leading-twist LCDA $\phi_\eta(u)$ has the divergent piece

$$\phi_\eta^{(1)}(u)|_{\text{div.}} = \frac{2}{\varepsilon} \left[\left(1 + \frac{1}{u_0 - u} \right) \frac{u}{u_0} \theta(u_0 - u) + \left(1 + \frac{1}{\bar{u}_0 - \bar{u}} \right) \frac{\bar{u}}{\bar{u}_0} \theta(u - u_0) \right]_+, \quad (\text{D.10})$$

and the finite piece

$$\begin{aligned} \phi_\eta^{(1)}(u; \mu) = & 2 \left\{ \left(\log \frac{\mu^2}{m_\eta^2(u_0 - u)^2} - 1 \right) \left[\left(1 + \frac{1}{u_0 - u} \right) \frac{u}{u_0} \theta(u_0 - u) + \left(\begin{array}{c} u \leftrightarrow \bar{u} \\ u_0 \leftrightarrow \bar{u}_0 \end{array} \right) \right] \right\}_+ \\ & + 4 \left\{ \frac{u\bar{u}}{(u_0 - u)^2} \right\}_{++} + 2\delta'(u - u_0) \left(2u_0\bar{u}_0 \log \frac{u_0}{\bar{u}_0} + u_0 - \bar{u}_0 \right). \end{aligned} \quad (\text{D.11})$$

The subleading-twist LCDA associated to the pseudoscalar current, $\phi_P(u)$, is given by

$$\phi_P^{(1)}(u)|_{\text{div.}} = \frac{2}{\varepsilon} \left[\left(1 + \frac{1}{u_0 - u} \right) \theta(u_0 - u) + \left(\begin{array}{c} u \leftrightarrow \bar{u} \\ u_0 \leftrightarrow \bar{u}_0 \end{array} \right) \right]_+, \quad (\text{D.12})$$

and

$$\begin{aligned} \phi_P^{(1)}(u; \mu) = & 2 \left\{ \left(\log \frac{\mu^2}{m_\eta^2(u_0 - u)^2} - 1 \right) \left[\left(1 + \frac{1}{u_0 - u} \right) \theta(u_0 - u) + \left(\begin{array}{c} u \leftrightarrow \bar{u} \\ u_0 \leftrightarrow \bar{u}_0 \end{array} \right) \right] \right\}_+ \\ & + 4u_0\bar{u}_0 \left(\left\{ \frac{1}{(u_0 - u)^2} \right\}_{++} + \delta'(u - u_0) \log \frac{u_0}{\bar{u}_0} \right) + 2 \left\{ \frac{u_0 - \bar{u}_0}{u_0 - u} \right\}_+, \end{aligned} \quad (\text{D.13})$$

with the appropriate plus-distributions

$$\begin{aligned} \int_0^1 du \{ \dots \}_+ f(u) & \equiv \int_0^1 du \{ \dots \} (f(u) - f(u_0)), \\ \int_0^1 du \{ \dots \}_{++} f(u) & \equiv \int_0^1 du \{ \dots \} (f(u) - f(u_0) - f'(u_0)(u - u_0)). \end{aligned} \quad (\text{D.14})$$

The subleading-twist LCDA associated to the pseudotensor current, $\phi_\sigma(u)$, simply reads

$$\phi_\sigma(u) = 2 \left[\frac{u}{u_0} \theta(u_0 - u) + \left(\begin{array}{c} u \leftrightarrow \bar{u} \\ u_0 \leftrightarrow \bar{u}_0 \end{array} \right) \right] + \mathcal{O}(\alpha_s). \quad (\text{D.15})$$

Note that the 3-particle LCDA $\phi_{3\eta}$ is not provided in [119].

The one-loop corrections to the prefactors that accompany the subleading-twist LCDAs read

$$\begin{aligned} \frac{\mu_\eta}{m_\eta} & = 1 + \frac{\alpha_s(\mu)C_F}{4\pi} \left(\frac{3}{\varepsilon} + 3 \log \frac{\mu^2}{m_q m_{\bar{q}}} - 3 \frac{m_q - m_{\bar{q}}}{m_q + m_{\bar{q}}} \log \frac{m_q}{m_{\bar{q}}} + 4 \right) + \mathcal{O}(\alpha_s^2), \\ \frac{\tilde{\mu}_\eta}{m_\eta} & = \frac{\alpha_s(\mu)C_F}{4\pi} \left(\frac{6}{\varepsilon} + 6 \log \frac{\mu^2}{m_q m_{\bar{q}}} - 6 \frac{m_q - m_{\bar{q}}}{m_q + m_{\bar{q}}} \log \frac{m_q}{m_{\bar{q}}} + 8 \right) + \mathcal{O}(\alpha_s^2), \end{aligned} \quad (\text{D.16})$$

where $m_\eta \simeq m_q^{\text{os}} + m_{\bar{q}}^{\text{os}}$ in the on-shell scheme.

D.2 Leading Endpoint Contributions of Two-Loop Moments

We study the cancellation of leading poles $\sim \frac{\alpha_s^2}{\delta^2 \varepsilon^2}$ in δ and ε at two-loops. They arise from the double-soft, double-collinear and the mixed soft-collinear region of all possible two-loop diagrams in the full theory. Once we trust the naive factorisation formula Eq. (6.67), they can be determined from corresponding contributions to the appearing moments. Replacing all moments of 3-particle LCDAs via the equations of motion, we need to compute all endpoint-divergent moments of 2-particle LCDAs in the desired approximation.

If the endpoint contributions exponentiate in a similar way as in the Sudakov form factor, $\xi_\eta \stackrel{?}{\sim} (2\gamma)^{-F}$, we expect the following structure for the leading poles in the bare calculation (up to $\mathcal{O}(\alpha_s^3)$ contributions in the second line):

$$\begin{aligned} \log(2\gamma)^{-F_{\text{div.}}^{(1)}/\varepsilon} &= \lim_{\delta \rightarrow 0} \exp \left\{ F_{\text{div.}}^{(1)} \left[\frac{1}{\delta \varepsilon} \left(\frac{\nu}{2\gamma m_{\bar{q}}} \right)^\delta - \frac{1}{\delta \varepsilon} \left(\frac{\nu}{m_{\bar{q}}} \right)^\delta \right] \right\} \\ &\simeq \lim_{\delta \rightarrow 0} \left\{ 1 + \frac{F_{\text{div.}}^{(1)}}{\varepsilon} \left[\frac{1}{\delta} \left(\frac{\nu}{2\gamma m_{\bar{q}}} \right)^\delta - \frac{1}{\delta} \left(\frac{\nu}{m_{\bar{q}}} \right)^\delta \right] + \frac{(F_{\text{div.}}^{(1)})^2}{2\varepsilon^2} \left[\frac{1}{\delta} \left(\frac{\nu}{2\gamma m_{\bar{q}}} \right)^\delta - \frac{1}{\delta} \left(\frac{\nu}{m_{\bar{q}}} \right)^\delta \right]^2 \right\}, \end{aligned} \quad (\text{D.17})$$

where $F_{\text{div.}}^{(1)}$ is the divergent coefficient of the bare one-loop anomaly. In particular, we expect that the poles in the double-soft region come with the same coefficient as in the double-collinear region, which is exactly minus one half the coefficient in the mixed soft-collinear region. The latter can already be computed from the one-loop LCDAs for the \bar{B}_c meson and the η_c meson given in Eqs. (7.14) and (7.18). For this contribution we find

$$\begin{aligned} \xi_\eta^{(s-c)} &\simeq \frac{\xi_0 C_F}{m_\eta} \left(\frac{\alpha_s(\mu)}{4\pi} \right)^2 \left(\frac{\mu^2}{m_{\bar{q}}^2} \right)^{2\varepsilon} \left(\frac{\nu}{2\gamma m_{\bar{q}}} \right)^\delta \left(\frac{\nu}{m_{\bar{q}}} \right)^\delta \left(-\frac{4}{\delta^2 \varepsilon^2} \right) \\ &\quad \left[4C_F^2 \frac{1 + \bar{u}_0}{\bar{u}_0^3} - \frac{C_A C_F}{2} \frac{2 + \bar{u}_0}{\bar{u}_0^3} \right], \end{aligned} \quad (\text{D.18})$$

which we confirmed by calculating all relevant two-loop diagrams in the full theory in the soft-collinear region. Note that we ignored the double pole in ε from the ‘‘asymmetric’’ regulator at this point, since we only want to check the cancellation of divergences in δ .

The $1/\delta^2$ contributions to endpoint-sensitive two-loop moments can be calculated from diagrams with two spectator-quark propagators. In light-cone gauge ($n \cdot A_s = 0$ for soft moments and $\bar{n} \cdot A_c = 0$ for collinear moments) they are shown in Fig. D.1. We sketch the calculation in the soft sector for the two-loop ladder-type diagram. The contribution of this diagram to the perturbative expansion of the position-space matrix element that

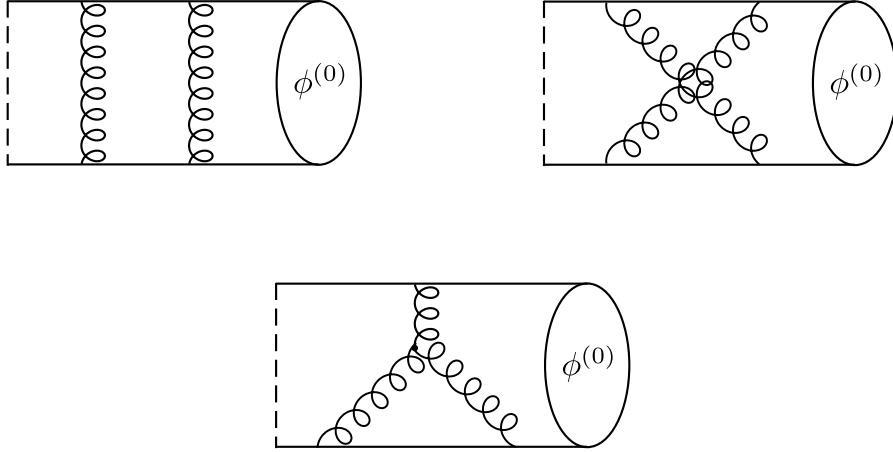


Figure D.1: Relativistic corrections to 2-particle LCDAs at two-loop. In light-cone gauge, only the diagrams shown in this figure contribute a double pole in δ to endpoint-sensitive moments. In Feynman gauge there are additional diagrams with gluons emitted from the Wilson line (dashed line).

defines the LCDAs reads with our regularisation prescription

$$\langle 0 | \bar{Q}_s(\tau n) \Gamma_{\pm} \mathcal{H}_v(0) | \bar{B}(v) \rangle \Big|_{\text{ladder}} = C_F^2 N_C g_s^4 \tilde{\mu}^{4\epsilon} \int \frac{d^d k}{(2\pi)^d} \left(\frac{\nu}{k_-} \right)^{\delta} \frac{d^d j}{(2\pi)^d} \left(\frac{\nu}{j_-} \right)^{\delta} e^{-i\tau k_+} \frac{\mathcal{T}^{\pm}(k, j)}{[k^2 - m_{\bar{q}}^2] [-2v \cdot k] [(k - j)^2] [j^2 - m_{\bar{q}}^2] [-2v \cdot j] [(j - m_{\bar{q}} v')^2]}, \quad (\text{D.19})$$

where all propagators in the second line are dressed with the proper $+i\epsilon$ prescription, whereas the analytic regulators are defined with a $-i\epsilon$. The loop momenta k and j are chosen as explained in the main text (cf. also Fig. 7.3). Furthermore, $\Gamma_+ = \frac{\not{n}}{2} \gamma_5$ gives the projection onto $\tilde{\phi}_B^+(\tau)$ and $\Gamma_- = \frac{\not{n}}{4} \gamma_5$ onto $\tilde{\phi}_B^-(\tau)$ (with the appropriate prefactors that can be read off from Eqs. (6.41) and (6.42)). Note that we still use an ad-hoc regularisation prescription by introducing one regulator for each integration measure. The numerator structure is contained in the function $\mathcal{T}^{\pm}(k, j)$ defined as the following Dirac trace:

$$\mathcal{T}^{\pm}(k, j) = \text{tr} \left[\mathcal{M}_B \gamma^{\mu} (-\not{j} + m_{\bar{q}}) \gamma^{\nu} (-\not{k} + m_{\bar{q}}) \Gamma_{\pm} (1 + \not{\psi}) \gamma^{\tilde{\mu}} (1 + \not{\psi}) \gamma^{\tilde{\nu}} \right] \left[g_{\mu\tilde{\mu}} - \frac{n_{\mu}(j - m_{\bar{q}}v)_{\tilde{\mu}} + n_{\tilde{\mu}}(j - m_{\bar{q}}v)_{\mu}}{j_+ - m_{\bar{q}}} \right] \left[g_{\nu\tilde{\nu}} - \frac{n_{\nu}(k - j)_{\tilde{\nu}} + n_{\tilde{\nu}}(k - j)_{\nu}}{k_+ - j_+} \right], \quad (\text{D.20})$$

with the Dirac projector of the heavy \bar{B}_c meson

$$\mathcal{M}_B = \frac{if_B M_B}{2N_C} \frac{1 + \not{\psi}}{2} \gamma_5. \quad (\text{D.21})$$

Note that at leading power the b -quark propagator reduces to a HQET propagator.

The intergral in Eq. (D.19) is well-defined in d dimensions as are all contributions to the perturbative expansion of this operator. However, when we consider inverse moments endpoint divergences occur. After Fourier transform, $\tau \rightarrow \omega$, the n -th inverse moment of the LCDA under consideration amounts to replacing $e^{-i\tau k_+} \rightarrow k_+^{-n}$ in the integrand. We perform the k_- and j_- integration with contour methods. The pole-structure of the various propagators is depicted in Fig. D.2. Note that due to the analytic regulators additional branch-cuts are located in the upper half-plane (UHP), and hence, closing the contour in the lower half-plane (LHP) is advisable.

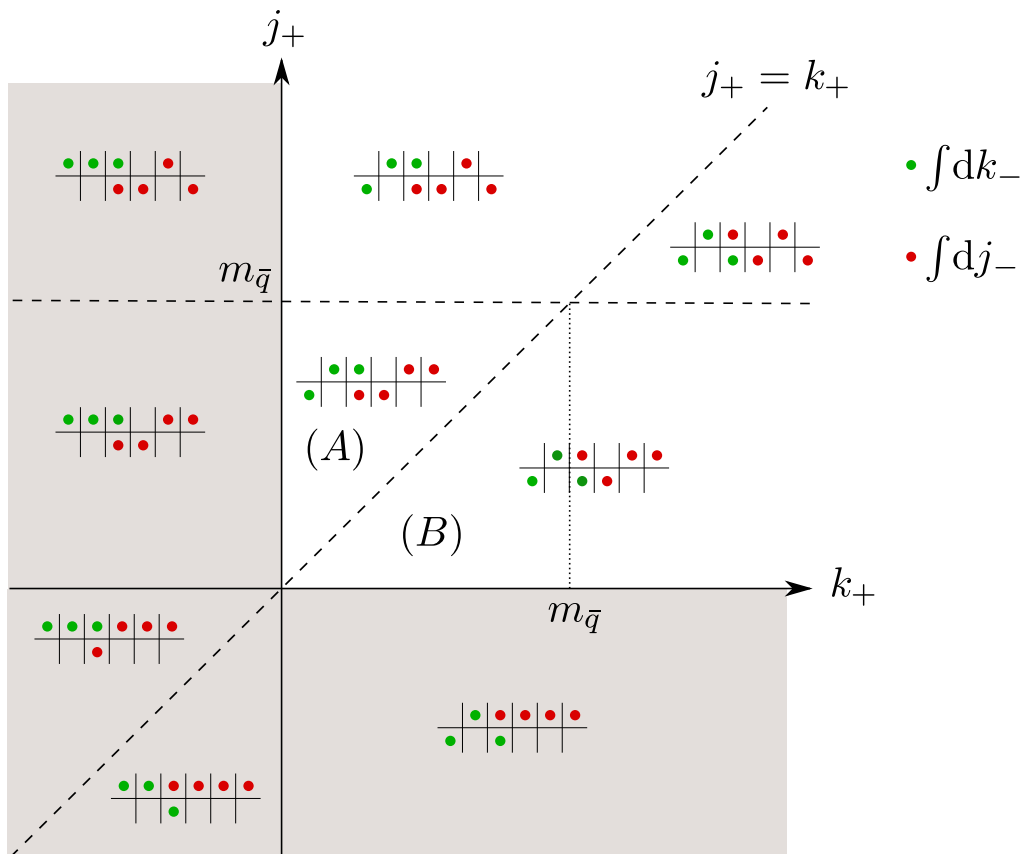


Figure D.2: Location of poles of the example two-loop ladder-type integral. Green dots denote poles in k_- and red dots in j_- , which are located either in the UHP (upper row) or the LHP. The gray shaded area gives no contribution since all poles in either k_- or j_- are in the UHP. Branch cuts from the analytic regulator lie in the UHP as well.

Endpoint divergences arise in the limit $\omega \rightarrow 0 \Leftrightarrow k_+ \rightarrow 0$. In the approximation that we are interested in, it is thus sufficient to investigate region (A) and (B) in Fig. D.2. The explicit calculation shows that in all diagrams double poles in δ arise only when the two following criteria are fulfilled:

1. We only have to consider regions where we subsequently can take the limits $k_+ \rightarrow 0$ and afterwards $j_+ \rightarrow 0$. In our example this is only region (A) since in (B) the limit $k_+ \rightarrow 0$ forces $j_+ \rightarrow 0$ simultaneously.

2. If we close the contour in the LHP, double poles in δ arise only when both spectator-quark propagators go on-shell, $k_- \rightarrow \frac{m_{\bar{q}}^2 - k_+^2}{k_+}$ and $j_- \rightarrow \frac{m_{\bar{q}}^2 - j_+^2}{j_+}$.

The integration domain in region (A) is a triangle, which we rescale according to

$$\int_0^{m_{\bar{q}}} dj_+ \int_0^{j_+} dk_+ f(k_+, j_+) = m_{\bar{q}}^2 \int_0^1 ds \int_0^1 dt s f(m_{\bar{q}}st, m_{\bar{q}}s). \quad (\text{D.22})$$

We then separate the poles in δ from $s \rightarrow 0$ and $t \rightarrow 0$ by the standard expansion in plus-distributions. Note that the rescaling has the effect that the regulators are now in the form $s^{2\delta} t^\delta$. The additional factor of two in the exponent is important for the exponentiation of the leading poles. The rescaling at higher orders generates the $1/n!$ coefficient in the exponential sum.

Performing these steps yields the following contribution to the double poles in δ and ε of the second inverse moment of $\phi_B^+(\omega)$ and the first inverse moment of $\phi_B^-(\omega)$:

$$\begin{aligned} \int_0^\infty \frac{d\omega}{\omega^2} \phi_B^{+, (2)}(\omega; \delta) \Big|_{\text{ladder}} &\simeq \frac{1}{m_{\bar{q}}^2} \left(\frac{\alpha_s(\mu) C_F}{4\pi} \right)^2 \left(\frac{\mu^2}{m_{\bar{q}}} \right)^{2\varepsilon} \left(\frac{\nu}{m_{\bar{q}}} \right)^{2\delta} \frac{2}{\delta^2 \varepsilon^2}, \\ \int_0^\infty \frac{d\omega}{\omega} \phi_B^{-, (2)}(\omega; \delta) \Big|_{\text{ladder}} &\simeq \frac{1}{m_{\bar{q}}} \left(\frac{\alpha_s(\mu) C_F}{4\pi} \right)^2 \left(\frac{\mu^2}{m_{\bar{q}}} \right)^{2\varepsilon} \left(\frac{\nu}{m_{\bar{q}}} \right)^{2\delta} \frac{6}{\delta^2 \varepsilon^2}. \end{aligned} \quad (\text{D.23})$$

We proceed similarly for the other two diagrams in Fig. D.1. We find that the non-planar diagram gives no contribution in our approximation and that the diagram with a non-abelian vertex gives a contribution to the first inverse moment of ϕ_B^- only. In the sum of all three diagrams we obtain:

$$\begin{aligned} \int_0^\infty \frac{d\omega}{\omega^2} \phi_B^{+, (2)}(\omega; \delta) &\simeq \frac{1}{m_{\bar{q}}^2} \left(\frac{\alpha_s(\mu)}{4\pi} \right)^2 \left(\frac{\mu^2}{m_{\bar{q}}} \right)^{2\varepsilon} \left(\frac{\nu}{m_{\bar{q}}} \right)^{2\delta} \frac{1}{\delta^2 \varepsilon^2} 2C_F^2, \\ \int_0^\infty \frac{d\omega}{\omega} \phi_B^{-, (2)}(\omega; \delta) &\simeq \frac{1}{m_{\bar{q}}} \left(\frac{\alpha_s(\mu)}{4\pi} \right)^2 \left(\frac{\mu^2}{m_{\bar{q}}} \right)^{2\varepsilon} \left(\frac{\nu}{m_{\bar{q}}} \right)^{2\delta} \frac{1}{\delta^2 \varepsilon^2} (6C_F^2 - C_A C_F). \end{aligned} \quad (\text{D.24})$$

In the collinear sector all three diagrams contribute, but no terms with the colour structure C_A arise for the leading-twist LCDA ϕ_η . We find the results:

$$\begin{aligned} \int_0^1 \frac{du}{\bar{u}^2} \phi_\eta^{(2)}(u; \delta) &\simeq \left(\frac{\alpha_s(\mu)}{4\pi} \right)^2 \left(\frac{\mu^2}{m_{\bar{q}}} \right)^{2\varepsilon} \left(\frac{\nu}{2\gamma m_{\bar{q}}} \right)^{2\delta} \frac{1}{\delta^2 \varepsilon^2} 2C_F^2 \frac{1 + \bar{u}_0}{\bar{u}_0^2}, \\ \int_0^1 \frac{du}{\bar{u}} \mu_\eta^{(0)} \phi_P^{(2)}(u; \delta) &\simeq - \int_0^1 \frac{du}{\bar{u}} \frac{\tilde{\mu}_\eta^{(1)}}{6} \phi_\sigma'^{(1)}(u; \delta) \\ &\simeq \left(\frac{\alpha_s(\mu)}{4\pi} \right)^2 \left(\frac{\mu^2}{m_{\bar{q}}} \right)^{2\varepsilon} \left(\frac{\nu}{2\gamma m_{\bar{q}}} \right)^{2\delta} \frac{m_\eta}{\delta^2 \varepsilon^2} \left(3C_F^2 \frac{1 + \bar{u}_0}{\bar{u}_0} - \frac{C_A C_F}{2} \frac{1}{\bar{u}_0} \right). \end{aligned} \quad (\text{D.25})$$

Plugging the corresponding expressions into the naive factorisation formula Eq. (6.67) gives

$$\begin{aligned} \left(\frac{\nu}{2\gamma m_{\bar{q}}}\right)^{-2\delta} \xi_{\eta}^{(c-c)} &\simeq \left(\frac{\nu}{m_{\bar{q}}}\right)^{-2\delta} \xi_{\eta}^{(s-s)} \\ &\simeq \frac{\xi_0 C_F}{m_{\eta}} \left(\frac{\alpha_s(\mu)}{4\pi}\right)^2 \left(\frac{\mu^2}{m_{\bar{q}}^2}\right)^{2\varepsilon} \left(\frac{2}{\delta^2 \varepsilon^2}\right) \left[4C_F^2 \frac{1+\bar{u}_0}{\bar{u}_0^3} - \frac{C_A C_F}{2} \frac{2+\bar{u}_0}{\bar{u}_0^3}\right]. \end{aligned} \quad (\text{D.26})$$

We observe a cancellation of divergences $\sim \frac{\alpha_s^2}{\delta^2 \varepsilon^2}$ at two-loop order in the sum of the soft-soft, the soft-collinear and the collinear-collinear region, and moreover, the structure is in agreement with the constraints from the exponentiation in Eq. (D.17). However, the coefficient in front of the logarithm is not simply one half the coefficient of the one-loop anomaly squared (compare to Eqs. (7.10) and (7.11)). This indicates that the resummed form factor contains several exponentials with different anomaly exponents F_i .

D.3 Solutions of the Recursion Relations

In this section we construct the explicit solutions to the recursion relations of the soft moments given in Eq. (7.25) in the approximation that is required to resum leading logarithms in the non-relativistic setup. That is, endpoint-finite moments of Ψ_{A-V} can be neglected since they do neither cause leading poles in δ nor in ε and their tree-level matrix element is zero. The endpoint-divergent moment of Ψ_{A-V} is replaced by the equation of motion Eq. (6.49). Note that we have to keep endpoint-finite moments whose tree-level matrix elements are non-zero. This leaves us with (we again ignore the double pole in ε for the moment)

$$\begin{aligned} \int_0^\infty \frac{d\omega}{\omega^2} \phi_B^{+, (n)}(\omega; \delta) &\simeq \frac{\alpha_s(\mu)}{4\pi} \left(\frac{\mu^2}{m_{\bar{q}}^2} \right)^\varepsilon \frac{2C_F}{\delta\varepsilon} \int_0^\infty \frac{d\omega}{\omega^2} \left(\frac{\nu\omega}{m_{\bar{q}}^2} \right)^\delta \phi_B^{+, (n-1)}(\omega; \delta), \\ \int_0^\infty \frac{d\omega}{\omega} \phi_B^{-, (n)}(\omega; \delta) &\simeq \frac{\alpha_s(\mu)}{4\pi} \left(\frac{\mu^2}{m_{\bar{q}}^2} \right)^\varepsilon \frac{2C_F}{\delta\varepsilon} \int_0^\infty d\omega \left(\frac{\nu\omega}{m_{\bar{q}}^2} \right)^\delta \\ &\quad \times \left\{ \frac{\phi_B^{-, (n-1)}(\omega; \delta)}{\omega} - \frac{C_{FA}}{C_F} m_{\bar{q}} \frac{\phi_B^{+, (n-1)}(\omega; \delta)}{\omega^2} \right\}, \end{aligned} \quad (\text{D.27})$$

for $n > 1$ and

$$\begin{aligned} \int_0^\infty \frac{d\omega}{\omega^2} \phi_B^{+, (1)}(\omega; \delta) &\simeq \frac{\alpha_s(\mu)}{4\pi} \left(\frac{\mu^2}{m_{\bar{q}}^2} \right)^\varepsilon \frac{2C_F}{\delta\varepsilon} \int_0^\infty \frac{d\omega}{\omega^2} \left(\frac{\nu\omega}{m_{\bar{q}}^2} \right)^\delta \phi_B^{+, (0)}(\omega), \\ \int_0^\infty \frac{d\omega}{\omega} \phi_B^{-, (1)}(\omega; \delta) &\simeq \frac{\alpha_s(\mu)}{4\pi} \left(\frac{\mu^2}{m_{\bar{q}}^2} \right)^\varepsilon \frac{2C_F}{\delta\varepsilon} \int_0^\infty d\omega \left(\frac{\nu\omega}{m_{\bar{q}}^2} \right)^\delta \\ &\quad \times \left\{ \frac{\phi_B^{-, (0)}(\omega)}{\omega} - \frac{C_{FA}}{C_F} m_{\bar{q}} \frac{\phi_B^{+, (0)}(\omega)}{\omega^2} + \frac{C_A}{2C_F} \frac{\phi_B^{+, (0)}(\omega)}{\omega} \right\}, \end{aligned} \quad (\text{D.28})$$

for $n = 1$. We distinguish the two cases since only for $n > 1$ we can set endpoint-finite moments to zero. Taking into account that the regulator is increased by one power of δ for each loop integration (see main text for details), we find the all-order resummation for the second inverse moment of ϕ_B^+ :

$$\begin{aligned} \int_0^\infty \frac{d\omega}{\omega^2} \phi_B^+(\omega; \delta) &= \sum_{n=0}^\infty \int_0^\infty \frac{d\omega}{\omega^2} \phi_B^{+, (n)}(\omega; \delta) \\ &\simeq \int_0^\infty \frac{d\omega}{\omega^2} \phi_B^{+, (0)}(\omega) \sum_{n=0}^\infty \frac{1}{n!} \left\{ \frac{\alpha_s(\mu)}{4\pi} \left(\frac{\mu^2}{m_{\bar{q}}^2} \right)^\varepsilon \frac{2C_F}{\delta\varepsilon} \left(\frac{\nu\omega}{m_{\bar{q}}^2} \right)^\delta \right\}^n \\ &= \int_0^\infty \frac{d\omega}{\omega^2} \phi_B^{+, (0)}(\omega) \exp \left\{ \frac{\alpha_s(\mu)}{4\pi} \left(\frac{\mu^2}{m_{\bar{q}}^2} \right)^\varepsilon \frac{2C_F}{\delta\varepsilon} \left(\frac{\nu\omega}{m_{\bar{q}}^2} \right)^\delta \right\} \\ &\equiv \frac{1}{m_{\bar{q}}^2} \exp \left\{ \frac{F_{\text{div.}}^{(1)}}{\delta} \left(\frac{\nu}{m_{\bar{q}}} \right)^\delta \right\}, \end{aligned} \quad (\text{D.29})$$

where we identify the divergent contribution of the one-loop anomaly as given in Eq. (7.29).

To construct the solution of the complete system in Eqs. (D.27) and (D.28) to all orders we define the matrix

$$A \equiv \begin{pmatrix} 1 & 0 & 0 \\ -\frac{C_{FA}}{C_F} & 1 & 0 \\ 0 & 0 & 0 \end{pmatrix}. \quad (\text{D.30})$$

The recursion formulas can then be cast into the following form:

$$\begin{aligned} \int_0^\infty d\omega \vec{M}^{(n)} &\simeq \frac{F_{\text{div.}}^{(1)}}{\delta} \int_0^\infty d\omega \left(\frac{\nu\omega}{m_{\bar{q}}^2} \right)^\delta A \cdot \vec{M}^{(n-1)} \quad (n > 1), \\ \int_0^\infty d\omega \vec{M}^{(1)} &\simeq \frac{F_{\text{div.}}^{(1)}}{\delta} \int_0^\infty d\omega \left(\frac{\nu\omega}{m_{\bar{q}}^2} \right)^\delta B \cdot \vec{M}^{(0)}, \end{aligned} \quad (\text{D.31})$$

with the vector \vec{M} defined in Eq. (7.34) and the matrix B defined in Eq. (7.43). The solution to the system can be constructed in the following way:

$$\begin{aligned} \int_0^\infty d\omega \vec{M} &\equiv \sum_{n=0}^\infty \int_0^\infty d\omega \vec{M}^{(n)} \\ &= \int_0^\infty d\omega \left\{ 1 + \sum_{n=1}^\infty \frac{1}{n!} \left[\frac{F_{\text{div.}}^{(1)}}{\delta} \left(\frac{\nu\omega}{m_{\bar{q}}^2} \right)^\delta \right]^n A^{n-1} \cdot B \right\} \cdot \vec{M}^{(0)} \\ &= \int_0^\infty d\omega \exp \left(\frac{F_{\text{div.}}^{(1)}}{\delta} \left(\frac{\nu\omega}{m_{\bar{q}}^2} \right)^\delta B \right) \cdot \vec{M}^{(0)}. \end{aligned} \quad (\text{D.32})$$

Here we used that $A^{n-1} \cdot B = B^n$. In the matrix exponential of B only terms proportional to C_F end up in the exponent whereas the other colour structures remain as factors multiplying the tree-level moments. The solution Eq. (D.32) encompasses the result for the endpoint-divergent moment of ϕ_B^+ that we already derived, as well as the trivial result for the endpoint-finite first inverse moment of ϕ_B^+ . The expression for the resummed leading poles in δ of the first inverse moment of ϕ_B^- reads:

$$\begin{aligned} \int_0^\infty \frac{d\omega}{\omega} \phi_B^-(\omega; \delta) &\simeq \int_0^\infty d\omega \left\{ \frac{\phi_B^{-,(0)}(\omega)}{\omega} \exp \mathcal{E} \right. \\ &\quad \left. - m_{\bar{q}} \frac{C_{FA}}{C_F} \frac{\phi_B^{+,(0)}(\omega)}{\omega^2} \mathcal{E} \exp \mathcal{E} + \frac{C_A}{2C_F} \frac{\phi_B^{+,(0)}(\omega)}{\omega} (\exp \mathcal{E} - 1) \right\}, \end{aligned} \quad (\text{D.33})$$

where the abbreviation for the factors in the exponent is defined in Eq. (7.31). Expanding this result up to $\mathcal{O}(\alpha_s^2)$ reproduces the expressions Eqs. (7.18) and (D.24) of the explicit one- and two-loop calculation.

D.4 The Collinear Anomaly Argument in the Presence of Operator Mixing

In Section 5.4 we found that a simple product of two collinear functions exponentiates by demanding the expression to be independent of the artificial rapidity scale ν :

$$J_c(L_{\nu,Q}) J_{\bar{c}}(L_{\nu Q,m^2}) = J_c^{(0)} J_{\bar{c}}^{(0)} \left(\frac{Q^2}{m^2} \right)^{-J_c^{(1)}/J_c^{(0)}}. \quad (\text{D.34})$$

Here $J_{c,\bar{c}}^{(n)}$ are coefficients in a Taylor series in the logarithms that are generated through the expansion in δ . The regulator then must drop out in the prefactor (the remainder function R) and the exponent (the collinear anomaly F) separately, which we checked at one-loop order.

In this appendix we show that demanding the ν -independence is sufficient to resum large rapidity logarithms in an expression of the form

$$\mathcal{J}(Q^2/m^2) = J_{c1}(L_{\nu,Q}) J_{\bar{c}1}(L_{\nu Q,m^2}) + J_{c2}(L_{\nu,Q}) J_{\bar{c}2}(L_{\nu Q,m^2}). \quad (\text{D.35})$$

This can be considered as two products of inverse moments as they arise in the naive factorisation of ξ_η . The new feature here is that the J_i can mix among each other which results in a more complicated structure than in Eq. (D.34).

We proceed similarly as in Section 5.4 and write the various J_i as Taylor series in their logarithms. The ν -independence then results in the recurrence relation

$$n \left(J_{c1}^{(n)} J_{\bar{c}1}^{(m-1)} + J_{c2}^{(n)} J_{\bar{c}2}^{(m-1)} \right) + m \left(J_{c1}^{(n-1)} J_{\bar{c}1}^{(m)} + J_{c2}^{(n-1)} J_{\bar{c}2}^{(m)} \right) = 0, \quad \forall n, m \geq 1, \quad (\text{D.36})$$

which holds for different values of m and n that can be chosen independently. A strategy to solve this set of equations is the following. We can use the two equations with fixed values $m = 1$ and $m = 2$ and bring them into a form that only contains J_{c1} :

$$J_{c1}^{(n)} - \frac{F_1 + F_2}{n} J_{c1}^{(n-1)} + \frac{F_1 F_2}{n(n-1)} J_{c1}^{(n-2)} = 0. \quad (\text{D.37})$$

At this point F_1 and F_2 are just abbreviations for certain rational functions of the coefficients in the Taylor series:

$$F_1 + F_2 = \frac{2J_{\bar{c}1}^{(0)} J_{\bar{c}2}^{(2)} - 2J_{\bar{c}1}^{(2)} J_{\bar{c}2}^{(0)}}{J_{\bar{c}1}^{(1)} J_{\bar{c}2}^{(0)} - J_{\bar{c}1}^{(0)} J_{\bar{c}2}^{(1)}}, \quad F_1 F_2 = \frac{2J_{\bar{c}1}^{(2)} J_{\bar{c}2}^{(1)} - 2J_{\bar{c}1}^{(1)} J_{\bar{c}2}^{(2)}}{J_{\bar{c}1}^{(1)} J_{\bar{c}2}^{(0)} - J_{\bar{c}1}^{(0)} J_{\bar{c}2}^{(1)}}. \quad (\text{D.38})$$

Similar relations hold for the other J_i . However, Eq. (D.36) guarantees that in all of them the same coefficients F_1 and F_2 appear. In particular, the relation (D.37) is also true for J_{c2} whereas for $J_{\bar{c}1}$ and $J_{\bar{c}2}$ one simply needs to replace $F_1 \rightarrow -F_1$ and $F_2 \rightarrow -F_2$.

The solution to this recurrence relation is a sum of two exponentials involving two different anomalies F_1 and F_2 . If we take the first two coefficients in the Taylor series to fix the boundary conditions we end up with

$$J_{c1,c2} = J_{c1,c2}^{(0)} \frac{F_1 \left(\frac{\nu}{Q}\right)^{F_2} - F_2 \left(\frac{\nu}{Q}\right)^{F_1}}{F_1 - F_2} + J_{c1,c2}^{(1)} \frac{\left(\frac{\nu}{Q}\right)^{F_1} - \left(\frac{\nu}{Q}\right)^{F_2}}{F_1 - F_2}, \quad (\text{D.39})$$

and similarly for $J_{\bar{c}1,\bar{c}2}$ with the appropriate scales and $F_i \rightarrow -F_i$ ($i = 1, 2$).

Plugging these solutions into Eq. (D.35) gives the (by construction ν -independent) result

$$\begin{aligned} \mathcal{J}(Q^2/m^2) &= \left(J_{c1}^{(0)} J_{\bar{c}1}^{(0)} + J_{c2}^{(0)} J_{\bar{c}2}^{(0)} \right) \frac{F_1 \left(\frac{Q^2}{m^2}\right)^{-F_2} - F_2 \left(\frac{Q^2}{m^2}\right)^{-F_1}}{F_1 - F_2} \\ &+ \left(J_{c1}^{(1)} J_{\bar{c}1}^{(0)} + J_{c2}^{(1)} J_{\bar{c}2}^{(0)} \right) \frac{\left(\frac{Q^2}{m^2}\right)^{-F_1} - \left(\frac{Q^2}{m^2}\right)^{-F_2}}{F_1 - F_2}, \end{aligned} \quad (\text{D.40})$$

that resums all rapidity logarithms. Note that all eight parameters (the four $J_i^{(0)}$, the two $J_{c1}^{(1)}$ as well as F_1 and F_2) are independent if we make no further assumptions. Their choice is however not unique since we could use Eq. (D.36) to define a different set of independent coefficients.

For later use let us introduce the matrices γ , defined by the two relations

$$\begin{pmatrix} J_{c1}^{(2)} \\ J_{c2}^{(2)} \end{pmatrix} \equiv \frac{\gamma}{2} \cdot \begin{pmatrix} J_{c1}^{(1)} \\ J_{c2}^{(1)} \end{pmatrix} \quad \text{and} \quad \begin{pmatrix} J_{c1}^{(1)} \\ J_{c2}^{(1)} \end{pmatrix} \equiv \gamma \cdot \begin{pmatrix} J_{c1}^{(0)} \\ J_{c2}^{(0)} \end{pmatrix}, \quad (\text{D.41})$$

and $\tilde{\gamma}$ defined analogously for the $J_{\bar{c}i}$. Equation. (D.36) implies that $\tilde{\gamma} = -\gamma^T$, and furthermore, we find

$$\text{tr } \gamma = \gamma_{11} + \gamma_{22} = F_1 + F_2 \quad \text{and} \quad \det \gamma = \gamma_{11}\gamma_{22} - \gamma_{12}\gamma_{21} = F_1 F_2. \quad (\text{D.42})$$

This can be used to replace the $J_{c1,c2}^{(1)}$ via some γ_{ij} in Eq. (D.40).

Now consider solving a rapidity RGE in ν for the various J_i . By equating the coefficients one finds that γ is exactly the anomalous dimension matrix:

$$\frac{d}{d \log \nu} \begin{pmatrix} J_{c1}(L_{\nu}, Q) \\ J_{c2}(L_{\nu}, Q) \end{pmatrix} = \gamma \cdot \begin{pmatrix} J_{c1}(L_{\nu}, Q) \\ J_{c2}(L_{\nu}, Q) \end{pmatrix}, \quad (\text{D.43})$$

and

$$\frac{d}{d \log \nu} \begin{pmatrix} J_{\bar{c}1}(L_{\nu Q}, m^2) \\ J_{\bar{c}2}(L_{\nu Q}, m^2) \end{pmatrix} = -\gamma^T \cdot \begin{pmatrix} J_{\bar{c}1}(L_{\nu Q}, m^2) \\ J_{\bar{c}2}(L_{\nu Q}, m^2) \end{pmatrix}. \quad (\text{D.44})$$

Since γ itself is ν -independent we can solve this system of differential equations. We find

$$J_{c1}(\nu) = J_{c1}(\nu_c) \frac{(\gamma_{11} - F_2) \left(\frac{\nu}{\nu_c}\right)^{F_1} - (\gamma_{11} - F_1) \left(\frac{\nu}{\nu_c}\right)^{F_2}}{F_1 - F_2} + J_{c2}(\nu_c) \gamma_{12} \frac{\left(\frac{\nu}{\nu_c}\right)^{F_1} - \left(\frac{\nu}{\nu_c}\right)^{F_2}}{F_1 - F_2}, \quad (\text{D.45})$$

and similar solutions for the other J_i . Here we would define the anomalies F_1 and F_2 as the eigenvalues of γ , consistent with Eq. (D.42). Equation (D.35) then becomes

$$\begin{aligned} \mathcal{J}(Q^2/m^2) = & [J_{c1}(\nu_c)J_{\bar{c}1}(\nu_{\bar{c}}) + J_{c2}(\nu_c)J_{\bar{c}2}(\nu_{\bar{c}})] \frac{F_1\left(\frac{\nu_c}{\nu_{\bar{c}}}\right)^{-F_2} - F_2\left(\frac{\nu_c}{\nu_{\bar{c}}}\right)^{-F_1}}{F_1 - F_2} \\ & + [\gamma_{11} J_{c1}(\nu_c)J_{\bar{c}1}(\nu_{\bar{c}}) + \gamma_{12} J_{c2}(\nu_c)J_{\bar{c}1}(\nu_{\bar{c}}) \\ & + \gamma_{21} J_{c1}(\nu_c)J_{\bar{c}2}(\nu_{\bar{c}}) + \gamma_{22} J_{c2}(\nu_c)J_{\bar{c}2}(\nu_{\bar{c}})] \frac{\left(\frac{\nu_c}{\nu_{\bar{c}}}\right)^{-F_1} - \left(\frac{\nu_c}{\nu_{\bar{c}}}\right)^{-F_2}}{F_1 - F_2}. \end{aligned} \quad (\text{D.46})$$

Note that the four γ_{ij} are not independent and the solution is again defined by eight independent parameters (for example the four entries of γ and the four J_i at their natural scales). In particular, when we identify the renormalised J_i at their natural scale with the first coefficient in the Taylor series, $J_i(\nu_{c,\bar{c}}) = J_i^{(0)}$, and set $\nu_c \rightarrow Q$ and $\nu_{\bar{c}} \rightarrow m^2/Q$ to their typical scales, this result agrees with the previous result in Eq. (D.40).

Thus, we showed that for the specific structure assumed for \mathcal{J} , the collinear anomaly argument is equivalent to the solution of a rapidity RGE. The reason why this is the case is that the anomalous dimension that governs the running in ν is itself independent of ν . In contrast, the anomalous dimension that governs the running in μ depends on μ via an explicit logarithm and through the β -function. In other words, the coupling $\alpha_s = \alpha_s(\mu)$ depends on the renormalisation scale μ , whereas the rapidity scale ν is an artefact introduced to keep the mass dimensions homogeneous and thus only arises in the corresponding logarithms.

Lastly, we show qualitatively how the various structures observed in the ν -evolved soft form factor ξ_η in Eq. (7.56) arise by considering different limits of Eq. (D.46).

- (a) *No mixing*: In this case $\gamma_{12} = \gamma_{21} = 0$ which implies $\gamma_{11} = F_1$ and $\gamma_{22} = F_2$ (or vice versa). Then \mathcal{J} has the expected form with two independent anomalies:

$$\mathcal{J}(Q^2/m^2) = J_{c1}(\nu_c)J_{\bar{c}1}(\nu_{\bar{c}}) \left(\frac{\nu_c}{\nu_{\bar{c}}}\right)^{-F_1} + J_{c2}(\nu_c)J_{\bar{c}2}(\nu_{\bar{c}}) \left(\frac{\nu_c}{\nu_{\bar{c}}}\right)^{-F_2}. \quad (\text{D.47})$$

- (b) *Mixing with endpoint-finite moments*: The case where two (or more) moments are endpoint-finite is trivial. When only one moment is endpoint-finite, we have e.g. $\gamma_{21} = \gamma_{22} = 0$ which implies that $F_2 = 0$ and $\gamma_{11} = F_1 \equiv F$ (or vice versa):

$$\begin{aligned} \mathcal{J}(Q^2/m^2) = & J_{c1}(\nu_c)J_{\bar{c}1}(\nu_{\bar{c}}) \left(\frac{\nu_c}{\nu_{\bar{c}}}\right)^{-F} + J_{c2}(\nu_c)J_{\bar{c}2}(\nu_{\bar{c}}) \\ & + \frac{\gamma_{12}}{F} J_{c2}(\nu_c)J_{\bar{c}1}(\nu_{\bar{c}}) \left(\left(\frac{\nu_c}{\nu_{\bar{c}}}\right)^{-F} - 1 \right). \end{aligned} \quad (\text{D.48})$$

In the last term we identify one of the non-trivial structures that we found in ξ_η .

- (c) *Resummation of leading logarithms*: In this approximation both anomalies can be identified with the evolution kernel, $F_{1,2} \rightarrow A \equiv A_{\gamma_{\text{cusp}}}(\mu_s, \mu)$, which gives the

logarithmic contributions found in ξ_η :

$$\begin{aligned}
 \mathcal{J}(Q^2/m^2) &= [J_{c1}(\nu_c)J_{\bar{c}1}(\nu_{\bar{c}}) + J_{c2}(\nu_c)J_{\bar{c}2}(\nu_{\bar{c}})] \left(\frac{\nu_c}{\nu_{\bar{c}}}\right)^{-A} \left(1 + A \log \frac{\nu_c}{\nu_{\bar{c}}}\right) \\
 &\quad - [\gamma_{11} J_{c1}(\nu_c)J_{\bar{c}1}(\nu_{\bar{c}}) + \gamma_{12} J_{c2}(\nu_c)J_{\bar{c}1}(\nu_{\bar{c}}) \\
 &\quad + \gamma_{21} J_{c1}(\nu_c)J_{\bar{c}2}(\nu_{\bar{c}}) + \gamma_{22} J_{c2}(\nu_c)J_{\bar{c}2}(\nu_{\bar{c}})] \left(\frac{\nu_c}{\nu_{\bar{c}}}\right)^{-A} \log \frac{\nu_c}{\nu_{\bar{c}}}. \quad (\text{D.49})
 \end{aligned}$$

Note that in the LL approximation all entries γ_{ij} are proportional to A , as we found for example in the anomalous dimension matrices in Section 7.3.2.

Bibliography

- [1] ATLAS collaboration, G. Aad et al., *Observation of a new particle in the search for the Standard Model Higgs boson with the ATLAS detector at the LHC*, *Phys.Lett.* **B716** (2012) 1–29, [1207.7214].
- [2] CMS collaboration, S. Chatrchyan et al., *Observation of a new boson at a mass of 125 GeV with the CMS experiment at the LHC*, *Phys.Lett.* **B716** (2012) 30–61, [1207.7235].
- [3] P. W. Higgs, *Broken Symmetries and the Masses of Gauge Bosons*, *Phys. Rev. Lett.* **13** (1964) 508–509.
- [4] F. Englert and R. Brout, *Broken Symmetry and the Mass of Gauge Vector Mesons*, *Phys. Rev. Lett.* **13** (1964) 321–323.
- [5] M. E. Peskin and D. V. Schroeder, *An Introduction to quantum field theory*. Addison-Wesley, Reading, USA, 1995.
- [6] J. F. Donoghue, E. Golowich and B. R. Holstein, *Dynamics of the standard model*, *Cambridge Monographs on Particle Physics, Nuclear Physics and Cosmology* **2** (1992) 1–540.
- [7] PARTICLE DATA GROUP collaboration, C. Patrignani et al., *Review of Particle Physics*, *Chin. Phys.* **C40** (2016) 100001.
- [8] M. D. Schwartz, *Quantum Field Theory and the Standard Model*. Cambridge University Press, 2014.
- [9] T. Muta, *Foundations of Quantum Chromodynamics: An Introduction to Perturbative Methods in Gauge Theories*, (3rd ed.), vol. 78 of *World scientific Lecture Notes in Physics*. World Scientific, Hackensack, N.J., 2010.
- [10] N. Cabibbo, *Unitary Symmetry and Leptonic Decays*, *Phys.Rev.Lett.* **10** (1963) 531–533.
- [11] M. Kobayashi and T. Maskawa, *CP Violation in the Renormalizable Theory of Weak Interaction*, *Prog.Theor.Phys.* **49** (1973) 652–657.
- [12] D. J. Gross and F. Wilczek, *Asymptotically Free Gauge Theories - I*, *Phys. Rev.* **D8** (1973) 3633–3652.
- [13] H. D. Politzer, *Reliable Perturbative Results for Strong Interactions?*, *Phys. Rev. Lett.* **30** (1973) 1346–1349.

- [14] LHCb collaboration, R. Aaij et al., *Observation of $J/\psi p$ Resonances Consistent with Pentaquark States in $\Lambda_b^0 \rightarrow J/\psi K^- p$ Decays*, *Phys. Rev. Lett.* **115** (2015) 072001, [1507.03414].
- [15] M. Neubert, *Heavy quark symmetry*, *Phys. Rept.* **245** (1994) 259–396, [hep-ph/9306320].
- [16] A. V. Manohar and M. B. Wise, *Heavy quark physics*, *Camb. Monogr. Part. Phys. Nucl. Phys. Cosmol.* **10** (2000) 1–191.
- [17] T. Mannel, *Effective Field Theories in Flavor Physics*, *Springer Tracts Mod. Phys.* **203** (2004) 1–175.
- [18] A. G. Grozin, *Heavy quark effective theory*, *Springer Tracts Mod. Phys.* **201** (2004) 1–213.
- [19] T. Mannel, W. Roberts and Z. Ryzak, *A Derivation of the heavy quark effective Lagrangian from QCD*, *Nucl. Phys.* **B368** (1992) 204–217.
- [20] N. Isgur and M. B. Wise, *Weak Decays of Heavy Mesons in the Static Quark Approximation*, *Phys. Lett.* **B232** (1989) 113–117.
- [21] N. Isgur and M. B. Wise, *Weak Transition Form-Factors Between Heavy Mesons*, *Phys. Lett.* **B237** (1990) 527–530.
- [22] M. Artuso et al., *B , D and K decays*, *Eur. Phys. J.* **C57** (2008) 309–492, [0801.1833].
- [23] M. Antonelli et al., *Flavor Physics in the Quark Sector*, *Phys. Rept.* **494** (2010) 197–414, [0907.5386].
- [24] LHCb collaboration, R. Aaij et al., *Implications of LHCb measurements and future prospects*, *Eur. Phys. J.* **C73** (2013) 2373, [1208.3355].
- [25] A. J. Buras and J. Girrbach, *Towards the Identification of New Physics through Quark Flavour Violating Processes*, *Rept. Prog. Phys.* **77** (2014) 086201, [1306.3775].
- [26] BELLE, BABAR collaboration, A. J. Bevan et al., *The Physics of the B Factories*, *Eur. Phys. J.* **C74** (2014) 3026, [1406.6311].
- [27] M. Beneke, G. Buchalla, M. Neubert and C. T. Sachrajda, *QCD factorization for $B \rightarrow \pi\pi$ decays: Strong phases and CP violation in the heavy quark limit*, *Phys. Rev. Lett.* **83** (1999) 1914–1917, [hep-ph/9905312].
- [28] M. Beneke, G. Buchalla, M. Neubert and C. T. Sachrajda, *QCD factorization for exclusive, nonleptonic B meson decays: General arguments and the case of heavy light final states*, *Nucl. Phys.* **B591** (2000) 313–418, [hep-ph/0006124].

-
- [29] M. Beneke, G. Buchalla, M. Neubert and C. T. Sachrajda, *QCD factorization in $B \rightarrow \pi K, \pi\pi$ decays and extraction of Wolfenstein parameters*, *Nucl. Phys.* **B606** (2001) 245–321, [[hep-ph/0104110](#)].
- [30] A. V. Efremov and A. V. Radyushkin, *Factorization and Asymptotical Behavior of Pion Form-Factor in QCD*, *Phys. Lett.* **94B** (1980) 245–250.
- [31] G. P. Lepage and S. J. Brodsky, *Exclusive Processes in Quantum Chromodynamics: Evolution Equations for Hadronic Wave Functions and the Form-Factors of Mesons*, *Phys. Lett.* **87B** (1979) 359–365.
- [32] G. P. Lepage and S. J. Brodsky, *Exclusive Processes in Perturbative Quantum Chromodynamics*, *Phys. Rev.* **D22** (1980) 2157.
- [33] J. D. Bjorken, *Topics in B Physics*, *Nucl. Phys. Proc. Suppl.* **11** (1989) 325–341.
- [34] G. Bell, *NNLO vertex corrections in charmless hadronic B decays: Imaginary part*, *Nucl. Phys.* **B795** (2008) 1–26, [[0705.3127](#)].
- [35] G. Bell, *NNLO vertex corrections in charmless hadronic B decays: Real part*, *Nucl. Phys.* **B822** (2009) 172–200, [[0902.1915](#)].
- [36] M. Beneke, T. Huber and X.-Q. Li, *NNLO vertex corrections to non-leptonic B decays: Tree amplitudes*, *Nucl. Phys.* **B832** (2010) 109–151, [[0911.3655](#)].
- [37] G. Bell, M. Beneke, T. Huber and X.-Q. Li, *Two-loop current–current operator contribution to the non-leptonic QCD penguin amplitude*, *Phys. Lett.* **B750** (2015) 348–355, [[1507.03700](#)].
- [38] M. Beneke and S. Jäger, *Spectator scattering at NLO in non-leptonic b decays: Tree amplitudes*, *Nucl. Phys.* **B751** (2006) 160–185, [[hep-ph/0512351](#)].
- [39] N. Kivel, *Radiative corrections to hard spectator scattering in $B \rightarrow \pi\pi$ decays*, *JHEP* **05** (2007) 019, [[hep-ph/0608291](#)].
- [40] V. Pilipp, *Hard spectator interactions in $B \rightarrow \pi\pi$ at order α_s^2* , *Nucl. Phys.* **B794** (2008) 154–188, [[0709.3214](#)].
- [41] M. Beneke and S. Jäger, *Spectator scattering at NLO in non-leptonic B decays: Leading penguin amplitudes*, *Nucl. Phys.* **B768** (2007) 51–84, [[hep-ph/0610322](#)].
- [42] T. Feldmann, *Non-Leptonic Heavy Meson Decays - Theory Status*, in *12th Conference on Flavor Physics and CP Violation (FPCP 2014) Marseille, France, May 26-30, 2014*, 2014. 1408.0300.
- [43] S. Kränkl, T. Mannel and J. Virto, *Three-body non-leptonic B decays and QCD factorization*, *Nucl. Phys.* **B899** (2015) 247–264, [[1505.04111](#)].
- [44] G. P. Korchemsky, D. Pirjol and T.-M. Yan, *Radiative leptonic decays of B mesons in QCD*, *Phys. Rev.* **D61** (2000) 114510, [[hep-ph/9911427](#)].

- [45] S. Descotes-Genon and C. T. Sachrajda, *Factorization, the light cone distribution amplitude of the B meson and the radiative decay $B \rightarrow \gamma \ell \nu(\ell)$* , *Nucl. Phys.* **B650** (2003) 356–390, [[hep-ph/0209216](#)].
- [46] E. Lunghi, D. Pirjol and D. Wyler, *Factorization in leptonic radiative $B \rightarrow \gamma e$ decays*, *Nucl. Phys.* **B649** (2003) 349–364, [[hep-ph/0210091](#)].
- [47] S. W. Bosch, R. J. Hill, B. O. Lange and M. Neubert, *Factorization and Sudakov resummation in leptonic radiative B decay*, *Phys. Rev.* **D67** (2003) 094014, [[hep-ph/0301123](#)].
- [48] M. Beneke and J. Rohrwild, *B meson distribution amplitude from $B \rightarrow \gamma \ell \nu$* , *Eur. Phys. J.* **C71** (2011) 1818, [[1110.3228](#)].
- [49] M. Beneke, V. M. Braun, Y. Ji and Y.-B. Wei, *Radiative leptonic decay $B \rightarrow \gamma \ell \nu_\ell$ with subleading power corrections*, [1804.04962](#).
- [50] BABAR collaboration, B. Aubert et al., *Search for the radiative leptonic decay $B^+ \rightarrow \gamma \ell^+ \nu_\ell$* , [0704.1478](#).
- [51] BABAR collaboration, B. Aubert et al., *A Model-independent search for the decay $B^+ \rightarrow \ell^+ \nu_\ell \gamma$* , *Phys. Rev.* **D80** (2009) 111105, [[0907.1681](#)].
- [52] V. M. Braun, D. Yu. Ivanov and G. P. Korchemsky, *The B meson distribution amplitude in QCD*, *Phys. Rev.* **D69** (2004) 034014, [[hep-ph/0309330](#)].
- [53] M. Beneke and T. Feldmann, *Symmetry breaking corrections to heavy to light B meson form-factors at large recoil*, *Nucl. Phys.* **B592** (2001) 3–34, [[hep-ph/0008255](#)].
- [54] M. Beneke and T. Feldmann, *Factorization of heavy to light form-factors in soft collinear effective theory*, *Nucl. Phys.* **B685** (2004) 249–296, [[hep-ph/0311335](#)].
- [55] J. Charles, A. Le Yaouanc, L. Oliver, O. Pene and J. C. Raynal, *Heavy to light form-factors in the heavy mass to large energy limit of QCD*, *Phys. Rev.* **D60** (1999) 014001, [[hep-ph/9812358](#)].
- [56] P. Böer, T. Feldmann and D. van Dyk, *QCD Factorization Theorem for $B \rightarrow \pi \pi \ell \nu$ Decays at Large Dipion Masses*, *JHEP* **02** (2017) 133, [[1608.07127](#)].
- [57] F. Kruger and J. Matias, *Probing new physics via the transverse amplitudes of $B^0 \rightarrow K^{*0}(\rightarrow K^- \pi^+) l^+ l^-$ at large recoil*, *Phys. Rev.* **D71** (2005) 094009, [[hep-ph/0502060](#)].
- [58] W. Altmannshofer, P. Ball, A. Bharucha, A. J. Buras, D. M. Straub and M. Wick, *Symmetries and Asymmetries of $B \rightarrow K^* \mu^+ \mu^-$ Decays in the Standard Model and Beyond*, *JHEP* **01** (2009) 019, [[0811.1214](#)].
- [59] C. Bobeth, G. Hiller and D. van Dyk, *The Benefits of $\bar{B} \rightarrow \bar{K}^* l^+ l^-$ Decays at Low Recoil*, *JHEP* **07** (2010) 098, [[1006.5013](#)].

-
- [60] T. Feldmann, B. Müller and D. van Dyk, *Analyzing $b \rightarrow u$ transitions in semileptonic $\bar{B}_s \rightarrow K^{*+}(\rightarrow K\pi)\ell^-\bar{\nu}_\ell$ decays*, *Phys. Rev.* **D92** (2015) 034013, [1503.09063].
- [61] U.-G. Meißner and W. Wang, *$B_s \rightarrow K^{(*)}\ell\bar{\nu}$, Angular Analysis, S-wave Contributions and $|V_{ub}|$* , *JHEP* **01** (2014) 107, [1311.5420].
- [62] P. Böer, T. Feldmann and D. van Dyk, *Angular Analysis of the Decay $\Lambda_b \rightarrow \Lambda(\rightarrow N\pi)\ell^+\ell^-$* , *JHEP* **01** (2015) 155, [1410.2115].
- [63] S. Faller, T. Feldmann, A. Khodjamirian, T. Mannel and D. van Dyk, *Disentangling the Decay Observables in $B^- \rightarrow \pi^+\pi^-\ell^-\bar{\nu}_\ell$* , *Phys. Rev.* **D89** (2014) 014015, [1310.6660].
- [64] M. Beneke and M. Neubert, *QCD factorization for $B \rightarrow PP$ and $B \rightarrow PV$ decays*, *Nucl. Phys.* **B675** (2003) 333–415, [hep-ph/0308039].
- [65] M. Beneke, J. Rohrer and D. Yang, *Branching fractions, polarisation and asymmetries of $B \rightarrow VV$ decays*, *Nucl. Phys.* **B774** (2007) 64–101, [hep-ph/0612290].
- [66] M. Beneke and T. Feldmann, *Spectator interactions and factorization in $B \rightarrow \pi\ell\nu$ decay*, *Eur. Phys. J.* **C33** (2004) S241–S243, [hep-ph/0308303].
- [67] M. Beneke, A. P. Chapovsky, M. Diehl and T. Feldmann, *Soft collinear effective theory and heavy to light currents beyond leading power*, *Nucl. Phys.* **B643** (2002) 431–476, [hep-ph/0206152].
- [68] V. M. Braun and I. E. Filyanov, *Conformal Invariance and Pion Wave Functions of Nonleading Twist*, *Z. Phys.* **C48** (1990) 239–248.
- [69] G. Hiller and R. Zwicky, *(A)symmetries of weak decays at and near the kinematic endpoint*, *JHEP* **03** (2014) 042, [1312.1923].
- [70] I. Sentitemsu Imsong, A. Khodjamirian, T. Mannel and D. van Dyk, *Extrapolation and unitarity bounds for the $B \rightarrow \pi$ form factor*, *JHEP* **02** (2015) 126, [1409.7816].
- [71] D. van Dyk et al., *EOS — A HEP program for Flavor Observables*, 2016. <https://eos.github.io>.
- [72] PARTICLE DATA GROUP collaboration, J. Beringer et al., *Review of Particle Physics (RPP)*, *Phys. Rev.* **D86** (2012) 010001.
- [73] A. Khodjamirian, T. Mannel, N. Offen and Y. M. Wang, *$B \rightarrow \pi\ell\nu_l$ Width and $|V_{ub}|$ from QCD Light-Cone Sum Rules*, *Phys. Rev.* **D83** (2011) 094031, [1103.2655].
- [74] X.-W. Kang, B. Kubis, C. Hanhart and U.-G. Meißner, *B_{14} decays and the extraction of $|V_{ub}|$* , *Phys. Rev.* **D89** (2014) 053015, [1312.1193].

- [75] U.-G. Meißner and W. Wang, *Generalized Heavy-to-Light Form Factors in Light-Cone Sum Rules*, *Phys. Lett.* **B730** (2014) 336–341, [1312.3087].
- [76] C. Hambrock and A. Khodjamirian, *Form factors in $\bar{B}^0 \rightarrow \pi\pi\ell\bar{\nu}_\ell$ from QCD light-cone sum rules*, *Nucl. Phys.* **B905** (2016) 373–390, [1511.02509].
- [77] C. Bourrely, I. Caprini and L. Lellouch, *Model-independent description of $B \rightarrow \pi\ell\nu$ decays and a determination of $|V_{ub}|$* , *Phys. Rev.* **D79** (2009) 013008, [0807.2722].
- [78] C. Becchi, A. Rouet and R. Stora, *Renormalization of gauge theories*, *Annals of Physics* **98** (1976) 287 – 321.
- [79] M. Z. Iofa and I. V. Tyutin, *Gauge invariance of spontaneously broken non-abelian theories in the bogolyubov–parasyuk–hepp–zimmermann method*, *Theoret. and Math. Phys.* **27** (1976) 316–322.
- [80] J. C. Collins, *Renormalization: An Introduction to Renormalization, the Renormalization Group and the Operator-Product Expansion*. Cambridge Monographs on Mathematical Physics. Cambridge University Press, 1984, 10.1017/CBO9780511622656.
- [81] H. Lehmann, K. Symanzik and W. Zimmermann, *Zur Formulierung quantisierter Feldtheorien*, *Nuovo Cimento* **1** (1955) 205–225.
- [82] J.-y. Chiu, F. Golf, R. Kelley and A. V. Manohar, *Electroweak Sudakov corrections using effective field theory*, *Phys. Rev. Lett.* **100** (2008) 021802, [0709.2377].
- [83] J.-y. Chiu, F. Golf, R. Kelley and A. V. Manohar, *Electroweak Corrections in High Energy Processes using Effective Field Theory*, *Phys. Rev.* **D77** (2008) 053004, [0712.0396].
- [84] B. Jantzen and V. A. Smirnov, *The Two-loop vector form-factor in the Sudakov limit*, *Eur. Phys. J.* **C47** (2006) 671–695, [hep-ph/0603133].
- [85] M. Beneke and V. A. Smirnov, *Asymptotic expansion of Feynman integrals near threshold*, *Nucl. Phys.* **B522** (1998) 321–344, [hep-ph/9711391].
- [86] B. Jantzen, *Foundation and generalization of the expansion by regions*, *JHEP* **12** (2011) 076, [1111.2589].
- [87] T. Becher, A. Broggio and A. Ferroglia, *Introduction to Soft-Collinear Effective Theory*, *Lect. Notes Phys.* **896** (2015) pp.1–206, [1410.1892].
- [88] T. Becher and G. Bell, *Analytic Regularization in Soft-Collinear Effective Theory*, *Phys. Lett.* **B713** (2012) 41–46, [1112.3907].

-
- [89] C. W. Bauer, S. Fleming and M. E. Luke, *Summing Sudakov logarithms in $B \rightarrow X_s \gamma$ in effective field theory*, *Phys. Rev.* **D63** (2000) 014006, [hep-ph/0005275].
- [90] C. W. Bauer, S. Fleming, D. Pirjol and I. W. Stewart, *An Effective field theory for collinear and soft gluons: Heavy to light decays*, *Phys. Rev.* **D63** (2001) 114020, [hep-ph/0011336].
- [91] C. W. Bauer and I. W. Stewart, *Invariant operators in collinear effective theory*, *Phys. Lett.* **B516** (2001) 134–142, [hep-ph/0107001].
- [92] C. W. Bauer, D. Pirjol and I. W. Stewart, *Soft collinear factorization in effective field theory*, *Phys. Rev.* **D65** (2002) 054022, [hep-ph/0109045].
- [93] M. Beneke and T. Feldmann, *Multipole expanded soft collinear effective theory with nonAbelian gauge symmetry*, *Phys. Lett.* **B553** (2003) 267–276, [hep-ph/0211358].
- [94] R. J. Hill and M. Neubert, *Spectator interactions in soft collinear effective theory*, *Nucl. Phys.* **B657** (2003) 229–256, [hep-ph/0211018].
- [95] J.-Y. Chiu, A. Jain, D. Neill and I. Z. Rothstein, *A Formalism for the Systematic Treatment of Rapidity Logarithms in Quantum Field Theory*, *JHEP* **05** (2012) 084, [1202.0814].
- [96] T. Becher and M. Neubert, *Drell-Yan Production at Small q_T , Transverse Parton Distributions and the Collinear Anomaly*, *Eur. Phys. J.* **C71** (2011) 1665, [1007.4005].
- [97] A. M. Polyakov, *Gauge Fields as Rings of Glue*, *Nucl. Phys.* **B164** (1980) 171–188.
- [98] R. A. Brandt, F. Neri and M. Sato, *Renormalization of Loop Functions for All Loops*, *Phys. Rev.* **D24** (1981) 879.
- [99] I. A. Korchemskaya and G. P. Korchemsky, *On lightlike Wilson loops*, *Phys. Lett.* **B287** (1992) 169–175.
- [100] B. O. Lange and M. Neubert, *Factorization and the soft overlap contribution to heavy to light form-factors*, *Nucl. Phys.* **B690** (2004) 249–278, [hep-ph/0311345].
- [101] A. V. Manohar and I. W. Stewart, *The Zero-Bin and Mode Factorization in Quantum Field Theory*, *Phys. Rev.* **D76** (2007) 074002, [hep-ph/0605001].
- [102] M. Beneke and D. Yang, *Heavy-to-light B meson form-factors at large recoil energy: Spectator-scattering corrections*, *Nucl. Phys.* **B736** (2006) 34–81, [hep-ph/0508250].
- [103] M. Beneke, Y. Kiyo and D. S. Yang, *Loop corrections to subleading heavy quark currents in SCET*, *Nucl. Phys.* **B692** (2004) 232–248, [hep-ph/0402241].

- [104] B. O. Lange and M. Neubert, *Renormalization group evolution of the B meson light cone distribution amplitude*, *Phys. Rev. Lett.* **91** (2003) 102001, [[hep-ph/0303082](#)].
- [105] T. Becher, G. Bell and M. Neubert, *Factorization and Resummation for Jet Broadening*, *Phys. Lett.* **B704** (2011) 276–283, [[1104.4108](#)].
- [106] T. Becher and M. Neubert, *Factorization and NNLL Resummation for Higgs Production with a Jet Veto*, *JHEP* **07** (2012) 108, [[1205.3806](#)].
- [107] I. W. Stewart, F. J. Tackmann, J. R. Walsh and S. Zuberi, *Jet p_T resummation in Higgs production at NNLL' + NNLO*, *Phys. Rev.* **D89** (2014) 054001, [[1307.1808](#)].
- [108] T. Becher and G. Bell, *Enhanced nonperturbative effects through the collinear anomaly*, *Phys. Rev. Lett.* **112** (2014) 182002, [[1312.5327](#)].
- [109] T. Becher and X. Garcia i Tormo, *Factorization and resummation for transverse thrust*, *JHEP* **06** (2015) 071, [[1502.04136](#)].
- [110] G. Bell, R. Rahn and J. Talbert, *Two-loop anomalous dimensions of generic dijet soft functions*, [1805.12414](#).
- [111] T. Binoth and G. Heinrich, *An automatized algorithm to compute infrared divergent multiloop integrals*, *Nucl. Phys.* **B585** (2000) 741–759, [[hep-ph/0004013](#)].
- [112] G. Bell, *Higher order QCD corrections in exclusive charmless B decays*. PhD thesis, Munich U., 2006. [0705.3133](#).
- [113] G. Heinrich, *Sector Decomposition*, *Int. J. Mod. Phys.* **A23** (2008) 1457–1486, [[0803.4177](#)].
- [114] G. Bell, T. Feldmann, Y.-M. Wang and M. W. Y. Yip, *Light-Cone Distribution Amplitudes for Heavy-Quark Hadrons*, *JHEP* **11** (2013) 191, [[1308.6114](#)].
- [115] H. Kawamura, J. Kodaira, C.-F. Qiao and K. Tanaka, *B-meson light cone distribution amplitudes in the heavy quark limit*, *Phys. Lett.* **B523** (2001) 111, [[hep-ph/0109181](#)].
- [116] S. J. Lee and M. Neubert, *Model-independent properties of the B-meson distribution amplitude*, *Phys. Rev.* **D72** (2005) 094028, [[hep-ph/0509350](#)].
- [117] V. M. Braun, A. N. Manashov and N. Offen, *Evolution equation for the higher-twist B-meson distribution amplitude*, *Phys. Rev.* **D92** (2015) 074044, [[1507.03445](#)].
- [118] V. M. Braun, Y. Ji and A. N. Manashov, *Higher-twist B-meson Distribution Amplitudes in HQET*, *JHEP* **05** (2017) 022, [[1703.02446](#)].

-
- [119] G. Bell and T. Feldmann, *Modelling light-cone distribution amplitudes from non-relativistic bound states*, *JHEP* **04** (2008) 061, [0802.2221].
- [120] P. Ball, *Theoretical update of pseudoscalar meson distribution amplitudes of higher twist: The Nonsinglet case*, *JHEP* **01** (1999) 010, [hep-ph/9812375].
- [121] B. A. Thacker and G. P. Lepage, *Heavy quark bound states in lattice QCD*, *Phys. Rev.* **D43** (1991) 196–208.
- [122] G. P. Lepage, L. Magnea, C. Nakhleh, U. Magnea and K. Hornbostel, *Improved nonrelativistic QCD for heavy quark physics*, *Phys. Rev.* **D46** (1992) 4052–4067, [hep-lat/9205007].
- [123] G. T. Bodwin, E. Braaten and G. P. Lepage, *Rigorous QCD analysis of inclusive annihilation and production of heavy quarkonium*, *Phys. Rev.* **D51** (1995) 1125–1171, [hep-ph/9407339].
- [124] M. Beneke, A. Signer and V. A. Smirnov, *Top quark production near threshold and the top quark mass*, *Phys. Lett.* **B454** (1999) 137–146, [hep-ph/9903260].
- [125] A. Pineda and J. Soto, *Effective field theory for ultrasoft momenta in NRQCD and NRQED*, *Nucl. Phys. Proc. Suppl.* **64** (1998) 428–432, [hep-ph/9707481].
- [126] A. Pineda and J. Soto, *The Lamb shift in dimensional regularization*, *Phys. Lett.* **B420** (1998) 391–396, [hep-ph/9711292].
- [127] N. Brambilla, A. Pineda, J. Soto and A. Vairo, *Potential NRQCD: An Effective theory for heavy quarkonium*, *Nucl. Phys.* **B566** (2000) 275, [hep-ph/9907240].
- [128] I. Moul, I. W. Stewart, G. Vita and H. X. Zhu, *First Subleading Power Resummation for Event Shapes*, 1804.04665.
- [129] Y.-Y. Keum, H.-n. Li and A. I. Sanda, *Fat penguins and imaginary penguins in perturbative QCD*, *Phys. Lett.* **B504** (2001) 6–14, [hep-ph/0004004].
- [130] Y. Y. Keum, H.-N. Li and A. I. Sanda, *Penguin enhancement and $B \rightarrow K\pi$ decays in perturbative QCD*, *Phys. Rev.* **D63** (2001) 054008, [hep-ph/0004173].
- [131] A. Bharucha, T. Feldmann and M. Wick, *Theoretical and Phenomenological Constraints on Form Factors for Radiative and Semi-Leptonic B-Meson Decays*, *JHEP* **09** (2010) 090, [1004.3249].
- [132] T. Feldmann and M. W. Y. Yip, *Form Factors for $\Lambda_b \rightarrow \Lambda$ Transitions in SCET*, *Phys. Rev.* **D85** (2012) 014035, [1111.1844].
- [133] D. Das and R. Sinha, *New Physics Effects and Hadronic Form Factor Uncertainties in $B \rightarrow K^*\ell^+\ell^-$* , *Phys. Rev.* **D86** (2012) 056006, [1205.1438].
- [134] C. Hambroek and G. Hiller, *Extracting $B \rightarrow K^*$ Form Factors from Data*, *Phys. Rev. Lett.* **109** (2012) 091802, [1204.4444].

Danksagung

Bedanken möchte ich mich zuerst bei meinem Doktorvater Prof. Dr. Thorsten Feldmann sowie meinem Co-Betreuer Prof. Dr. Guido Bell, welche mir die Gelegenheit gegeben haben, mich mit höchst interessanten Forschungsfragen der Elementarteilchenphysik auseinanderzusetzen, und stets bereit waren in teils stundenlangen Diskussionen meine Fragen zu beantworten.

Für eine sehr hilfreiche und angenehme Betreuung zu Beginn meiner Promotion möchte ich Dr. Danny van Dyk danken. Weiterhin möchte ich Dr. Jan Piclum, Dr. Björn O. Lange, sowie Stefan Schmidt und Katja Jäschke für das Korrekturlesen und viele nützliche Kommentare zu dieser Arbeit danken. Besonders danke ich Jan sowie auch Dr. Tobias Huber für ihren Einsatz, mir beim Lösen diverser Integrale behilflich gewesen zu sein.

Des Weiteren danke ich Prof. Dr. Thomas Mannel, der mich während des ganzen Studiums unterstützt hat und mir während der Promotion das Vertrauen schenkte, ihm als sein persönlicher Referent zur Seite zu stehen. Ebenso danke ich ihm für seine berüchtigten Grill- und Glühweinpartys. Aleksey Rusov möchte ich für zahlreiche angenehme Reisen zu diversen Konferenzen und Sommerschulen sowie ausgiebigen Diskussionen über physikalische Fragestellungen danken. Allen anderen Mitgliedern der Arbeitsgruppe “Theoretische Physik 1” danke ich für die angenehme Zeit, die spannenden Diskussionen, die Weihnachtsmarktbesuche, die Fußballturniere, . . . uvm.

Der größte Dank gilt allerdings meiner Familie und Svenja, die mich mit viel Geduld und Unterstützung durch meine Promotion begleitet haben.

This work was supported by the Bundesministerium für Bildung und Forschung (BMBF), and by the Deutsche Forschungsgemeinschaft (DFG) within Research Unit FOR 1873 (Quark Flavour Physics and Effective Field Theories).